Molecular mechanisms that drive functional imbalance of circulating CD4+ T cell subsets in granulomatosis with polyangiitis patients

Kim, Sangmi

Awarding institution:
King's College London

Molecular mechanisms that drive functional imbalance of circulating CD4+ T cell subsets in granulomatosis with polyangiitis patients

Sangmi Kim

Thesis submitted for
the Degree of Doctor of Philosophy in
Immunobiology at King's College London,
University of London

Abstract

Granulomatosis with polyangiitis (GPA) is a systemic autoimmune disease. The underlying pathology is primarily caused by the formation of anti-neutrophil cytoplasmic antibodies (ANCA), leading to ANCA associated vasculitis (AAV). While ANCA produced by B cells are a key mediator of the underlying pathogenic process, there is increasing evidence from human and murine studies to strongly support a role for CD4+ T cells in GPA pathogenesis. Previous studies using peripheral blood mononuclear cells (PBMCs) and whole blood from GPA patients suggest that CD4+ T cell subsets, particularly regulatory T cells (Treg) and circulating follicular helper T (cTfh), may be altered in frequencies and/or function in GPA patients.

The aim of this thesis was to identify and compare Treg and cTfh frequencies in GPA patients and healthy controls (HC) and to investigate potential cell intrinsic dysregulation and/or extracellular factor(s) responsible for the functional imbalance in these CD4+ T cell subsets in GPA.

Phenotypic profiling of CD4 T cells by FACS, revealed the aberrant presence of CD25 expression on GPA naive CD4+ T cells. The data reveal a significant increase in Tfh-like phenotypes in GPA, with GPA CD4+ T cells exhibiting elevated expression of BCL6 (a key transcription factor for Tfh differentiation) and IL-21 (a Tfh signature cytokine).

Microarray analysis was performed on naïve CD4+ T cells, from GPA and HC donors, with and without TCR stimulation. These data revealed that antimicrobial genes were the main differentially expressed genes irrespective of stimulation, a finding consistent with the previously accepted notion that chronic infection is an important underlying driver in GPA pathogenesis. Additionally, TCR activation induced the expression of key genes associated with Tfh lineage, such as BCL6 and TRIM8, consistent with the observation of increased Tfh-like phenotypes in GPA.

Significantly, the microarray data suggested the down-regulation of the IL-2/STAT5 pathway in GPA naïve CD4+ T cells. Furthermore, IL2-induced STAT5 activation was confirmed to be decreased in GPA naïve CD4 T cells, by western blot analysis. As the IL2/STAT5 signalling module is a major negative regulator of Tfh differentiation, these findings provide a molecular mechanism for the aberrant enhanced development of Tfh cells in GPA for the first time.

In contrast, frequencies of Tregs and their capacity to suppress effector T cell proliferation were comparable between CD4+ T cells from GPA patients and HC. However, cytokine analysis of supernatants from the suppression assays, reveal significantly that GPA Tregs failed to specifically inhibit the expression of the pro-inflammatory cytokine GM-CSF, which has previously been shown to be a critical mediator of neutrophil activation during the development of GPA pathogenesis.

Finally, the contribution of extracellular factors in plasma to CD4+ T cell dysregulation was assessed by co-culture assays and mass spectrometry. Factors present in plasma could induce expression of CD25 on CD4 T cells from healthy donors. Pro-inflammatory cytokine IL-18 was elevated in plasma from GPA patients. Intriguingly, a comparative mass-spectrometry analysis of plasma samples suggested a potential dysregulation of lipid metabolism in GPA.

In conclusion, this study presents key novel evidence for the involvement of both cell intrinsic dysregulation and extracellular factors in the imbalance of CD4+ T cell differentiation in GPA.

Acknowledgements

First, I would like to hugely thank Dr. Susan John for her great support, encouragement and advice throughout the period of this project, and in fact ever since my masters course. I have been really lucky to have her as my supervisor and life mentor! I would also like to thank my second supervisor, Prof. David D'Cruz for his generous support and helping me to find the necessary funding for this project. Prof. Jo Spencer has also provided me with helpful advice and support. Thank you to Dr. Alina Casian and Louise Nel for recruiting patients and collecting blood samples every Friday morning. I would like to thank Dr Estefania Nova Lamperti for helpful discussion and guidance with experiments and thank you also to Dr Jennie Yang for invaluable advice and help with microsuppression assays. Thank you to Steven Lynham from the CEMS Proteomics Facility at KCL for mass spectrometry support, and Dr. Paul Lavender for support with microarray analysis. Thank you to Yasmin Haque for FACS expertise. Thank you also to Dr. Ben Afzali for helpful discussions and advice, and to my thesis committee members Prof. Stuart Neil and Dr. Chad Swanson. A big thank you to the School of Immunology and Microbial Sciences at KCL for providing significant support to help me complete my studies. Importantly, I want to thank all the patients and healthy donors whose donation of blood samples has made this study possible, and I hope that the findings will be helpful to sufferers of this disease in the future. A big thank you to the Wegener's Trust for providing financial support for this project.

I would like to say a massive thank to all my friends for supporting me, my family in Korea who always send me unconditional support. Lastly, massive massive thank you to my husband Matthew Dicks for helping me to get through all this writing!

Table of contents

Table of Figures

Table of Tables

Abbreviations

AAV	ANCA associated vasculitis
ANOVA	ANalysis Of VAriance
ANCA	Anti-neutrophil cytoplasmic antibodies
Ab	Antibody
ADCC	Antibody-dependent cellular cytotoxicity
APC	Antigen presenting cells
BCR	B cell receptor
BCL	B-cell lymphoma
BATF	Basic Leucine Zipper ATF-Like Transcription Factor
BM-DC	Bone marrow dendritic cell
CTV	Cell Trace Violet
Tcm	Central memory T cell
CXCR / CCR	Chemokine receptor
CSR	Class switch recombination
CD	Cluster of differentiation
cDNA	Complementary DNA
CI	Confidence interval
cpm	Counts per minute
CBA	Cytometric bead array
CTL	Cytotoxic T lymphocyte
DC	Dendritic cell
DNA	Deoxyribonucleic acid
dNTP	Deoxyribonucleotide triphosphate
DMSO	Dimethyl Sulfoxide
ds	Double stranded
DLN	Draining lymph node
Tem	Effector memory T cell
Teff	Effector T cell
ELISA	Enzyme-linked immunosorbant assay
EDTA	Ethylenediaminetetraacetic acid
FcR	Fc Receptor
FACS	Fluorescence-activated cell sorting

FCS	Foetal calf serum
FO	Follicular
FDC	Follicular dendritic cell
Tfr	Follicular regulatory T cells
GC	Germinal Centre
GM-CSF	Granulocyte macrophage colony stimulating factor
GPA	Granulomatosis with Polyangitis
HC	Healthy control
h	Hour
IC	Immune complex
Ig	Immunoglobulin
IPA	Ingenuity Pathway Analysis
IFN	Interferon
IRF	Interferon regulatory factor
IL	Interleukin
IU	International units
ICS	Intracellular staining
kb	Kilobase
kDa	Kilodalton
KCL	King's College London
KO	Knock-out
LPS	Lipopolysaccharide
LN	Lymph node
MHC	Major histocompatibility complex
MZ	Marginal Zone
MS	Mass Spectrometry
mBC	Memory B cell
MEM	Minimum essentials medium
MAPK	Mitogen activated protein kinase
M-MuLV	Moloney Murine Leukemia Virus
mAb	Monoclonal antibody
MPO	Myeloperoxidase
NK	Natural Killer
NET	Neutrophil extracellular trap

NLR	NOD-like receptors
NF-κB	Nuclear factor kappa B
PAMP	Pathogen associated molecular patterns
PRR	Pattern recognition receptors
PPIA	Peptidylprolyl isomerase A
PBMC	Peripheral blood mononuclear cells
PMA	Phorbol 12-myristate 13-acetate
PBS	Phosphate buffered saline
PCR	Polymerase chain reaction
PVDF	Polyvinylidene difluoride
PCA	Principal Component Analysis
PR3	Proteinase 3
qRT-RCP	Quantitative Reverse Transcription PCR
Treg	Regulatory T cell
g	Relative centrifugal force
Tresp	Responder T cells
rpm	Revolutions per minute
RNA	Ribonucleic acid
RLR	RIG-1-like receptor
RNF	Ring finger protein
RTX	Rituximab
RT	Room temperature
RPMI	Roswell Park Memorial Institute
s	Second
SLO	Secondary lymphoid organs
STAT	Signal transducer and activator of transcription
SPIA	Single primer isothermal amplification
SDS-PAGE	Sodium dodecyl sulfate polyacrylamide gel electrophoresis
SHM	Somatic hypermutation
SCS	Subcapsular sinus
Th	T helper cell
TCR	T-cell Receptor
Tfh	T-follicular helper cell
TMT	Tandem Mass Tag

TLR	Toll-like receptor
TGF	Transforming growth factor
TNF	Tumour necrosis factor

1. Introduction

Our immune system has developed to protect the body from foreign pathogens. To eliminate an invading pathogen, the immune system mounts a selective response upon recognition of non-self antigen. Distinguishing between self and non-self antigen is crucial for an effective immune system - immune self tolerance ensures that there is no reactivity to self-antigen. A failure in the mechanism of immune self-tolerance leads to immune responses being raised against self-antigen (autoimmunity) and inflammatory disease. This inflammatory response can either be confined to local tissues (organ specific autoimmune disease) or can affect multiple organs /tissues (non-organ specific/systemic autoimmune disease). Approximately 3-5% of the general population is affected by autoimmune diseases, and cases of autoimmune diseases have increased over the past few decades (Bach, 2018). Despite significant increase advances in scientific and improved treatments, autoimmune diseases remain incurable and morbidity and mortality remain high.

Granulomatosis with polyangiitis (GPA, formerly known as Wegener's granulomatosis) is one of the systemic autoimmune small vessel vasculitis syndromes that are associated with anti-neutrophil cytoplasmic antibodies (ANCA) (Cartin-Ceba *et al.*, 2012; Mckinney *et al.*, 2014). As is the case for many autoimmune diseases, GPA is a polygenic disease. It is believed that the initial source of inflammation may be from activated neutrophils but the mechanism is unclear and may involve complement, proinflammatory cytokines, infection, or combination of all three factors. Although ANCA is a laboratory marker of GPA, it is not directly involved in the disease pathogenesis. Increasing evidence suggests

that a functional imbalance between Treg and Tfh cells in GPA patients may be one of the underlying causes of disease progression.

This introduction will begin by providing a basic overview of the immune system, and then progress to reviewing the current literature regarding the role of CD4+ T cells in GPA pathogenesis.

1.1. The immune system

The body is protected from infection, physical damage and other harmful foreign agents by having an immune system. To protect from pathogens, the immune system must first be able to distinguish between foreign (non-self) antigens, and self-antigens, so that the immune system can specifically target foreign antigen only. Upon antigen recognition, the, immune system generates immunological memory which allows the body to respond quicker when it is re-challenged by the same antigen. However, redundant immune responses or self-reactive immune responses can cause unwanted damage in tissue. To prevent this, the immune system is exquisitely controlled by immune regulatory mechanisms (Murphy *et al.*, 2008).

The immune system can be divided into two parts; innate immunity and adaptive immunity. Innate immunity is a rapid, first line of defence mechanism, while adaptive immunity is a more delayed response but has extremely high specificity against non-self antigens, and provides immunological memory and immune regulation (Murphy *et al.*, 2008).

1.1.1. Innate immunity

Innate immunity is activated immediately upon sensing of foreign antigens.

Foreign antigens are recognized by a family of pattern recognition receptors (PRRs) on innate immune cells. PRRs include Toll like receptors (TLR), Retinoid acid-inducible gene I (RIG-I)-like receptors (RLR) and nucleotide-binding oligomerization domain (NOD)-like receptors (NLR), mannose receptors, scavenger receptors and CD14. The ligands of PRRs are pathogen-associated molecular patterns (PAMPs). PAMPs include distinct evolutionarily conserved molecular structures on pathogens that are not present in mammalian cells. Each different type of PRR recognises its own specific PAMP, for example TLR4 specifically recognises lipopolysaccharides (LPS). PAMP recognition by PRRs activates specific signalling pathways in innate immune cells. As a result, innate immune cells can upregulate and/or secrete specific signalling molecules such as cytokines and chemokines, and antimicrobial proteins depending upon the nature of the antigen recognised (Medzhitov, 2007; Murphy *et al.*, 2008; Mogensen, 2009). Activation of the innate immune system leads to inflammation – a signal that the body is alerted to the presence of an invading of pathogen. Blood flow to the infected site is increased to allow rapid recruitment of other immune cells and the subsequent initiation of adaptive immunity.

1.1.1.1. Innate immune cells

Innate immune cells include epithelial cells, Innate lymphoid cells (ILCs), phagocytes (Neutrophils, macrophages and dendritic cells, (DC)) and leukocytes (Basophils, eosinophils, mast cells and natural killer (NK) cells). Basophils, eosinophils and mast cells are involved in protection from parasites. While mast cells are mucosal tissue resident, basophils and eosinophils are recruited by blood

circulation to the infected site. NK cells defend the host from viral infections and kill infected cells. DCs are professional antigen presenting cells (APCs), and play an important role in bridging between innate immunity and adaptive immunity. DCs process antigen after phagocytosis, and present antigenic peptides on major histocompatibility (MHC) class II molecules. Presented antigen on MHC class II is recognised by cognate T cell receptors (TCR) on naive CD4+ T cells, initiating CD4+ T cell differentiation. Neutrophils and macrophages are important phagocytes in host defence from many pathogens. Activated macrophages release proinflammatory cytokines such as interleukin1β (IL-1β), IL-6 and tumor necrosis factor (TNF) to recruit other effector cells such as NK and CD4+ T cells (Medzhitov, 2007; Murphy *et al.*, 2008).

1.1.1.2. Defence mechanisms in innate immunity

1.1.1.2.1. Neutrophil extracellular traps

Neutrophils are the first cells to migrate through blood vessels and be recruited to the inflammatory site. Functions of neutrophils in host defense include phagocytosis, degranulation (release of an assortment of antimicrobial agents) and production of neutrophil extracellular traps (NETs). NET is a host defense mechanism particular to neutrophils. It is a web-like DNA structure decorated with a variety of proteins including several cytosolic and granule proteins with bactericidal activity such as myeloperoxidase (MPO), cathepsin G, proteinase 3 (PR3), elastase, cathelicidin (LL37) and defensins(Delgado-Rizo *et al.*, 2017; Papayannopoulos, 2018). Pertinent to this thesis, auto-reactive antibodies against MPO and / or PR3 are believed to be the primary cause of the autoimmune disorder Granulomatosis with Polyangiitis (GPA).(Mckinney *et al.*, 2014; Jorch and Kubes, 2017).

There are two NET formation pathways; lytic NETosis (a lytic pathway involving neutrophil death) and non-lytic NETosis (Figure 1.1). Lytic NETosis can be inducedby phorbol-12-myristate-13-acetate (PMA), auto-reactive antibodies and cholesterol crystals. Upon induction of NETosis, reactive oxygen species (ROS) are generated by activated NADPH oxidase. ROS generation activates MPO and neutrophil elastases (NE), promoting their translocation to the nucleus. In the nucleus, NE and MPO promote chromatin decondensation and disruption of the nuclear membrane. Granular and cytosolic proteins associate with released chromatin in cytosol, then the NET structure is released upon neutrophil death. This NETosis method occurs over several hours after neutrophil activation(Jorch and Kubes, 2017; Papayannopoulos, 2018). In contrast, non-lytic NETosis does not result cell death, and can occur within minutes after neutrophil activation. Non-lytic NETosis is initiated with stimuli such as *Staphylococcus aureus*, LPS, fungi and *Esherichia coli* through TLR2, TLR4 and CR3 (a complement receptor, consisting of CD11b (integrin α_M) and CD18 (integrin β_2)(Delgado-Rizo *et al.*, 2017; Papayannopoulos, 2018). Upon activation, neutrophils immediately undergo NET formation as in lytic NETosis, but proteins and the associated NET is released in a vesicle. The plasma membrane therefore remains intact after NET release, allowing the neutrophil to survive and continue to perform anti-microbial functions. This rapid, non-lytic NETosis mechanism commonly occurs in neutrophils that first arrive at the site of infection (Papayannopoulos, 2018).

The formation of NETs is induced not only by foreign antigens but also by products of inflammation such as complement C5a, granulocyte-macrophage colony-stimulating factor (GM-CSF), activated platelets and adhesion molecules on

epithelial cells. (Delgado-Rizo *et al.*, 2017; Jorch and Kubes, 2017; Grover and Mackman, 2018; Papayannopoulos, 2018).

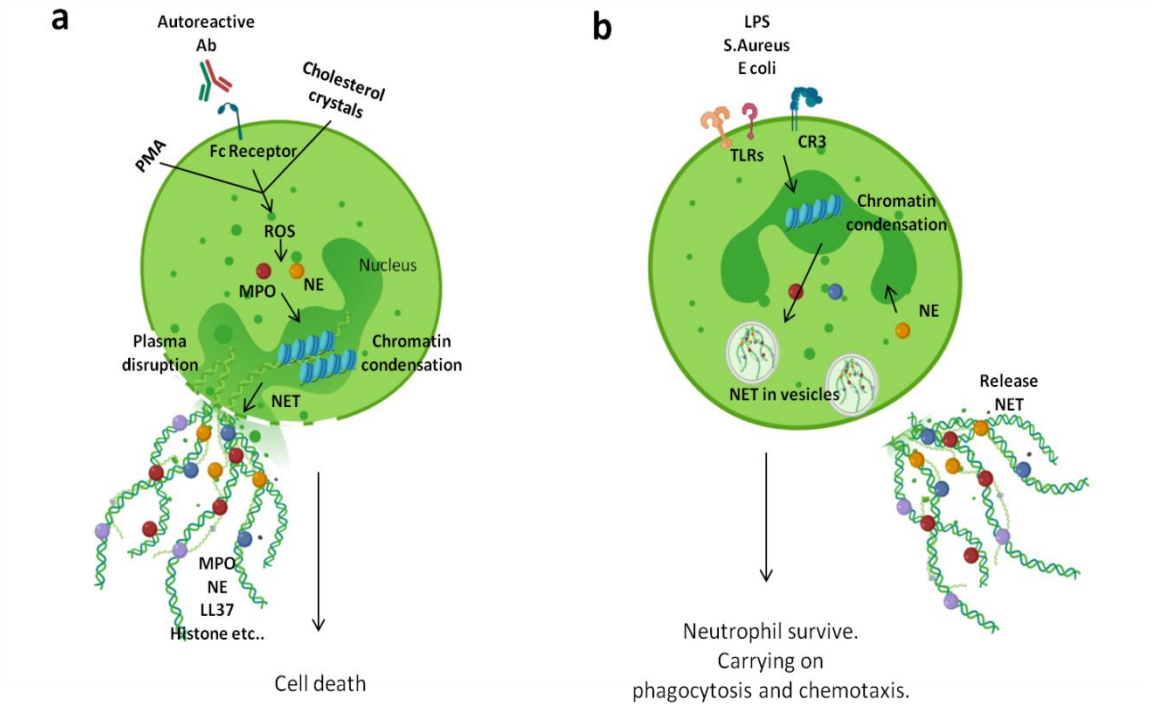

Figure 1.1. Overview of NETosis. **(a)** lytic NETosis.**(b)** non-lytic NETosis. Adapted from (Jorch and Kubes, 2017).

1.1.1.2.2. Coagulation system

An additional function of NETosis is to enhance coagulation in blood vessels. The coagulation system is activated during infection to prevent the spread of infection by making thrombin. Released NETs from neutrophils lead to an increase in the size of thrombi by capturing more platelets. In addition, inflammation upregulates adhesion molecules such as P-selectin on vascular epithelial cells to recruit neutrophils to the site of infection. Engagement between adhesion molecules and receptors on neutrophils activates neutrophils, which leads to NETosis. (Grover and Mackman, 2018; De Bont *et al.*, 2019).

1.1.1.2.3. Anti-microbial peptides and Type I interferons

Defensins, a class of antimicrobial peptides, are also produced by innate immune cells particularly by neutrophils and almost all epithelial cells. These small peptides are generally stored in granules and they are released during phagocytosis. Defensins are amphipathic peptides so they are thought to kill bacteria by interrupting the bacterial cell membrane (Ganz, 2003).

Although innate immune cells are more specialized and focused towards the immune response to pathogens, other host cells also have defence mechanisms upon infection. Type I interferons (IFNs) are produced by almost cells in the body in response to viral infection and induce expression of antiviral response genes. It also has been shown that bacterial infection can induce type I IFNs through TLR engagement (Gonzalez-Navajas *et al.*, 2012).

1.1.1.2.4. Complement

Another innate host defence mechanism is complement activation. Activated innate immune cells produce pro-inflammatory cytokines such as IL-1β and IL-6. Consequently, these proinflammatory cytokines leads to release of acute-phase proteins such as C-reactive protein (CRP), serum amyloid protein A (SAA) and mannose-binding protein (MBP) from the liver. These acute-phase proteins result in activation of complement system (Medzhitov, 2007; Murphy *et al.*, 2008).

The complement system includes a large range of plasma proteins and cell-surface proteins which are predominantly protease enzymes. These proteins circulate in body fluid and tissues as inactive proteases until they become activated. Complement activation is initiated at the site of infection and inflammation. It

occurs on the pathogen surface via three different pathways; classical, lectin and alternative. The classical pathway is initiated through engagement between C1q (C1 serine protease complex) and the Fc region of an antibody attached to the pathogen surface. The lectin pathway is initiated through the recognition of arrays of mannose residues on the surface of a pathogen by mannose binding lectin (MBL). In contrast to the classical and lectin pathways, the alternative pathway does not require pathogen binding proteins for its initiation. It is initiated through the spontaneous hydrolysis of C3 (which is abundant in plasma). Activated complement initiates a proteolytic enzyme cascade, resulting in the generation of proinflammatory mediators (anaphylatoxins: C3a, C4a and C5a), formation of a membrane attack complex to lyse infected cells (MAC: C5b to C9) and opsonisation by coating the surface of the pathogen (C3b). (Murphy *et al.*, 2008; Dunkelberger and Song, 2010).

1.1.2. Adaptive immunity

Adaptive immune cells consist of two major lymphocyte types: B cells and T cells. B cells secrete glycoprotein molecules termed immunoglobulins (also known as antibodies). T cells display membrane anchored immunoglobulins on their surface (T cell receptors, TCR) which recognise antigens displayed in complex with MHC molecules on the surface of APCs.

An adaptive immune response takes longer to develop compared to innate immunity, but adaptive immunity has two key advantages; a vast diversity of highly specific antigen receptors acquired during lymphocyte development, and the generation of immunological memory. While the diversity of PRRs in innate immunity is limited to the recognition of certain PAMPs, B cell receptors (BCR) and

T cell receptors (TCR) are far more varied and customized for specific epitopes located within a pathogen derived antigen. A series of gene recombination events leads to a huge diversity of BCRs and TCRs during B cell and T cell development in the bone marrow and thymus respectively. Antigen engagement with these receptors, together with additional signals (including from cytokines and co-stimulatory receptors) results in the activation and differentiation of these cells into effector populations. A subpopulation of 'antigen-experienced' cells gains immunological memory to prepare for a future challenge with the same pathogen. These 'memory' cells remain after elimination of the pathogen and respond more rapidly when the antigen stimulus is reintroduced (Murphy *et al.*, 2008).

1.1.2.1. B cells

1.1.2.1.1. B cell development and maturation

In adaptive immunity, the key role of B cells is to provide a humoral response by generating antibodies. B cell development occurs in adult human bone marrow. Hematopoietic stem cells undergo V(D)J DNA segment rearrangement to generate functional BCRs (IgM form) on immature B cells(Murphy *et al.*, 2008). These immature B cells leave from the bone marrow and migrate to the spleen for maturation. The immature B cells go through transitional stages, called T1 and T2. After transitional stages, they develop into two types of naive B cell; follicular (FO) B cells and marginal zone (MZ) B cells. During B cell development, random V(D)J rearrangement also generates a subset of BCRs that are less specific for particular antigens and instead recognise multiple microbial patterns. Most of these 'innate-like' BCRs are expressed on MZ B cells. Both FO B cells and MZ B cells circulate in the periphery and migrate to secondary lymphoid organs (SLO) such as the spleen and lymph nodes where B cells typically encounter antigen. FO B cells migrate into

B cell follicles and MZ B cells migrate to the marginal zone in spleen or marginal zone like sites in SLOs (Mcheyzer-Williams *et al.*, 2011; Heesters *et al.*, 2016).

During infection, antigens drain into SLOs as small soluble molecules or as membrane associated antigen presented on the surface of APCs including macrophages and DCs and follicular dendritic cells (FDC) (Figure 1.2). In naive B cell priming, these APCs in SLOs use receptors instead of MHC molecules for presentation of unprocessed antigens including complement receptors (CR1, CR2 and CR3), DC-Specific ICAM3-Grabbing Non-integrin (DC-SIGN) and low-affinity F_c receptor for IgG (FCγRIIB). Antigen engagement with BCRs leads to naive B cell priming for further activation (Batista and Harwood, 2009).

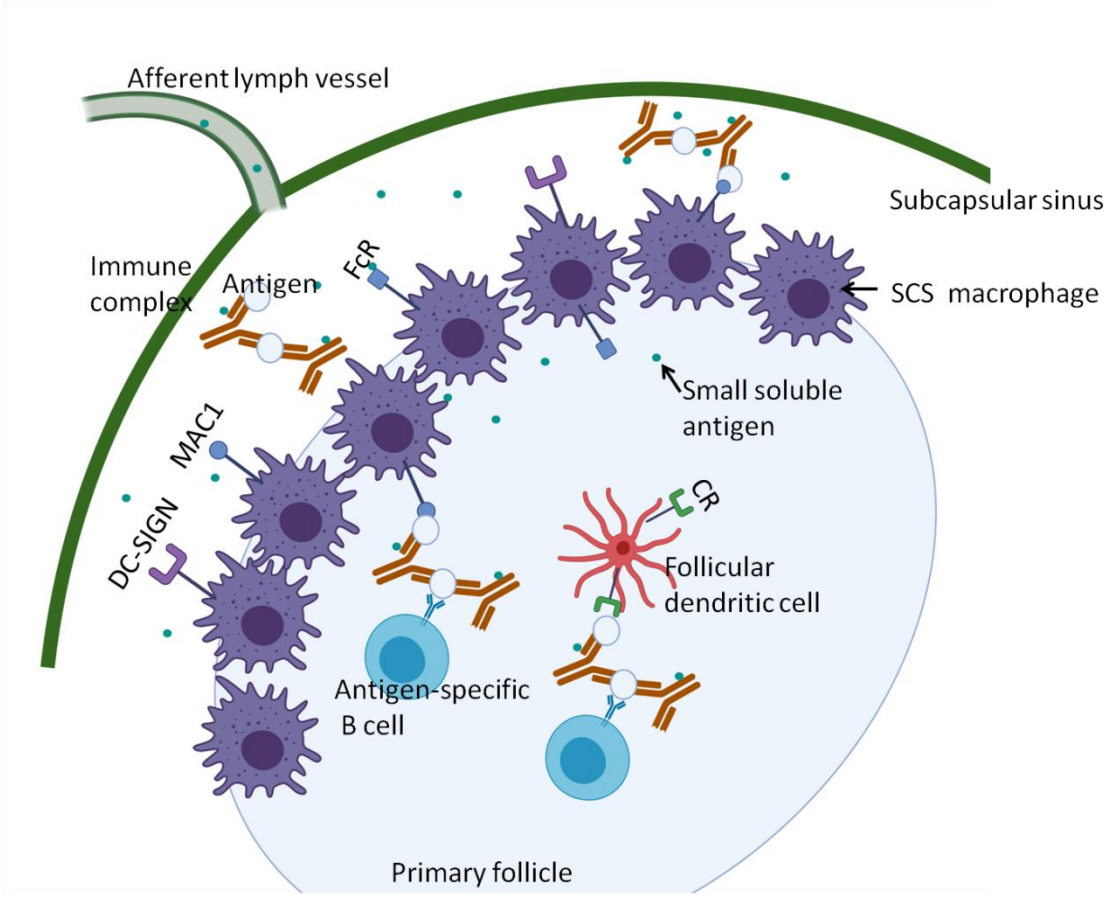

Figure 1.2. B cell maturation in the spleen. Antigens are presented to B cells in the spleen by subcapsular sinus (SCS) macrophages and follicular dendritic cells. Unprocessed antigens are recognised by B cells as small soluble antigens or in the form of immune complexs. Adapted from (Batista and Harwood, 2009).

1.1.2.1.2. B cell activation

There are two mechanisms of B cell activation, T- Dependent (TD) activation and T-Independent (TI) activation. This classification is based on the degree of T cell involvement in B cell activation(Batista and Harwood, 2009; Schmitt and Williams, 2013; Heesters *et al.*, 2016).

1.1.2.1.2.1. T- Dependent (TD) B cell activation

FO B cell activation in germinal centres is the best representative mechanism of TD activation (Figure 1.3). Presented antigens to FO B cells are internalised by BCRs and processed for presentation on MHC class II molecule on the B cell surface. These antigen presenting B cells move to the B cell-T cell border within SLOs (Batista and Harwood, 2009). Peptide-MHC class II complexes on B cells engage with cognate TCRs on CD4+ T cells. In addition to TCR engagement, secondary signals from interactions between CD40, CD80 and CD86, and cytokine receptors on B cells, and their cognate ligands on CD4+ T cells and cytokines released from CD4+ T cells initiate B cell proliferation and differentiation into effector cells. These proliferative B cells either differentiate into short lived plasma cells which produce low affinity antibody (IgM) or continue proliferation in the follicle leading to the formation of a germinal centre (GC) (Batista and Harwood, 2009; Mcheyzer-Williams *et al.*, 2011; Schmitt and Williams, 2013; Heesters *et al.*, 2016).

GC resident B cells undergo the process of Ig class switch recombination (CSR) and somatic hypermuation (SHM) to generate high affinity antibody producing plasma cells and memory cells (Mcheyzer-Williams *et al.*, 2011). In this GC reaction, the role of follicular helper T cells (Tfh) and FDCs are important (see Figure 1.3). FO B cells that have recently entered GCs undergo clonal expansion in the dark zone of the GC. During clonal expansion, SHM and CSR occur to generate BCR diversity. Following clonal expansion, GC B cells move to the light zone of the GC and BCRs are scanned by FDCs to check their ability to bind presented antigen. While a failure of antigen recognition by the BCR leads to cell apoptosis, positive antigen recognition by BCRs generates a signal allowing GC B cells to encounter cognate Tfh cells. Engagement with cognate Tfh cells results in further CSR and survival of GC B cells with high affinity BCRs. After interaction with Tfh cells, GC B cells either exit the GC as effector cells (long-lived plasma cells or plasma cells) or re-enter the GC cycle for further BCR re-diversification (Batista and Harwood, 2009; Mcheyzer-Williams *et al.*, 2011; Schmitt and Williams, 2013; Heesters *et al.*, 2016; Wing *et al.*, 2019).

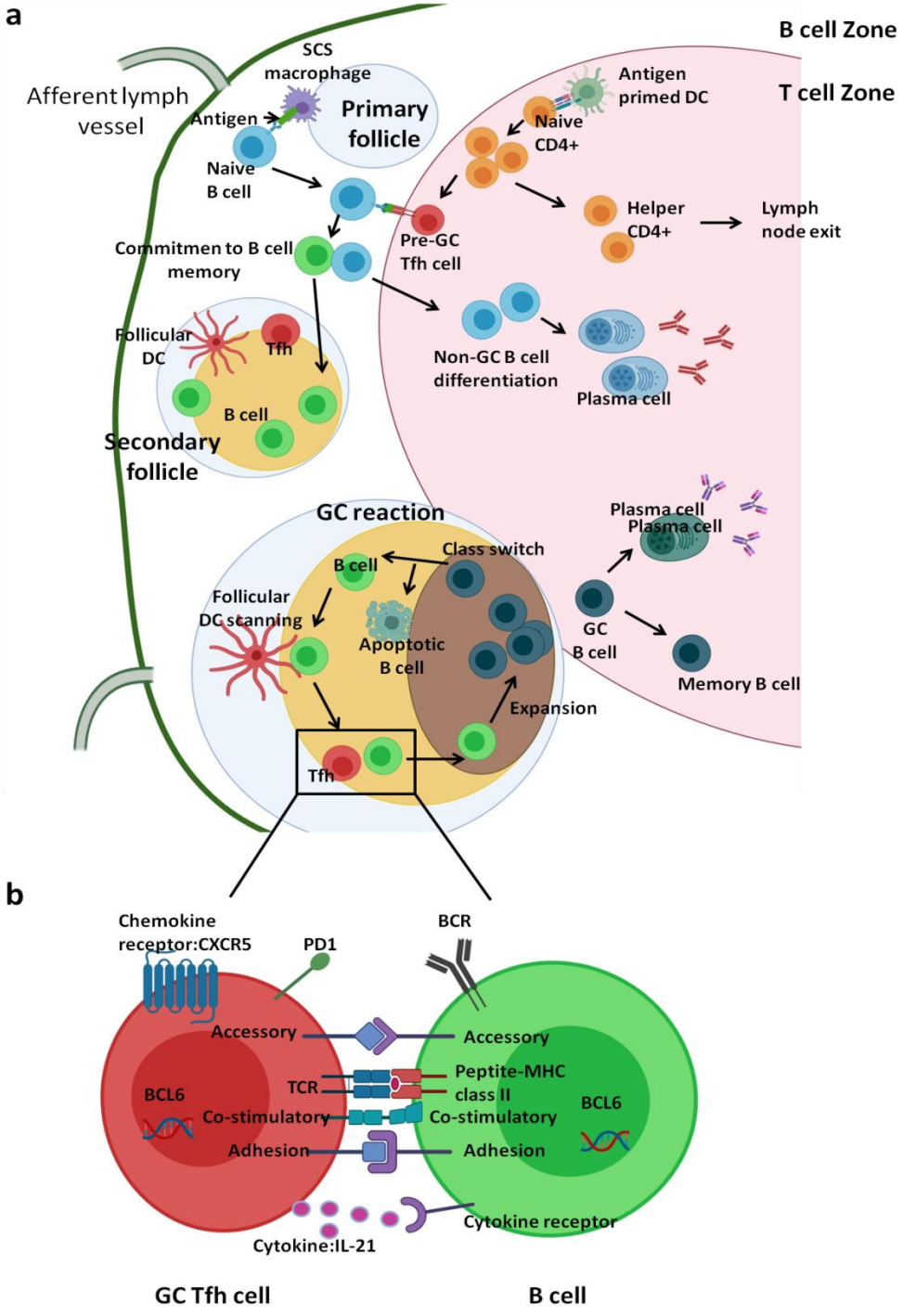

Figure 1.3. T-dependent B cell activation and differentiatio. (a) Overview of B cell differentiation and germinal centre (GC) reaction. **(b)** GC Tfh and B cell engagement during GC reaction. Adapted from (Mcheyzer-Williams *et al.*, 2011).

1.1.2.1.2.2. T-Independent (TI) B cell activation

In contrast to FO B cells, MZ B cells do not necessarily require T cell help to become activated. Therefore, MZ B cells migrate to marginal zones in the spleen or marginal zone like sites in other SLOs which contain an abundance of antigen and very large macrophage and DC populations. Polyreactive BCRs on MZ B cells engage highly repetitive epitopes on bacteria such as capsular polysaccharide molecules via clustering of BCRs. In addition to BCRs, TLRs on MZ B cells are involved in dual engagement of conserved microbial antigen such as LPS. As a result of strong BCR signalling alone, MZ B cells are activated and become low affinity antibody producing plasma cells (Batista and Harwood, 2009; Mcheyzer-Williams *et al.*, 2011; Cerutti *et al.*, 2013; Schmitt and Williams, 2013; Heesters *et al.*, 2016).

1.1.2.1.3. Antibodies and the B Cell Receptor

Antibodies play a major role in three humoral immune mechanisms; neutralization, opsonisation and complement activation. Neutralisation may involve antibodies binding to pathogen surfaces to prevent pathogen adhering to and/or infecting host cells. This antibody mediated neutralisation can also defend host cells from bacterial toxins. Antibody coating of antigens promotes targeting by phagocytes since the Fc region of antibodies are recognised by receptors on the surface of phagocytes – a process termed opsonisation. Antigen-antibody complexes may also initiate the classical complement activation pathway (Murphy *et al.*, 2008).

Antibodies are essentially secreted forms of the membrane anchored B cell receptor immunoglobulin. The basic structure of an antibody is shown in Figure

1.4. Antibodies consist of a complex of four polypeptide chains (two identical heavy chains and two identical light chains) attached via disulfide bonds. The complex is functionally divided into variable regions (highly variable between antibodies – the sites of antigen-binding) and constant regions (the organisation of which determines the immunoglobulin isotype) (Murphy *et al.*, 2008).

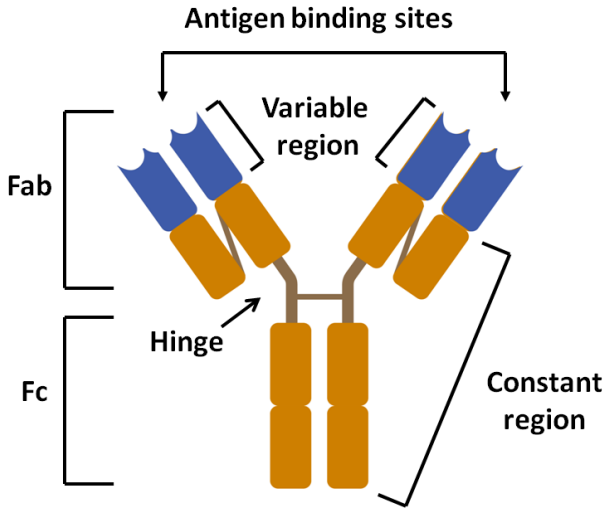

Figure 1.4. Basic structure of antibody.

The initial form of the B cell immunoglobulin is generated by V(D)J gene recombination. There are three gene segments: variable (V), diversity (D) and joining (J) in genetic loci for each polypeptide heavy chain (the D segment is absent in light chain loci). Each segment has number of different copies - therefore gene recombination generates immunoglobulin diversity in adaptive immunity. A similar process occurs during T cell development to generate T cell receptor diversity.

During B cell maturation, immunoglobulins undergo somatic hypermutation (SHM) and class switch recombination (CSR). These processes result in the generation of high affinity antibodies, secreted by plasma B cells. SHM occurs during B cell clonal expansion through high rates of point mutation within variable gene regions. CSR occurs within constant gene regions – this process generates different isotypes of antibodies within B cell populations. In humans there are five different Ig isotypes: IgM, IgD, IgA, IgG (subclasses are IgG_1, IgG_2, IgG_3 and IgG_4) and IgE. Each antibody isotype is structurally and functionally distinctive (see Table 1.1).

Type of Ab	Function
IgM	Neutralization, opsonization, active complement system
IgG	Neutralization, opsonization, active complement system Mediate antibody dependent cellular cytotoxicity mediated by NK cells Four subclasses (IgG1, IgG2, IgG3 and IgG4)
IgA	Neutralization, opsonization, active complement system
IgE	Sensitization of mast cells

Table 1.1. Antibody isotypes and their function.

Naive B cells express IgM and IgD isotypes initially. However, during B cell activation, exposure of certain cytokines in SLOs, particularly those produced by CD4+ T cells, can trigger CSR and direct switching to a different antibody isotype class. (Murphy *et al.*, 2008)

1.1.2.2. T cells

1.1.2.2.1. T cell development

While BCRs and antibodies interact with native antigen directly, and their affinity is variable depending on B cell activation, αβ T cell receptors (TCR) recognise antigen presented as peptides by MHC molecules. The specificity and affinity of TCRs are determined after T cell development in thymus. TCRs consist of two polypeptide chains, and their structure is similar to the Fab region of an antibody (Figure 1.4). TCRs on conventional T cells are composed of an α chain and β chain (Vroom *et al.*, 1991; Murphy *et al.*, 2008). However, about 5% of T cells express TCRs consisting of a γ chain and δ chain (γδ TCR). γδ T cellsrecognise a range of antigens through non-classical MHC molecules. These cells exhibit cytotoxic activity and also play a role in activation of other immune cells. Their roles in oncology and autoimmunue disease have become increasingly appreciated in recent years but are not yet understood to the same extent as conventional T cells (Lawand *et al.*, 2017; Melandri *et al.*, 2018). Therefore, in this thesis use of the term 'TCR' will refer to conventional αβ T cell receptors.

T cells have two major lineages, CD4+ T cells and CD8+ T cells. Cluster of differentiation (CD)4 and CD8 are cell surface glycoproteins. They are associated with TCRs and act as co-receptors for antigen presenting MHC molecules during antigen recognition. CD4 and CD8 co-receptors recognise different types of MHC molecules; CD4 recognises MHC class II and CD8 recognises MHC class I molecules(Murphy *et al.*, 2008)

These lineages are determined in thymus after migration of T cell committed lymphoid progenitors from bone marrow (Figure 1.5). In the thymus, progenitors

first undergo V(D)J gene recombination to generate TCR specificities. Prior to this stage, T cells are termed double negative (DN) thymocytes as they express neither CD4 nor CD8 on their surface. Co-receptor molecules are first expressed during the pre-TCR development phase, during which T cells express a premature form of the TCR consisting of a non-rearranged α chain and mature rearranged β chain. Double positive (DP) thymocytes which express both CD4 and CD8 then complete TCR maturation and undergo positive selection by interacting with epithelial cells in the cortex. Cortical thymic epithelial cells (cTEC) express self-peptides on MHC class I and class II molecules and an engagement between DP thymocytes and self-peptides generates a survival signal to DP thymocytes. This engagement also promotes differentiation of DP thymocytes into CD4 or CD8 single positive (SP) T cells, determined by the TCRs preference for interaction with MHC class II or MHC class I, respectively. The failure of a thymocyte to interact with self- peptide:MHC complexes will lead to apoptosis (Germain, 2002; Murphy *et al.*, 2008) .

Positively selected CD4 or CD8 SP T cells then migrate into the medulla for negative selection. Negative selection is an important process, required for elimination of auto reactive T cells. In the medulla, almost all self-antigen recognising T cells are eliminated by apoptosis. In general, interactions between high affinity TCRs and self-peptides:MHC molecules by APCs such as medullary thymic epithelial cells (mTEC), DCs and macrophages induce clonal deletion. However, some of these high affinity auto-reactive T cells survive and become differentiated into tTreg cells. Although the exact mechanism of how TCR signalling directs clonal deletion, tTreg generation or conventional T cell generation remains unclear, studies in mice show that ubiquitous auto-antigen binding induces clonal deletion but binding to tissue restricted antigen (TRA) may

induce tTreg generation (Legoux *et al.*, 2015; Malhotra *et al.*, 2016). Peptides from TRAs are processed and presented under the control of transcription factors such as autoimmune regulator (AIRE) and FEZ family zink finger 2 (Fezf2) in mTEC. Still, most T cells auto-reactive to TRAs are deleted – the mechanisms involved in tTreg differentiation and release to the periphery are unknown. In addition, negatively selected T cells, which have low affinity TCRs to self-antigens can also be released to periphery as naive CD4+ or CD8+ T cells after effective maturation. (Kieback *et al.*, 2016; Takaba and Takayanagi, 2017; Lee and Lee, 2018)

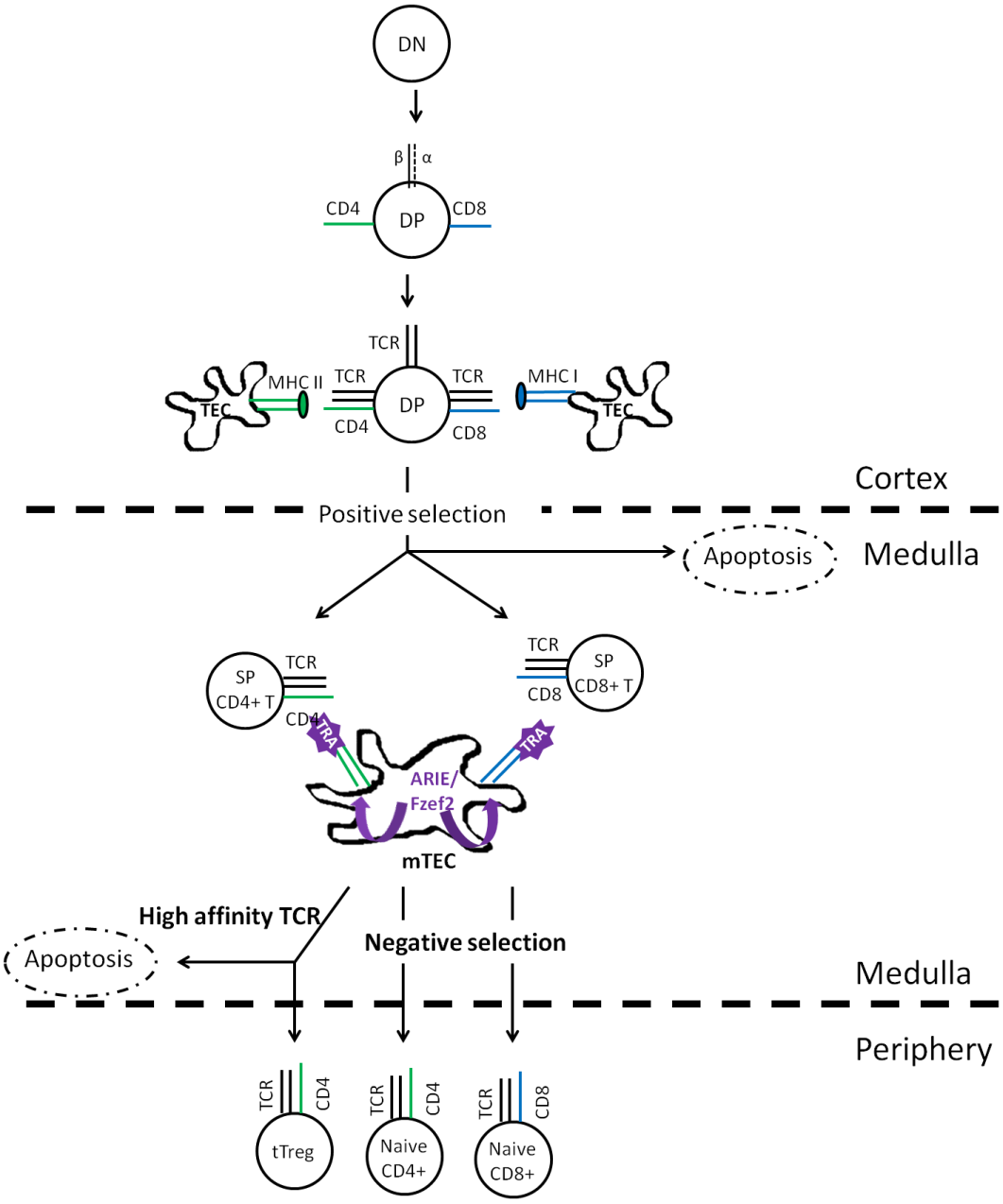

Figure 1.5. T cell development in the thymus. Double negative (DN) thymocytes become double positive (DP) thymocytes that express both CD4 and CD8 on their surface. By engaging with self peptide presented by MHC on thymic epithelial cells (positive selection), they become single positive (SP) T cells in the cortex. In the medulla, most SP T cells possessing high affinity TCR undergo apoptosis after interaction with tissue restricted antigen (TRA) (negative

selection), but a few survive to become thymic Tregs and are released into the periphery.

1.1.2.2.2. T cell activation

Newly formed naive T cells are released from the thymus into peripheral blood. They circulate between SLOs (such as spleen and tonsils), and the blood. Until they experience antigen presented within SLOs, naive T cells are homogeneous and quiescent. In humans, naive T cells express CD45RA (ligand as yet unknown), and lymphoid homing receptors such as CC- chemokine receptor7 (CCR7) and CD62 ligand (CD62L). However, once they become activated by cognate antigen presented by APCs, CD45RA expression is down-regulated and CD45RO, (a memory associated marker), becomes up regulated (Van Den Broek *et al.*, 2018).

Upon infection, naive T cells become activated by interacting with APCs presenting cognate non-self antigens (Figure 1.6). Activated T cells undergo differentiation into effector T cells., T cells recognising peptide:MHC complexes on the surface of APCs also require a second co-stimulatory signal for full T cell activation to occur. The primary co-stimulatory signalling molecule on naive T cells is CD28. CD28 binds to CD80 (also known as B7-1) or CD86 (also known as B7-2) on APCs. CD80/CD86 molecules are up-regulated on APCs that have detected the presence of non-self antigens via pattern recognition receptor stimulation. Therefore, the requirement for a 'second' co-stimulatory signal acts an additional mechanism to prevent auto-reactive T cell activation. T cells that engage antigen:MHC complexes without a simultaneous co-stimulatory signal become functionally inactivated – a process termed T cell anergy (Murphy *et al.*, 2008; Chen and Flies, 2013).

T cell activation (from simultaneous antigen recognition and co-stimulation) triggers three main signal transduction pathways; the nuclear factor κB (NFκB) pathway, the mitogen activated protein kinase (MAPK) pathway, and the calcium-calcineurin pathway. Together these signals induce the rapid and potent expression of the key immune cytokine, IL-2. CD25 (IL-2 receptor α chain) is also upregulated, which promotes autocrine IL-2 signalling, leading to T cell clonal proliferation and subsequent effector T cell differentiation. For activated CD4+ T cells, a 'third signal' from environmental cytokines is required to direct differentiation into specific effector helper T cell subtypes. (Murphy *et al.*, 2008)

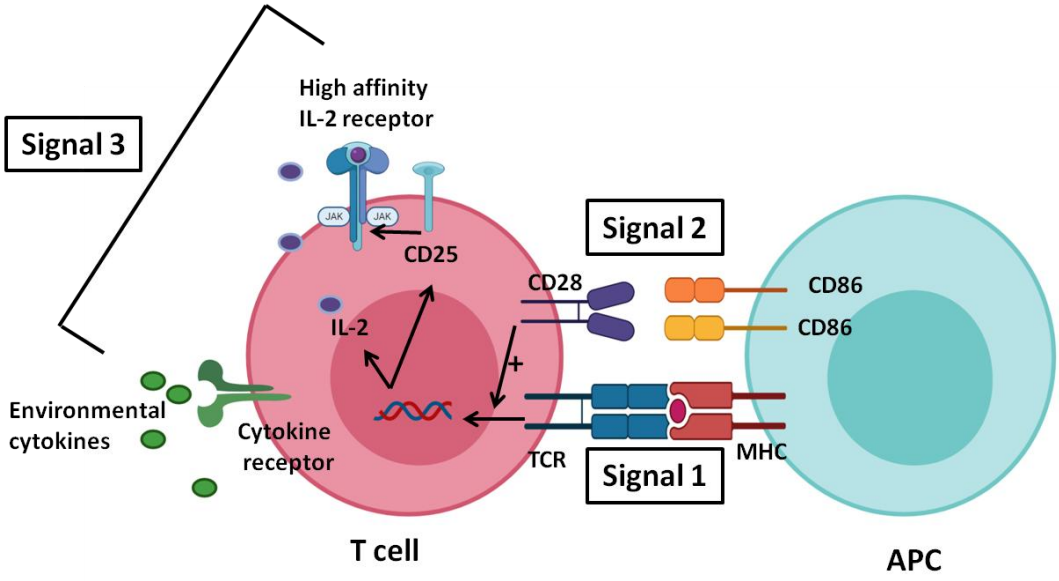

Figure 1.6. T cell activation by signal 1, 2 and 3. Adapted from (Snanoudj *et al.*, 2007)

1.1.2.2.3. Effector T cells

1.1.2.2.3.1. Effector CD8+ T cells

Naive CD8+ T cells are activated through recognition of presented antigen in the form of peptide:MHC class I complexes on the surface of infected cells or APCs in SLOs. Effector CD8+ T cells are important for mediating immune defence against

intracellular pathogens including viruses and intracellular bacteria. CD8+ T cells are also known as cytotoxic T lymphocyte (CTL) due to their ability to selectively kill infected cells. Effector CD8+ T cells induce cell death by releasing cytotoxic granules such as perforin and granzymes. Perforin interrupts cell membranes to create a pore that results in target cell lysis. Granzymes are serine proteases and induce target cell apoptosis. They trigger activation of a caspase cascade, which eventually leads to nuclease activation and degradation of DNA in target cells. Activated CD8+ T cells also upregulate FAS ligand (known as apoptosis antigen 1) (FASL). The interaction between FASL on CD8+ T cells and FAS on infected cells also results in activation of the caspase cascade and induction of apoptosis. Activated CD8+ T cells also secrete proinflammatory cytokines including IFNγ and TNFα that contribute to elimination of pathogens (Murphy *et al.*, 2008; Cox and Zajac, 2010).

1.1.2.2.3.2. Effector CD4+ T cell differentiation

In SLOs, naive CD4+ T cells are activated by engaging with antigen presented on MHC class II complexes by APCs. Activated naive CD4+ T cells become differentiated into effector CD4+ T helper (Th) cells. Th cells primarily act to augment the function of other cells types instead of killing infected cells directly. They help to activate CTLs and macrophages to target infected cells and stimulate B cells to generate high affinity antibodies by inducing SHM and CSR.

Activated CD4+ T cells can become differentiated into a variety of CD4+ T helper subsets. Each Th cell subset has different phenotypic and functional characteristics. The lineage differentiation is determined by the strength of TCR signalling and nature of cytokine stimulation. The combination of signals from TCR and cytokines

up and/or down- regulates specific transcription factors. In particular, cytokine stimulation of cognate receptors activates the canonical JAK-STAT signalling pathway. Latent cytoplasmic tyrosine kinases JAKs, which are loosely associated with cytoplasmic domains of cytokine receptors get activated upon ligand binding to receptors. Activated JAKs phosphorylate the cytokine receptor to create specific docking sites for latent signalling/transcription factors, Signal transducers and activators of transcription (STATs) (Figure 1.7). Phosphorylated and activated STATs directly bind DNA and induce gene expression of lineage specific master regulators. There have been seven mammalian STAT family members identified; STAT1, STAT2, STAT3, STAT4, STAT5a, STAT5b, STAT6. Different cytokines induce specific STAT(s) activation that results in specific Th cell subset differentiation. (Christie and Zhu, 2014; Tripathi and Lahesmaa, 2014; O'shea *et al.*, 2015; Zhu, 2018).

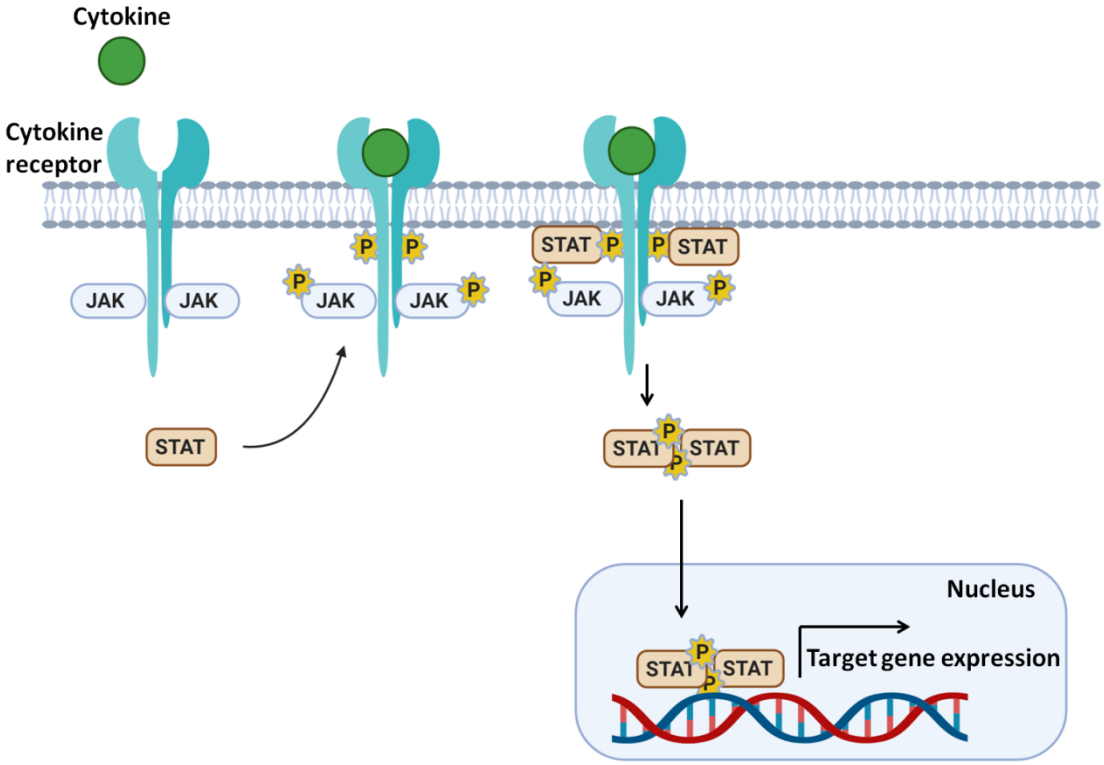

Figure 1.7 Schematic of JAK/STAT activation via cytokine receptors. Interaction between cytokines and cytokine receptors leads to phosphorylation of

JAK proteins. Intracellular cytokine receptors are utilised as docking sites for STAT protein phosphorylation. Phosphorylated STATs dimerise, and translocate to the nucleus to initiate target gene expression.

Although cytokine induced STAT activation is critical for regulation of CD4+ T cell differentiation, there are several additional transcription factors that also become up and/or down-regulated during CD4+ T cell activation. Moreover, these master regulators and transcription factors cross regulate each other. Therefore, this fine-tuned network of factors contributes towards generating a variety of Th cell subsets.

During Th cell differentiation, cytokines are key mediators in determining Th cell lineage fates. In turn, the different Th cell lineages are also the major sources of specific cytokine production in the immune system. Functional characteristics of Th cell subset can be distinguished by their specific cytokine secretion profiles. Although IL-2, IL-6, IL-10, tumor necrosis factor α (TNFα), and granulocyte macrophage colony stimulating factor (GM-CSF) are produced by all Th cells, there are additional signature effector cytokines produced by each Th cell subset. (Christie and Zhu, 2014; Tripathi and Lahesmaa, 2014; Zhu, 2018).

Since the concept of distinct functional Th cell subsets, T helper 1 (Th1) and T helper 2 (Th2), was introduced in the 1980s, the range of Th cell subsets has expanded considerably. This has been achieved through advances in immune phenotyping techniques including flow cytometry, fluorescence-activated cell sorting (FACS), genetic tools, and proteomics. Currently, five major Th cell subsets have been defined; Th1, Th2, Th17, T follicular helper (Tfh) and regulatory T (Treg)

cells including thymus derived Treg (tTreg) and peripherally induced Treg (pTreg). (Christie and Zhu, 2014; Tripathi and Lahesmaa, 2014; Zhu, 2018).

1.1.2.2.3.2.1. T helper 1 cells

Differentiation towards a Th1 cell phenotype is generally induced by IL-12 stimulation, predominantly produced by activated APCs such as macrophages and DCs (Figure 1.8). IL-12 signalling activates STAT4, which in turn induces upregulation of Th1 specific genes including *IL2Rβ, IFNγ* and *Tbx21* (encoding Th1 master transcription factor, Tbet). STAT4 induced Tbet regulates Th1 related gene expression including IFNγ upregulation. As a result, the collaboration of STAT4 and Tbet induces IFNγ production from Th1 cells. Moreover, a positive feedback mechanism is initiated, since IFNγ signalling further upregulates Tbet expression via STAT1 activation. (Christie and Zhu, 2014; Tripathi and Lahesmaa, 2014; Zhu, 2018).

Tbet not only upregulates Th1 specific genes but also inhibits expression of genes that would direct CD4+ T cells towards differentiation into other subtypes. It inhibits Th2 cell differentiation by down-regulating IL-4 and GATA Binding Protein 3 (GATA3; the Th2 master transcription factor) expression. Additionally, Tbet binds to Runx1 and Runx3 to block induction of the Rorc gene (encoding Th17 master transcription factor, RORγt), and inhibits expression of B-cell lymphoma 6 protein (BCL6; Tfh master transcription regulator), resulting in inhibition of Th17 and Tfh cell differentiation, respectively.

Th1 cells are critical for host defence mechanisms against intracellular pathogens such as viruses, protozoa and bacteria. One of the major functions of Th1 cells is production of IFNγ, that activates macrophages and induces B cells to generate

complement fixing and opsonising IgG antibodies. (Christie and Zhu, 2014; Tripathi and Lahesmaa, 2014; Zhu, 2018).

1.1.2.2.3.2.2. T helper 2 cells

Th2 cell differentiation is directed by IL-4 stimulation. IL-4 signalling activates STAT6, which in turn induces Th2 master transcription factor, GATA3. GATA3 induces IL-4 production and additionally production of IL-5 and IL-13 (Figure 1.8). Moreover, IL-2 also indirectly promotes Th2 cell differentiation by activating STAT5 and STAT3 (Stritesky *et al.*, 2011)Activated STAT5 binds to *IL-4* gene regulatory elements leading to IL-4 upregulation, and also induces IL-4Rα expression (Liao *et al.*, 2008).Similar to the role of Tbet in Th1 differentiation, GATA3 is also involved in inhibition of other Th subsets such as Th1 and Th17 through down-regulation of their main transcriptional regulators. Th2 cells are important in immune responses against extracellular parasites (e.g. helminths) Through secretion of IL-4, IL-5 and IL13, Th2 cells also induce IgG1 and IgE production from B cells. These cytokines can also activate eosinophils and macrophages (Christie and Zhu, 2014; Tripathi and Lahesmaa, 2014; Zhu, 2018).

1.1.2.2.3.2.3. T helper 17 cells

Th17 cell differentiation is induced by signals from a combination of cytokines (including IL-6, IL-21, and IL-23) that activate STAT3. Activated STAT3 increases expression of the Th17 master transcription factor, RORγt (Zhou *et al.*, 2007). RORγt is also induced by TGFβ and IL-1β signaling via activation of NF-κB members RelA (p65) and c-Rel (Figure 1.8)(Chen *et al.*, 2011). In addition to RORγt, several transcription factors including RUNX1 (which upregulates RORγt)(Zhang *et al.*, 2008),Interferon regulatory factor 4 (IRF4)(Brustle *et al.*, 2007), Basic

leucine zipper transcription factor, ATF-like (BATF) (Miao *et al.*, 2013) and Hypoxia-inducible factor 1-alpha (HIF1α)(Dang et al., 2011) also promote Th17 cell differentiation.

Th17 cells have been shown to be important in immune defence against extracellular bacteria and fungi such as Candida albicans. However, an overactive Th17 response can be responsible for inflammatory tissue damage and autoimmune disease by over-production of pro-inflammatory cytokines such as IL-17A and IL-17F, and a dual functional (can be protective or inflammatory) cytokine IL-22 (Sanjabi et al., 2009; Khan and Ansar Ahmed, 2015).

1.1.2.2.3.2.4. Follicular helper T cells

Human Tfh cell differentiation is initiated by activation of STAT3 via signalling from a combination of IL-12, IL-6, IL-21 and TGFβ (Figure 1.8). However, these cytokine signals, under different conditions can also promote Th1 and Th17 differentiation. Therefore, strong TCR signalling and co-stimulatory signalling (especially signalling through ICOS) is also critical to direct cells towards Tfh differentiation (Schmitt *et al.*, 2014; Qi, 2016). Attenuation of STAT5 activation is also important to enable upregulation of BCL6, the master transcription factor for Tfh differentiation. IL-2, IL-7 and IL-15 induced STAT5 activation leads to high Blimp-1 expression that inhibits BCL6 expression (Johnston *et al.*, 2009; Crotty *et al.*, 2010; Ballesteros-Tato *et al.*, 2012) Like other master regulators, BCL6 upregulation simultaneously inhibits differentiation into other Th subsets. BCL6 directly binds to *Tbet* and *Rorγc* promoters, negatively regulating their expression, and GATA3 is also downregulated by BCL6 . In sum, Tfh lineage specific genes including Tfh signature cytokine IL-21 are induced through a combination of

signals from transcription factors including BCL6, BATF, IRF4, c-Maf and Ascl2, and attenuation of STAT5 (Qi, 2016; Vinuesa *et al.*, 2016; Webb and Linterman, 2017; Wu *et al.*, 2018).

While other effector Th cell subsets migrate to sites of infection and mediate antigen clearance, Tfh cells remain resident within SLOs and migrate into GCs. Within GCs, Tfh cells help B cells to generate high affinity antibody (see section 1.1.2.1.1 and Figure 1.3) (Wu *et al.*, 2018). To promote migration into B-cell follicles, Tfh cells express the key follicle homing marker CXCR5, a chemokine receptor for CXCL13. CXCR13 is abundantly expressed within follicles so Tfh cells migrate via chemotaxis, following a CXCL13 gradient. The interaction between Tfh and B cells leads to B cell maturation. These activated B cells further differentiate into plasma B cells (that can produce antibodies) or memory B cells. Therefore, Tfh cells are regarded as specialised T cell subsets for B cell maturation and antibody production in the immune system (Ma *et al.*, 2012; Shekhar and Yang, 2012). Other distinctive Tfh cell surface markers include PD1 and ICOS. Although the role of PD1 on Tfh cells is unclear, it is thought that PD1 expression may be the result of strong TCR activation (inhibiting hyper proliferation of Tfh cells)(Vinuesa and Cyster, 2011) .ICOS is believed to be critical for inducing IL-21 expression through the PI3K signaling pathway (Qi, 2016; Webb and Linterman, 2017; Wu *et al.*, 2018).

CD4+ T cells expressing CXCR5 have also been reported in peripheral blood and are termed peripheral Tfh (pTfh) cells (He *et al.*, 2013). This subset is highly heterogeneous, and although additional markers including CXCR3, CCR7, ICOS and PD1 have been associated with peripheral Tfh cells, a definitive phenotype remains unclear (He *et al.*, 2013; Pissani and Streeck, 2014). Interestingly, a recent study

has indicated that circulating IL-21^{+} CD4^{+} T cells may be more functionally similar to the bona fide Tfh cells found in germinal centres than previously reported pTfh cell phenotypes (Schultz *et al.*, 2016).

1.1.2.2.3.2.5. Regulatory T cells

For an effective immune system, maintaining immunological self-tolerance and control of excessive and potentially damaging responses is as important as elimination of antigen. Treg cells are a specific T cell subset that acts as the key mediator in immune suppression. The majority of Treg cells develop in the thymus (thymus driven Treg, tTreg) during positive and negative selection (see section 1.1.2.2.1 and Figure 1.5). During T cell thymic development, some immature CD4 single positive T cells express CD25 (IL-2 receptor α chain) on their surface. These CD25+ CD4 single positive cells (tTreg precursor cells) express transcription factor Forkhead Box P3 (Foxp3) which is the Treg master regulator and become fully committed tTregs upon stimulation from IL-2 and IL-15 and subsequent activation of STAT5 (Lio and Hsieh, 2008; Wing *et al.*, 2019). Although Foxp3 is the master Treg transcription factor and principal marker of the Treg subset, the commitment of a T cell towards the Treg lineage is determined prior to Foxp3 expression by high affinity TCR engagement. Therefore, strong TCR signalling is the main determinant of tTreg fate (Sakaguchi *et al.*, 2007; Hsieh *et al.*, 2012; Kitagawa and Sakaguchi, 2017; Lee and Lee, 2018).

Treg cells also can be generated in the periphery from naive CD4+ T cells. These 'induced' Treg cells are called iTreg when they generated *in vitro*, or 'peripherally induced' Treg (pTreg) when they generated *in vivo*. Upon stimulation from TGFβ and IL-2, naive CD4+ T cells can become induced Tregs (Figure 1.8). TGFβ leads to

activation of transcription factors Smad2 and Smad3 that induce Foxp3 expression. IL-2 induced STAT5 also directly binds to the *Foxp3* promoter to enhance Foxp3 expression (Christie and Zhu, 2014; Kanamori *et al.*, 2016).

The phenotypic markers of Treg cells are similar to activated CD4+ T cells in humans. The key surface marker CD25 and transcription factor Foxp3 can be expressed by CD4+ T cells upon activation. Moreover, CTLA4, GITR and CD95 (also known as FAS) may also be expressed on activated CD4+ T cells. Treg cells are commonly identified by the phenotype $CD25^{high}$ $CD127^{low}$ (CD127 is IL-7 receptor α-chain) - cells displaying this phenotype typically suppress effector T cell function in *in vitro* suppression assays. However, activated CD4+ T cells also tend to express low levels of CD127 (Sakaguchi *et al.*, 2007; Sakaguchi *et al.*, 2008; Sakaguchi *et al.*, 2010).

The suppressive ability of Treg cells is mediated through a variety of mechanisms; cell to cell contact (CTLA4 on Treg to CD80/CD86 on APCs, LAG3 on Treg to MHC molecules on APCs), secretion of anti-inflammatory cytokines (such as IL-10, TGFβ and IL-35) and metabolic disruption (Tregs express CD39/CD73 which degrades ATP to cAMP, an important second messenger signaling molecule in many biological processes, which is subsequently taken up by effector T cells. In addition, effector T cells are competitively deprived of IL-2 through expression of a high affinity IL-2 receptor on Tregs) (Sakaguchi *et al.*, 2010; Schmitt and Williams, 2013).

Tregs can be also divided into three sub-populations based on expression of CD45RA and intensity of CD25 expression; population I (CD25+CD45RA+ Tregs:

resting Tregs), population II (CD25++CD45RA- Treg: activated Tregs) and population III (CD25+CD45RA- Tregs: memory Tregs)(Miyara *et al.*, 2009). Population I and population II have shown suppressive function *in-vitro*. However, the function of population III has been controversial. Although it has been showed that the suppressive function of this subset was reduced *in vitro* (Miyara *et al.*, 2009), other studies suggested that the population may in fact be a mixture of Tregs and non-Tregs (Cuadrado *et al.*, 2018; Wing *et al.*, 2019).

Treg cells exhibit significant functional plasticity; an ability to switch between different functional subsets, influenced by the specific pathological microenvironment (Kleinewietfeld and Hafler, 2013; Pandiyan and Zhu, 2015). A well-documented example of plasticity is between Treg and Th17 cell subsets. In the presence of IL-1β, Treg population III, (CD4+CD25hiCD127loCD45RA-) cells can express the natural killer cell marker, CD161, and produce IL-17 (Tr17), while still retaining their suppressive function, despite a decrease in FoxP3 expression (Afzali *et al.*, 2013). Tr17 cells are regarded as potentially "dangerous" rather than immunoregulatory under pathological conditions, as they secrete proinflammatory cytokine IL-17 in an already inflammatory microenvironment. Treg cells can also be found in B cell follicles and they display phenotypic characteristics of both Treg cells and Tfh cells. These cells are called follicular regulatory T (Tfr) cells. Tfr cells have the ability to suppress both B cell and Tfh cell immune responses (Fonseca *et al.*, 2017; Lee and Lee, 2018).

1.1.2.2.3.2.6. Newly identified CD4+ T cell subsets: Th9, Th22 and Th_{GM} cells

Th9 and Th22 cells have recently been identified as functionally distinct Th subsets (Figure 1.8). Th9 T cells are closely related to Th2 cells. Th9 cell differentiation is

initiated by IL-4 and TGF-β stimulation, leading to STAT6 activation and subsequent upregulation of master transcription factors PU.1 and IRF4. Th9 cells produce the signature cytokine IL-9 and are involved in host defence against extracellular parasites and may also be involved in the progression of autoimmnunity. Th22 cell differentiation is induced by cytokines IL-6 and TNF-alpha, and upregulation of master transcription factor AhR via activation of STAT3. However, the molecular mechanism involved in Th22 differentiation is still unclear. Th22 cells are the main source of IL-22, and their primary function is protection of epithelial barriers including skin and the lungs.

GM-CSF secreting Th cells (Th_{GM} cells) were first observed in mouse models of autoimmune neuroinflammation. Differentiation appears to be triggered through STAT5 activation via IL-7 (and probably IL-2) stimulation (Figure 1.9b). (Sheng *et al.*, 2014; Tripathi and Lahesmaa, 2014; Eyerich and Eyerich, 2015; Neurath and Kaplan, 2017; Owen and Farrar, 2017).

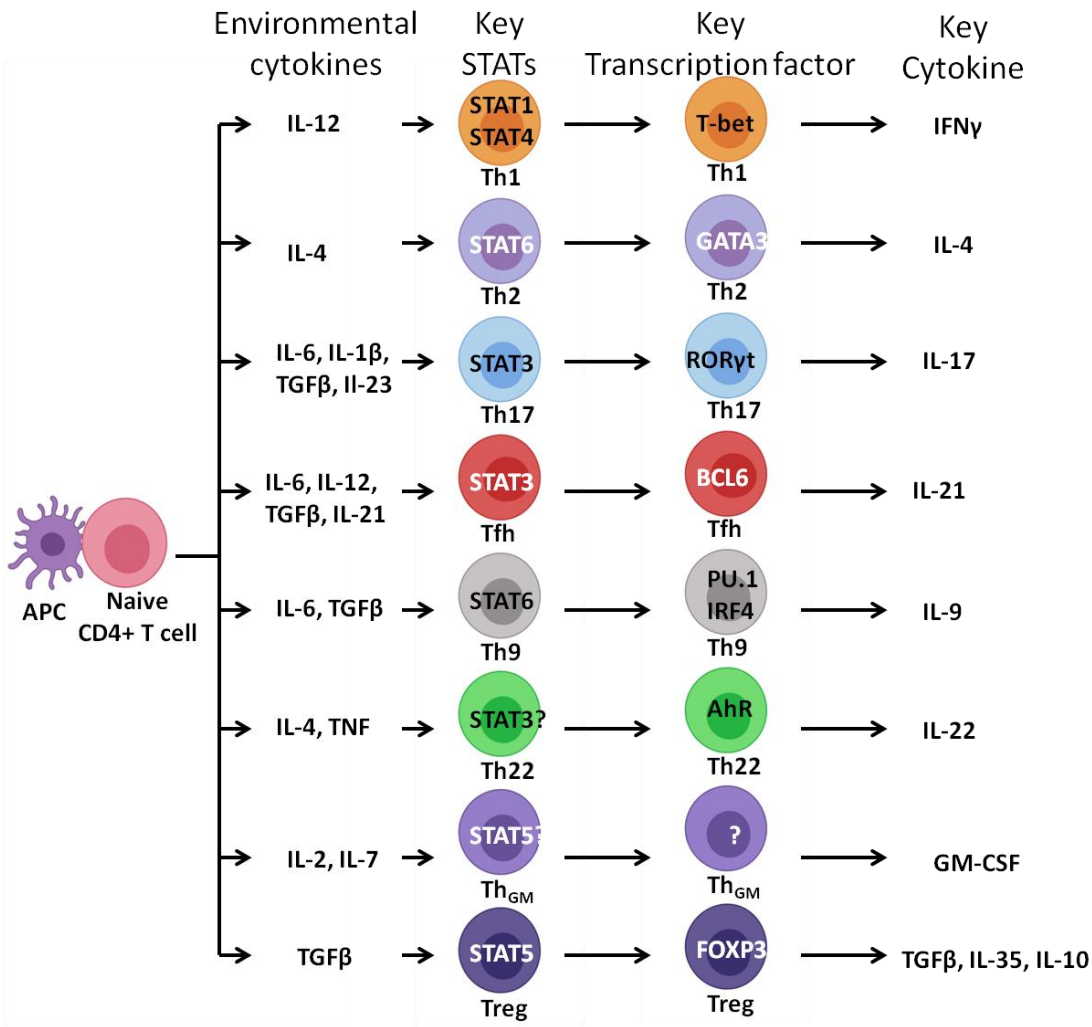

Figure 1.8 Th differentiation and subsets. Exposure of activated naïve CD4+ T cells to different cytokines leads to activation of different STAT proteins. STAT activation determines Th cell lineage commitment, leading to expression of key transcription factors for each Th subset. Adapted from (Tripathi and Lahesmaa, 2014).

1.1.2.2.4. IL-2/STAT5 in CD4+ T cell differentiation

In additional to TCR engagement and co-stimulation, a 'third signal' from the cytokine environment (typically transduced via STAT transcription factors) is critical to determine Th cell lineage. STAT5 is one of the essential transcription

factors in many aspects of T cell biology. It is activated by multiple cytokines including IL-2, IL-4, IL-7, IL-9, , IL-15 and GM-CSF(Owen and Farrar, 2017)

There are two STAT5 family members, STAT5A and STAT5B that share 90% amino acid sequence identity (Lin *et al.*, 1996). Both play essential roles in the immune system, particularly during lymphocyte development, but the full spectrum of functional differences between the family members are not fully understood yet. However, a few studies have suggested that STAT5B is more important for the function of immune cells. In mice, STAT5B expression is more abundant than STAT5A in both T effectors and Tregs (Villarino *et al.*, 2016), and STAT5B deficiency is linked to failure of Treg development in humans through dysregulation of Foxp3 gene expression, despite normal STAT5A expression in these patients (Jenks *et al.*, 2013; Kanai *et al.*, 2014; Villarino *et al.*, 2016).

IL-2 is a critical cytokine in CD4+ T cell development, proliferation and differentiation, and signals initiated through IL-2 receptor activation are transduced through STAT5. IL-2 is among the earliest cytokines secreted by CD4+ T cells upon TCR activation. Upon TCR activation, several transcription factors such as activator protein 1 (AP1), NFκB, nuclear factor of activated T cells (NFAT) and Foxp3, upregulate IL-2 expression. IL-2 is primarily produced by activated CD4+ T cells, though it is also secreted by other cell types such as CD8+ T cells, DC's and NK cells (Granucci *et al.*, 2003; Kim *et al.*, 2006; Spolski *et al.*, 2018).

There are two functional IL-2 receptor forms; a high affinity form and an intermediate affinity form. The high affinity IL-2 receptor consists of three IL-2 receptor subunits - IL-2R alpha chain (IL-2Rα, CD25), IL-2Rβ chain (IL-2Rβ, CD122)

and common gamma chain (γc, CD132). The intermediate affinity IL-2 receptor form consists of IL-2Rβ and γc chains. Upon IL-2 binding and receptor activation, signal transduction occurs via the cytoplasmic domains of IL-2Rβ and γc chains (Liao *et al.*, 2011). CD25 expression increases the affinity of the IL-2 receptor for IL-2 but is not involved in signal transduction directly. IL-2Rβ and γc chains are constitutively expressed on the surface of immune cells such as resting T cells and NK cells, while CD25 is expressed on DCs, Tregs oractivated T cells upon TCR stimulation or IL-2 signalling (Figure 1.9a) (Granucci *et al.*, 2003; Spolski *et al.*, 2017; Spolski *et al.*, 2018).

Blockade of IL-2 stimulation inhibits both Th1 and Th2 differentiation(Mcdyer *et al.*, 2002). STAT5, activated via IL-2 signalling, promotes upregulation of IL-12Rβ and IL-4Rα in Th1 and Th2 cells, respectively. In contrast, Th17 and Tfh cell differentiation is inhibited by activated STAT5 via IL-2. Both Th17 and Tfh differentiation require STAT3 activation. During Th17 cell differentiation, STAT5 and STAT3 compete for binding to the same DNA binding site at the *IL-17* gene locus. Furthermore, STAT5 supresses IL-6R expression – IL-6 signalling promotes STAT3 activation in Th17 cells. In Tfh cell differentiation, STAT5 suppresses BCL6 expression directly and indirectly via BLIMP1 mediated repression of BCL6. STAT5 activation via IL-2 signalling is essential for Treg cell development, maintenance and function. Deletion of STAT5B decreases Treg cell populations in both humans and mice. In tTreg development, tTreg precursor (CD25+CD4 single positive) cells require IL-2/STAT5 activation to express Foxp3 and become mature tTregs. In pTreg differentiation, IL-2 induced STAT5 contribute in upregulation of Foxp3 expression. Moreover, in mature Treg cells, IL-2/STAT5 signals stabilize Foxp3 expression to prevent conversion of Treg cells into effector Th cells under

inflammatory conditions (Figure 1.9b) (Liao *et al.*, 2011; Johnston *et al.*, 2012; Owen and Farrar, 2017; Spolski *et al.*, 2017; Abbas *et al.*, 2018; Mitra and Leonard, 2018; Spolski *et al.*, 2018).

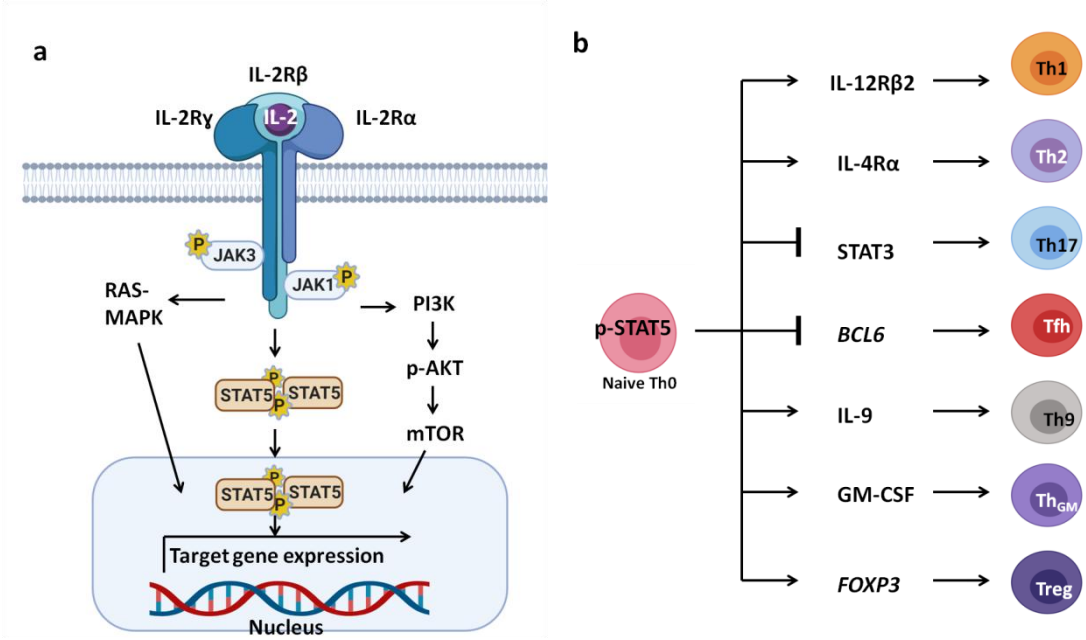

Figure 1.9. IL-2 signalling pathways and STAT5 activation in CD4+ T cell differentiation. (a) IL-2 signalling. Along with JAK- STAT5 activation, PI3K and MAPK pathways are also upregulated upon IL-2 stimulation in CD4+ T cell. PI3K pathway induces mTOR activation that leads to metabolic state change (will discuss section 1.1.2.2.7). MAPK activation enhances cell proliferation. Adapted from (Mitra and Leonard, 2018). **(b)**CD4+ Th cell lineage differentiation regulated by STAT5. Adapted from (Owen and Farrar, 2017).

1.1.2.2.5. Memory T cell subsets

After pathogen elimination, most effector T cells undergo apoptosis; this is termed the contraction phase of the response. However, some effector T cells persist after the contraction phase as memory T cells. They require signals from cytokines IL-7 and IL-15 to maintain homeostatic proliferation, independent of antigen

stimulation. Memory T cells have been classified into two main subsets; effector memory T cells (T_{EM}) and central memory T cells (T_{CM}). T_{CM} cells express secondary lymphoid homing receptor, CCR7 and CD62L, so rapidly proliferate upon antigenic re-encounter and are less dependent on co-stimulatory signals compared to naive T cells. T_{EM} cells reactivate effector functions more rapidly compared to T_{CM} cells. T_{EM} cells express lower levels of secondary lymphoid homing receptors compared to T_{CM} but they display chemokine receptors that promote migration to inflamed tissues. Although CD45RA is mainly associated with the naive T cell phenotype, some T_{EM} cells re-express CD45RA on their surface, are so are termed T_{EMRA} (table 1.2) (De Rosa *et al.*, 2001; Lee *et al.*, 2004; Sallusto *et al.*, 2004; Tian *et al.*, 2017; Jameson and Masopust, 2018).

	Naïve T	T_{CM}	T_{EM}	T_{EMRA}
CD45RA	+	-	-	+
CD45RO	-	+	+	-
CCR7	+	+	-	-
CD62L	+	+	+/-	+/-

Table 1.2. Naive and Memory T cell surface markers.

1.1.2.2.6. T cell exhaustion

Persistent antigen stimulation such as in the case of chronic infection or cancer may lead to T cell exhaustion. Exhausted T cells exhibit some effector T cell phenotypes but lose their effector functions. These cells exhibit a decrease in cytokine secretion and a resistance to reactivation and differentiation into memory cells (Wherry, 2011; Mckinney *et al.*, 2015; Wherry and Kurachi, 2015). Originally, T cell exhaustion was described in CD8+ T cells after chronic viral infection. It is

thought that CD8+ T cell exhaustion occurred not only due to continuous antigen exposure, but also lack of CD4+ T cell help (Matloubian *et al.*, 1994). Although CD4+ T cell exhaustion is not well understood, a few studies have suggested that the mechanism may involve skewing towards a Tfh-like phenotype. In mice, chronic infection increases Tfh-like cell phenotypes, characterized by upregulation of markers such as BCL6, CXCR5 and IL-21 in CD4+ T cells (Fahey *et al.*, 2011; Crawford *et al.*, 2014; Greczmiel *et al.*, 2017; Vella *et al.*, 2017).

1.1.2.2.7. Co-inhibitory receptors and exhaustion

In addition, multiple inhibitory receptors such as programmed cell death protein 1 (PD1), cytotoxic T lymphocyte antigen 4 (CTLA4), lymphocyte activation gene 3 (LAG3) and T cell immunoglobulin domain and mucin domain-containing protein 3 (TIM3; also known as HAVCR2) are highly expressed on exhausted T cell surfaces. During T cell activation to generate functional effector T cells, inhibitory receptors are upregulated to create a negative feedback system for the T cell activation pathway. Signalling through inhibitory receptors generates regulatory signals within the T cell that act to oppose co-stimulatory activation and limit effector functions, with the ultimate aim to limit the immune response. The balance between co-stimulatory and co-inhibitory signals determines the magnitude and duration of the immune response. Co-signalling (co-stimulatory and co-inhibitory) receptors and counter ligands are expressed on almost all cell types. In adaptive immunity, co-signalling is critical to fine control immune responses (Chen and Flies, 2013; Wherry and Kurachi, 2015).

1.1.2.2.8. Metabolic changes upon activation of Th subsets

Metabolic flux through pathways involved in biosynthesis and ATP generation

switches upon T cell activation. In the quiescent state, CD4+ T cells focus on mitochondrial oxidative phosphorylation to generate ATP, the energy currency in the cell, by utilising fatty acids or amino acids as the key metabolites. Upon TCR activation, CD4+ T cells become proliferative and require more energy to generate new cellular structures and biological macromolecules such as nucleotides, amino acids and fatty acids for daughter cells. Therefore, focus of metabolism within CD4+ T shifts from oxidative metabolism to biosynthetic metabolism by increasing flux through glycolysis in the cytoplasm and the tricarboxylic acid *cycle* (TCA cycle) in mitochondria. Glucose is either metabolised into pyruvate or enters into the pentose phosphate pathway or serine biosynthesis pathway in the cytosol. Pyruvate, amino acids and fatty acids enter into mitochondria and are metabolised in the TCA cycle.

This shift in metabolic state is initiated by signals from TCR activation and transcription factor activation. Activated TCR and co-stimulatory signals activate the phosphoinositide 3 kinse (PI3K) –AKT pathway resulting in mechanistic target of rapamycin (mTOR) signalling (Figure 1.10). Acitvated mTOR leads to activation of transcription factors such as HIF1α, MYC and SREBP that upregulate biosynthetic metabolism such as glycolysis, fatty acid synthesis and amino acid synthesis. Each Th subset has a distinct metabolic program, and changes in metabolic flux can also direct lineage differentiation. Th1, Th2 and Th17 cells rely heavily on glycolysis via mTOR signalling, while the Tfh master regulator, BCL6, suppresses glycolysis.

Treg cells are characterised by low levels of active mTOR signalling. In Treg cells, high expression of PTEN regulates the PI3K–AKT- mTOR pathway that promotes

Treg cell homeostasis and survival. Moreover, rapamycin treatment which suppresses mTOR activation can induce Treg differentiation *in vitro*. (Buck *et al.*, 2015; Bantug *et al.*, 2018; Dumitru *et al.*, 2018)

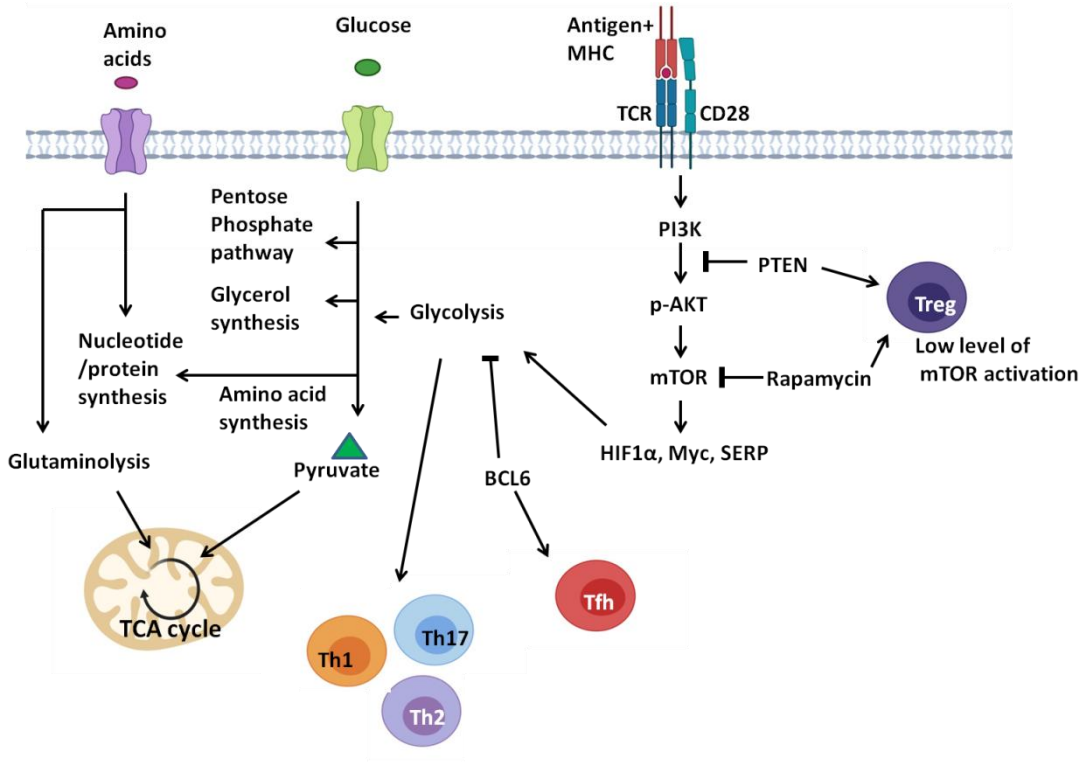

Figure 1.10. Metabolic changes in effector T cell maturation. PI3K-AKT-mTOR activation upon TCR signalling upregulates glycolysis leading to effector Th subset differentiation. BCL6 negatively regulates glycolysis in Tfh cells. Inhibiting mTOR activation by through inhibiting of PI3K-AKT-mTOR signalling results in Treg development.

1.2. Autoimmunity

Autoimmune diseases arise when the immune system loses the ability to

distinguish self from non-self. This leads to the generation and activation of autoreactive T cells, B cells, the production of auto-antibodies, and a general decrease in immune regulation. This functional imbalance between effector and regulatory immune responses results in the development of a chronic inflammatory condition, which is potentially life threatening without treatment (Rosenblum *et al.*, 2015; Wang *et al.*, 2015).

Although most autoreactive lymphocytes are eliminated before they are released into the periphery during T cell and B cell development, a very small number of potentially autoreactive lymphocytes escape deletion. These released autoreactive lymphocytes are predominantly eliminated upon recognition of self-antigen. However, an extremely low number of autoreactive lymphocytes and auto-antibodies are still detected in the healthy condition. In particular, auto-antibodies with low affinity and poly-reactivity are believed to be important in the clearance of degraded self-antigen and maintenance of cellular homeostasis in healthy individuals (Avrameas, 2016; Avrameas *et al.*, 2018).

However, when the finely tuned immunological balance between effector and regulatory responses is broken, these autoreactive lymphocytes and auto-antibodies can become involved in the development of autoimmune disease. The factor(s) that trigger disease are still unclear but it is believed that autoimmune diseases are caused by a combination of genetic and environmental factors. A number of genetic studies including genome wide association studies (GWAS) have revealed that mutation within MHC gene loci may contribute to autoimmune disease development (Matzaraki *et al.*, 2017). Many other genetic mutations in genes such at CD25, AIRE and Foxp3 may also contribute, as well as epigenetic

mechanisms. There have also been a variety of environmental factors associated with autoimmune diseases. Pathogenic infection, host microbiota, chemical substances, deficiencies in nutrition, and tissue damage (leading to development of a proinflammatory environment) can all trigger activation of autoreactive lymphocytes (Rosenblum *et al.*, 2015; Wang *et al.*, 2015).

These autoimmune disease triggers, both genetic and environmental factors, not only induce activation of autoreactive lymphocytes but also hinder regulatory functions. Therefore, a simultaneous reduction of Treg function and increase in frequency and function of effector T cells such as Th17 and Tfh cells is commonly observed in autoimmune disease (Rosenblum *et al.*, 2015; Wang *et al.*, 2015).

1.3. Granulomatosis with polyangiitis (GPA)

Vasculitis is an inflammation of the blood vessels. When the inflammatory condition affects several organs and tissues, it is called 'systemic vasculitis'. The primary cause of systemic vasculitis is still unclear but a combination of factors such as drug use, autoimmune disease and infections can lead to inflammation of blood vessels (Mansi *et al.*, 2002; Di Martino *et al.*, 2013). Since the association between anti-neutrophil cytoplasmic antibodies (ANCA) and vasculitis was firstly reported in 1982, ANCA have been used as a key laboratory marker for the diagnosis of a subtype of small vessel vasculitis, ANCA associated vasculitis (AAV). AAV is considered as the most common cause of small vessel vasculitis (Mansi *et al.*, 2002; Broeders *et al.*, 2018). Granulomatosis with polyangiitis (GPA, formerly known as Wegener's granulomatosis) is one of the AAV subtypes, along with microscopic polyangiitis (MPA) and eosinophilic granulomatosis with polyangiitis (EGPA; formerly known as Churg Strauss syndrome) (Jennette *et al.*, 2013). The classification of AAV subtypes is based on the type of ANCA, presence of granuloma,

and other clinical features. However, AAV, especially GPA, is a markedly heterogeneous disease and a certified diagnostic system is not available yet. Therefore, diagnosis of GPA is still challenging (Houben *et al.*, 2016). In addition to the difficulty of diagnosis of GPA, measurement of disease activity in GPA is also challenging due to the heterogeneous symptoms. Although the Birmingham Vasculitis Activity Score (BVAS) is widely used in GPA disease assessment, without specific training, BVAS cannot be performed even by experienced doctors (Flossmann *et al.*, 2008).

<table>
<tr><th></th><th colspan="4">Criteria</th><th>Name of diease</th><th>Dominant ANCA type</th></tr>
<tr><td rowspan="6">Vasculitis</td><td colspan="4">Large-vessel vasculitis</td><td>Giant cell arteritis, Takayasu's disease</td><td>N/A</td></tr>
<tr><td colspan="4">Medium-vessel vasculitis</td><td>Polyarteritis nodosa, Kawasaki's disease</td><td>N/A</td></tr>
<tr><td rowspan="4">Small-vessel vasculitis</td><td colspan="3">Non-ANCA small-vessel vasculitis</td><td>Inflammatory bowel disease vasculitis, Lupus vasculitis, Rheumatoid arthritis</td><td>N/A</td></tr>
<tr><td rowspan="3">ANCA associated small-vessel vasculitis (AAV)</td><td colspan="2">Non-granuloma</td><td>MPA</td><td>p-ANCA</td></tr>
<tr><td rowspan="2">Granuloma</td><td>Asthma and eosinophilia</td><td>EGPA</td><td>p-ANCA</td></tr>
<tr><td>Non-Asthma and Non-eosinophilia</td><td>GPA</td><td>c-ANCA</td></tr>
</table>

Table 1.3. Classification of vasculitis.

The common clinical phenotype of GPA is granulomatous inflammation of the upper airway and lungs. It also has been reported that 75% of GPA patients develop into renal necrotising vasculitis or glomerulonephritis. Although almost any organ can be involved, 5% of patients display only limited regional inflammation which primarily affects the upper respiratory tract (Tarzi and Pusey, 2014). Without proper medical treatment, GPA can develop rapidly into a life threatening inflammatory condition and result in a high rate of mortality within one year (Mckinney *et al.*, 2014).

1.3.1. Antineutrophil cytoplasmic antibody (ANCA)

The laboratory marker of GPA is the generation of ANCA, either against proteinase 3 (PR3) (in approximately 80% of patients) or against myeloperoxidase (MPO) or both (Iannella *et al.*, 2016). There are two major types of ANCA, cytoplasmic ANCA (c-ANCA) and perinuclear ANCA (p-ANCA) based on their immunofluorescence staining localisation pattern in neutrophils. c-ANCA is mainly against PR3 and p-ANCA is against myeloperoxidase MPO. PR3 and MPO are present in neutrophil granules or presented on the cell surface and/or secreted by activated neutrophils and ANCA recognise these auto antigens.(Mansi *et al.*, 2002; Lepse *et al.*, 2011) Among the three AAV diseases, GPA is the most associated with generation of c-ANCA. Although a high circulating level of ANCA is common in active AAV, ANCA may not be the key driver of disease progression (Cartin-Ceba *et al.*, 2012). In approximately 20% of AAV cases including GPA, ANCA is reported as negative and clinical benefit is observed prior to ANCA level reduction following B cell depletion therapy with Rituximab, a chimeric monoclonal anti-CD20 antibody (Mckinney *et al.*, 2014). Moreover, as in other AAV diseases, since immune complexes are not observed in GPA it is called a 'pauci-immune' vasculitis. As immunoglobulin deposition is not detected in AAV, it is thought that binding of ANCA to these antigens triggers an autoinflammatory response rather than causing direct toxicity and/or tissue damage (Cartin-Ceba *et al.*, 2012; Lutalo and D'cruz, 2014; Mckinney *et al.*, 2014; Tarzi and Pusey, 2014).

1.3.2. PR3 and GPA

PR3 is the autoantigen recognised by c-ANCA which is associated with disease in the majority of GPA patients. PR3 is a serine proteinase in neutrophils. It has been shown that PR3 can trigger the differentiation of neutrophils (Bories *et al.*, 1989)

and activate cytokine IL-8 (Padrines *et al.*, 1994). Unlike MPO (autoantigen for p-ANCA), PR3 can be expressed on neutrophils without activation and patients possessing a high proportion of PR3 expressing neutrophils have a high chance of developing vasculitis (Witko-Sarsat and Thieblemont, 2018). PR3 is also found in neutrophil extracellular traps but more interestingly, studies have shown that PR3 is preferentially expressed on apoptotic neutrophils (Durant *et al.*, 2004; Kantari *et al.*, 2007). PR3 expressing apoptotic neutrophils are removed by macrophages, resulting in the production of pro-inflammatory cytokines such as IL-1β, IL-6 and TNFα by macrophages. Moreover, a study in a murine model suggests that induction of PR3 positive apoptotic neutrophils leads to an increase in pro-inflammatory macrophages and plasmacytoid DCs that induce Th2/Th9/Th17 cells but reduce the Treg response (Millet *et al.*, 2015).

1.3.3. Factors trigger GPA

The GPA incidence rate varies between countries. The annual incidence of GPA is approximately 4.9 – 10.6 cases per million people, but it is more prevalent within Northern European Caucasian individuals. Studies in the U.S.A and New Zealand suggest that individuals that have Northern European ancestry have a higher GPA incidence rate compared to other ethnicities (Cartin-Ceba *et al.*, 2012; Mckinney *et al.*, 2014).

1.3.3.1. Genetic factor

A Swedish familial aggregation study of GPA report a relative risk of 1.56 for developing the disease if one has first degree relatives with GPA (Knight *et al.*, 2008). Like other autoimmune diseases, multiple genetic predispositions were reported in MHC and non- MHC genes in GPA patients. Several gene association

studies confirmed that GPA is associated with gene variation in *HLA-DPB1* that encodes MHC class II molecule *DPB1*. A GWAS study also confirmed single nucleotide polymorphism (SNP) in this gene. Furthermore, GWAS study analysis revealed genetic segregation between c-ANCA and p-ANCA AAV patients. c-ANCA patients were strongly associated with *HLA-DP* polymorphisms while p-ANCA patients were associated with *HLA-DQ* polymorphisms (Cartin-Ceba *et al.*, 2012; Lyons *et al.*, 2012).

Polymorphisms in other, non-HLA genes, have also been associated with GPA susceptibility including *PRTN3* and *SERPINA1*, especially in c-ANCA patients. *PRTN3* encodes PR3 and *SERPINA1* encodes the major PR3 inhibitor, alpha 1 anti-trypsin (α-1-AT). Polymorphisms in *CTLA4* have also been reported to be associated with GPA (Cartin-Ceba *et al.*, 2012; Mckinney *et al.*, 2014).

1.3.3.2. Environmental factor

Environmental factors including cigarette smoke, pollution, and heavy metal exposure may induce GPA development. In addition, infection with microorganism is believed to be one of the main triggers of disease progression. Lysosome-associated membrane protein 2 (LAMP2) was identified as a possible auto-antigen for ANCA. The sequence of LAMP2 has significantly similarity to a bacterial protein FimH. It is plausible that infection may trigger GPA development through molecular mimicry. (Cartin-Ceba *et al.*, 2012; Mckinney *et al.*, 2014). In another example, *Staphylococcous auresus (S. aureus)* possesses a protein with a high degree of homology to complementary *PRTN3* (cPR3). Furthermore, GPA patients classified as *S. aureus* nasal carriers are at higher risk of relapse than non-carriers (Popa *et al.*, 2007).

1.3.4. Pathogenesis of GPA

A combination of genetic and environmental factors can trigger GPA pathogenesis, leading to production of pro-inflammatory cytokines and/or complement activation (particularly activation of the alternative complement pathway) (Figure 1.11). Primed neutrophils express ANCA- specific autoantigen PR3 and MPO on their surface. ANCA bind to their auto-antigens and Fc receptors simultaneously. ANCA bound neutrophils become further activated, leading to release of ROS and lytic enzymes. Highly activated neutrophils ultimately undergo NETosis. NET formation causes direct damage to epithelial tissue on vessels, and also leads to release of more autoantigens. These autoantigens are taken up by APCs and presented to naive T cells, which become activated and differentiate into effector Th cells. Effector Th cells directly contribute to tissue damage through release of pro-inflammatory cytokines (which also activates neutrophils). A proportion of CD4+ T cells differentiate into Tfh cells and help B cell activation and differentiation into plasma cells, and consequently generating more ANCA. Hence a positive feedback loop becomes established, which enhances the progression and severity of GPA pathogenesis (Morgan *et al.*, 2006; Cartin-Ceba *et al.*, 2012; Mckinney *et al.*, 2014; Nakazawa *et al.*, 2019).

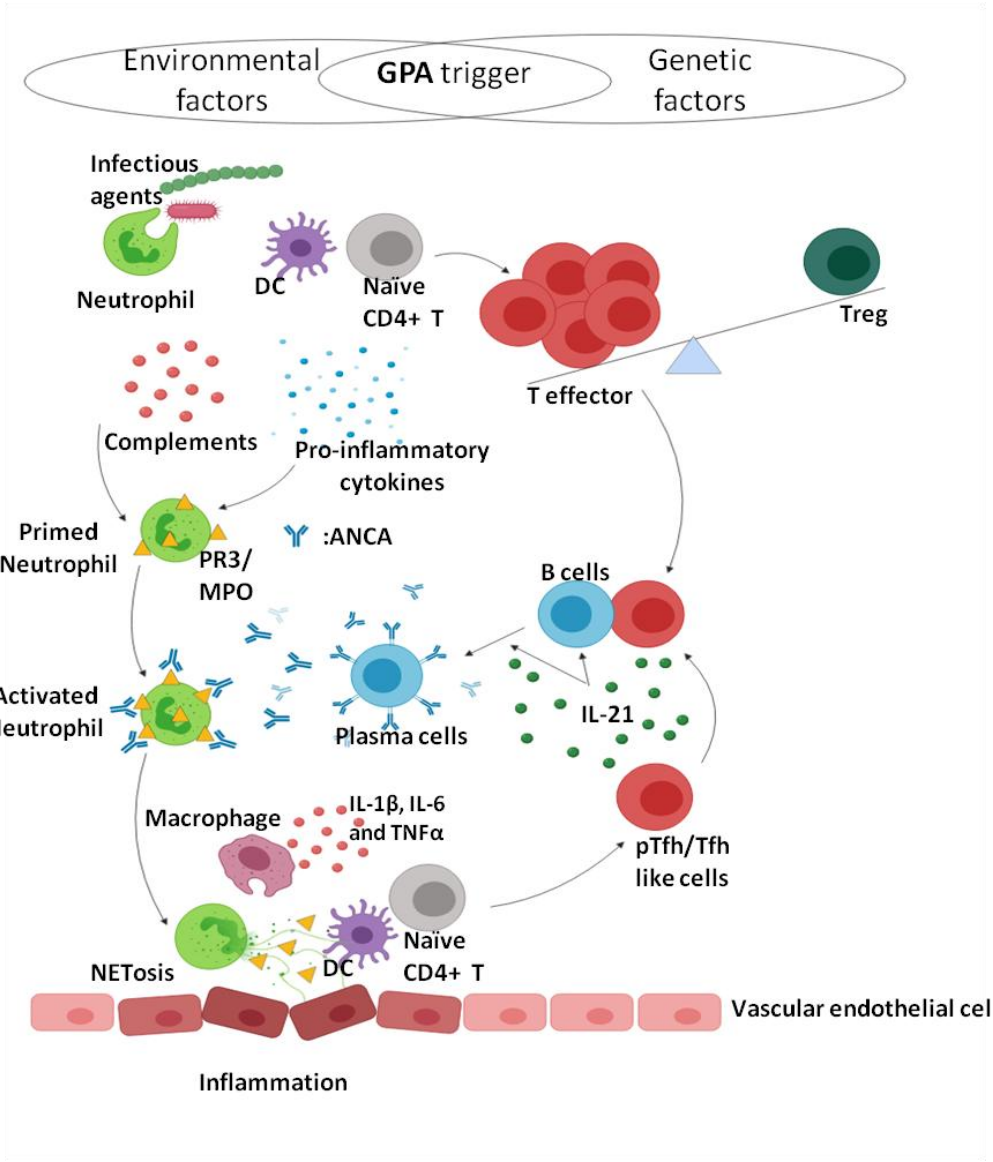

Figure 1.11. Factors contributing to progression of GPA pathogenesis.

Currently, a combination of immune suppressive drugs, steroids and antibiotics are given to GPA patients to induce remission of disease (Geetha *et al.*, 2015).However the relapse risk for GPA and PR-3-ANCA positive patients is significantly higher than for other AAV patients. However, the increase in ANCA titre during remission is not strongly associated with relapse, and no clear biomarkers for predicting relapse have as yet been identified. Due to the absence of specific biomarkers, many physicians rely on clinical monitoring of symptoms and inflammatory markers to detect relapse at an early stage. As a result, the

duration of immunosuppression treatment is often longer than required (Tarzi and Pusey, 2014; Geetha *et al.*, 2015).

Although ANCA produced by B cells are the key diagnostic markers of GPA, there is increasing evidence from both human and murine studies to support an important role for CD4 T cells in the development GPA pathogenesis (Komocsi *et al.*, 2002; Ruth *et al.*, 2006; Abdulahad *et al.*, 2007; Abdulahad *et al.*, 2009). Necrotizing granulomatous inflammation involving T cells, B cells and neutrophils is a clinical feature of GPA (Cartin-Ceba *et al.*, 2012). In a murine model, transfer of MPO specific T cells into *Rag*1$^{-/-}$ mice induced necrotizing glomerulonephritis (Ooi *et al.*, 2012). Moreover, observation of germinal centre like structures where T cells and B cells aggregated without follicular DCs in GPA and evidence of high-affinity class-switched antibodies in ANCA indicate T-cell involvement in ANCA production and AAV pathogenesis (Mueller *et al.*, 2008; Cartin-Ceba *et al.*, 2012; Mckinney *et al.*, 2014). Despite the achievement of effective remission in many patients, a high risk of relapse still exists after Rituximab treatment (Geetha *et al.*, 2015).

1.3.5. T cells in GPA

1.3.5.1. CD8+ T cells in GPA

Patients with ANCA associated vasculitis including GPA exhibit lower ratios of CD4$^+$ to CD8$^+$ T cells. However, it is not clear whether this phenotype is due to an expansion of the CD8$^+$ T cell population or a contraction of the CD4$^+$ T cell population. Though little is known about the role of CD8$^+$ T cells in GPA, a reduction in the frequency of CD8$^+$ T cells displaying an 'exhausted' phenotype is typically observed in active autoimmune disease. A recent transcriptomics study by McKinney *et al*. suggested that a signature of high CD8+ T cell exhaustion and

low expression of CD4+ T cell co-stimulatory molecules may be used to predict better long-term disease outcomes in AAV (Mckinney *et al.*, 2015). These data suggest a strong T cell component in the etiology of GPA.

1.3.5.2. CD4+ T cells in GPA

Several studies have reported abnormal expression of $CD4^+$ T cell surface markers in GPA. T cell activation markers such as IL-2 receptor alpha (CD25), HLA-DR and CD137 have been reported to have higher expression on CD4+ T cells from GPA patients. In particular, elevated expression of CD25 was reported predominantly on naive CD4+ T cells. Paradoxically, other signal transduction receptors associated with T cell activation, such as CD28 and IL-2Rβ (CD122), have been reported to have lower expression levels on CD4+T cells in GPA (Marinaki *et al.*, 2005; Berden *et al.*, 2009; Mckinney *et al.*, 2014; Nakazawa *et al.*, 2019).

1.3.5.2.1. Th1 and Th2 cells in GPA

Elevated concentrations of Type 1 helper CD4+ T cell (Th1) cytokines such as IFN-gamma and IL-2 have been reported in localised disease, but this cytokine profile shifts towards a Type 2 helper CD4+ T cell (Th2) profile upon development of generalised disease, with elevated levels of cytokines such as IL-4 reported (Lamprecht *et al.*, 2003; Berden *et al.*, 2009; Tarzi and Pusey, 2014). In addition to the classical Th1 and Th2 $CD4^+$ T cell subsets, the importance of follicular helper T cells (Tfh), T helper 17 cells (Th17) and regulatory T cells (Treg) in autoimmune disease has been increasingly recognised in recent years.

1.3.5.2.2. Th17 cells in GPA

Interleukin 17 (IL-17) is mainly produced by Th17 cells and has a protective role against certain fungal and bacterial pathogens such as extracellular bacteria including *Staphylococcus aureus* and *Candida albicans*, promoting recruitment of innate immune cells to sites of infection at epithelial and mucosal barriers (Jin and Dong, 2013; Levy *et al.*, 2016). However, deregulation of IL-17 production results in chronic inflammation and tissue damage (Park *et al.*, 2005; Rovedatti *et al.*, 2009) Many autoimmune diseases exhibit high levels of IL-17 production and an increase in the frequency of Th17 cells (Nistala and Wedderburn, 2009; Jin and Dong, 2013).

GPA patients also have high serum IL-17 levels, and *ex vivo* PR3 stimulation of PBMCs from GPA patients induces IL-17 expression (Abdulahad *et al.*, 2008; Rani *et al.*, 2015). However, the expansion of the Th17 population in GPA appears to be independent of disease activity, as the expanded Th17 population is sustained in GPA patients in remission (Wilde, Thewissen*, et al.*, 2012).

1.3.5.2.3. Tfh cells in GPA

Tfh cells are predominantly located in germinal centres but they are also detected in the periphery. It is believed that the surface marker expression of peripheral Tfh cells is similar to GC Tfh cells; namely high expression of CXCR5 and PD1. The key transcription factor of the Tfh cell lineage is BCL6, and the signature cytokine produced by Tfh cells is IL-21. The main function of Tfh cells is to help B cells to generate high affinity antibodies. IL-21 stimulates B cells to differentiate into plasma cells and also alleviates CD8+ T cell exhaustion during lymphocytic choriomeningitis virus (LCMV) infection (Tian and Zajac, 2016; Long *et al.*, 2019). Though the function and origin of pTfh cells is still unclear, high frequencies of

circulating CXCR5+CD4+ T (pTfh) cells have been found in autoimmune diseases such as systemic lupus erythematous (SLE) and rheumatoid arthritis (RA) (Shekhar and Yang, 2012). Similarly, a study by Zhao *et al* found an increase in the CXCR5+PD1+CD4+ T cell (pTfh) population in peripheral blood from both active and inactive GPA patients (Zhao *et al.*, 2014). The frequency of IL-21 expressing CD4+ T cells in blood is also significantly higher in both ANCA+ and ANCA- GPA patients. Interestingly, significantly higher BCL6 expression in peripheral CD4+ T cells is only observed in ANCA+ GPA patients (Abdulahad *et al.*, 2013). Even though these studies indicate an increase in pTfh cell frequencies in GPA patients, the relationship between these observed phenotypes and Tfh cell function remains unclear. However, it may be hypothesized that elevated Tfh cell frequencies could exacerbate the accumulation of auto-reactive antibodies in GPA.

1.3.5.2.4. Treg cells in GPA

Treg cells are critical regulators of immune responses in health that function by suppressing immune responses other than those actively involved in fighting infection. The two well characterized types of Tregsare tTreg (also called natural Treg ;nTreg), generated from the thymus, and induced Treg (iTreg), converted from naïve CD4+ T cells in the periphery. (Sakaguchi *et al.*, 2008; Adalid-Peralta *et al.*, 2011). Both nTreg and iTreg cells display the signature Treg markers; high expression of IL-2 receptor alpha chain (CD25) and most express the transcription factor FoxP3. They also exhibit low expression of the IL-7 receptor (CD127), and both express immunosuppressive cytokine IL-10 (Kleinewietfeld and Hafler, 2013; Pandiyan and Zhu, 2015).

While there is a positive correlation between autoimmune disease progression and the frequency of Th17 and Tfh cells, in contrast, Treg cells often exhibit an impaired immune-suppressive function or are present in lower numbers (Nistala and Wedderburn, 2009). Observations regarding the relative frequencies and function of Treg cells in GPA patients have been inconsistent. Some studies have reported no difference in the numbers of Treg cells, defined by FoxP3 expression, in circulating CD4+ T cells from GPA patients compared to healthy controls (Marinaki *et al.*, 2005; Abdulahad *et al.*, 2006). In contrast, one study reported an increase in the $CD4^{+}CD25^{high}FoxP3^{+}$ Treg population in GPA patients, but also showed that these cells were defective in their immune suppressive function in an *in vitro* co-culture assay (Abdulahad *et al.*, 2007). Interpretation of these studies is complicated, since the principal Treg marker, FoxP3, is also transiently up-regulated following T cell activation in effector T cells (Sakaguchi *et al.*, 2008). Interestingly, a recent study showed that Treg cells as defined by the phenotype $CD4^{+}CD25^{high}CD127^{low}$ have lower frequencies in GPA compared to healthy donors, but exhibited no defect in immune-suppressive function in a co-culture assay(Zhao *et al.*, 2014). Thus, there is currently no clear consensus on the status of Tregs in GPA, and further studies are required to identify the nature of the Treg deficiency.

While further investigations regarding the frequencies and functions of Tregs in GPA are required, based on current findings so far it could be hypothesised that the pathogenesis of GPA may be due, in part, to a decline in Treg mediated immune regulation. This may be the consequence of lower Treg frequencies or an intrinsic defect in the immune-suppressive function of Treg cells in GPA patients. The result, is a functional imbalance between immune-suppressive Tregs and pro-

inflammatory Th17 and/or Tfh populations (Wilde, Thewissen*, et al.*, 2012; Zhao *et al.*, 2014; Rani *et al.*, 2015).

1.4. Aims of thesis

The overarching goal of this study is to understand the contribution of CD4+ T cells to GPA pathology, with the hope of identifying potential avenues for therapeutic intervention and/or biomarkers for disease stratification.

GPA pathology is characterized by severe chronic inflammation, driven by auto-antibody production. Given the important role of CD4 T cells in both these immune processes, few previous studies have varyingly described dysregulation in numbers and/or function of Treg and Tfh cell subsets in GPA. However, the underlying factors contributing to the observed reduction in Treg function and increase in Tfh-like phenotypes in GPA remain poorly understood.

Thus, the hypothesis of this study is that CD4+ T cells in GPA patients have a predisposition to adopt abnormal differentiation profiles due to dysregulation of intrinsic molecular signaling pathways and / or changes in the levels of extracellular factors within patient plasma.

The specific aims of this thesis are:

Chapter three aims to determine the frequency of Treg and Tfh cells in peripheral blood from GPA patients and compare to healthy individuals. Phenotypic characteristics of CD4+ T cells including cytokine production and expression of key transcription factors will also be compared between GPA patients and healthy donors.

Chapter four aims to investigate the molecular mechanisms responsible for the pre-disposition of naïve CD4+ T cells in GPA to differentiate towards a Tfh-like phenotype. This chapter will address the hypothesis that intrinsic dysregulation of specific molecular signalling pathways in naive CD4 T cells may contribute to the functional imbalance of CD4 T cell subsets in GPA.

Chapter five aims to investigate the functional capacity of conventional Tregs and a dysregulated population of naïve CD25+CD4+ T cells from GPA patients to suppress proliferation and cytokine production of T effector cells.

Chapter six aims to investigate the contribution of extracellular factor(s) present in GPA plasma to the dysregulation of CD4+ T cell subset differentiation, and to establish the identity of proteins present in GPA plasma to provide a preliminary understanding of factors/pathways that may contribute to cellular pathology.

2. Materials and Methods

2.1. Methods: Sample preparation

2.1.1. Blood sample collection from individuals

Ethics approval for this study has been granted by the UK Research Ethics Committee (REC no. 11/LO/1433). Blood samples from GPA patients were routinely collected in the systemic vasculitis clinic in the Louise Coote Lupus Unit at Guy's hospital. Up to 50ml of blood was collected from 50 GPA patients and 20 healthy donors in total over 3 years (Table 2.1). All patients in this study were given combinations of steroids, immunosuppressive drugs and antibiotics (but they had either not received RTX or had received RTX but relapsed). In each of the studies in this thesis, samples were selected and their age, gender and ANCA types are described in appendix (sTable 9.1-4). Samples were collected in sodium heparin coated blood collection tubes (BD), and banked separately as plasma and PBMCs. Note: samples for microarray assay were immediately processed, isolating naive CD4 T cells from freshly prepared PBMCs. Plasma and PBMCs were prepared as described in the following section.

	Total number	Mean age (range)	F/M	ANCA type (c-ANCA/p-ANCA/negative)
HC	20	48.55 (26-73)	14/6	N/A
GPA	50	49.6 (25-73)	21/29	30/15/5

Table 2.1 Patients and healthy control information.

2.1.2. Plasma and PBMC isolation

For plasma isolation, 10ml of blood was centrifuged at 1000 × g for 10 minutes. The top clear plasma layer was harvested and transferred into microcentrifuge tubes (500µl per tube). Aliquoted plasma samples were immediately stored at -80°C. The cellular fraction was added to the remaining blood for PBMC isolation (see below).

2.1.3. PBMC isolation

Blood was diluted in an equal volume of Mg^{2+} and Ca^{2+} free phosphate-buffered saline (PBS) and layered onto Lymphoprep (Axis Shield, UK). Layered blood was spun at 450 × g for 30 minutes at room temperature. Peripheral blood mononuclear cells (PBMCs) were carefully collected and transferred into 50ml falcon tubes, then spun at 300 × g for 10 minutes at 4 °C. PBMC pellets were re-suspended in 10ml of Mg^{2+} and Ca^{2+} free PBS and cells were counted using a haemocytometer.

2.1.4. Cryopreservation

Isolated PBMCs in PBS were centrifuged at 300 x g for 10 minutes, then re-suspended at a concentration of 10^6 PBMCs per 1ml of freezing media (90% heat inactivated foetal bovine serum (FBS) and 10% DMSO). The re-suspended PBMCs were frozen slowly by cooling the cells at a rate of -1°C per minute in a -80°C freezer. Frozen PBMCs were transferred to liquid nitrogen for long term storage.

2.1.5. Thawing out PBMCs

Frozen PBMCs were thawed rapidly at 37°C, and added drop-wise to pre-warmed RPMI media containing 50% FBS. Thawed PBMCs were centrifuged at 300 × g for

10 minutes at room temperature and the cell pellet was re-suspended in RPMI supplemented with 10% FBS.

2.2. Method: Cell isolation

2.2.1. CD4 isolation by Dynabead isolation

CD4+ T cells were isolated by using Dynabeads untouched human CD4+ T cells kit (Invitrogen) by following manufacturer's protocol.

2.2.2. Naive CD4 isolation by Dynabead isolation

Naive CD4+ T cells were isolated by using MagniSort™ Human CD4 Naïve T cell Enrichment Kit (Invitrogen) by following manufacturer's protocol. Purity of naive CD4+ T cells were assessed by flow cytometry and the mean of purity in GPA and HC was 74.36% and 70.36% respectively (Figure 2.1).

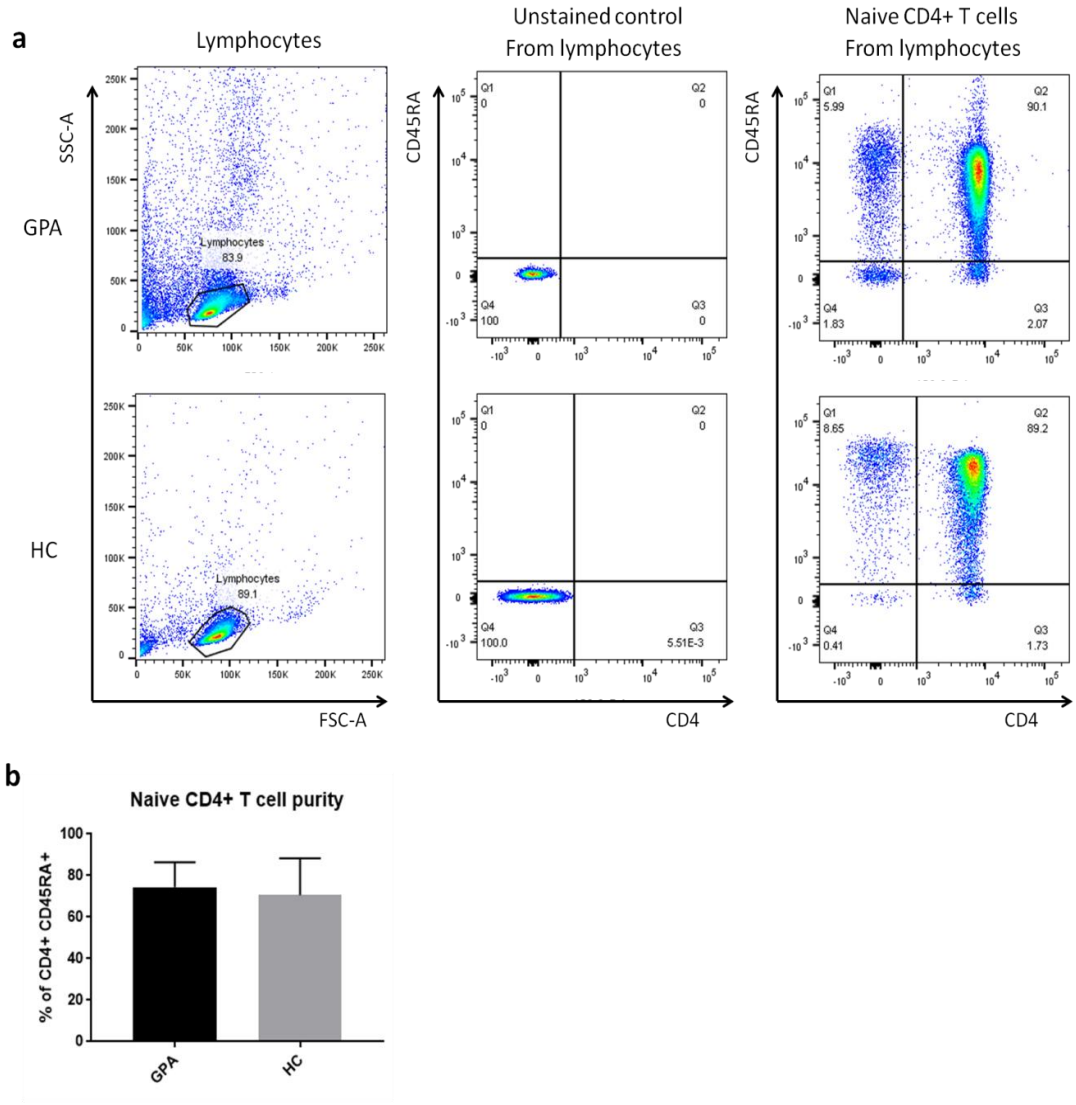

Figure 2.1 Naive CD4+ T cell purity check after isolation.

(a) CD45RA+CD4+ T cell gating from isolated naive CD4+ T cells from GPA (upper row) and HC (bottom row). The gating strategy was based on unstained control. **(b)** The frequencies of naive CD4+ T cells after isolation were compared between GPA patients and HC to assess purity (GPA n=18, HC n=12).

2.2.3. Cell sorting by flow cytometry

2.2.3.1. Antibody staining for bulk sorting

Thawed PBMCs were stained with panel of fluorochrome-conjugated antibodies (Figure 2.2h) following described method for antibody staining for flow cytometry

(Method 2.3.1.2). After staining, cells were resuspended in 500 µl of flow cytometry staining buffer (1% EDTA, 1% FBS in Mg^{2+} and Ca^{2+} free PBS) for sorting.

2.2.3.2. Antibody staining for sorting cells for micro-suppression assay

Thawed PBMCs were stained with a panel of antibodies (Figure 2.2h) by following method described in section methods 2.3.1.2. Note: Antibody staining was performed with flow cytometry buffer containing heat inactivated human serum instead of FBS. After staining, cells were resuspended at 500 µl of flow cytometry buffer (2mM EDTA and 1% heat inactivated human serum (HS) in Mg^{2+} and Ca^{2+} free PBS) for sorting.

2.2.3.3. Flow cytometry cell sorting

Antibody stained cells were sorted using the BD FACSAria III (BD) at PII flow cytometry facility in KCL. Each indicated population from Figure 5.2 was sorted and collected into 15ml falcon tubes. Each indicated population from Figure 5.3 and Figure 5.4 was sorted directly into 96 well V-bottom plates (Greiner Bio-one).

2.3. Method: Antibody staining for flow cytometry analysis and antibody panels

2.3.1. Flow cytometry staining

2.3.1.1. Cell Trace Violet (CTV) staining for proliferation assay

Pelleted cells were resuspended at a concentration of 10^6 cells per ml in PBS containing 1µM of Cell Trace Violet (CTV) dye (Life Technologies) warmed to 37°C. Cells were incubated at 37°C for 20 minutes in the dark, then the reaction was quenched by adding three times the volume of cold FBS. Cells were pelleted at 300

× g for 5 minutes, then resuspended in pre-warmed culture medium prior to incubation for 10 minutes at 37°C.

2.3.1.2. Surface marker staining in 12 x 75 mm tubes

Thawed PBMCs were washed with PBS 300 × g for 5 minutes and incubated in 100ul of flow cytometry staining buffer (1% EDTA and 1% FBS in Mg^{2+} and Ca^{2+} free PBS) containing each of the surface marker antibodies for 30 minutes at 4°C. Note: Chemokine receptor CCR7 staining was performed prior to addition of other surface markers. Briefly, CCR7 antibody was added to the PBS wash, and incubated with PBMCs at 37°C for 15 minutes. After incubation, a mixture of antibodies against other surface marker proteins was immediately added. Stained cells were washed twice with flow cytometry buffer by pelleting cells at 300 × g for 5 minutes after each wash. After the final wash, cells were re-suspended in 200µl flow cytometry buffer for analysis on a BD FACSCanto II flow cytometer. Intracellular staining (ICS), if required, was performed after surface staining as described below.

2.3.1.3. Transcription factor intracellular staining (ICS) in 12 x 75 mm tubes

ICS was performed with eBioscience™ Foxp3 / Transcription Factor Staining Buffer Set (Invitrogen), according to manufacturer's protocol.

2.3.1.4. Surface marker staining in 96 well plates

96 well plates containing cultured cells were centrifuged at 2000rpm for 1 minute. Culture supernatants were collected and transferred into new 96 well plates prior to storage at -80°C if required for cytokine profiling (otherwise supernatants were

discarded). 200ul PBS (Mg^{2+} and Ca^{2+} free) was added to each well, and cells were pelleted again. If a LIVE/DEAD marker was required, as for Figure 4.1 and Figure 4.2, cells were re-suspended with 50µl of PBS (Mg^{2+} and Ca^{2+} free) plus 1:1000 diluted LIVE/DEAD™ Fixable aqua dead cell dye (Invitrogen) and incubated for 30 minutes at room temperature prior to a further wash with Mg^{2+} and Ca^{2+} free PBS. A cocktail of antibodies against surface marker proteins were added in a total volume 50ul of PBS (Mg^{2+} and Ca^{2+} free) per well, and incubated with cells for 10 minutes at 4°C. Stained cells were washed three times with flow cytometry buffer prior to re-suspension in 200µl flow cytometry buffer for analysis on a BD FACSCanto II flow cytometer. If required, intracellular staining was performed after surface staining according to protocols described below.

2.3.1.5. Transcription factor intracellular staining (ICS) in 96 well plates

ICS was performed with eBioscience™ Foxp3 / Transcription Factor Staining Buffer Set (Invitrogen) according to manufacturer's protocol.

2.3.1.6. Cytokine intracellular staining (ICS) in 96 well plates

Cells were stimulated for 5 h at 37 °C with 25ng/ml of phorbol 12-myristate 13-acetate (PMA) (Sigma) and 1µg/ml ionomycin (Sigma) in the presence of 1X Brefeldin A (Invitrogen) and a 1:1000 dilution of Monensin, a protein transport inhibitor (BD). Cells were pelleted at 300 × g before being re-suspended in 200µl of Fixation buffer (BD) and incubated for 30 minutes at room temperature in the dark. Following fixation, cells were pelleted by centrifugation at 600 × g for 5 minutes, and the fixation buffer discarded. Cells were washed in 200ul of Perm buffer III (BD), prior to addition of antibodies. Cells were resuspended in a cocktail

of antibodies against intracellular cytokines in Perm buffer III (BD) (50 µl per well) and incubated for 30 minutes at room temperature in the dark. Cells were washed twice with Perm buffer III (BD) and resuspended in a final volume of 200ul PBS for analysis on a BD FACSCanto II flow cytometer.

2.3.2. Flow cytometry antibody panels

a

Treg/Tfh panel			
Cell marker	**Fluorochrome**	**Company**	**Volume (µl/100µl)**
CD4	APC-eFluor780	ebioscience	2
CD25 (Clone 2A3)	PE	BD	3
CD25 (Clone M-A251)	PE	BD	3
CD127	Brilliant Violet 711	BioLegend	3
CD45RA	Brilliant Violet 605	BioLegend	2
CXCR5	PerCP-Cy 5.5	BioLegend	2
PD1	PE-Cy7	BioLegend	2
Foxp3	Alexa Fluor 488	BioLegend	3

b

CD25+ on naive CD4+ T cell panel 1			
Cell marker	**Fluorochrome**	**Company**	**Volume (µl/100µl)**
CD4	APC-eFluor780	ebioscience	2
CD45RA	Brilliant Violet 605	BioLegend	2
CD25 (Clone 2A3)	PE	BD	3
CD25 (Clone M-A251)	PE	BD	3
CD62L	Pacific blue	BioLegend	5
CD11a	APC	BioLegend	3
CD57	FITC	BioLegend	3
CD28	PE-Cy7	BioLegend	2

c

CD25+ on naive CD4+ T cell panel 2			
Cell marker	**Fluorochrome**	**Company**	**Volume (µl/100µl)**
CD4	APC-eFluor780	ebioscience	2
CD25 (Clone 2A3)	PE	BD	3
CD25 (Clone M-A251)	PE	BD	3
CCR7	APC	BioLegend	5
CD45RA	Brilliant Violet 605	BioLegend	2

d

Naive and Memory proliferation sorting panel			
Cell marker	**Fluorochrome**	**Company**	**Volume (µl/100µl)**
CD4	APC-eFluor780	ebioscience	2
CD25 (Clone 2A3)	PE	BD	3
CD25 (Clone M-A251)	PE	BD	3
CD45RA	Brilliant Violet 605	BioLegend	2
CD45RO	FITC	Dako	1

e

Naive purity panel			
Cell marker	**Fluorochrome**	**Company**	**Volume (µl/100µl)**
CD4	APC-eFluor780	ebioscience	2
CD45RA	Brilliant Violet 605	BioLegend	2

f

BCL6 after *in vitro* differentiation panel			
Cell marker	**Fluorochrome**	**Company**	**Volume (µl/50µl)**
CD4	PE	BD	5
CXCR5	PerCP-Cy 5.5	BioLegend	2
PD1	PE-Cy7	BioLegend	2
BCL6	Alex Flour 647	BD	1

g

IL-21 after *in vitro* differentiation panel			
Cell marker	**Fluorochrome**	**Company**	**Volume (µl/50µl)**
CD4	APC-eFluor780	ebioscience	2
CXCR5	PerCP-Cy 5.5	BioLegend	2
PD1	PE-Cy7	BioLegend	2
IL-21	PE	BioLegend	3

h

Treg sorting panel			
Cell marker	**Fluorochrome**	**Company**	**Volume (µl/100µl)**
CD4	APC-eFluor780	ebioscience	5
CD25 (Clone 2A3)	PE	BD	10
CD25 (Clone M-A251)	PE	BD	10
CD127	Brilliant Violet 711	BioLegend	5
CD45RA	Brilliant Violet 605	BioLegend	5

i

Treg/Tfh after plasma co-culture panel			
Cell marker	**Fluorochrome**	**Company**	**Volume (µl/50µl)**
CD4	APC-eFluor780	ebioscience	2
CD25 (Clone 2A3)	PE	BD	3
CD25 (Clone M-A251)	PE	BD	3
CD127	Brilliant Violet 711	BioLegend	3
CXCR5	PerCP-Cy 5.5	BioLegend	2
PD1	PE-Cy7	BioLegend	2

Figure 2.2 Flow cytometery antibody panels.

2.4. Method: Cell culture

2.4.1. CD4+ T cell culture for cytokine profile

For TCR stimulation, 96-well tissue culture plates were pre-coated with 10µg/ml of anti-CD3 (BD Bioscience) and 2µg/ml of anti-CD28 (BD Bioscience) antibodies in 150 µl per well of PBS at 4 °C overnight. Prior to adding cells, PBS/antibody mixture was carefully discarded from plates. Isolated CD4+ T cells were re-suspended in RPMI media containing 10% FBS and 1X Penicillin/Streptomycin (Sigma) antibiotic. Cells were plated at 100,000 cells/well in a total volume of 200µl then incubated at 37°C in 5% CO_2. After five days culture, plates were spun at 1200rpm for 3 minutes to pellet cells and supernatants (for cytokine measurement) were transferred into a new plate and stored at -80°C.

2.4.2. Memory and naive CD4+ T cell culture for cell proliferation assay

PBMCs were stained with CTV (Method 2.3.1.1.) prior to surface marker staining (Method 2.3.1.2, Figure 2.2d) for naive and memory CD4+ T cell sorting by FACS. For TCR stimulation, 96-well tissue culture plates were pre-coated with 10µg/ml anti-CD3 (BD Bioscience) and 2µg/ml anti-CD28 (BD Bioscience) antibodies in PBS prior to addition of 100,000 cells/well. 40 IU of IL-2 (Biolegend) was added to stimulate cell proliferation. Cells were incubated for five days at 37°C in 5% CO_2.

2.4.3. *In vitro* Tfh differentiation

Isolated naive CD4+ T cells (Method 2.2.2) were resuspended in serum free X-VIVO (Lonza) culture media then plated at 75,000 cells per well of a 96 well cell culture plate in a total volume of 250µl. For TCR activation, 2 µl of Dynabeads Human T-Activator anti-CD3/anti-CD28 beads (Life Technologies) were added per well plus addition of 4ng/ml of recombinant human IL-7(Biolegend). For Tfh differentiation,

in addition to TCR activation, 5ng/ml of recombinant human IL-12 (PeproTech) and 1ng/ml of recombinant human TGF-β (Biolegend) were added in culture. Plates were prepared in duplicate, one plate to perform transcription factor ICS and the other to perform cytokine ICS. Cells were cultured for five days at 37°C in 5% CO_2. Supernatants were harvested after 5 days of *in vitro* culture and cells were stained with panel of antibodies listed in either Figure 2.2f or Figure 2.2g.

2.4.4. Treg suppression assay by flow cytometry

Activated Tregs, Responder T cells (Tresp) and naive CD25+CD4+ T cells (population shown in Figure 5.2) were FACS sorted in bulk into 15ml falcon tubes. Sorted activated Tregs and naive CD25+CD4+ T cells were resuspended in warm RPMI culture media containing 10% FBS (Gibco) and 1X penicillin streptomycin. Sorted Tresp cells were stained with CTV (Method 2.3.1.1) and plated at 2000 cells/well in U bottom 96 well plates. Tresp were cultured with autologous or allergenic Tregs/naive CD25+CD4+ T cells at a Tresp : Tregs/naive CD25+CD4+ T cell ratio of 1:0, 1:1, 2:1 or 4:1 with TCR stimulation provided by addition of 2000 beads of Dynabeads Human T-Activator anti-CD3/anti-CD28 beads per well. Cells were co-cultured for 6 days at 37°C in 5% CO_2 prior to measurement of dilution of CTV by flow cytometry analysis on a BD FACSCanto II flow cytometer.

2.4.5. Micro-Treg suppression assay by H^3 thymidine incorporation

Tregs, Tresp and naive CD25+CD4+ T cells (population shown in Figure 5.3 and Figure 5.4) were directly sorted into V bottom 96 well plates containing 150µl ice cold X-VIVO (Lonza) culture media including 10% human serum (Sigma) and 1X penicillin streptomycin (Sigma). 500 Tresp cells per well were sorted with autologous or allergenic Tregs/naive CD25+CD4+ T cells at a Tresp : Tregs/naive

CD25+CD4+ T cell ratio of 1:0, 1:1, 2:1 or 4:1 (an additional 0.5:1 ratio was included for Tresp : naive CD25+CD4+ T cells). After cell sorting, 500 Dynabeads (Human T-Activator anti-CD3/anti-CD28 beads) per well were added by FACS for TCR stimulation. Immediately afterwards, plates were centrifuged at 400 × g for 4 minutes then incubated for 5 days at 37°C in 5% CO_2. After 5 days *in vitro* co-culture, 75µl of supernatant was harvested and kept at -80°C to assess cytokine profile, then 75µl of warm culture media containing 0.5 mCi/well [^{3}H] thymidine (Perkin Elmer) was added prior to another 18 hours *in vitro* co-culture to enable tritiated thymidine incorporation into newly synthesized DNA of dividing cells. Cells were harvested on a glass filterer (Perkin Elmer) with automated harvester (Packard Filtermat Cell Harvester) then filters were dried by microwaving for 1 minute. Dried filters were sealed in a plastic sample bag (Perkin Elmer) with 5 mL of liquid scintillation (Perkin Elmer) so the filter was covered with liquid scintillation evenly. ^{3}H thymidine incorporation was measured using a liquid scintillation counter (Wallac Trilux 1450 Microbeta) and the level of proliferation was determined by measuring counts per minute (cpm). The percentage of suppression was calculated by using the formula (for example, to calculate Treg suppression):

% suppression = 100 - (cpm with Tregs / cpm without Tregs × 100).

Cell harvesting and ^{3}H thymidine incorporation were performed with assistance from Dr. Jennie Yang (KCL).

2.4.6. CD4+ T cell culture for measuring STAT activation

Isolated CD4+ T cells were resuspended in RPMI culture supernatant containing 10% FBS and 1X penicillin streptomycin (Sigma). Cells were plated in 6-well plates at 1,000,000 cells per well and incubated overnight. Rested cells were washed and resuspended in fresh culture media. In a new micro-centrifuge tube, 200,000 cells in a total volume of 200µl were transferred and stimulated with 100IU/ml of IL-2 (R&D) for 20 minutes at 37°C in 5% CO_2. After stimulation, cells were immediately cooled on ice and centrifuged at 300 × g for 5 minutes at 4°C. Then cells were lysed in 50µl of Laemmli buffer for western blot analysis. For a negative control, rested cells without stimulation were also prepared for western blotting.

2.4.7. Naive CD4+ T cell culture for measuring STAT activation

Isolated naive CD4+ T cells (100,000 cells/well) were cultured in 200µl of RPMI culture media containing 10% FBS and 1X penicillin streptomycin (Sigma) for 48 hours at 37°C in 5% CO_2 in 96 well plates that were pre-coated with anti-CD3 and anti-CD28 antibodies, as described previously (Method 2.4.1). After the 48 hr, pre-activation, naive CD4+ T cells were transferred into micro-centrifuge tubes and washed with fresh culture media by centrifuging at 300 × g for 5 minutes. Pelleted cells were resuspended in fresh culture media and plated in 6 well plates at 1,000,000 cells per well prior to resting overnight at 37°C in 5% CO_2. Rested cells were washed and resuspended in fresh culture media. In a new micro-centrifuge tube, 100,000 cells in a total volume of 200µl were transferred and stimulated with indicated cytokines (50IU/ml of IL-2, 75ng/ml IL-15 or 10ng/ml of IL-6) for indicated times at 37°C in 5% CO_2. After stimulation, cells were immediately cooled on ice and centrifuged at 300 × g for 5 minutes at 4°C. Supernatant was discarded

and cells lysed in 50µl of Laemmli buffer for western blot analysis. For a negative control, rested cells without stimulation were also prepared for western blotting.

2.4.8. Plasma co-culture with HC PBMCs

PBMCs from healthy donors were plated at 200,000 cells per well in RPMI culture media containing 10% FBS, 1X penicillin streptomycin (Sigma) and 10% plasma from GPA patients or healthy donors in a 96 well plate. Cells were incubated for 5 days at 37°C in 5% CO_2, and after 5 days culture, supernatant were stored at -80°C for cytokine measurement, and cells were stained with a panel of antibodies (Figure 2.2i) for flow cytometry analysis.

2.5. Cytokine measurement

2.5.1. Cytometric bead array (CBA)

Cytokines in supernatant from TCR stimulated CD4+ T cells (Method 2.4.1) and plasma samples were measured by using Cytometric bead array (CBA) human Th1/Th2/Th17 cytokine kit (BD) according to manufacturer's protocol. Culture supernatant samples and plasma samples were diluted at 1 in 5 during the sample incubation step. Cytokines measured were IL-2, IL-4, IL-6, IL-10, TNFα, IFNγ and IL-17A. Assay was performed on a BD LSR II flow cytometer (BD) to acquire data and cytokine concentrations were calculated using BD FACS DIVA software (BD).

2.5.2. Luminex assay

Cytokines in plasma and culture supernatants from *in vitro* differentiation (Method 2.4.3), micro-suppression assay (Method 2.4.5) and plasma co-culture assays (Method 2.4.7) were measured using the ProcartaPlex human Th1/Th2/Th9/Th17/Th22/Treg 18plex kit according to manufacturer's protocol.

Culture supernatants from plasma co-culture assays were diluted at 1 in 5 and plasma samples were diluted at 1 in 7.145. These samples were incubated for 2 hours at room temperature during the sample incubation step. Culture supernatants from *in vitro* differentiation assays were diluted 1 in 2 and supernatants from micro-suppression assays were tested neat. Samples from these assays were incubated overnight at 4°C during the sample incubation step. Cytokines tested were GM-CSF, IFNγ, TNFα, IL-10, IL-12p70, IL-13, IL-17A, IL-18, IL-1β, IL-2, IL-21, IL-22, IL-23, IL-27, IL-4, IL-5, IL-6, IL-9. Assay was performed on a FlexMap3D machine, which operates on Xponent 4.0 software for data acquisition.

2.5.3. IL-21 ELISA assay

IL-21 in supernatants from TCR stimulated CD4+ T cells (Method 2.4.1) was measured by using a LEGEND MAX™ Human IL-21 ELISA Kit (Biolegend) with pre-coated plates according to manufacturer's protocol. Culture supernatant samples were diluted 1 in 5 during the sample incubation step. Standard curve is shown in appendix sFigure 9.1. Assay was performed on Benchmark plus micropalte spectrophoto meter (Bio-Rad) and microplate manager software version 5.2.1.

2.6. Gene expression analysis

2.6.1. Quantitative reverse-transcription PCR (qRT-PCR)

2.6.1.1. Sample preparation – analysis from rested CD4+ T cells

Isolated CD4+ T cells were resuspended in RPMI culture supernatant containing 10% FBS and 1X penicillin streptomycin (Sigma). Cells were plated in 6-well plates at 1,000,000 cells per well and incubated overnight prior to harvest (200,000 cells were lysed in 200ul of Trizol).

2.6.1.2. RNA isolation by Trizol extraction.

RNA samples in Figure 3.6 and Figure 4.4 were prepared by Trizol extraction. Cell pellets were lysed in 200µl of TRIzol reagent (Life Technologies). After mixing gently, lysate was incubated at room temperature for 5 minutes and then centrifuged at 12000 × g for 15 minutes at 4°C. The upper layer containing RNA was transferred to new tubes and 10µg of glycogen (Ambion) was added per tube. An equal volume of isopropyl alcohol (VWR) was then added prior to centrifugation at 12000 × g, at 4°C for 10 minutes. The resulting supernatants were discarded and the RNA pellets washed with 75% ethanol, followed by centrifugation for 5 minutes at 7500 × g, 4°C. The ethanol was removed and the pellets were air dried at room temperature before adding 50µl of sterile TE buffer (1 M Tris-Cl (pH 8.0) and 0.2 mL 0.5M EDTA (pH 8.0) to dissolve the pellets. The RNA concentration was measured on a Nanodrop spectrophotometer (Invitrogen).

2.6.1.3. RNA isolation by using Allprep DNA/RNA micro kit

RNA samples for microarray analysis and for the experiment shown in Figure 4.8 were prepared by using Allprep DNA/RNA micro kit (Qiagen) according to manufacturer's protocol.

2.6.1.4. cDNA synthesis

To prepare cDNA for all relevant experiments except Figure 3.6, up to 250ng of RNA was incubated at 70°C for 5 min in the presence of 200ng of random hexamer primer (MWG) in sterile nuclease free water in a total volume of 20µl. Denatured RNA was promptly cooled on ice then added to a mixture of 8 µl of 5X reaction buffer (Thermofisher Scientific), 20mM of dNTP (Biogene), 40 IU of RNase-out (Invitrogen) and sterile nuclease free water to a total volume of 39 µl. After 5

minutes incubation, at 25°C, 1 µl of RevertAid M-MuLV Reverse Transcriptase enzyme (Thermofisher Scientific) was added per sample and samples incubated at 25°C for 10 minutes, 40°C for 1 hr, to perform reverse transcription then 70°C for 10 minutes to inactivate reverse transcriptase enzyme and terminate the reaction.

2.6.1.5. cDNA synthesis by using qPCRBIO cDNA Synthesis kit

To prepare cDNA samples for Figure 3.6 only, 100ng of RNA was converted into cDNA with the qPCRBIO cDNA Synthesis kit (PCR Biosystems) according to manufacturer's instructions.

2.6.1.6. Real time quantitative polymerase chain reaction (qRT-PCR)

Reactions were performed in 384 well plates, in a total volume of 20µl per well. Each well contained 10µl of SYBR mastermix (Primer Design Ltd and Thermofisher Scientific), 1µl of primer mix (each primer at a final concentration of 10pmol) (Table 2.3), 4µl sterile nuclease free water and 5µl cDNA (diluted four-fold in sterile nuclease free water). qRT-PCR was performed using a 4-stage protocol (Table 2.2) with stage 4 generating a dissociation curve:

Stage 1	Stage 2	Stage 3 (40 cycles)	Stage 4
50˚C for 2'	95˚C for 10'	95˚C for 15 s 60˚C for 1'	95˚C for 15 s 60˚C for 15 s

Table 2.2. qRT-PCR thermal cycler program.

Real time PCR data was analysed by using the comparative Ct method (delta Ct (ΔCt)). The peptidylprolyl isomerase A (PPIA) gene was used as reference for all qRT-PCR experiments. Relative target gene expression was calculated as described below;

1) ΔCt = Ct (target gene) – Ct (reference gene)

2) Relative gene expression = 2^-ΔCt.

3) Triplicates of relative gene expression (2^-ΔCt) were averaged to calculate mean.

2.6.2. Microarray analysis

2.6.2.1. Sample preparation

Naive CD4+ T cells were isolated from freshly prepared PBMCs. Isolated naive CD4+ T cells were incubated in RPMI culture media containing 10% FBS and 1X penicillin streptomycin (Sigma) in 6 well plates (1,000,000 cells per well) overnight at 37°C in 5% CO_2. After overnight incubation, 200,000 cells were pelleted and lysed in 300µl of RLT buffer (Qiagen) containing 10µl of 2-Mercaptoethanol. Alternatively, cells were stimulated on anti-CD3 and anti-CD28 pre-coated 96 well plates for 2 hrs prior to lysis.

2.6.2.2. RNA isolation and cDNA synthesis

RNA was isolated as described in Method 1.6.1.3 and the quality and quantity of RNA was measured by using a Bio-analyser (Agilent) following manufacturer's protocol. Double stranded cDNA was amplified using Ovation PicoSL WTA System V2 (Nugen) and purified by using Agencourt RNAClean XP beads (Beckman). After cDNA purification, cDNA bound to beads was amplified by using Single primer isothermal amplification (SPIA) and cleaned with Qiagen MinElute reaction cleanup kit (Qiagen). The quality of dsDNA was measured by using a Bio-analyser (Agilent) and the quantity of cDNA was determined by using a Nano-drop (Invitrogen) following manufacturer's instructions.

2.6.2.3. Microarray assay

Prepared cDNA was labelled with biotin using Ovation PicoSL WTA System V2 (Nugen), purified using Qiagen MinElute PCR purification kit (Qiagen), and quantified using a Nano-drop (Invitrogen). Biotin labelled cDNA was hybridised on Human HT-12 v4 Expression Bead Chips (Illumina) and microarray scanning was performed in the BRC Genomics facility (KCL). Hybridisation and microarray scanning was performed by Dr. Paul Lavender (KCL).

2.6.2.4. Microarray data analysis

Raw data containing fluorescent hybridization signal intensities (above background levels) was exported and analysed by Partek genomics suite analysis software (Partek) to identify differentially expressed genes between GPA patients and healthy individuals. To assess whether global gene expression is different between GPA patients and healthy individuals, a principle component analysis (PCA) was performed using Partek software. To detect differently expressed genes between groups of patients, Partek software was used to calculate fold-change values and to perform analysis of variance (ANOVA). Since this study had an unbalanced data set due to differing numbers of samples between GPA and HC groups (Table 2.3), multi-way ANOVA was performed using Least squares mean (LSmean) to generate an unbiased estimate of the mean of each experiment group.

a

Time/Donor	GPA	HC
0h	7	4
2h	7	4

b

Donor/ Time/Group	GPA Group1	GPA Group2	HC HC
0h	5	2	4
2h	5	2	4

Table 2.3. Microarray samples experiment factor annotation and number. (a) Samples used to generate a differently expressed gene list between GPA vs HC in

each time point and (b) between GPA group1 vs HC, GPA group2 vs HC in each time point.

To analyse lists of genes differentially expressed between GPA vs HC using Partek software, the following factors were applied to ANOVA analysis; 'donor' and 'time' were specified as fixed factors, 'batch type' was specified as a random factor, and interaction of 'donor*time' was added. To calculate fold change in gene expression between GPA vs HC at each time point, contrast between 'GPA*0h' and 'HC*0h', and contrast between 'GPA*2h' and 'HC*2h' were included in the analysis. To identify differently expressed genes between GPA group1 vs HC, and GPA group2 vs HC, the following factors were applied to ANOVA analysis; 'donor', 'time' and 'group' were specified as fixed factors, batch type was specified as a random factor, and interaction of 'donor*time*group' was added. To calculate fold change between GPA group1 vs HC, and GPA group2 vs HC at each time point, contrast 'GPA*0h*group1' and 'HC*0h*HC,' 'GPA*0h*group2' and 'HC*0h*HC', 'GPA*2h*group1' and 'HC*2h*HC', and 'GPA*2h*group2' and 'HC*2h*HC' were included in the analysis. The data from ANOVA analysis was exported, and lists of differentially expressed genes were generated by using fold change greater than 1.5 and P-value lower than 0.05. False discovery rate (FDR) analysis was not applied in generating these gene lists. To increase confidence in the genes identified as differentially expressed by microarray, qRT-PCR was also employed to assess the expression of selected genes (Figure 4.8). Further bioinformatic analysis was applied to these gene lists using Ingenuity Pathway Analysis (IPA) (Qiagen). 'Core analysis' in IPA was performed with gene lists including P-value and fold change data to predict putative functional changes in biological processes, pathways and molecular networks.

2.7. Quantification of protein levels

2.7.1. Mass spectrometry

Samples were prepared, and mass spectrometry assay and data extraction performed by Steve Lynham at the Centre of excellence for mass spectrometry proteomics facility at KCL. Briefly, total protein levels of plasma samples were measured by the Bradford reagent method (Biorad). The total protein content was comparable between samples (ranging from 71.4 µg/µl to 84.2 µg/µl). A reference sample was generated by pooling an equal volume of each of the individual samples. Each individual sample together with the reference sample was then lyophilized prior to enzymatic digestion. Each individual sample was labelled with a unique TMT10plex label (ThermoFisherScientific) and fractionated using isoelectric focussing (IEF, Agilent Technologies, UK). Fractionated TMT labelled peptide samples were analysed by using Liquid chromatography (LC) with mass spectrometry (MS)/MS analysis. Raw data from LC-MS/MS analysis was uploaded into Scaffold 4 (v4.8.4) software for qualitative protein/peptide measurement (150 proteins were detected following database searching and 95% CI filtering and the same number of proteins were detected in the TMT labelled fraction after TMT label filter was applied; therefore there was a 100% labelling efficiency at the protein level (95% CI)). Proteome Discoverer (v1.4) software was used for quantitative protein/peptide analysis. Data from Proteome Discoverer was exported into Microsoft Excel for further analysis. Experiment details in appendix- see appendix 9.1 Method: mass spectrometry.

2.7.1.1. Mass spectrometry data analysis

TMT reporter ions values for each protein were calculated using Proteome Discoverer. The median values per group were calculated in Microsoft Excel. Fold change in protein levels in each group was calculated by dividing median of patients sample group by median of healthy control group. P-value was calculated by performing a two-tailed student t test in Microsoft Excel. Lists of differentially abundant proteins between groups (fold change greater than 1.3) were used for bioinformatics analysis by Ingenuity Pathway Analysis (IPA) (Qiagen).

2.7.2. Western blotting

Cell lysates in Laemmli buffer were resolved on a 10% acrylamide SDS-PAGE gel in 1X Tris-Glycine-SDS PAGE Buffer (National Diagnostics), run at 125 V for 2 hours. Separated proteins on the gel were electro-transferred to Immobilon Polyvinylidene difluoride (PVDF) membrane (Thermofisher Scientific) with 1X Tris-Glycine Electroblotting Buffer (National diagnostics) at 35 V for 90 minutes, using an XCell II blot module (ThermoFisher Scientific). Following transfer, membranes were incubated in 20ml blocking buffer (5% skimmed milk (Marvel) in PBS including 0.1% Tween 20 solution (MP) for 1 hr at room temperature. Following blocking, membranes were incubated with primary antibodies directed against proteins of interest in 10ml of blocking buffer at 4°C overnight. After three washes with PBS containing 0.1% tween for 10 minutes each, membranes were incubated with appropriate species secondary HRP-conjugated antibodies in 10ml of blocking buffer for 1 hour at room temperature. After secondary antibody incubation, membranes were washed three times and developed using Clarity MAX™ Western ECL substrate (Bio-RAD) and visualized on an Imagequant LAS 4000 instrument (GE). For phosphoprotein blots, phosphoproteins were detected first then blots were re-hybridized to detect total target protein by repeating the

primary antibody incubation using an antibody (raised in a different species) (Table 2.4) recognising both phosphorylated and non-phosphorylated protein (i.e pSTAT5/STAT5A or pan-STAT5/STAT5B, pSTAT3/STAT3). Western blot quantifications were performed using ImageQuant software (GE).

2.8. Data analysis

2.8.1. Flow cytometry data analysis

All data from flow cytometry experiments were analysed by using FlowJo version 10 (TreeStar).

2.8.2. Bioinformatic analysis by Ingenuity Pathway Analysis (IPA) software

Ingenuity Pathway Analysis (IPA) (Qiagen) was used for bioinformatic functional analysis. Lists of differentially expressed or abundant genes or proteins from microarray and mass spectrometry analyses respectively were uploaded into IPA software. IPA, a web-based functional analysis software, identified the most relevant signalling and metabolic pathways, canonical pathways, disease indications, and predicted upstream regulators involved in GPA by clustering differentially expressed genes and comparing to an IPA database that has been formulated from previous literature. IPA also computed a statistical quantity, activation Z- score, to assess the predicted relevance of each biological function / pathway. A positive z-score indicates a predicted activation/increase of biological function in a pathway, while a negative z-score indicates inhibition/decrease of biological function in a pathway.

2.8.3. Statistical analysis

In this study, all statistical analyses between groups were performed with non-parametric tests as indicated using GraphPad Prism software (Graph Pad). Mann-

Whitney tests were performed to analyse un-paired data, while paired data were analysed by Wilcoxon matched-pairs signed rank test. Correlations were analysed by Spearman correlation. A p-value of <0.05 was considered statistically significant throughout.

2.9. Materials

Gene name	Primer direction	Sequence 5'-3'
PPIA	Foward	TGGGCAACATAGTGAGACG
	Reverse	TGTACAGTGGCATGATAATAGC
BCL6	Foward	CTGCAGCTGGAGCAATGTTGT
	Reverse	TCTTCACGAGGAGGCTTGAT
RNF144A	Foward	GACCTGGCCTGAAGACATTT
	Reverse	TGTGGTCATCGCAGAACAGT
BATF	Foward	ACACAGAAGGCCGACACC
	Reverse	CTTGATCTCCTTGCGTAGAGC
IRF4	Foward	GCCAAGATTCCAGGTGACTC
	Reverse	CTGGCTAGCAGAGGTTCTACG
cMAF	Foward	AGCGGCTTCCGAGAAAAC
	Reverse	TGCGAGTGGGCTCAGTTA
IL-2Rβ	Foward	GCCCCCATCTCCCTCGAAGT
	Reverse	AGGGGAAGGGCGAAGACAGC
Cathepsin G	Foward	ACACCCAGCAACACATCACTGC
	Reverse	GGTTCACGTTTCGATTCCGTCTG
Peli 2	Foward	CGCGCGCGGATTTGACTCTT
	Reverse	CTGGGTGAAGCCCCCTCGTG
PTEN	Foward	TGAGTTCCCTCAGCCGTTACCT
	Reverse	GAGGTTTCCTCTGGTCCTGGTA
IL-21	Foward	CCAAGGTCAAGATCGCCACATG
	Reverse	TGGAGCTGGCAGAAATTCAGGG
STAT5A	Foward	CCGTGACAGAGGAGAAGTTC
	Reverse	AGAGTCTTCACCTGGAACAC
STAT5B	Foward	TCAGACTTGATACACTTTCAGGTT
	Reverse	CTCAGGGAAGCCACACTCAT

Table 2.3 List of qRT-PCR primers.

Primary antibody				
Antigen	**Company**	**Catalogue number**	**Host**	**Dilution**
phospho STAT5	Cell Signal Technology	9351L	Rabbit	1:1000
phospho STAT3	Cell Signal Technology	9145S	Rabbit	1:1000
STAT5A	SantaCruz	SC-74442	Mouse	1:1000
STAT5B	SantaCruz	SC-1656X	Mouse	1:1000
Pan STAT5	BD	611819	Rabbit	1:1000
βactin	SantaCruz	SC-1615	Goat	1:2000
Secondary antibody				
Antigen	**Company**	**Catalogue number**	**Host**	**Dilution**
anti-mouse IgG-HRP	GE	NA931V	Sheep	1:5000
anti-rabbit IgG-HRP	GE	NA934V	Donkey	1:5000
anti-goat IgG-HRP	SantaCruz	SC-2020	Donkey	1:5000

Table 2.4 List of antibodies for western blot.

Cell marker	Fluorochrome	Company	Cat number
CD4	APC-eFluor780	ebioscience	47-0048-42
CD25 (Clone 2A3)	PE	BD	341011
CD25 (Clone M-A251)	PE	BD	555432
CD127	Brilliant Violet 711	BioLegend	351328
CD45RA	Brilliant Violet 605	BioLegend	304134
CXCR5	PerCP-Cy 5.5	BioLegend	356910
PD1	PE-Cy7	BioLegend	329918
Foxp3	Alexa Fluor 488	BioLegend	320012
CCR7	APC	BioLegend	353214
CD62L	Pacific blue	BioLegend	304826
CD11a	APC	BioLegend	301212
CD57	FITC	BioLegend	322306
CD28	PE-Cy7	BioLegend	302926
IL-21	PE	BioLegend	513004
BCL6	Alex Flour 647	BD	561525
CD45RO	FITC	Dako	F0800
Alexa Fluor® 488 Mouse IgG1, κ Isotype Ctrl (ICFC) Antibody	Alexa Fluor 488	Biolegend	400133
Alexa Fluor® 647 Mouse IgG1 κ Isotype Control	Alex Flour 647	BD	557714

Table 2.5 List of antibodies for Flow cytometry.

Reagent / Consumable	Supplier	Catalogue Number
dNTPs	Biogene	300-114
[^{3}H] thymidine	Perkin-Elmer	NET027X001MC
12 x 75mm FACS tubes	Falcon	352058
15mL centrifuge tubes	Corning	430791
2-Mercaptoethanol	Sigma	M3148
384 well qRT-PCR plate	Applied Biosystems	4309849
50mL centrifuge tubes	Corning	430829
6-well tissue culture plates	Costar	3516
Allprep DNA/RNA micro Kit	QIAGEN	80284
anti-CD28	BD bioscience	555725
anti-CD3	BD bioscience	555329
Betaplate scint for betaplate	Perkin Elmer	6013621
Blood collection tubes, heparin coated	BD	5125277
Brefeldin A	Invitrogen	450651
Cell Trace Violet dye	Life Technologies	C34571
Clarity MAX™ Western ECL substrate	BioRad	1705062
Cytometric bead array (CBA) human Th1/Th2/Th17 cytokine Kit	BD	560484
Dimethyl suloxide (DMSO)	Sigma	D8418
DNAase / RNAse free water	Ambion	AM9937
Dynabeads Human T-Activator anti-CD3/anti-CD28 beads	Life Technologies	11131D
Dynabeads untouched human CD4+ T cells Kit	Invitrogen	793131
eBioscience™ Foxp3 / Transcription Factor Staining Buffer Set	Invitrogen	00-5523-00
Ethanol	VWR	20821.33
Ethylenediaminetetraacetic acid (EDTA)	Fluka	3690
Fixation Buffer	BD	554655
Fœtal Bovine Serum (FBS)	Gibco	16140071
Glass filter	Perkin-Elmer	1450-421
Glycogen	Ambion	7510
Human AB serum	Sigma	SLBT0322V
Immobilon polyvinylidene difluoride (PVDF) membrane	Thermofisher Scientific	88518
Ionomycin	Sigma	I0634
Isopropanol	VWR	437423R
LEGEND MAX™ Human IL-21 ELISA Kit	BioLegend	433808
LIVE/DEAD® Aqua dye	Invitrogen	L34965
Lymphoprep	Axis Shield, UK	NYC-1114544
MagniSort™ Human CD4 Naïve T cell Enrichment Kit	Invitrogen	8804-6214-74
Micro-centrifuge tubes	Costar	3621
Penicillin / Streptomycin solution	Sigma	P4333
Perm Buffer III	BD	558050
Phorbol 12-myristate 13-acetate (PMA)	Sigma	P8139
Phosphate Buffered Saline (PBS), Mg2+ and Ca2+ free	Gibco	14190-094
ProcartaPlex human Th1/Th2/Th9/Th17/Th22/Treg 18plex Kit	Invitrogen	EPX180-12165-901
Protein transport inhibitor (containing Monesin)	BD	51-2092KZ
qPCRBIO cDNA Synthesis kit	PCR Biosystems	PB30.11-10
Random hexamer primer	Invitrogen	100026484
Recombiant human IL-2	R&D	202-IL-010
Recombinant human IL-10	BioLegend	571002
Recombinant human IL-12	PeproTech	200-12
Recombinant human IL-15	BioLegend	570302
Recombinant human IL-6	BioLegend	570802
Recombinant human IL-7	BioLegend	581902
Recombinant human TGF-β	BioLegend	580702
RevertAid H Minus Reverse Transcriptase	Thermofisher Scientific	EP0452
RNAse out	Invitrogen	100000840
RPMI-1640	Gibco	21875-034
SYBR Mastermix	Primer Design Ltd	PPLUS-machine type
SYBR Mastermix	Thermofisher Scientific	A25743
Tris-Glycine Electroblotting Buffer	National Diagnostics	EC880
Tris-Glycine-SDS PAGE Buffer	National Diagnostics	EC870
TRIzol reagent	Life Technologies	15596018
Tween-20	MP	TWEEN201
U bottom plates, 96-well	Costar	3799
V bottom plates, 96-well	Greiner Bio-one	651161
X-VIVO media, serum free	Lonza	BE02-060F

Table 2.6 List of reagents and consumables.

3. Chapter 3. CD4+ T cells from GPA patients may become polarized toward a Tfh-like phenotype.

3.1. Introduction

A number of previous studies have suggested that a functional imbalance between effector CD4+ T cells and Treg cells in GPA may contribute significantly to disease pathogenesis. Furthermore, it is believed that Tfh/cTfh cells may play a particularly important role in GPA, a disease associated with auto-reactive antibodies, given the ability of Tfh cells to provide help to B cells for generation of high affinity antibodies. Studies have suggested an increase in cTfh cell populations (characterised by a high frequency of CXCR5+PD1+CD4+ T cells, high expression of BCL6 in these cells and, high production of IL-21) in GPA blood compared to HC (Abdulahad *et al.*, 2013; Zhao *et al.*, 2014) In other studies, PMA with ionomycin or PR3 peptide stimulation of isolated PBMCs or whole blood from GPA patients showed an expansion of Th17 subsets (Abdulahad *et al.*, 2008; Wilde, Thewissen, *et al.*, 2012; Rani *et al.*, 2015).. However, since the majority of studies have involved PMA/ionomycin stimulation of whole blood or PBMC (rather than isolated CD4+ T cells) it has been difficult to understand whether expansion of the Th17/cTfh population is intrinsically programmed in GPA, or whether these cells are responding to changes in the cytokine and antigenic environment during GPA pathogenesis. Moreover, signalling through PMA/ionomycin stimulation bypasses membrane receptor complexes and activates internal signalling pathways, many of

which are not naturally induced by TCR engagement (Ai *et al.*, 2013; Olsen and Sollid, 2013). It has been shown that the effects of altered membrane receptor expression on AAV/GPA CD4+ T cell activation (CD25, CD28 and IL-2 receptor β (CD122)) may be masked by using PMA/ionomycin stimulation (Marinaki *et al.*, 2005; Morgan *et al.*, 2011; Wilde *et al.*, 2014a).

While an increase in Th17 and cTfh population has been reported in GPA, the frequency of Treg cells and the ability of these cells to suppress effector T cell function in GPA patients remain controversial. Some studies show higher frequencies of Tregs in GPA compared to HC (Treg defined as $CD25^{high}$Foxp3+). Other studies show no change in Treg numbers (Treg defined as CD25+Foxp3+) although GPA Tregs exhibited a defect in their immune suppression function. A further study showed lower frequencies of Treg cells in GPA (Treg defined as $CD25^{high}CD127^{low}$) but no difference in their ability to suppress Teff function compared to HC (Marinaki *et al.*, 2005; Abdulahad *et al.*, 2007; Mckinney *et al.*, 2014; Zhao *et al.*, 2014).

Although the phenotypic definition of Treg cells in terms of expression of surface markers varies between studies, Treg cells are typically defined as CD25 positive.. Interestingly, higher frequencies of naive ($CD45RB^{high}$) CD4+ T cells from AAV patients (not exclusively GPA patients) expressed CD25 compared to HC (Marinaki *et al.*, 2005). This study suggested that the increased frequency of naive CD25+CD4+ T cells from AAV patients may not reflect a global expansion of the Treg population (since no difference in Foxp3 mRNA expression in total CD4+ T cells was observed) but may instead represent increased persistence of T cell activation.. It would seem that CD25 expression, specifically on naïve CD4+ T cells,

may be related to AAV pathogenesis. Investigation of the immunology underlying this phenotype, may be important in understanding the role of CD4+ T cells in progression of AAV/GPA.

Additionally, the majority of previous studies in this area have focused on cellular immunology (e.g. T cell surface expression markers / cytokine production) rather than molecular immunology (e.g. expression of transcription regulatory factors). Therefore our understanding of the underlying molecular mechanisms responsible for the phenotype of GPA CD4+ T cells remains limited. It is unclear whether the functional imbalance between cTfh/Th17 and Treg cells in GPA is due to intrinsic changes in expression of transcription regulatory factors in GPA CD4+ T cells, or whether these phenotypes are predominantly caused by factors within the extracellular environment.

This chapter aims to characterise the frequencies of Treg cells and Tfh cells and analyze the expression of CD25 on CD4+ T cells by flow cytometry. Differences in cytokine production, and expression of key transcription factors in CD4+ T cells from GPA an HC will also be investigated.

3.2.Results

3.2.1. The frequencies of circulating Treg and Tfh populations between active GPA patients and healthy donors.

To assess the frequencies of CD4+ T cell subsets by flow cytometry, cryopreserved peripheral blood mononuclear cells (PBMCs) from eight active GPA patients and seven age matched healthy controls were stained with a panel of fluorochrome-conjugated antibodies described in Figure 2.2a. The gating strategy and data from this experiment is shown in Figure 3.1. Identification of CD4+ T cells from PBMC is shown in Figure 3.1a .Tregs were defined in two ways based on previous studies; either $CD25^{high}CD127^{low}$ Tregs (Zhao *et al.*, 2014) or $CD25^{high}$Foxp3+ Tregs (Abdulahad *et al.*, 2007). The mean frequency of circulating Tregs in active GPA patients (5.5% for $CD25^{high}CD127^{low}$ and 3.8% for $CD25^{high}$Foxp3+) was not statistically significantly different from that of healthy controls (5.7% and 4.1%, respectively) (Figure 3.1b). Also, no differences were found in the frequencies of circulating Tfh cells ($CD4+CXCR5^{high}PD1^{high}$) (Figure 3.1c) between GPA patients and healthy controls. CXCR5 and PD1 expression on CD4+ T cells were also analysed and there was a significant reduction in the frequencies of PD1+CD4+ T cells in GPA compared to HC (Figure 3.1e) while there was no differences in frequencies of CXCR5+CD4+ T cells between GPA and HC (Figre 3.1d).

Tfh cells were first described in germinal centres, and were shown to display $CXCR5^{high}$ and $PD1^{high}$ markers on CD4+ T cell surfaces. The same gating strategy has also been applied to identify circulating Tfh cells (Zhao *et al.*, 2014). In the current study, circulating Tfh cells were gated as in previous studies ($CD4+CXCR5^{high}PD1^{high}$) but since gating of this population could be subjective, the broader CD4+CXCR5+PD1+ population was also analysed (Figure 3.1c). No

differences were found in frequencies of circulating Tfh cells between GPA patient and HC groups using either definition of Tfh (CD4+CXCR5^{high}PD1^{high} or CD4+CXCR5+PD1+) (Figure 3.1c).

Frequencies of CXCR5+ CD4+ T cells and PD1+CD4+ T cells were also analysed. There was a significant reduction in the frequencies of PD1+CD4+ T cells in GPA compared to HC (Figure 3.1e) while there was no difference in frequencies of CXCR5+CD4+ T cells between GPA and HC groups (Figure 3.1d).

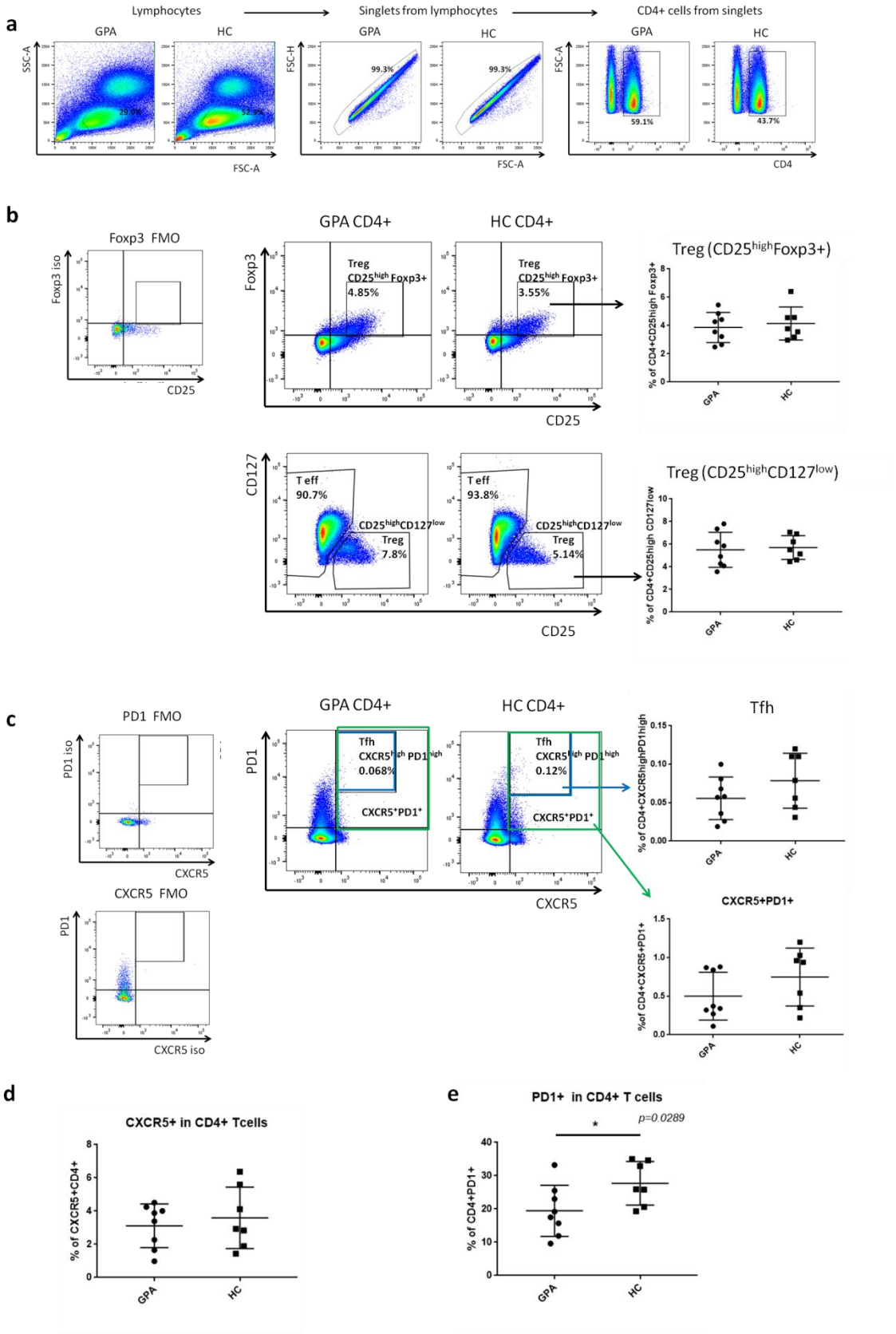
a
Lymphocytes
Singlets from lymphocytes
CD4+ cells from singlets
GPA
HC
SSC-A
FSC-A
FSC-H
99.3%
59.1%
43.7%
CD4
b
Foxp3 FMO
Foxp3 iso
CD25
GPA CD4+
HC CD4+
Foxp3
Treg CD25high Foxp3+ 4.85%
Treg CD25high Foxp3+ 3.55%
Treg (CD25highFoxp3+)
% of CD4+CD25high Foxp3+
CD127
Teff 90.7%
CD25highCD127low Treg 7.8%
Teff 93.8%
CD25highCD127low Treg 5.14%
Treg (CD25highCD127low)
% of CD4+CD25high CD127low
c
PD1 FMO
PD1 iso
CXCR5
CXCR5 FMO
CXCR5 iso
PD1
Tfh CXCR5high PD1high 0.068%
Tfh CXCR5high PD1high 0.12%
CXCR5+PD1+
Tfh
% of CD4+CXCR5highPD1high
%of CD4+CXCR5+PD1+
d
CXCR5+ in CD4+ Tcells
% of CXCR5+CD4+
e
PD1+ in CD4+ T cells
p=0.0289
% of CD4+PD1+

Figure 3.1. Circulating Treg and Tfh populations in CD4+ cells. (a) CD4+ T cell gating from stained, cryopreserved PBMCs was performed following doublet exclusion from the lymphocyte population. **(b)** Treg cells were defined in two ways. **Top row**: CD4+CD25^{high}Foxp3+ Treg cells identified by gating based on CD25 and Foxp3 expression from CD4+ T cells gated from (a) with Foxp3+ cells determined using Foxp3 fluorescence minus one (FMO) control. The frequency of Treg (CD4+CD25^{high}Foxp3+) cells was compared between GPA and HC. **Bottom row:** Treg (CD4^{+}CD25^{high}CD127^{low}) and T effector (Teff) (CD4^{+}CD127^{+}CD25^{low}) cell identification was performed by gating based on CD25 and CD127 expression. Frequencies of these T cell subsets was compared between PBMC from GPA patients and HC (bottom row). **(c)** Circulating Tfh cells (CD4^{+}CXCR5^{high} PD1^{high}) and CD4+CXCR5+PD1+ cells were identified by gating based on CXCR5 and PD1 expression using CXCR5 FMO and PD1 FMO controls. The frequencies of both cells were compared between GPA patients and HC **(d)** Frequencies of CXCR5+CD4+ T cells in PBMCs were compared between GPA patients and HC **(e)** Frequencies of PD1+ CD4+ T cells in PBMC were compared between GPA patients and HC. Data shows mean frequencies of cell subsets. No statistically significant differences were observed between GPA and HC samples by Mann Whitney test.

3.2.2. Patients with active GPA have higher expression of CD25 expression on naïve (CD45RA+) CD4+ T cells than healthy individuals.

To investigate the level of CD25 expression on naive CD4+ T cells in GPA patients versus healthy controls, CD4^{+} T cells from PBMCs were gated on marker CD45RA (which is highly expressed on naïve but not memory CD4^{+} T cells) and CD25. GPA patients had significantly higher frequencies of CD4^{+}CD45RA^{+}CD25^{+} cells compared to healthy controls (Figure 3.2a), in agreement with previously

published observations (Marinaki *et al.*, 2005). To address whether this observation is due to an increase in the Treg population, Foxp3 levels was measured in these cells by intra cellular staining. There was no observed difference in Foxp3 expression in CD4+CD45RA+CD25+ cells between GPA patients and healthy controls (Figure 3.2b).

To ensure that Tregs were excluded from the CD4+CD45RA+CD25+ cell population, in further experiments CD4+ T cells from PBMCs were first gated on markers CD25 and CD127 (Figures 3.2c-h). The remainder of the CD4+ T cell population after Treg ($CD25^{high}CD127^{low}$) exclusion were defined as T effector (Teff) cells. Teff cells from GPA patients and HC were then analyzed for expression of markers CD45RA (which is expressed on naive CD4+ T cells) and CD25, as shown in representative plots in Figure 3.2c. To further confirm these data with more samples, further analyses on eight GPA and seven healthy control samples using a similar gating strategy to that shown in Figure 3.2c is shown in Figure 3.2d-h. These additional samples were stained with a panel of fluorochrome-conjugated antibodies described in Figure 2.2h. Even after excluding Tregs, frequencies of CD4+CD45RA+CD25+ cells within the Teff population were higher in GPA patients compared to healthy controls (Figure 3.2e). Moreover, the mean frequencies of CD4+CD45RA+CD25+ cells within the total CD4+ T cell population in GPA patients (9.3%) and healthy controls (3.4%) (Figure 3.2f) was comparable to that within the Teff population alone (GPA patients 9.94%, HC 3.74% Figure 3.2e). In contrast, frequencies of CD4+CD45RA-CD25- cells were lower in GPA patients than in healthy controls (Figure 3.2g). There were no statistically significant differences in frequencies of CD4+CD45RA+CD25- cell populations or CD4+CD45RA-CD25+ cell populations between GPA patients and healthy controls (Figure 3.2 d and h). This

observation suggested that naive CD4+ T cells in GPA may express higher levels of CD25. However, in this panel, only CD45RA was used as a naive/memory marker. Therefore, it is possible that the CD45RA+ T cells identified here are in fact a mixture of T_{EMRA} and naive CD4+ T cells.

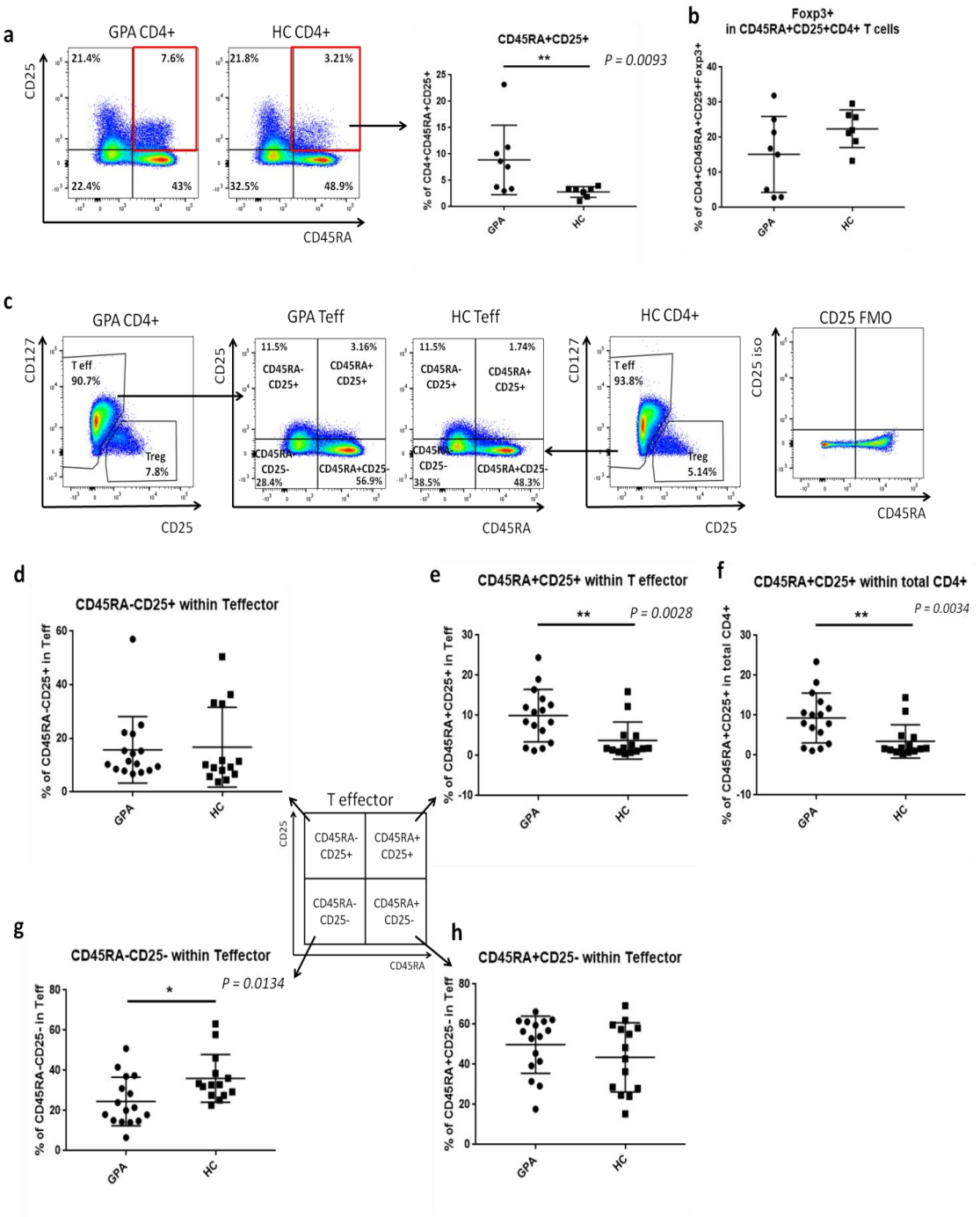

Figure 3.2 CD25 expression on CD45RA+andCD45RA- CD4+T cells in GPA patients and healthy controls. (a) PBMCs from GPA patients and healthy controls were isolated, stained with a panel of fluorochrome-conjugated antibodies and analysed by flow cytometry. CD4+ T cells were gated using the strategy shown in Figure 3.1a. CD45RA- and CD45RA+CD25+CD4+ T cells were identified based on CD45RA and CD25 expression. Representative data from a single GPA patient blood sample (first from left) and from a single healthy control blood sample (second from left) are shown. Frequencies ofCD45RA- and CD45RA+ CD25+CD4+ T cells in GPA patient (GPA, n=8) and healthy control (HC, n=7) samples is shown (third from left). **(b)** CD45RA+CD25+CD4+ T cells from Figure 3.2a were analyzed for expression of Foxp3. Percentages of CD45RA+ CD25+CD4+ T cells expressing Foxp3 are shown **(c)**. In an alternative gating strategy, Treg ($CD25^{high}CD127^{low}$) cells were identified and excluded from the remainder of the CD4+ T cell population (defined as T effector (Teff) cells). prior to gating of CD45RA+CD25+ CD4+ T cells as shown previously in Figure 3.2a (GPA first and second from left, HC third and fourth from left). Representative data from a single GPA patient and a single HC sample are shown. The gating strategy for CD25 expression was determined based on CD25 FMO control (fifth from left). **(d-f)** The gating strategy from Figure 3.2c was used to assess the frequencies of four Teff cell populations from GPA (n= 16) and HC (n=14) samples: **(d)** CD45RA-CD25+, **(e)** CD45RA+CD25+, **(g)** CD45RA-CD25- and **(h)** CD45RA+CD25-. **(f)** For comparison, the frequency of CD45RA+CD25+ cells within the total CD4+ T cell population (including Tregs) was compared between GPA and HC. Data show mean frequencies of cell subsets, and statistical analysis performed by Mann Whitney test.

3.2.3.The frequency of CD25 expression on comprehensively phenotyped circulating naive CD4+T cells in GPA patients is higher than in healthy controls.

The flow cytometry data presented above shows a significant increase in CD25 expression on naive (CD45RA+) CD4+ T cells from GPA patients compared to healthy controls. CD45RA is among the principal markers of naive T cells but it is also expressed on T_{EMRA} cells. To confirm that these CD25+CD45RA+CD4+ T cells are bona fide naive CD4+ T cells, two further panels of fluorochrome-conjugated antibodies (Figure 2.2b and Figure 2.2c) suited to comprehensive identification of naive CD4+ T cells were used to stain GPA and HC PBMCs (Figure 3.3). CD25 expression on comprehensively phenotyped naive CD4+ T cells as defined by De Rosa *et al* (De Rosa *et al.*, 2001) (CD4+CD28+CD45RA+CD62L+CD11a^{dim}CD57-) was again significantly higher on cells from GPA patients compared to HC (Figure 3.3a).

Chemokine receptor, CCR7 is another important marker in distinguishing between naive T cells and T_{EMRA} cells. Therefore, a second fluorochrome-conjugated antibody panel was developed following a study from Tian and colleagues (Tian *et al.*, 2017)(Figure 3.3c). There was a trend towards higher CD25 expression on naive (CD4+CCR7+CD45RA+) cells in GPA compared to HC (Figure 3.3c).

It is noted that apparent frequencies of CD25+ naive CD4+ T cells tended to be higher when naïve CD4+ T cells were comprehensively phenotyped, particularly within the GPA patient group (Figure 3.3a vs Figure 3.3c). We hypothesize that this is likely to be due to the fact that the total comprehensively phenotyped naïve CD4+ T cell population, defined by the expression of six different markers (De Rosa

et al., 2001), is smaller than the CD4+CCR7+CD45RA+ population (a comparison of gating strategy is shown in Supplementary Figure 9.4). The frequencies of CD25+ comprehensively phenotyped naïve CD4+ T cells and CD25+CCR7+CD45RA+CD4+ T cells as a percentage of total CD4+ T cells were compared (Figure 3.3b and 3.3d). Frequencies of CD25+ naïve CD4+ T cells as a percentage of total CD4+ T cells were comparable using both gating strategies and frequencies of these cells were higher in GPA patients compared to HC (Figure 3.3b and d). This observation supports our hypothesis, and suggests that there was no significant discrepancy between the experiments shown in Figure 3.3a-b and Figure 3.3c-d, despite the use of different patient samples.

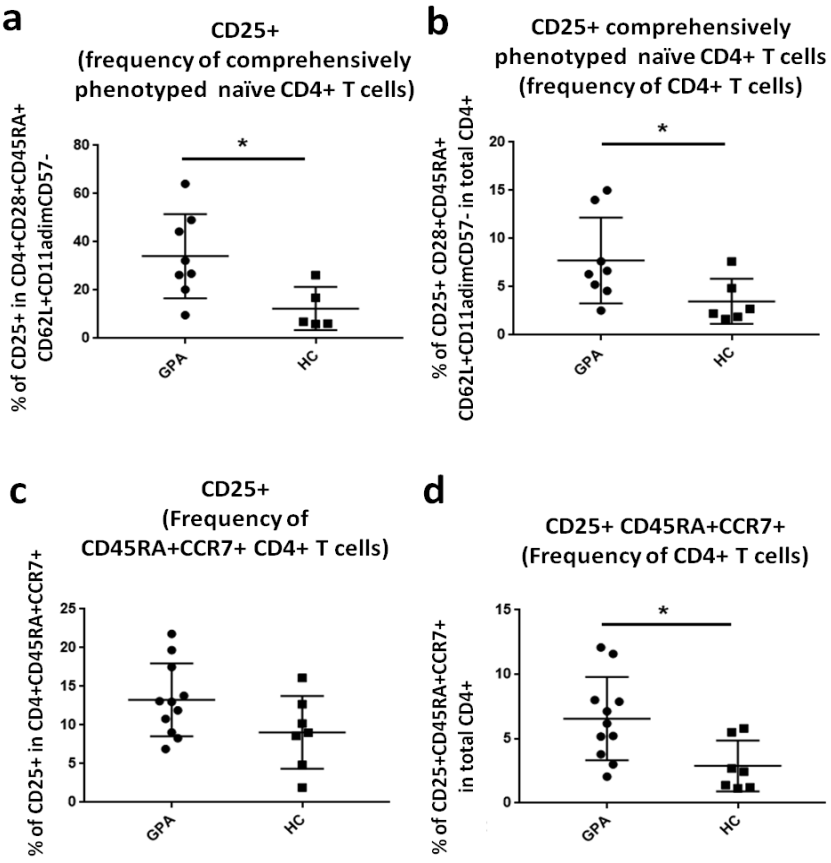

Figure 3.3 CD25 expression on comprehensively phenotyped naive CD4+ T cells. (a-b) Frequency of CD25 expression on naïve (CD4+CD28+CD45RA+CD62L+CD11a^{dim}CD57-) T cells from PBMC was assessed by flow cytometry. **(a)** Frequencies of CD25+ cells within naive CD4+ T cells and **(b)** frequencies of CD25+ naive CD4+ T cells within the total CD4+ T cell population from GPA patients (n=8) and HC (n=5). **(c-d)** Frequency of CD25 expression on naïve (CD4+CCR7+CD45RA+) T cells from PBMC was assessed by flow cytometry **(c)** Frequencies of CD25+ cells within naive (CD4+CCR7+CD45RA+) T cells and **(d)** CD25+CCR7+CD45RA+CD4+ T cells within the total CD4+ T cell population was compared between GPA (n=11) and HC (n=7). Data show mean frequencies of cell subsets, and statistical analysis performed by Mann Whitney test.

3.2.4. Cytokine production from isolated CD4+ T cells upon TCR activation.

To investigate whether there are intrinsic differences in the capacity of CD4+ T cells from GPA patients to produce cytokines upon TCR stimulation, in the absence of additional T cell polarization signals (Dupage and Bluestone, 2016) CD4$^+$ T cells were isolated from total PBMC from both GPA patients and healthy controls, and cultured with anti-CD3 and anti-CD28 antibodies to simulate TCR stimulation. Culture supernatants of TCR stimulated CD4$^+$ T cells were analyzed for cytokine concentration by cytometric bead array (CBA) for a range of cytokines (IL-4, IL-17A, TNF-alpha, IFN-gamma, IL-10, IL-6 and IL-2) and by ELISA for IL-21. Test sample values were background subtracted (media only, n=3).

Production of a key Tfh cell cytokine, IL-21, was significantly higher from GPA CD4+ T cells upon TCR activation compare to HC, albeit at low overall levels of expression (Figure 3.4a). In contrast, significantly lower levels of IL-4 were

secreted from GPA CD4+ T cells compare to HC (Figure 3.4b). While some previous published studies have suggested an increase in IL-17 secretion in GPA CD4+ T cells upon PMA and ionomycin activation, here there was no statistically significant difference in IL-17 secretion from isolated CD4+ T cells upon TCR activation between GPA and HC (Figure 3.4c). No difference in production of other cytokines including TNF -alpha, IFN-gamma, IL-10, IL-6 and IL-2 from TCR activated CD4+ T cells was observed between GPA and HC (see appendix sFigure 9.2).

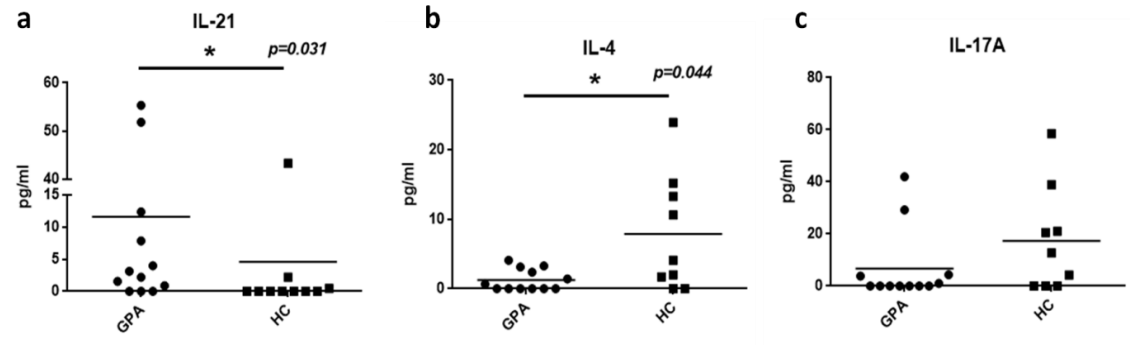

Figure 3.4 Cytokine production in TCR stimulated CD4+ T cell culture supernatants. $CD4^+$ T cells from GPA patients or healthy controls were isolated using Dynabeads from cryopreserved PBMCs and cultured for 4 days in the presence of anti-CD3 and anti-CD28 to mimic TCR stimulation. **(a)** After 4 days, IL-21 concentration within culture supernatants was measured by ELISA. **(b)** IL-4 and **(c)** IL-17A concentration in culture supernatant was measured by CBA assay. GPA n=12, HC n=10. Data show mean concentration of cytokine in culture supernatants, and statistical analysis performed by Mann Whitney test.

3.2.5. Naive and memory CD4+ T cells from GPA patients have comparable TCR induced proliferative ability.

The data presented above show that TCR activated CD4+ T cells from GPA patients and HC differ in their profile of cytokine production. *In vitro* cytokine production is also related to ability of a cell to proliferate. In a previous study, CD4+ T cells from AAV patients, especially memory CD4+ T cell subsets, had a higher proliferative ability after weak TCR activation but not strong TCR activation compared to HC (Marinaki *et al.*, 2005).

The observed differences in cytokine production in Figure 3.4 may be due to an abnormal proliferative ability in memory and naive CD4+ T cells in GPA patients compared to HC. To assess *in vitro* proliferative capacity in response to TCR stimulation, CD4+ T cells labelled with Cell Trace Violet (CTV) dye were sorted into naïve and memory CD4+ T cell subsets by fluorescence activated cell sorting (FACS). To avoid the suppressive function of Tregs confounding the analysis, Treg cells were excluded prior to sorting (Figure 3.5a). Sorted cells were cultured with anti-CD3, anti-CD28 and IL-2 to mimic TCR stimulation for 5 days before analysis by flow cytometry (Figure 3.5b-c). As expected, the proliferative capacity of sorted memory CD4+ T cells was significantly greater than naïve CD4+ T cells (Figure 3.5c). However, there were no significant differences between the proliferative capacity of cells isolated from GPA patients compared to those isolated from healthy controls. (Figure 3.5c). To assess whether there were differences in the rate of cell proliferation in this assay between GPA and HC, frequencies of cells in each of the proliferative peaks shown in Figure 3.5b were calculated using FlowJo software (sFigure 9.5). The frequency of non-divided cells (Division 0) was higher in memory CD4+ T cells from HC compared to GPA, but there were no differences in the frequencies of cells at Divisions 1-6 (sFigure 9.5b), hence the rate of proliferation of GPA and HC memory CD4+ T cells was comparable. However, since

the frequency of non-divided memory CD4+ T cells was higher in HC, it may be that these memory cells in GPA have a higher propensity to proliferate. There were no differences in frequencies of naïve CD4+ T cells at Division 0-6 between GPA and HC (sFigure 9.5c).

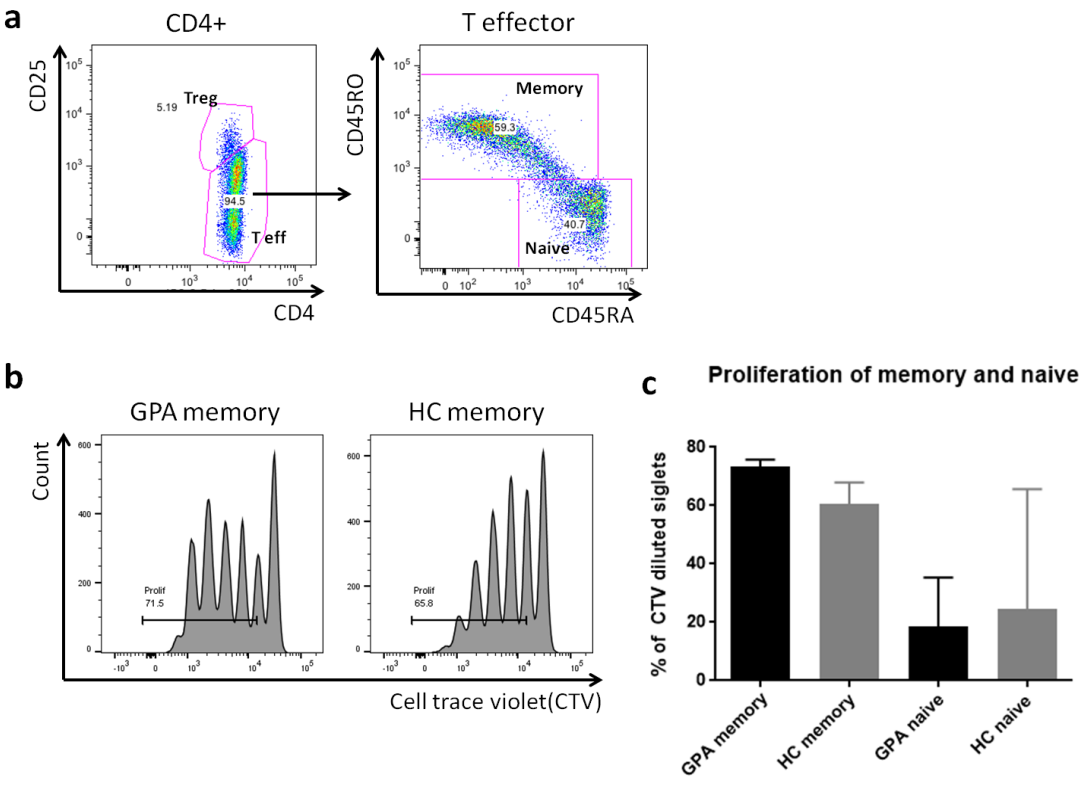

Figure 3.5 Proliferative capacity of naïve and memory CD4+ T cells in GPA. PBMCs from GPA patients or healthy controls were labelled with Cell Trace Violet (CTV) dye to track cell division and stained with fluorochrome-conjugated antibodies. CD4+ T cells were identified, and Teff subsets were sub-gated into naïve and memory cell subsets for cell sorting. **. (a)** Gating strategy of naive and memory CD4+ T cells for cell sorting. Teff (CD4+CD25+/-) and Treg (CD4+CD25^{high}) cell populations were gated based on CD25 and CD4 expression. Teff cells sub-gated into memory and naive CD4+ T cells based on CD45RA and CD45RO expression. Naive (CD45RA+CD45RO-) and memory (CD45RA^{low}/-CD45RO+) CD4+

T cells were sorted for *in vitro* proliferation assay. Note cell sorting was performed and gating strategy plots were provided by Estefania Nova Lamperti (DTIMB, KCL) **(b)** Sorted cells from Figure 3.5a were cultured for five days with anti-CD3, anti-CD28 and IL-2 (40IU/ml). Cell proliferation was tracked by dilution of CTV dye, measured by flow cytometry. Representative data from a single GPA patient's memory CD4+ T cell population (first from left) and a single HC memory CD4+ cell population (second from left) is shown. **(c)** Percentage of naïve and memory CD4+ T cells having undergone at least one cell cycle (GPA n=3, HC n=3, graph shows mean and standard deviation).

3.2.6. Expression of Tfh associated/regulatory genes in active GPA CD4+ T cells.

Further experiments were conducted to understand whether observed differences in cytokine production between CD4+ T cells in GPA and HC may be due to intrinsic changes in Tfh related regulators and/or transcription factor expression. Levels of mRNA expression of Tfh master transcription factor, BCL6, and Tfh/Th17 related regulatory factors such as RNF144A, BATF, IRF4 and c-MAF were measured by quantitative RT-PCR (qRT-PCR). Although not a transcription factor, IL-2Rβ expression was also measured, as IL-2 signaling negatively regulates Tfh / Th17 differentiation though STAT5 activation (Liao *et al.*, 2011; Ballesteros-Tato *et al.*, 2012; Johnston *et al.*, 2012; Owen and Farrar, 2017).

BCL6 and RNF144A expression was significantly higher in $CD4^+$ T cells from GPA patients compared to HC (Figure 3.6a-b). In contrast, BATF expression was significantly lower in CD4+ T cells from GPA patients compared to HC (Figure 3.6 c). There were no statistically significant differences in IRF4, c-MAF and IL-2Rβ

expression between GPA and HC, although there was a trend towards higher IRF4 and lower IL-2Rβ expression in GPA CD4+ T cells (Figure 3.6 d-f).

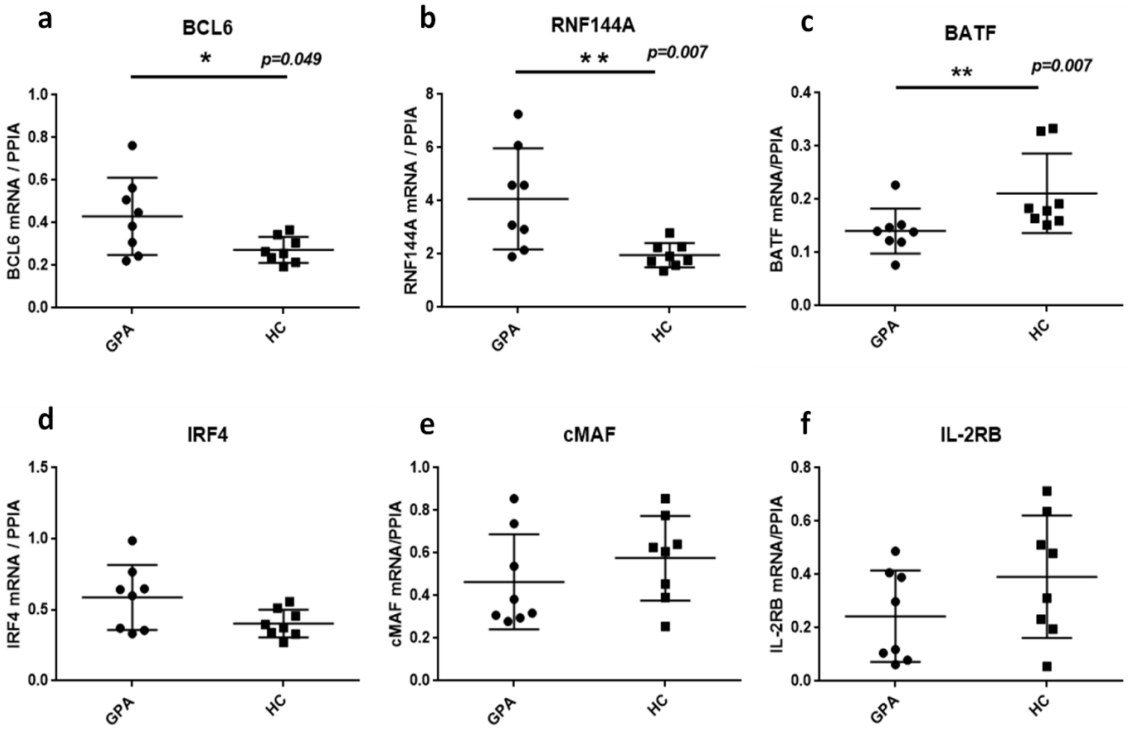

Figure 3.6 Levels of mRNA expression of factors relating to Tfh and Th17 differentiation in CD4+ T cells from GPA patients and healthy controls. CD4+ T cells from GPA patients (n=8) and healthy controls (n=8) were isolated from PBMC using Dynal beads. RNA from $CD4^+$ T cells was isolated by trizol extraction for qRT-PCR analysis. Relative mRNA expression of **(a)** BCL6 **(b)** RNF144A **(c)** BATF **(d)** IRF4 **(e)** c-MAF and **(f)** IL-2Rβ compared to a housekeeping control gene (PPIA) was measured by qRT-PCR. Data show mean relative gene expression ($2^{-\Delta Ct}$), and statistical analysis performed by Mann Whitney test.

3.3. Discussion

The overall aim of this chapter was to characterise Treg and cTfh/Th17 CD4+ T cell subsets by phenotype and function in GPA and HC blood. To investigate the frequencies of Treg and cTfh cell subsets, flow cytometry was performed. There were no observed differences the frequency of Treg and cTfh cell populations between GPA and HC CD4+ T cells in this study. Commonly used markers for identifying Treg cells include CD25, CD127 and Foxp3 (Wing *et al.*, 2019). In this chapter, Treg cells were defined in two different ways following previous studies (Abdulahad *et al.*, 2007; Zhao *et al.*, 2014). However, both gating strategies showed no differences in Treg frequencies between GPA and HC. Previous studies have offered conflicting evidence regarding differences in the frequencies of Treg cell populations between GPA and HC (Marinaki *et al.*, 2005; Abdulahad *et al.*, 2007; Zhao *et al.*, 2014). A challenge regarding the identification of Treg cells is that all three of the commonly used Treg markers can also be present on activated CD4+ T cells under certain conditions. To strengthen a further analysis, additional Treg cell markers including Helios, ICOS, TIM3and TIGIT, could be included in a flow cytometry antibody staining panel (Wing *et al.*, 2019).

The frequency of circulating Tfh (cTfh) cells was also similar between GPA and HC in this study. Chemokine receptors such as Tfh marker CXCR5 have a tendency to show reduced expression upon cryopreservation of PBMCs; one possibility is that using cryopreserved PBMCs reduced the signal intensity of CXCR5 labelling, hindering identification of cTfh cells. However, in a pilot study comparing cryopreserved versus fresh PBMCs, only a slight reduction in CXCR5 staining intensity was observed (see appendix sFigure 9.3). It has previously been reported that the population of bona fide Tfh cells in blood is very low, making conclusions

regarding cTfh cell frequencies difficult (He *et al.*, 2013). Although a previous study showed a higher frequency of cTfh cells in freshly isolated PBMCs from GPA compare to HC, the mean frequencies of these cells in both GPA and HC were barely at the level of detection (GPA ~0.4%, HC ~0.2% of total CD4+ T cells (Zhao *et al.*, 2014)).

Another reason that no difference in the frequencies of cTfh between GPA and HC were observed may be that PD1 expression was lower on GPA CD4+ T cells. This observation was contrary to data from a previous study that reported an increase in PD1 expression on CD4+ T cells from GPA patients compared to HC (Wilde, Hua*,* *et al.*, 2012) The authors also suggested that the high levels of PD1 expression observed in GPA may imply continuous activation of GPA CD4+ T cells. However, PD1 expression was also higher on CD25-CD4+ T cells in their study, which actually suggests that these cells were not activated CD4+ T cells. Moreover, although TCR activated CD4+ T cells upregulate PD1 expression, the role of PD1 is typically believed to generate an inhibitory signal that leads to reduction of CD4 T cell activation (Simon and Labarriere, 2017). For this reason, higher PD1 expression on T cells often represents T cell exhaustion (Wherry and Kurachi, 2015). Furthermore, it has been also reported in a different study that T cells from active GPA patients displayed a less exhausted phenotype (Mckinney *et al.*, 2015). Therefore, the observed reduction in PD1 expression in GPA in our study may indicate a reduction in frequencies of exhausted CD4+ T cells. However, this hypothesis needs to be tested further in future studies using other T cell exhaustion markers such as TIM3 and CTLA4 for phenotyping (Wherry and Kurachi, 2015). In addition, it will also be important to use more cTfh cell markers

for phenotyping this subset – including surface marker ICOS and transcription factor BCL6.

In this study, higher frequencies of naive CD25+CD4+ T cells were observed in GPA PBMCs compared to HC. Although a similar observation has been reported in AAV (Marinaki *et al.*, 2005), this is the first study, to our knowledge, describing this phenotype in GPA. It was important to investigate whether increased CD25 expression on naive CD4+ T cells represented an expansion of the Tregs that exhibit naïve phenotype in GPA patients. Although most effector Treg cells (Treg cells displaying an active immune suppressive function) exhibit memory phenotypes, some Treg cells display a naive phenotype like Treg population I (resting Tregs). (Dias *et al.*, 2017; Wing *et al.*, 2019).

Figure 3.2b indicates that the CD25 expressing naïve CD4+ T cells from GPA patients did not highly express Treg marker Foxp3, suggesting that these cells are unlikely to be Tregs. However, to further investigate whether increased CD25+ expression was on bona fide naive CD4+ T cells, an alternative gating strategy was developed to exclude Treg subsets ($CD25^{high}CD127^{low}$) prior to analysis of CD25+ naïve T cell frequencies (Figure 3.2c-h). After exclusion of Treg subsets, CD25+ naïve T cell frequencies remained statistically significantly higher in GPA patients compared to HC (Figure 3.2 e). This observation was reaffirmed upon more comprehensive phenotyping of naïve CD4+ T cells with staining for additional surface markers (Figure 3.3).

One other possible explanation for increased CD25 expression on naive CD25+ T cells is a persistence of T cell activation in GPA patients. In the healthy condition,

CD25 expression is rapidly upregulated upon TCR activation of naive CD4+ T cells, but these newly activated CD4+ T cells also rapidly downregulate the expression of markers associated with the naive phenotype (Murphy *et al.*, 2008; Van Den Broek *et al.*, 2018). Therefore, if T cell activation is persistent in GPA, high frequencies of naive CD25+CD4+ T cells may reflect this pathogenic condition. However, if this were true, one would also expect to observe an increase in memory CD25+CD4+ T cell populations. However, Figure 3.2d indicates that there was no difference in CD45RA-CD25+ Teff cell frequencies between GPA and HC. Moreover, in AAV studies, patients in remission still maintained higher frequencies of naive CD25+CD4+ T cell population compared to HC. Therefore, further studies are required to investigate the origins of the naive CD25+CD4+ T cell population in GPA and their role in disease progression.

Profiles of cytokine production from isolated CD4+ T cells also differed between GPA and HC. Although several studies have suggested expansion of Th17 cells in GPA patients (Abdulahad *et al.*, 2008; Rani *et al.*, 2015), in the current study IL-17 production from isolated CD4+ T cells upon TCR activation did not differ between GPA patients and HC (Figure 3.4c). In contrast, the production of IL-21 was higher in GPA compared to HC, but IL-4 production was lower from GPA CD4+ T cells (Figure 3.4 a and b). These data suggest that CD4+ T cells upon TCR activation may favour production of Tfh cytokines upon TCR activation, but produce lower levels of Th2 cytokines. Also, stimulation of IL-17 expression in CD4+ T cells from GPA patients may require additional signals that may be provided through PMA/Ionomycin activation.

This chapter also focused on understanding whether changes in the levels of transcription factors in CD4+ T cells in GPA contribute to the observed changes in CD4+ T cell phenotypes in this, and previous studies. Interestingly, isolated CD4+ T cells from GPA patients exhibited a Tfh-like phenotype by producing elevated IL-21 levels upon TCR activation (Figure 3.4) and higher expression of BCL6 and RNF144A mRNA (Figure 3.6) compared to HC. The cytokine IL-21 and transcription factor BCL6 are key signatures of Tfh cells. Moreover, RNF144A is a negative regulator of Th17 cell differentiation (Afzali et al, manuscript under revision) and was described in a previous study as among the top five direct target genes regulated by BCL6 in Tfh cells (Liu *et al.*, 2016). In addition to RNF144A, lower expression of BATF in CD4+ T cells from GPA (Figure 3.6) may be one of the reasons why TCR stimulation did not induce high IL-17 expression. BATF promotes Th17 cell differentiation by inducing IL-17 expression. On the other hand, BATF also induces Tfh cell differentiation by regulating BCL6 (Ise *et al.*, 2011). However, BCL6 expression was elevated in GPA CD4+ T cells, suggesting expression of BCL6 may be regulated independently of BATF in these cells. Observed reduction of IL-4 production (Figure 3.6) in GPA may be related to increased expression of BCL6 and lower expression of BATF. BCL6 inhibits Th2 differentiation (Kusam *et al.*, 2003), through post-transcriptional regulation of the master regulatory Th2 factor GATA3, which induces IL4 transcription , while BATF has been shown to be important in regulating IL-4 expression in Tfh and Th2 cells through direct binding to the IL-4 promoter region (Martinez and Dong, 2009; Sahoo *et al.*, 2015; Wu *et al.*, 2018). C-maf is a key Th2 transcription factor that controls IL4 expression (Kim *et al.*, 1999), and although the results did not reach statistical significance, the expression of this gene tended to be lower in GPA samples as compared to HC, consistent with the reduced IL4 expression noted here.

Due to limitations in quantity of extracted RNA from GPA CD4+ T cells, other key transcription factors, particularly Th17 transcription factor RORγt, were not measured in this analysis. Further studies are required to assess whether dysregulation of other CD4+ T cell differentiation pathways occurs in GPA.

In conclusion, an analysis of CD4+ T cell phenotypes revealed that GPA patients have higher frequencies of naive CD25+CD4+ T cells compared to HCs but their function and origin are still unclear. Genetic and functional characterization revealed that CD4+ T cells in GPA expressed higher levels of BCL6 and RNF144A mRNA, and TCR activation of these cells induced high production of IL-21 compared to HC. Although phenotypic analysis of peripheral blood by flow cytometry did not detect changes in the frequency cTfh ($CXCR5^{high}PD1^{high}$) cells in GPA, data from functional studies indicated that CD4+ T cells in GPA may become polarised towards a Tfh-like phenotype.

4. Chapter 4. Molecular characterisation of naive CD4+ T cells in GPA.

4.1. Introduction

The main observations from the previous chapter were i) an increase in circulating Tfh like CD4+ T cells in GPA compared to HC and ii) higher frequencies of naive CD25+CD4+ T cells in GPA compare to HC. However, it is not clear whether the naive CD25+CD4+ T cells observed are precursors of Tfh-like subsets in GPA patients.

Tfh cell subset development, requires strong TCR engagement and low IL-2 signalling (Ballesteros-Tato *et al.*, 2012). Several studies have clearly demonstrated the physiological importance of IL2 as a negative regulator of Tfh differentiation (Johnston *et al.*, 2012; Nurieva *et al.*, 2012). Paradoxically, recent studies in mice have shown that it is the IL-2-producing CD4 T cell that differentiates into a Tfh cell, while the IL2-non-producers become non-Tfh cells (Ditoro *et al.*, 2018). Mechanistically this is achieved by strong TCR engagement, resulting in a longer contact period between APC and naive CD4+ T cells, which induces IL-2 production from naive CD4+ T cells. Furthermore, those cells also express lower levels of CD25 thus, limiting IL-2 signalling and enabling subsequent Tfh differentiation (Ditoro *et al.*, 2018).

The observation, that in GPA patients there is an increased frequency of naive CD25+CD4+ T cells, with intermediate CD25 staining (Figure 3.2e), suggested the

possibility that these were precursor Tfh cells. A lower expression of the critical signalling subunit, IL-2 receptor beta (CD122) has also been reported in GPA CD4+ T cells, (Wilde *et al.*, 2014a), and together these observations are suggestive of a decreased IL-2 signalling pathway in naive CD4+ T cells in GPA.

In addition to lower levels of IL-2 signalling, the expression of key transcriptional regulatory factors are also important in Tfh development. In the previous chapter, it was shown that the expression of key Tfh transcription factor BCL6, was significantly increased in GPA CD4+ T cells. However, expression of a direct regulator of BCL6, BATF, was lower in GPA than healthy controls. This result suggests that intrinsic dysregulation of gene expression may contribute to the phenotypic changes observed in CD4+ T cells from GPA patients.

This chapter will investigate the hypothesis that intrinsic dysregulation of molecular signalling pathways in naive CD4 T cells may contribute to the functional imbalance of CD4 T cell subsets in GPA.

4.2. Results

4.2.1. The frequency of CXCR5^{+}PD1^{+}CD4+ T cells after *in vitro* Tfh differentiation.

To understand whether there were differences in the capacity of naive CD4+ T cells from GPA patients versus HC to differentiate towards Tfh cells, an *in vitro* Tfh differentiation assay was performed. CD4+ T cells were isolated from PBMCs from ten GPA patients and six healthy controls by Dynabead isolation. Isolated naive CD4+ T cells were cultured with either TCR stimulation (anti-CD3, anti-CD28) plus IL-7 alone (control Th0 (TCR) condition), or with TCR stimulation/IL-7 plus additional cytokines, TGFβ and IL-12 (Tfh differentiation) as described in a study from Locci et al (Locci *et al.*, 2016).

After a five-day culture, naive CD4+ T cells were stained with panels of fluorochrome-conjugated antibodies described in Figure 2.2f and Figure 2.2g. The gating strategy from this experiment is shown in Figure 4.1a. To address whether there is a change in frequency of cTfh (CXCR5+PD1+), CD4+ T cells were gated based on CXCR5 and PD1 expression. Due to limited cell numbers in isolated naive CD4+ T cell preparations, FMO controls for CXCR5 and PD1 were not included and instead unstained controls were used (Figure 4.1b).

Overall, there was no difference in cTfh cells between GPA and HC under both TCR/IL-7 alone and Tfh differentiation (TCR/IL-7+TGFβ+IL-12) conditions. However, Tfh differentiation (TCR+TGFβ+IL-12) condition induced significantly higher frequencies of CXCR5^{+}PD1^{+}CD4+ T cells compared to the control (TCR/IL-7 alone) condition in naive CD4+ T cells from both GPA patients and HC (Figure 4.1c). In particular, the frequency of CXCR5+PD1+CD4+ T cells strikingly increased in

GPA after Tfh differentiation compared to TCR stimulation alone (Figure 4.1c). This increase was driven by an increase in PD1 expression rather than CXCR5 expression on GPA CD4+ T cells (Figure 4.1d and e). In contrast, both PD1 and CXCR5 increased at the similar way in HC CD4+ T cells after Tfh differentiation. However, there was no statistically significant difference in the frequency of these subsets between GPA and HC after either condition.

Due to the absence of FMO controls, an additional gating strategy was tested to confirm that the CXCR5+PD1+CD4+ T cell population was correctly gated and whether an alternative gating strategy could reveal differences in CXCR5+PD1+ CD4+ T cell frequencies between GPA and HC under both *in vitro* skewing conditions (sFigure 9.6). In this re-analysis, only the cells with the lowest signal in the PE-Cy7 (PD1) and PerCP-Cy5.5 (CXCR5) channels in the unstained control were excluded (sFigure 9.6a). Again, there was no difference in cTfh frequencies between GPA and HC under both conditions (sFigure 9.6b), and the pattern of PD1 expression (sFigure 9.6c) and CXCR5 (sFigure 9.6d) expression, when analysed individually, was comparable to that observed in Figure 4.1d-e. However, there were no differences in the frequencies of double positive CXCR5+PD1+ populations in GPA between TCR alone and Tfh skewing conditions, while an increase in this population was still observed in HC after Tfh skewing (sFigure 9.6b). This discrepancy is likely to be due to the fact that the new gating strategy appears to overestimate the frequencies of PD1+ populations (mean frequencies of PD1+ cells were approximately 80% of total CD4+ T cells, Figure 9.6c). It would therefore seem that the more stringent exclusion gate applied in the analysis in Figure 4.1 is more appropriate.

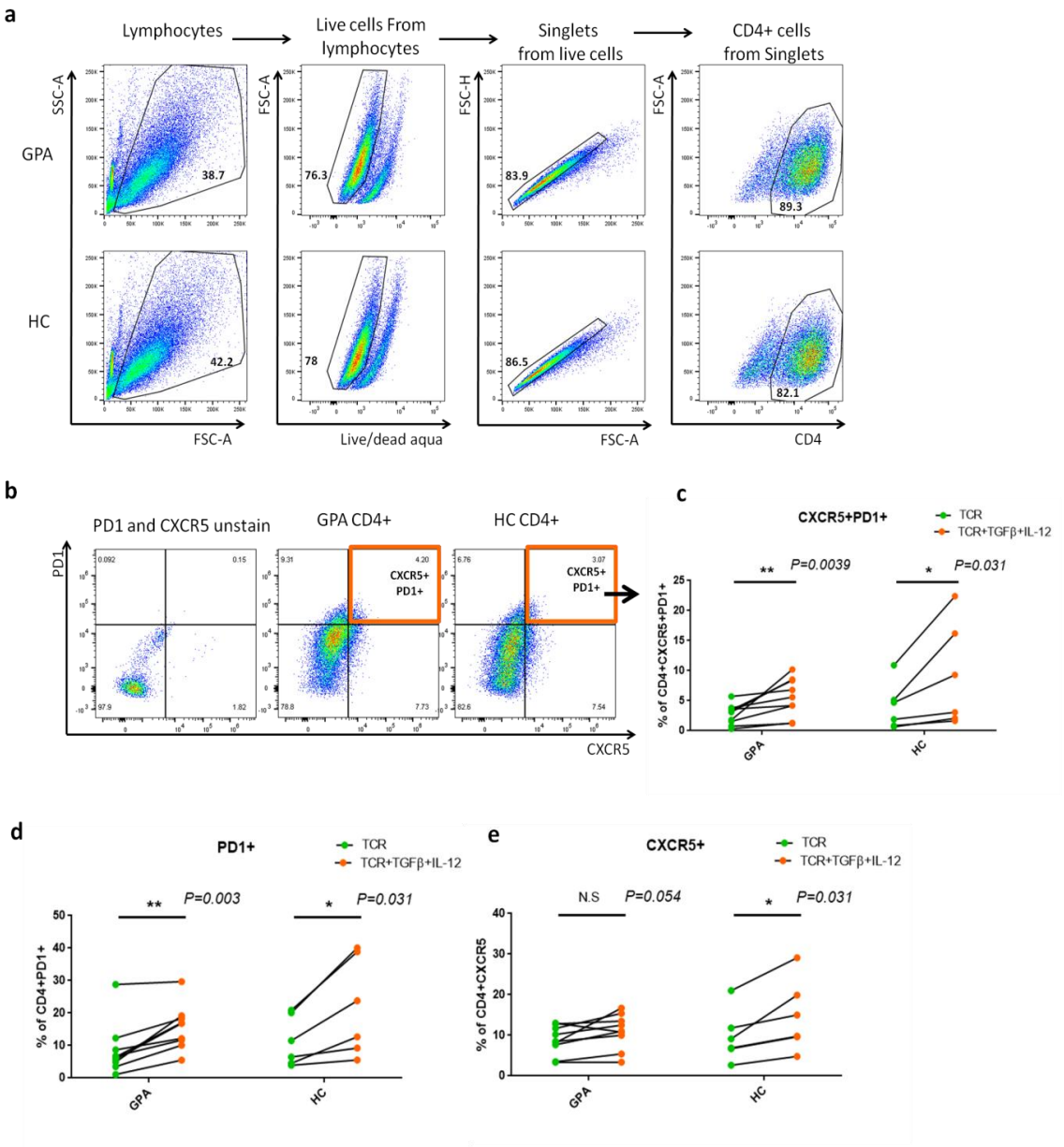

Figure 4.1 CXCR5+PD1+CD4+ T cells after Th0 (TCR) and Tfh (TCR+ TGFβ+IL-12) in vitro differentiation. (a) CD4+ T cell gating from stained naive CD4+ T cells stimulated for 5 days with anti-CD3, anti-CD28 and IL-7 (TCR) or TCR plus TGFβ and IL-12 (TCR+ TGFβ+IL-12) following doublet exclusion from the live population after lymphocytes gating. **(b)** CXCR5+PD1+CD4+ T cells were identified from gated CD4+ T cells from (a) by gating based on CXCR5 and PD1 expression using PD1 and CXCR5 unstained control. **(c)** The frequencies of CXCR5+PD1+CD4+ T cells were compared between GPA patients and HC naive CD4+ T cells cultured with TCR alone (green dot) or TCR+TGFβ+IL-21 (orange dot). Paired data points

from each donor sample are connected by a line. Statistical analysis was performed by Wilcoxon matched pairs signed rank test. n=9 (GPA) and (HC).

4.2.2. Intracellular expression of BCL6 and IL-21 in naive CD4+ T cells after *in vitro* Th0 and Tfh differentiation.

Thus far, data regarding the frequency of cTfh cells (Figure 3.1c and Figure 4.1b) suggest that there was no difference in the frequency of cTfh (CXCR5+PD1+CD4+) cells between GPA and HC. However, one potential issue may be that lower PD1 expression in GPA CD4+ T cells could confound identification of cTfh cells (Figure 3.1e). To investigate whether there were differences in the expression of other Tfh markers, BCL6 and IL-21 expression were measured by intracellular staining (ICS) in the same experiment described in Figure 4.1. For gating BCL6+ and IL-21+ populations, isotype controls for each markers were employed and the gating strategies for BCL6 and IL-21 detection are shown in Figure 4.2a and Figure 4.2d respectively.

Overall, both BCL6 and IL-21 expression were increased in CD4+ T cells after Tfh differentiation compared to TCR stimulation only (Figure 4.2b,c,e and f). Notably, the frequency of BCL6+CD4+ T cells was statistically significantly higher in GPA CD4+ T cells after only TCR stimulation compared to HC (Figure 4.2b). There was also a trend towards higher frequencies of BCL6+CD4+ T cells in GPA compared to HC after Tfh differentiation (Figure 4.2c). However, there were no differences in IL-21 expression between GPA and HC CD4+ T cells after either *in vitro* Th0 or Tfh differentiation.

It is noted that due to the method of gating based on histograms as described in Figure 4.2a, the analysis of BCL6+ cell frequencies in Figure 4.2b-c may have underrepresented the size of BCL6+ populations due to the tail on the isotype control peak (Figure 4.2a). The data were therefore reanalysed by Overton subtraction using Flowjo software (sFigure 9.7). While frequencies of BCL6+ cells were higher using this method as expected, the relationship between population frequencies in GPA patients compared to HC was comparable to data shown in Figure 4.2b-c.

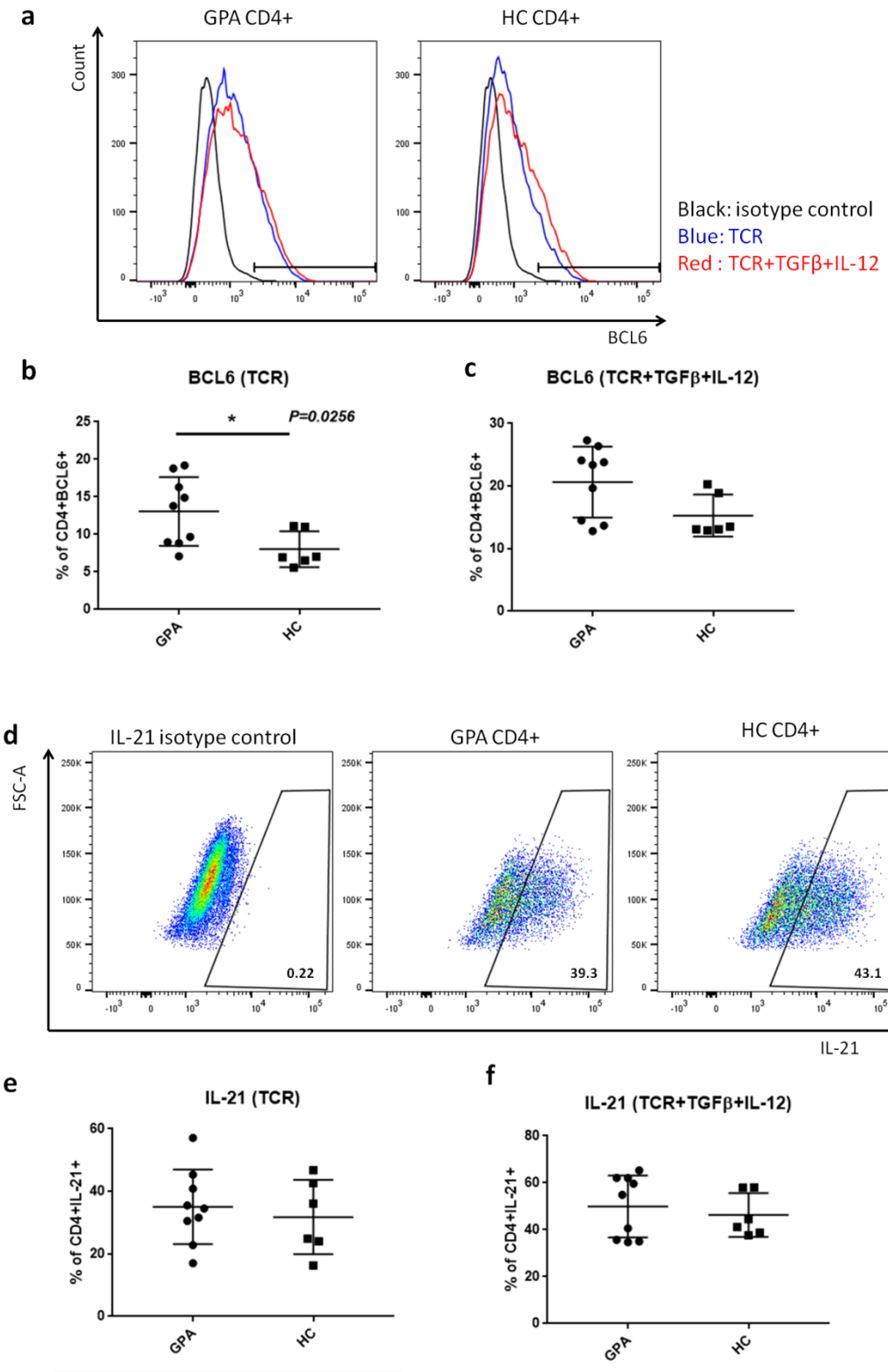

Figure 4.2 The intracellular expression of BCL6 and IL-21 in CD4+ T cells after Th0 and Tfh in vitro differentiation. (a and d) Flow cytometry analysing the intracellular expression of **(a)** BCL6 and **(d)** in naive CD4+ T cells 5 days cultured with Th0 (TCR) or Tfh (TCR+TGFβ+IL-12). BCL6^{+}CD4+ T cells were

identified from gated CD4+ T cells from (Figure 4.1a) by gating based on BCL6 and IL-21 expression using BCL6 and IL-21 isotope controls respectively. **(b and c)** The frequency of $BCL6^{+}CD4+$ T cells were compared between GPA patients and HC naive CD4+ T cells cultured with **(b)** Th0 (TCR) or **(c)** Tfh (TCR+TGFβ+IL-12) differentiation conditions. **(e and f)** The frequency of IL-21+CD4+ T cells were compared between GPA patients and HC naive CD4+ T cells cultured with **(e)** Th0 (TCR) or **(f)** Tfh (TCR+TGFβ+IL-12) differentiation conditions. Data show mean frequencies of cell subsets, and statistical analysis performed by Mann Whitney test. GPA n=9 HC n=6.

4.2.3. Secreted IL-21 from naive CD4+ T cells after *in vitro* Th0 and Tfh differentiation.

To measure IL-21 expression from CD4+ T cells by ICS in Figure 4.2, cells were cultured for 5 hours with PMA and ionomycin for boosting cytokine expression and in the presence of brefeldin and Protein transport inhibitor to prevent cytokine release prior ICS. Therefore, the IL-21 expression data described above might be affected by PMA/ionomycin stimulation, which may upregulate cytokine expression independently of receptor signalling. To exclude any additional non-TCR driven signalling effects of PMA/ionomycin, secreted cytokine levels in cell culture supernatant from PMA/ionomycin non-treated cells were measured by 18-plex Luminex assay (Figure 4.3).

Overall, both GPA and HC naive CD4+ T cells secreted more IL-21 after in vitro Tfh (TCR+TGFβ+IL-12) differentiation compared to Th0 (TCR alone) differentiation (Figure 4.3a, b). However, there were still no significant differences in secreted IL-

21 between GPA and HC cell culture supernatant, despite a trend towards higher IL-21 production in GPA samples.

Interestingly, there was a trend towards higher secreted IL-6 in GPA naive CD4+ T cells compared to HC after five-day *in vitro* Tfh differentiation (Figure 4.3d). Although statistically this trend was not significant by Mann Whitney test, the P value was very close to significance at 0.0519. Moreover, for three out of nine GPA samples and one out of six HC samples, IL-6 concentration data were unobtainable, since the values for these samples were above the top range of the standard curve measurements, and repeats at a higher dilution were not possible due to limited remaining sample availability. No difference in production of other cytokines (IL-4, IL-27, IL-10, IL-1β, IL-5, IL-12, IL-13, IL-17A, IL-9, IL-23, IL-18, IFNγ, GM-CSF, TNFα and IL-22) was observed between GPA and HC (see appendix sFigure 9.4).

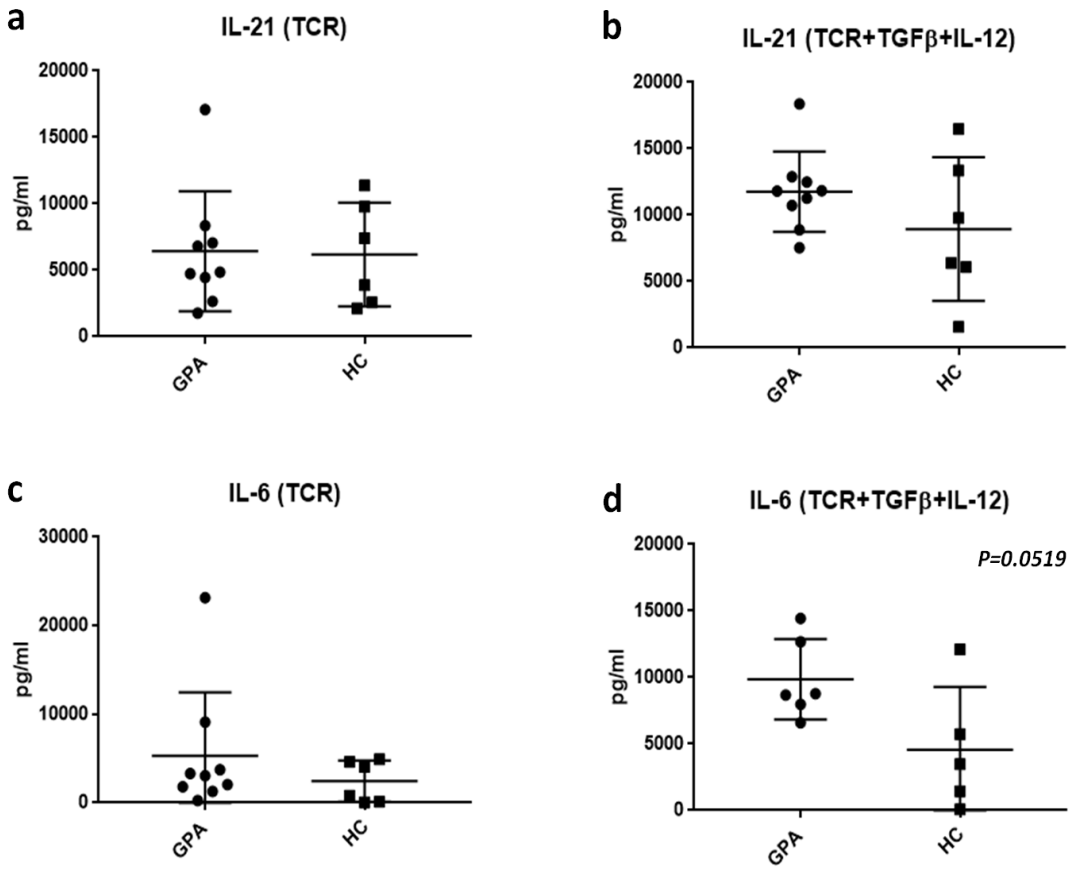

Figure 4.3. Secreted IL-21 and IL-6 levels from naive CD4+ T cells after in vitro Th0 and Tfh differentiation. Isolated naive CD4+ T cells from GPA patients or healthy controls were cultured for 5 days under Th0 (TCR alone) or Tfh (TCR+TGFβ+IL-12) differentiation conditions. Concentration of cytokines in cell culture supernatants was measured by Luminex assay. **(a and b)** IL-21 concentration within culture supernatants after **(a)** Th0 (TCR) or **(b)** Tfh ((TCR+TGFβ+IL-12) differentiation. **(c and d)** IL-6 concentration within culture supernatants after **(c)** Th0 (TCR) or **(d)** Tfh (TCR+TGFβ+IL-12) differentiation. Data show mean concentration of cytokine in culture supernatants, and statistical analysis performed by Mann Whitney test.

4.2.4. IL-21 mRNA expression after Tfh differentiation.

Although IL-21, expression from naive CD4+ T cells was not different between GPA and HC, there was a strong trend towards higher IL-6 expression in GPA naive CD4+ T cells after Tfh differentiation compared to HC (Figure 4.3d). IL-6 produced by CD4+ T cells can act in an autocrine manner to direct Th cell lineage differentiation (Naugler and Karin, 2008; Sofi *et al.*, 2009). Moreover IL-6 has been shown to induce Tfh differentiation and upregulate IL-21 production from CD4+ T cells (Diehl *et al.*, 2012; Chavele *et al.*, 2015). IL-6 is important for the expansion of Tfh cell differentiation by enabling differentiating cells to produce IL-2, while counteracting the inhibitory effects of IL-2 on Tfh cells. (Papillion *et al.*, 2018) Therefore, it was hypothesized that the increasing levels of IL-6 during Tfh differentiation may have the potential to enhance IL-21 expression in GPA naive CD4+ T cells at a later time point. To investigate this, IL-21 mRNA levels were measured from enriched naive CD4+ T cells stimulated for 6 days with Tfh (TCR+TGFβ+IL-12) differentiation conditions. Interestingly, there was a trend towards higher IL-21 mRNA expression in GPA naive CD4+ T cells after culture in Tfh differentiation conditions compared to HC (Figure 4.4) though more samples would be required to ascertain statistical significance.

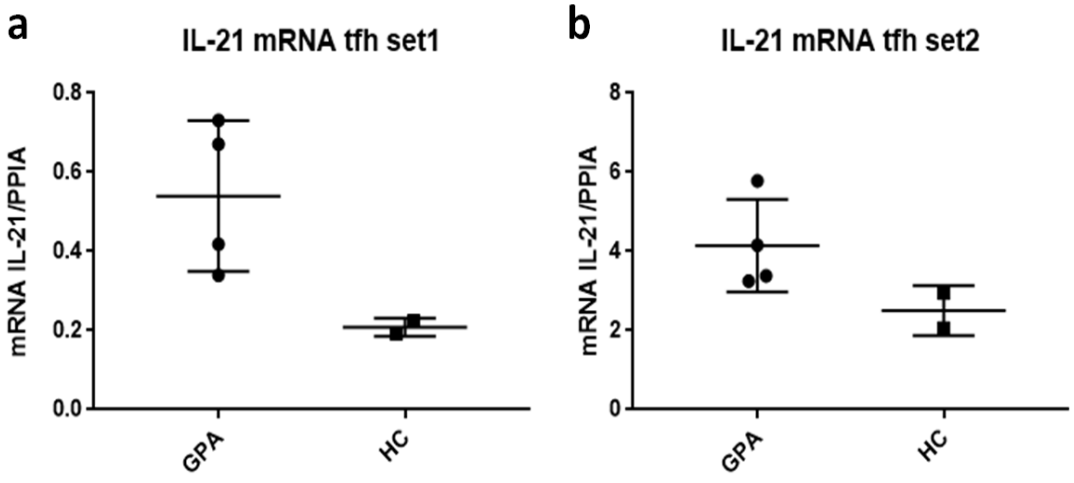

Figure 4.4 Level of mRNA expression in naive CD4+ T cells from GPA patients and HC after 6 days in vitro Th0 and Tfh differentiation. RNA from naive CD4+ T cells after 6 days culture with Tfh (TCR+TGFβ+IL-12) differentiation conditions was isolated by Trizol extraction for qRT-PCR analysis. Messenger RNA expression of IL-21 in GPA and HC naive CD4+ T cells was compared after culture with Tfh (TCR+TGFβ+IL-12) differentiation conditions relative to expression of a housekeeping control gene (PPIA) was measured by qRT-PCR in two independent experiments (a and b). **(a)** Set1 (n=3 (GPA) n=2 (HC)) **(b)** Set2 (n=3 (GPA) n=2 (HC)). Data show mean relative gene expression (2-ΔCt). Note, data from set 1 and set 2 treated separately due to different relative gene expression values between the two experiments.

4.2.5.Global gene expression in naive CD4+ T cells from GPA and HC.

The *in vitro* differentiation data described above, together wtih previous findings (Figure 3.4 and Figure 3.6) suggests that naive CD4+ T cells from GPA patients may favour differentiation towards a Tfh-like phenotype. To understand these observations at a molecular level, differences in global gene expression in resting and activated naive CD4+ T cells between GPA patients and healthy controls (HC), an Illumina microarray was performed. Naive CD4+ T cells were isolated using Dynal beads from blood samples from seven GPA patients and five HCs. GPA patient samples were selected that had similar medication histories (See appendix sTable 9.2). After resting overnight, RNA was isolated from rested naive CD4+ T cells (non-activated) and two-hour TCR activated naive CD4+ T cells. The two-hour time-point enabled investigation of early gene expression changes upon TCR stimulation but prior to cytokine mediated gene induction.

Strikingly, principle component analysis (PCA) showed that there are clear, distinctive gene expression profiles that differ between naive CD4+ T cells from GPA patients and healthy controls (Figure 4.5 a). Differentially expressed genes in GPA CD4+ T cells were identified by analysis of variance (ANOVA) using Partek software. Figure 4.5c, d provides a list of genes, which exhibited greater than a 1.5-fold difference between GPA and HC, for both rested and TCR activated cells. The list includes a number of genes involved in antimicrobial function that are expressed at higher levels in both rested and activated naive CD4+ T cells from GPA patients compared to healthy controls (Figure 4.5 c and d). This result agrees with a previously published study, in which microarray analysis was performed on total CD4+ T cells (including naïve, effector, memory and regulatory cells), comparing gene expression between GPA and HC (Kerstein *et al.*, 2017). In the current study, it was noted in the PCA analysis that samples from two out of seven GPA patients (GPA group 2) clustered differently to the other GPA samples (GPA group 1) – notably expression levels of antimicrobial genes were similar to HC (Figure 4.5b). To understand the differences in gene profiles between these two GPA groups and how these differences affected the 'all GPA' group analysis, differently expressed genes were identified by ANOVA. The majority of gene expression differences observed in both GPA group1 and group2 compared to HC were similar to the 'all GPA' group in both rested and activated states (Figure 4.5 c and d).

In general, genes differentially expressed between GPA and HC include: metabolism related genes such as TALDO1, CHUK and PTEN in rested cells (Figure 4.5c), TALDO1, GOT1 and SLC2A1 (GLUT1) in activated cells (Figure 4.5d), and adhesion molecules such as ITGAM and CD99L2 in rested cells (Figure 4.5c), ITGB7

in activated cells (Figure 4.5d). Interestingly, the most differently expressed genes between GPA group1 and GPA group2 were antimicrobial genes such as DEFA1, MPO, CAMP and CTSG (Figure 4.5 c and d). Genes related to T cell and/or Treg cell signalling and function such as CD28, PTEN, PTPN11, S1PR5 and TIM3 were also differentially expressed within these two groups in rested GPA naive CD4+ T cells (Figure 4.5c and d).

Most intriguingly, there were several STAT5 target genes dysregulated in both rested and activated GPA naive CD4+ T cells (Figure 4.5 c and d). The STAT5 target genes used for comparison here were taken from a previously published study (Kanai *et al.*, 2014), and seem to be predominantly down-regulated in GPA compared to HC. In rested GPA naive CD4+ T cells, expression of a key component of STAT5 signal induction, IL-2Rβ gene was lower than in HC cells (Figure 4.5c). Consistent with decreased IL2R/STAT5 activity, BCL6, a known STAT5-repressed gene, was upregulated in TCR activated naive CD4+ T cells from GPA patients (Figure 4.5d) (Choi *et al.*, 2013; Read *et al.*, 2016). Additionally, unpublished data from our lab has shown that the E3-ubiquitin ligase, Peli2 expression is also directly repressed by STAT5 binding to this locus (Peli2 expression: B Afzali, S Kim and S John unpublished data). CSF2 (encoding cytokine GM-CSF) had lower expression in activated GPA naive CD4+ T cells compared to HC (Figure 4.5d) has been shown to be positively regulated by STAT5 in CD4+ T cells (Sheng *et al.*, 2014).

In TCR stimulated naive CD4+ T cells, genes involved in TCR activation and differentiation were differentially expressed between GPA and HC samples (Figure 4.5d). Along with BCL6, another Tfh related gene, TRIM8, that enhances STAT3

activation was highly expressed in TCR activated GPA naive CD4+ T cells (Okumura *et al.*, 2010; Weinstein *et al.*, 2014) CD28, a key TCR co-stimulatory receptor and ETS2, a transcription repressor of IL-2 were highly expressed in GPA naive CD4 + T cells (Figure 4.5d)(Nunes *et al.*, 1996; Panagoulias *et al.*, 2016). Th1 differentiation related gene STAT4 was highly expressed, while Eomes and DNMT3A were down-regulated in GPA naive CD4+ T cells (Figure 4.5d) (Yang *et al.*, 2008; Pham *et al.*, 2013). Taken together, data from the current study suggest IL-2 signalling may be dysregulated in naïve CD4+ T cells in GPA.

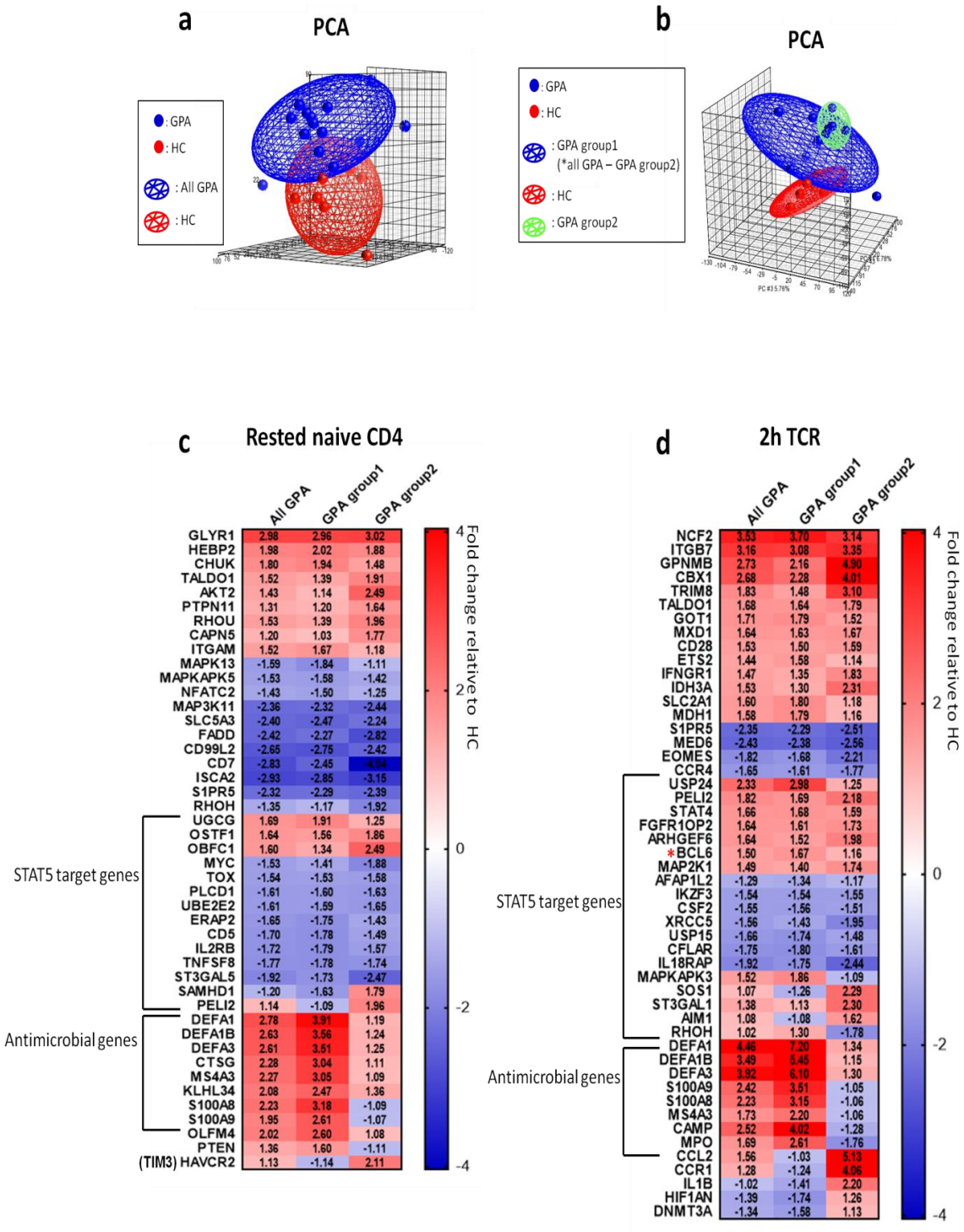

Figure 4.5 Microarray analysis: PCA and differently expressed genes in GPA naive CD4+ T cells. (a and b) PCA between GPA and HC samples. Data of GPA and HC were ellipsoid. **(c and d)** List of differently expressed genes in rested naive CD4+ T cells (c) and 2 hour TCR stimulated naive CD4+ T cells (d) from GPA

patients compare to HC. Fold change greater than 1.5 genes also have P-values lower than 0.05. BCL6 is labelled with a star. Full list of genes in sTable 9.5 and sTable 9.6.

4.2.6. Differently expressed genes in GPA CD4+ T cells: a comparison between naive and total CD4+ T cells.

To understand whether there are commonly dysregulated genes between naive and total CD4+ T cells, the list of differentially expressed genes from naive CD4+ T cells from this study was compared with that from a study using total CD4+ T cells (Kerstein *et al.*, 2017). Kerstein *et al* performed a microarray analysis with CD4+ T cells sorted by FACS (while negative selection by Dynal beads was used in this study). The raw data set was obtained from a public data repository (Gene Expression Omnibus, NCBI, https://www.ncbi.nlm.nih.gov/geo/, accession: GSE56481) and re-analysed by Partek software to gain a full range of gene sets.

Genes differentially expressed from HC (with a greater than 1.5 fold change) in GPA were compared between total CD4+ T cells, rested naïve CD4+ T cells, and TCR activated naïve CD4+ T cells (Figure 4.6).

Antimicrobial genes DEFA1B and DEFA3, and a gene encoding a key enzyme of pentose phosphate pathway, TALDO1, were highly expressed in all rested, activated GPA naïve and total GPA CD4+ T cells. In addition to this, several antimicrobial genes such as MS4A3, OLFM4, DEFA1 and S100P were commonly expressed between groups (Figure 4.6). Among them BCL6 and PELI2 were also high in total GPA CD4+ T cells. Moreover, MYD88, TLRs and CD14 were upregulated in GPA total CD4+ T cells, which Kerstein et al also showed in their study (Kerstein *et al.*, 2017). Also, CCR2 (chemokine receptor), IL-1β (cytokine)

and CCL2 (chemokine ligand) were highly expressed in total CD4+ T cells and they were also shown to be highly expressed in GPA group2 (Figure 4.6 and Figure 4.5d). Interestingly ETS, CCR7 and RNF144A was expressed at lower levels in GPA total CD4+ T cells compared to HC.

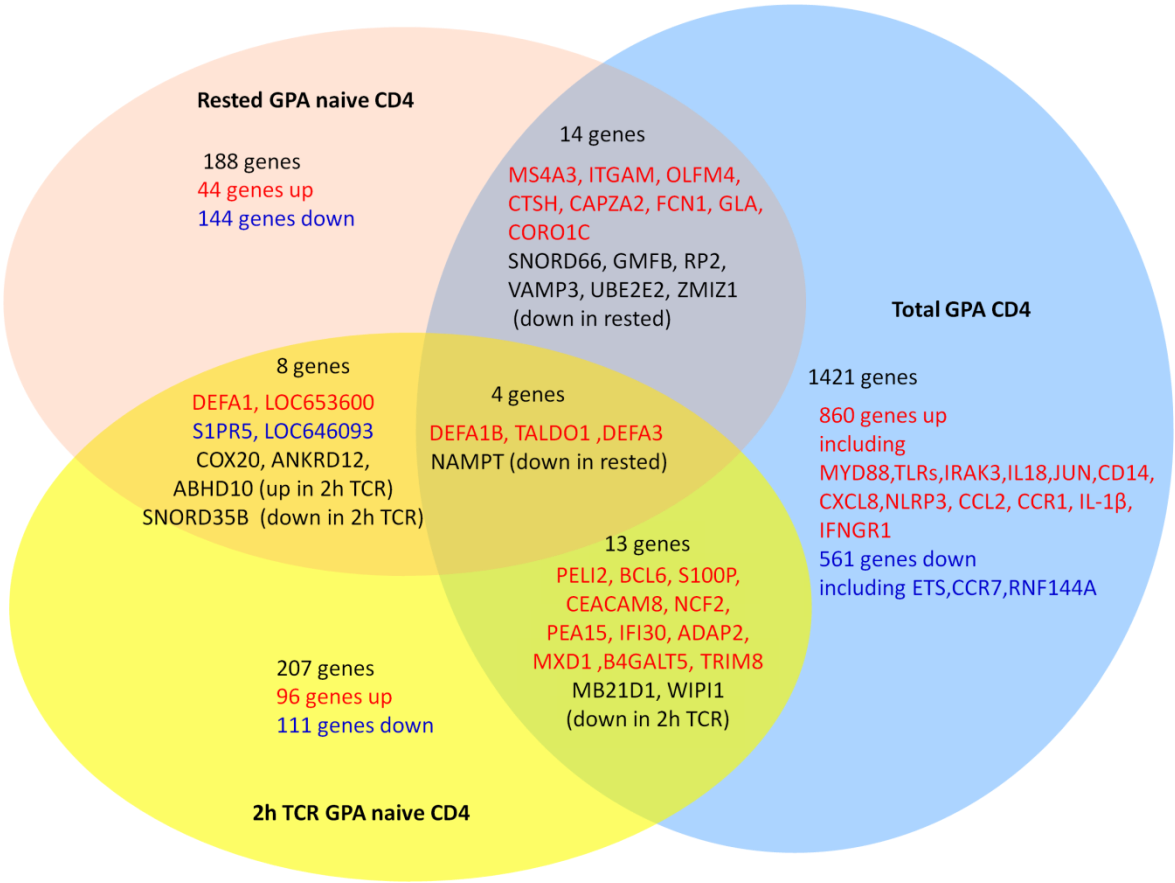

Figure 4.6 Venn diagram of differently expressed gene among rested, 2 hours TCR stimulated naive and total CD4+ T cells from GPA patients. Total number of genes, shared and unique (labelled in black colour) that have more than 1.5 fold change and lower than 0.05 P-value by ANOVA is shown for each of the comparisons between the three groups. Also indicated are the genes that were expressed in a reciprocal manner between groups (labelled in black), and the number of genes are highly increased in expression in GPA (in red) and the number that had lower expression in GPA (in blue) compared to HC.

4.2.7. Dysregulated pathways in GPA naive CD4+ T cells predicted by Ingenuity Pathway Analysis (IPA).

To identify the key molecular pathways and biological activities that may be dysregulated in naive CD4+ T cells in GPA, Ingenuity Pathway Analysis (IPA) on the gene expression array data was performed. As some antimicrobial genes were expressed differently between GPA group1 and GPA group2 (Figure 4.5c and d), these two groups were also analysed separately.

Overall, several key metabolic pathways were predicted to be dysregulated in both rested and TCR activated GPA naive CD4+ T cells. In IPA analysis, pathways are given a 'z-score'; a positive z-score indicating predicted activation of pathway components, a negative z-score indicating inhibition. Although not within the top 10 dysregulated pathways, production of nitric oxide (NO) and reactive oxygen species (ROS) in macrophages was predicted to be dysregulated with a positive Z score in both rested and activated GPA naive CD4+ T cells (Figure 4.7a and b). In rested naive CD4+ T cells, the p38 MAPK and STAT3 pathways were predicted to be dysregulated with negative Z scores in GPA group1 and GPA group2 respectively. The IL-8 signalling pathway was predicted to have a positive Z score in all GPA groupings (Figure 4.7a). In activated naive CD4+ T cells, VDR/RXR activation pathway was predicted to have a positive Z score but Th2 pathway to have a negative Z score in GPA group1 (Figure 4.7b).

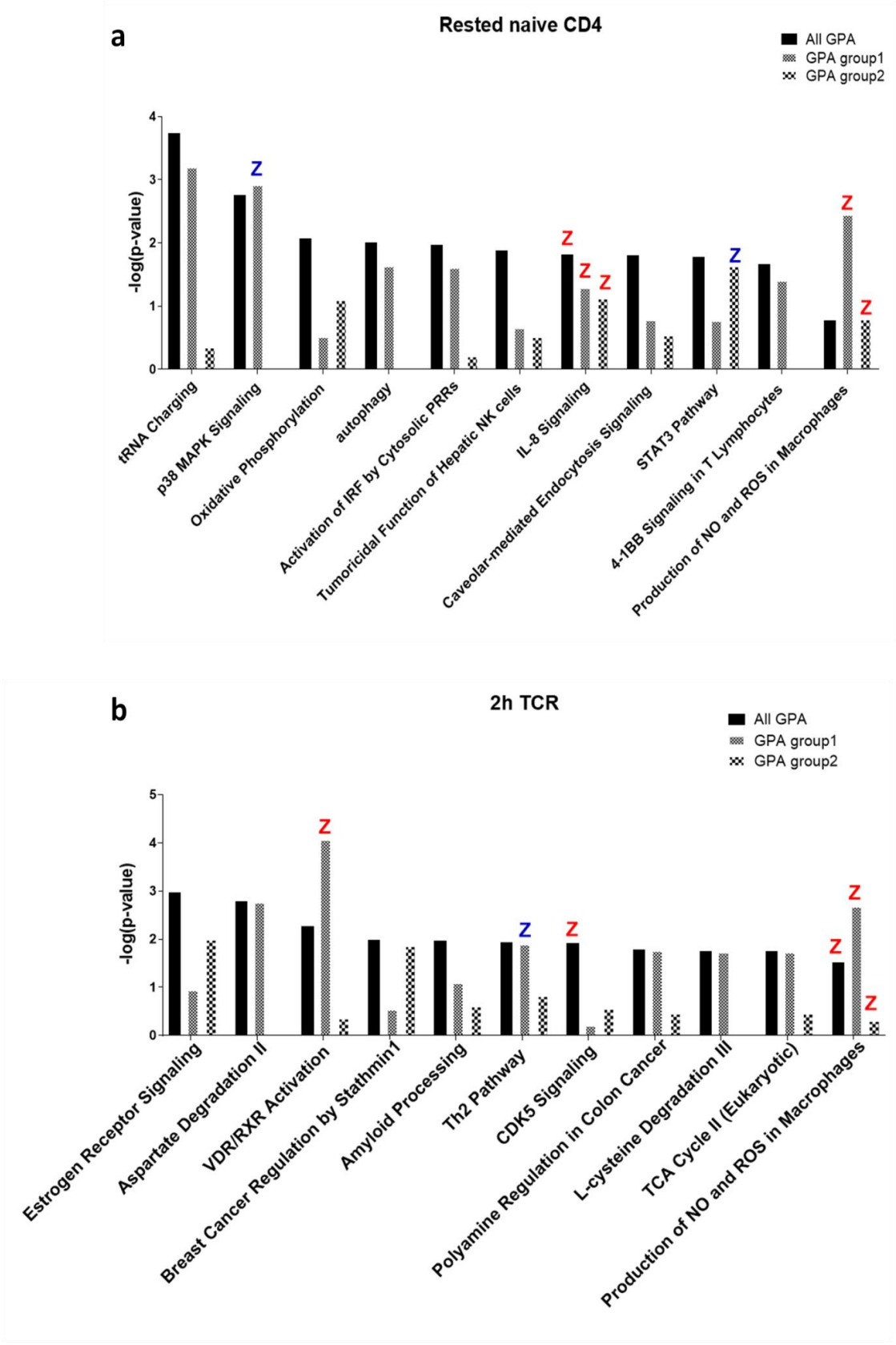

Figure 4.7 Top 10 pathways dysregulated in rested and activated GPA naive CD4+ T cells. Note: Production of NO and ROS in macrophages was not within top 10 pathways in either rested or 2h TCR activated naive CD4+ T cells. Dysregulated

pathways in **(a)** rested and **(b)** 2h TCR activated naive CD4+ T cells. Red coloured 'Z' represents positive Z score and blue coloured 'Z' represents negative Z score.

4.2.8. Upstream regulators in TCR activated GPA naive CD4+ T cells predicted by IPA.

To identify whether there are transcription factors or cytokines, which may explain the observed gene expression changes in GPA naive CD4+ T cells, upstream regulator analysis was performed.

As several antimicrobial genes were up regulated in GPA naive CD4+ T cells, microbial molecule lipopolysaccharide (LPS) was predicted with a positive (activated) Z score. This also agrees with previous bioinformatic analysis in total CD4+ T cells from GPA patients (Kerstein *et al.*, 2017). Notably, IL-2 was predicted to be inhibited with a negative Z score, while CD3, IRF4, IL-6 and IL-21 were predicted to be activated with positive z scores (Table 4.1)

Upstream Regulator	Activation z-score	p-value of overlap	Target molecules in dataset
lipopolysaccharide	0.756	5.88E-04	ANGPTL4,APP,ARHGEF3,BCL6,CCR4,CEACAM8,CFLAR,CSF2,EEF2,FOSB,FTH1,HLA-DQA1, IL18RAP,ITGB7,LYZ,MB21D1,MDH1,MED1,MXD1,NAMPT,NCF2,P4HB,REXO1,RFX7,RHOB, SLC30A1,STAT4,TALDO1,TRIM25
IRF4	0.447	2.25E-03	BCL6,CFLAR,CSF2,IL18RAP,MAPRE1,RHOB
IL12 (family)	-0.298	3.10E-03	BCL6,CFLAR,CSF2,IL18RAP,STAT4
IFNG	0.689	3.36E-03	ANGPTL4,APP,CFLAR,CSF2,FOSB,FTH1,GUSB,HLA-DQA1,IFI30,IL18RAP, KARS,MAP2K1,MB21D1,MED1,METAP2,NAMPT,NCF2,NUP98,PEA15,RHOB,STAT4,TRIM8
IL2	-1.271	5.55E-03	BCL6,CCR4,CFLAR,CSF2,EOMES,IL18RAP,ITGB7,MAP2K1,PEA15,RHOB,SLC30A1,STAT4
CD3	0.226	6.09E-03	BCL6,CCR4,CFLAR,CSF2,DEFA1 (includes others), EOMES,ITGB7,NAMPT,P4HB,RNF103,SF1,TAF15,TRIM25
IL6	2.491	1.35E-02	APP,BCL6,CCR4,CFLAR,CSF2,EOMES,HLA-DQA1,LYZ,MAP2K1,NAMPT,NCF2,STAT4,XRCC5
IL21	0.223	2.15E-02	BCL6,CSF2,EOMES,IL18RAP,STAT4

Table 4.1 Predicted upstream regulators in 2 hours TCR activated naive CD4+ T cells from GPA patients.

4.2.9. Validation of gene expression data from the microarray by qRT-PCR.

The microarray data suggested that genes involved in antimicrobial and STAT5 signalling pathways are dysregulated in GPA naive CD4+ T cells. As STAT5 signalling is a critical negative regulator of Tfh lineage differentiation, expression of STAT5 and STAT5-associated genes that were dysregulated in GPA were validated by qRT-PCR with three GPA patient and three HC samples that were used for microarray analysis.

Despite not being identified as differentially expressed in the microarray data, the mean relative gene expression (2-ΔCt) of both STAT5A and STAT5B were lower in GPA than HC although more data will be required to test the statistical significance of this observation. There was a trend towards lower IL-2Rβ mRNA levels and higher CSTG (Cathepsin G, a known post-translational regulator of STAT5 (Schuster *et al.*, 2007) mRNA levels in GPA rested naive CD4+ T cells compared to HC. In TCR activated naive CD4+ T cells, there was a trend toward higher PELI2

and PTEN mRNA expression in GPA. Due to the low number of samples tested (n=3), statistical analysis was of insufficient power to attribute significance to these findings, and future studies need to evaluate more samples. However, the observed trends were in agreement with the microarray data described above.

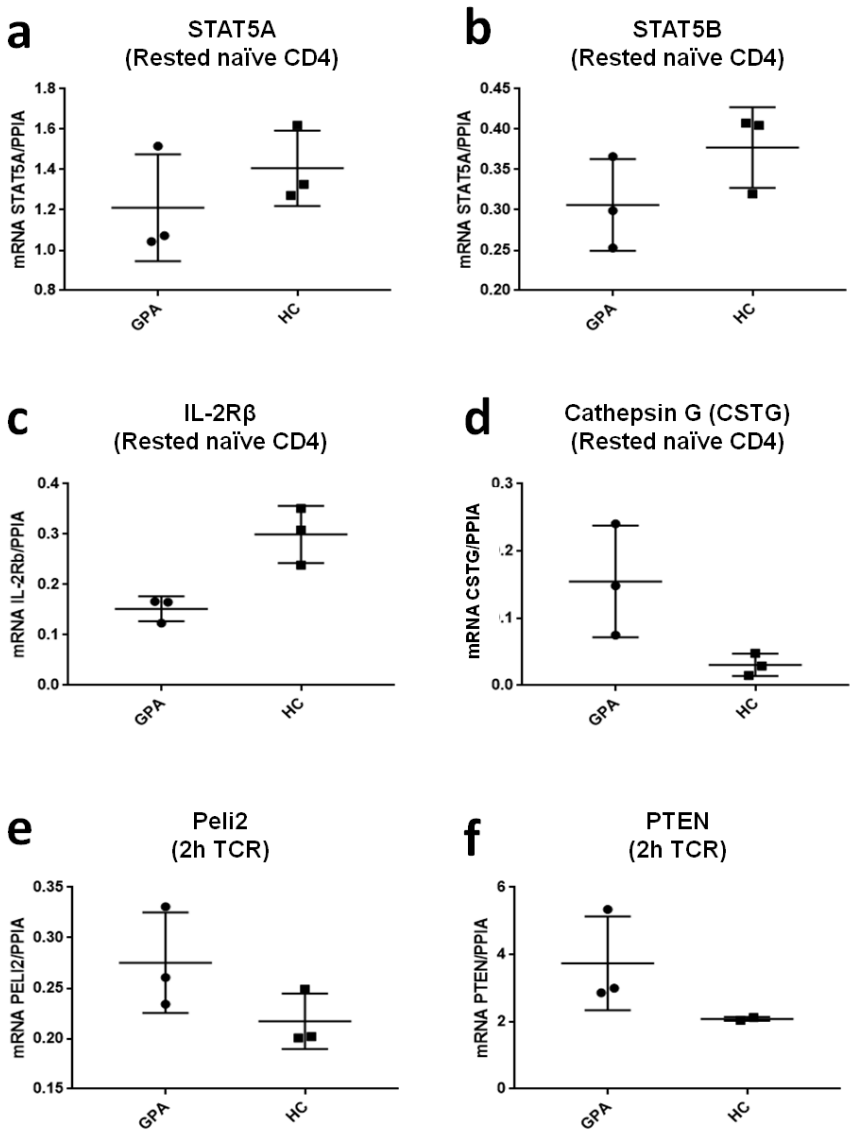

Figure 4.8 Levels of mRNA expression of genes differentially expressed in microarray data in naive CD4+ T cells from GPA patients and healthy controls. RNA samples from naive CD4+ T cells from GPA patients (n=3) and

healthy controls (n=3) that were used in the microarray analysis described in Figure 4.5 was isolated for qRT-PCR. Relative mRNA expression of **(a)** STAT5A **(b)** STAT5B **(c)** IL-2Rβ **(d)** Cathepsin G **(e)** PELI2 and **(f)** PTEN compared to a housekeeping control gene (PPIA) was measured by qRT-PCR. Data show mean relative gene expression (2-ΔCt) of n=3.

4.2.10. STAT5 and STAT3 activation and protein expression after IL-2 stimulation in total CD4+ T cells.

Thus far, the microarray data suggested that the STAT5 signalling pathway is down-regulated in GPA naive CD4+ T cells and this may contribute to the increase in Tfh-like cell phenotypes observed in GPA (Chapter 3). However, transcriptional dysregulation does not always result in changes to the rate of translation, protein production, or protein activity. Moreover, there was no obvious difference in mRNA levels of STAT5A and STAT5b expression in naive CD4+ T cells between GPA and HC. Therefore, the predicted down-regulation of the STAT5 signalling pathway in GPA naive CD4+ T cells may be the result of an inhibition of STAT5 activation.

Earlier, a published study showed increased expression of phospho-STAT5 (p-STAT5) and phospho-STAT3 (p-STAT3) after IL-2 and IL-10 activation in CD3+ T cells from AAV patient's PBMCs (Wilde *et al.*, 2014b). Since there are no data on STAT5 and STAT3 acitvation and expression levels in CD4+ T cell from GPA patients, the expression and phosphorylation state of these two proteins in isolated total CD4+ cells was assessed in GPA and HC by western blotting.

IL-2 stimulation of CD4+ T cells increased p-STAT5 and p-STAT3 levels in total CD4+ T cells from both GPA patients and HC. However there was no difference in levels of p-STAT5 and p-STAT3 compared to total STAT5A, STAT5B and STAT3 protein levels between GPA and HC (Figure 4.9 b,d and g). Moreover, the level of total STAT5A, STAT5B and STAT3 proteins was similar in both GPA and HC (Figure 4.9 c,e and h).

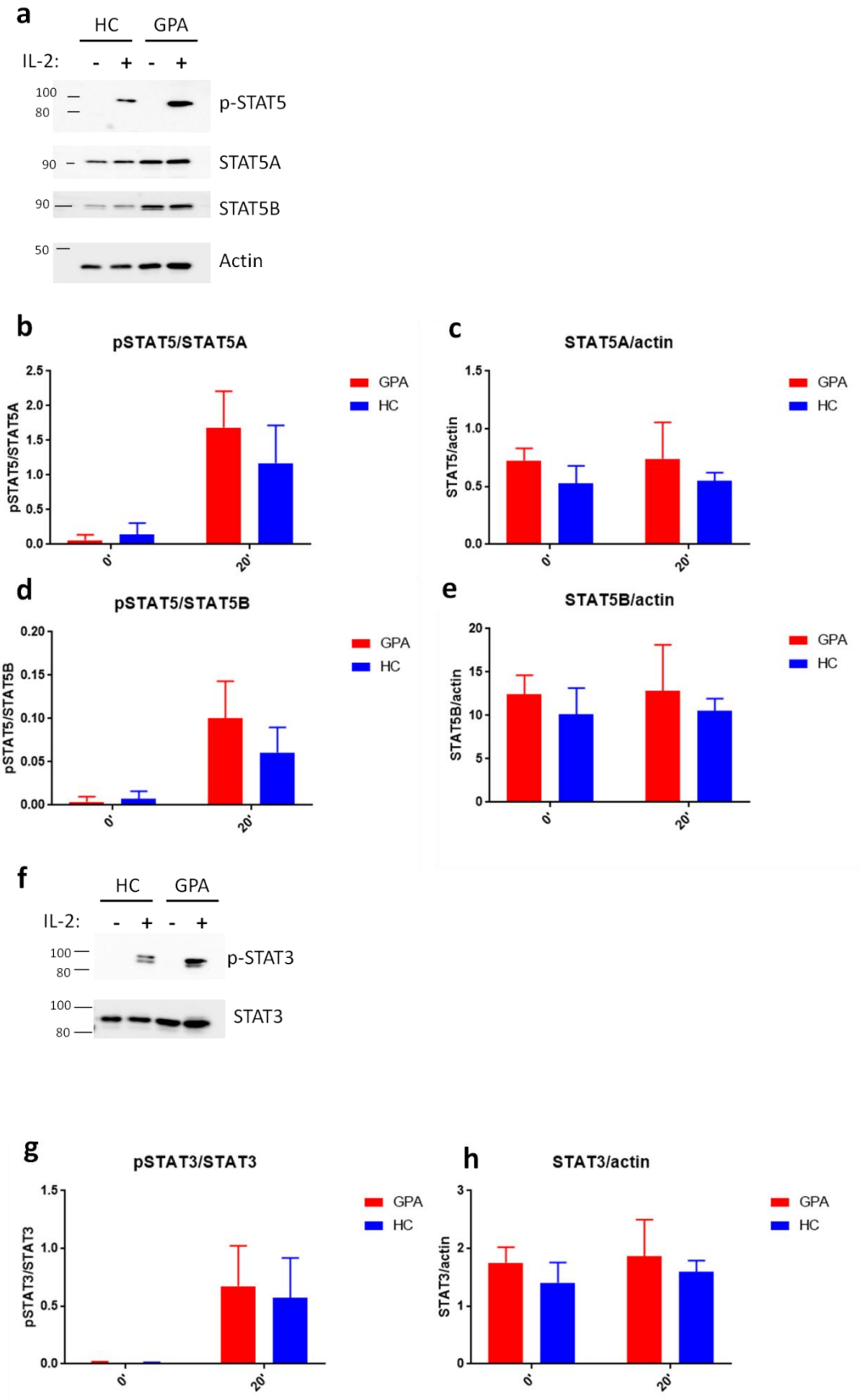
a
HC
GPA
IL-2:
- + - +
100
80
p-STAT5
90
STAT5A
90
STAT5B
50
Actin
b
pSTAT5/STAT5A
pSTAT5/STAT5A
GPA
HC
0'
20'
c
STAT5A/actin
STAT5/actin
GPA
HC
d
pSTAT5/STAT5B
pSTAT5/STAT5B
GPA
HC
e
STAT5B/actin
STAT5B/actin
GPA
HC
f
HC
GPA
IL-2:
- + - +
p-STAT3
STAT3
g
pSTAT3/STAT3
pSTAT3/STAT3
GPA
HC
h
STAT3/actin
STAT3/actin
GPA
HC

Figure 4.9 STAT5 and STAT3 activation and expressions in total CD4+ T cell. CD4+ T cells from GPA patients and healthy donors were isloated using Dynabeads then rested overnight. Lysates from rested CD4+ T cells (0') and CD4+ T cells stimulated with 100IU/ml of IL-2 for 20 minutes (20') were immunoblotted with anti-phospho-tryosine STAT5 (p-STAT5)/STAT3 (p-STAT3) (for measuring activated forms), and anti-STAT5A/B and anti-STAT3 (for measuring total protein expression) antibodies. Actin was blotted as a loading control. **(a)** Western blot of p-STAT5, STAT5A, STAT5B and actin in whole cell extracts of total CD4+ T cells from GPA and HC with or without IL-2 stimulation. Data shown is one representive example from n=5 of GPA and n=3 of HC. **(b-e)** Quantification of western blot **(b)** p-STAT5 level normalised to STAT5A **(c)** STAT5A expression level normalised to actin **(d)** p-STAT5 level normalised to STAT5B **(e)** STAT5B level normalised to actin. **(f)** Western blot of p-STAT3 and STAT3 in the same samples from (a) **(g-h)** Quantification of western blot **(g)** p-STAT3 level normalised to STAT3 **(h)** STAT3 level normalised to actin. All bar charts show the mean of normalised levels of quantified proteins, comparing GPA and HC samples

4.2.11. STAT5 activation and protein expression in naive CD4+ T cells.

To understand whether the STAT5 signalling pathway is defective specifically in naive CD4+ T cells from GPA patients, p-STAT5 level was measured from isolated naive CD4+ T cells with or without IL-2 stimulation. As naive CD4+ T cells are quiescent and exhibit very low responsiveness to cytokine stimulation until they are activated by TCR stimulation, isolated naive CD4+ T cells were pre-activated for 48 hours with anti-CD3 and anti-CD28 (TCR stimulation) prior to resting overnight in fresh media (without TCR stimulation). To understand the kinetic of

p-STAT5 expression, pre-activated naive CD4+ T cells were incubated with IL-2 for three different time periods; 15, 30 and 60 minutes.

Phosphorylation of STAT5, was induced by IL-2 stimulation in both GPA and HC naive CD4+ T cells (Figure 4.10a). There were no observed differences in the kinetics of pSTAT5 levels between GPA and HC naive CD4+ T cells (Figure 4.10a). The ratio of p-STAT5 compared to STAT5A protein level was similar between GPA and HC naive CD4+ T cells after IL-2 stimulation at all time points (Figure 4.10b). However, the total protein level of STAT5A in GPA naive CD4+ T cells was lower than in HC (Figure 4.10c). Interestingly, when p-STAT5 levels were related to total STAT5B expression, the activation level of p-STAT5B was lower in GPA compared to HC (Figure 4.10d), but the level of total STAT5B expression was similar in both GPA and HC (Figure 4.10e). In sum, the functional activation of STAT5 in GPA naive CD4+ T cells is reduced, either through lower protein levels of STAT5A, or lower phosphorylation of STAT5B. Due to the limited cell numbers in some samples an extended time course was only possible with two samples, and therefore statistical tests were not performed here.

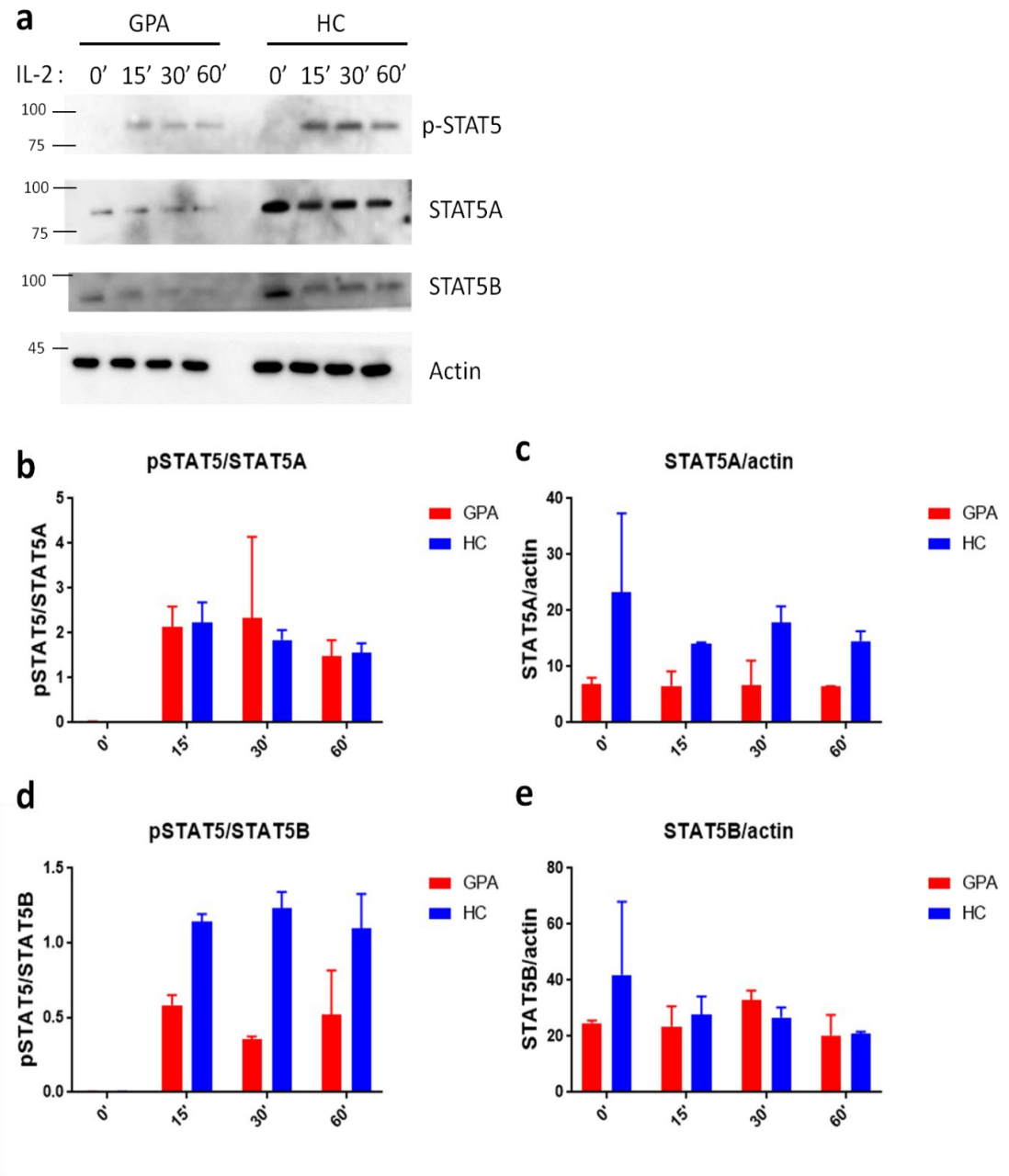

Figure 4.10 STAT5 activation and STAT5A and STAT5B protein expression in naive CD4+ T cells. Isolated naive CD4+ T cells from GPA and HC (isolation by dynal beads) were pre-activated for 48hours with anti-CD3 and anti-CD28. Pre-activated naive CD4+ T cells were washed and rested overnight with no stimulation. Pre-activated and rested naive CD4+ T cells were lysed after cultured with 50IU/ml of IL-2 for 15', 30' or 60', or without any stimulation (0'). Lysates from rested (0') and IL-2 stimulated (15',30' and 60') naive CD4+ T cells were immunoblotted with anti-phosphorylated STAT5 for measuring activated forms,

and anti-STAT5A/B for mearsuring the level of protein expression. Actin was blotted as a loading control. **(a)** Western blot of p-STAT5, STAT5A, STAT5B and actin in whole cell extracts of naive CD4+ T cells from GPA and HC with or without IL-2 stimulation. Data shown is one representive example from n=2 of GPA and n=2 of HC. **(b-e)** Quantification of western blots; **(b)** p-STAT5 level normalised by STAT5A **(c)** STAT5A expression level normalised by actin **(d)** p-STAT5 level normalised by STAT5B **(e)** STAT5B level normalised by actin. All bar charts show the mean of normalised level of quantified proteins bewteen GPA and HC.

4.2.12. STAT3 activation and protein expression in naive CD4+ T cells.

p-STAT3 and total STAT3 expression were also measured from the same samples as in experiment as Figure 4.10. p-STAT3 was also induced by IL-2 stimulation in both GPA and HC naive CD4+ T cells. The level of STAT3 activation and the STAT3 total protein were similar between GPA and HC. Again, due to the limited sample availability, statistical analysis could not be performed.

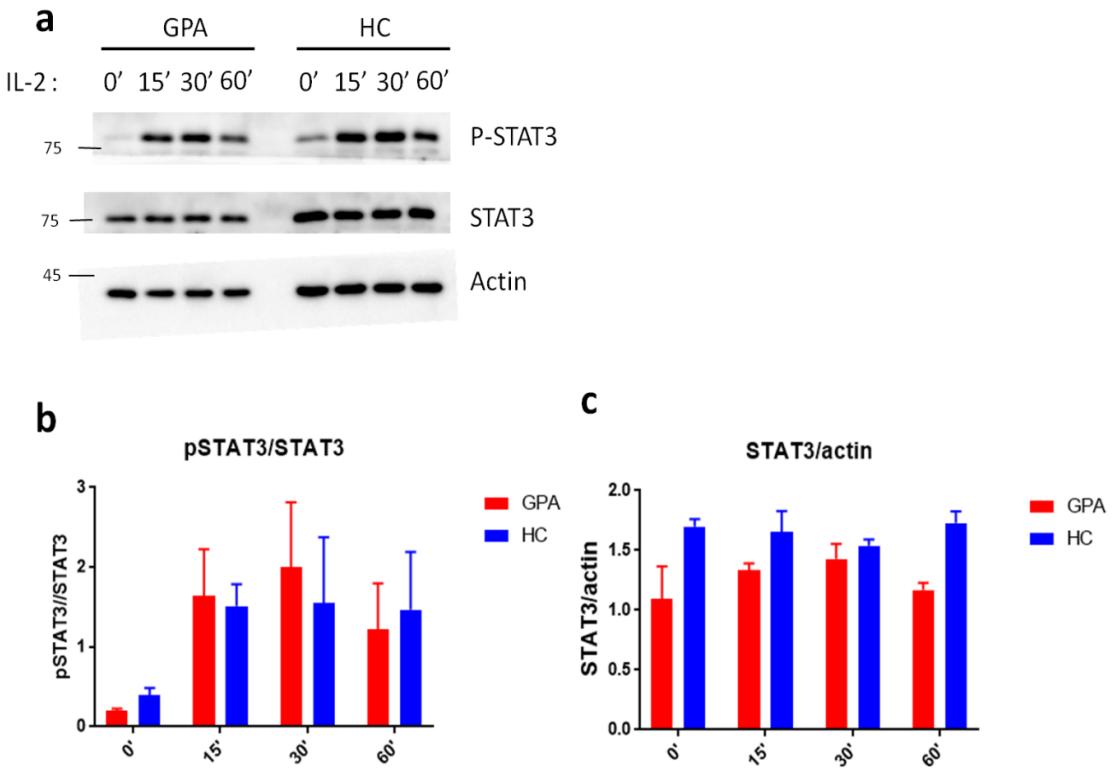

Figure 4.11 STAT3 activation and STAT3 protein expression in naive CD4+ T cells.

A similar experiment to that described in Figure 4.10 was performed to investigate STAT3 expression and activation, rather than STAT5. Lysates from rested (0') and IL-2 stimulated (15',30' and 60') naive CD4+ T cells were immunoblotted with anti-phosphorylated STAT3 for measuring activated forms, and anti-STAT3 for measuring the level of protein expression. Actin was blotted as loading control. **(a)** Western blot of p-STAT3 and STAT3 and actin in whole cell extracts of naive CD4+ T cells from GPA and HC with or without IL-2 stimulation. Data shown is one representive example from n=2 of GPA and n=2 of HC **(b-c)** Quantification of western blot; **(b)** p-STAT3 level normalised to STAT3 **(c)** STAT3 level normalised to actin levels. All bar charts show the mean of normalised level of quantified proteins bewteen GPA and HC.

4.2.13. STAT5 expression after IL-15 stimulation and STAT3 expression after IL-6 stimulation on naive CD4+ T cells.

IL-15 is an another cytokine that activates the STAT5 pathway by utilising the IL-2Rβ chain for its signal induction. As it had been observed that mRNA levels of IL-2Rβ were lower in GPA naive CD4+ T cells, pre-activated naive CD4+ T cells from GPA patients and HC were stimulated with IL-15. Levels of STAT5 activation (p-STAT5) were measured as described above. To measure total STAT5 protein levels, a pan STAT5 antibody was used, which detects both STAT5A and STAT5B proteins. p-STAT5 was not detected after IL-15 stimulation for 20 minutes (Figure 4.12a). One reason for this might be the unique signal induction mechanism for IL-15 called "trans-presentation"(Stonier and Schluns, 2010), where a complex of IL-15 and IL-15Rα is presented in trans to the beta-common (β_c) and gamma-common (γ_c) receptor chains on a T cell . In this study, although IL-15 was used at a high dose (75ng/ml) for stimulation (following a previous study (Cooley *et al.*, 2015)), it may not have been sufficient for STAT5 activation without IL-15Rα. Pan-STAT5 and anti-actin antibodies were used for immunoblotting and the levels of expression of total STAT5 and actin were detected and quantified. Consistent with earlier experiments, lower levels of STAT5 protein expression was observed in naive CD4+ T cell from GPA compared to HC, with the upper STAT5A band of the doublet (representing ~92KDa STAT5A and ~90KDa STAT5B), being clearly decreased in GPA (Figure 4.12 a and b).

Figure 4.11 showed that there are no differences in STAT3 activation and protein expression in naive CD4+ T cells between GPA and HC after IL-2 stimulation.

To investigate whether STAT3 activation or expression in naïve CD4+ T cells is affected by other cyokines, the major STAT3 activating cytokine IL-6 was used to

stimulate pre-activated naive CD4+ T cells from GPA and HC. There was no observed difference in STAT3 activation in naive CD4+ T cells between GPA and HC (Figure 4.12c and d). The total STAT3 level was not available for comparison between GPA and HC since the signal from loading control protein actin in HC samples was too strong for acurate quantification by immunoblotting. Nevetheless, it was clear that p-STAT3 signalling in GPA samples is comparable to HC samples while the total STAT3 levels were lower in GPA (Figure 4.12c).

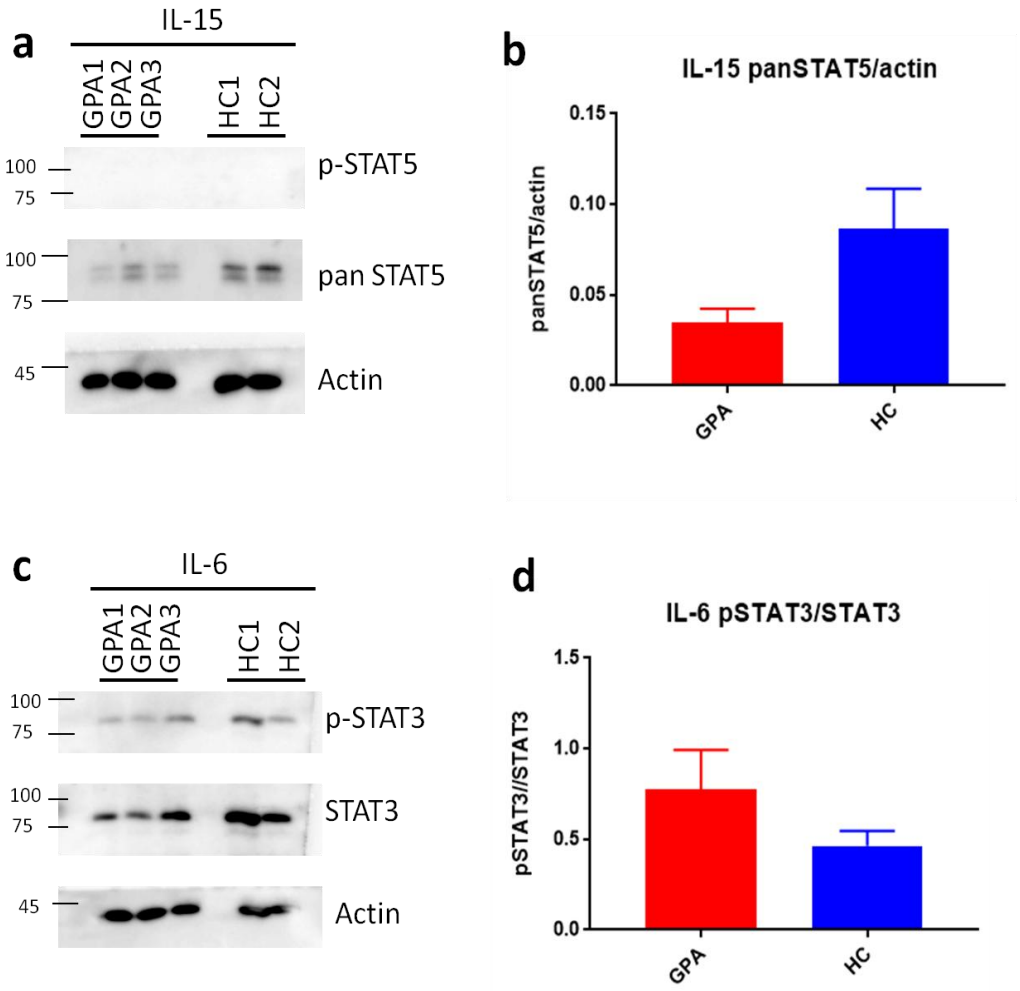

Figure 4.12. STAT5 expression after IL-15 stimulation and STAT3 expression after IL-6 stimulation on naive CD4+ T cells. Pre-activated and rested naive

CD4+ T cells were stimulated with IL-15 (75ng/ml) or IL-6 (10ng/ml) for 20 minutes. **(a)** Western blot of p-STAT5, pan STAT5 (antibody recognises both STAT5A and STAT5B) and actin in whole cell extracts of naive CD4+ T cells from GPA and HC with IL-15 stimulation. **(b)** Quantification of western blot from (a) of pan STAT5 normalised by actin. **(c)** Western blot of p-STAT3, STAT3 and actin in whole cell extracts of naive CD4+ T cells from GPA and HC with IL-6 stimulation. **(d)** Quantification of western blot from (a) of p-STAT3 relative to STAT3 expression. All bar charts show the mean of normalised levels of quantified proteins bewteen GPA and HC.

4.3. Discussion

The aim of this chapter was to understand whether naive CD4+ T cells from GPA patients are in some way 'programmed' to favour differentiation towards a Tfh-like phenotype. If so, what mechanism underlies the predisposition towards Tfh differentiation?

In vitro differentiation data with isolated naive CD4+ T cells did not identify any differences in the frequencies of CXCR5+PD1+CD4+ T cells after either TCR activation alone or Tfh differentiation between GPA and HC. This observation was in agreement with data from the previous chapter (Figure 3.1c). However, while lower PD1 expression was observed in total CD4+ T cells in GPA (Figure 3.1e), during *in vitro* differentiation studies with naïve CD4+ T cells, increased frequencies of CXCR5+PD1+CD4+ T cells were observed under Tfh differentiation conditions for both GPA and HC (Figure 4.1c). Taken together, these observations suggest that although ex-vivo homeostatic PD1 expression on GPA total CD4+ T cells was lower (Chapter 3, fig), GPA naïve CD4+ T cells do not have an impaired intrinsic ability to up-regulate PD1 during *in vitro* stimulation. Indeed, GPA naive CD4+ T cells more strongly increased PD1 expression upon Tfh differentiation compared to TCR stimulation alone (p-value <0.005 (Figure 4.1d). Therefore, it is possible that *in vivo,* physiological differences in extracellular factors in GPA may affect PD1 expression on CD4+ T cells.

Interesingly, GPA naïve CD4+ T cells expressed higher levels of BCL6 upon TCR activation alone compared to HC, suggesting an increased molecular predisposition towards Tfh. Consistently, the trend for higher BCL6 expression was also sustained following Tfh differentiation. The key cytokines for Tfh cell

promotion, maintenance and function are IL-6 and IL-21 (Jogdand *et al.*, 2016). Although there was no statistical difference in IL-21 expression and only a weak significance (p=0.05) in IL-6 expression between GPA and HC, there was a clear trend towards higher expression of both of these key Tfh cytokines in GPA naive CD4+ T cells after five days of in vitro Tfh differentiation.

IL-6 is one of the key cytokines involved in activation of STAT3 and the induction of IL-21 via c-maf, to promote differentiation and maintainance of active Tfh cells (Jogdand *et al.*, 2016). Moreover, a recent study in particular suggests IL-6 is important for sustaining Tfh phenotypes, (Papillion *et al.*, 2018). Taken together, these data suggest that given the propensity of naïve CD4+ T cells in GPA to express higher levels of IL-6 levels during Tfh differentiation, the Tfh-like phenotype may persist for longer in GPA. It is possible that, if the in-vitro Tfh differentiated cells had been cultured for longer than five days, other phenotypic differences between GPA and HC (e.g. IL-21 levels, BCL-6 levels) may have become more significantly evident. Indeed IL-21 mRNA expression was higher in GPA naive CD4+ T cells after Tfh differentiation for six days (Figure 4.4b). Further studies over a longer time period are required to confirm whether IL-21 cytokine production in naive CD4+ T cells differs between GPA and HC.

The significant difference in Bcl6 expression between GPA and HC naïve CD4+ cells with TCR activation alone, was indicative of underlying differences in intrinsic molecular signalling and/or transcriptional responses between these cells and hence the microarray study was undertaken. Global gene expression profiles differed substantially in naive CD4+ T cells between GPA and HC. Among the differentially expressed genes between GPA and HC, antimicrobial genes were

highly expressed in GPA naive CD4+ T cells (Figure 4.5). This result was consistent with the observations from a previous study using isolated total CD4+ T cells (Figure 4.6)(Kerstein *et al.*, 2017), and are in keeping with the observations that bacterial and viral infections are associated with the pathogenesis of ANCA-AAV (Kallenberg and Tadema, 2008; Csernok *et al.*, 2010). While the expression of antimicrobal genes are usually seen in innate immune cells such as granulocytes, they are sometimes known to be expressed in T cells under pathological conditions. The significantly elevated expression of these antimicrobial genes in T cells, may also be suggestive of an insufficient or dysregulated innate immune response to underlying infections. Consistent with this notion, studies with MPO-ANCA AAV patients have shown a significant reduction in TLR-driven signalling pathways in monocytes when cultured with anti-MPO antibodies (Popat *et al.*, 2017). In future studies, it would be interesting to understand if a similar defect in innate immune cell signalling exists in response to anti-PR3 antibodies treatment in GPA patients. However, two GPA patients (catagorised as GPA group2 in Figure 4.5, identified as a separate cluster in the PCA analysis) did not show elevated levels of these antimicrobial genes compared to HC. From the clinical information available on the patients used in the study (including ANCA type, gender, age, medication history) there was no obvious explanation for this difference, and no obvious differences between these patients and the rest of the GPA patient group. One possibility (although we do not have detailed medical records for these patients) is a difference in disease severity and/or phenotype that is currently not distinguished by the clinical criteria available. One other possible explanation for the two types of patient data maybe a technical anomaly. As mentioned earlier, the antimicrobial genes identified in the microarray data are particularly highly expressed in granulocytes. In this study, naive CD4+ T cells were isolated from

PBMCs isolated by density gradient separation methods that tends to separate granulocytes from the PBMC fraction However, it has been shown that there is an increase in low-density granulocytes (which may threfore infiltrate PBMC fractions) in AAV patients and this is associated with disease activity. It is therefore plausible that the increase in antimicrobial genes observed in GPA samples in this study may be due to a low level contamination of with low-density granulocytes (Grayson *et al.*, 2015). However, an argument against this maybe that in the total CD4 T cell microarray study, where the elevated expression of antimicrobial genes were also detected, the cells were isolated by FACS sorting and any contaminating granulocytes would have been excluded (Kerstein *et al.*, 2017). Furthermore, the expression of CTSG in GPA T cells was validated in our studies here (Figure 4.8d). Alternatively, patients from GPA group 2 may have less severe disease progression. However, a lack of information regarding severity of disease (such as BVAS score) limits our ability to interpret these data. Nevertheless, preparations of isolated naive CD4+ T cells should always be evaluated for low density granulocyte contamination in future studies.

While comparing lists of differentially expressed genes between GPA and HC from the microarray, it was noticed that RNF144A expression was lower in total CD4+ T cells (but not in naïve CD4+ T cell preparations). In Figure 3.6, observed mRNA levels of RNF144A were higher in rested GPA CD4+ T cells than HC by qRT-PCR. These contradictary results are likely due to the differences in the methods of CD4+ T cell isolation. The mRNA expression levels of RNF144A become spontaniously down-regulated upon T cell activation [S. Kim and S. John unpublished observations]. As mRNA for microarray analysis was isolated from

CD4+ T cells sorted by FACS (Kerstein *et al.*, 2017), the CD4+ T cells used for mRNA extraction may have been in a non-rested (partially activated) state.

Another interesting finding from the microarray data was that several genes differentially expressed between GPA and HC naive CD4+ T cells were involved in Th cell differentiation. Higher levels of STAT4, and lower levels of DNMT3A (Figure 4.5d) in were obseved in GPA; both of these genes have been shown to be important in Th1 development (Pham *et al.*, 2013). Higher expression of BCL6, TRIM8 and CD28 were also observed in GPA; higher CD28 expression may lead to greater TCR signalling intensity, which has previously been shown to promote Tfh cell differentiation (Figure 4.5d). STAT3 activation is critical in Tfh differentiation, and TRIM8 has been show to interact with protein inhibitor of activated STAT3 (PIAS3) that negatively regulates PIAS3 expression. This interaction results in an increase in activation of STAT3 (Okumura *et al.*, 2010). TRIM8, indeed, was shown to be highly expressed in Tfh cells (Weinstein *et al.*, 2014). Genes involved in STAT5 signalling also appear to be dysregulated in GPA, which may be an additional mechanism through which Tfh differentiation is favoured. Lower expression of IL-2Rβ (Figure 4.5c) and dysregulation of several STAT5 target genes (Figure 4.5 c and d) indicate a less active STAT5 pathway in GPA. Moreover, bioinformatic IPA analysis of predicted upstream regulators anticipated a reduction of IL-2 signalling (Table 4.1).

Based on the predictions of the IPA analysis that IL2 signalling is perturbed, STAT5 expression and activation by IL2 was investigated in GPA naive CD4+ T cells. Interestingly, down-regulation of STAT5 activation was only observed in GPA naive CD4+ T cells but not in total CD4+ T cells. Surprisingly, the decreased STAT5

activation, was not solely due to decreased tyrosine phosphorylation of STAT5A and STAT5B proteins, but also as a result of reduced STAT5A protein levels in naïve GPA CD4 levels. The selective decrease in STAT5A protein levels is not due to transcriptional differences in STAT5A (and STAT5B) mRNA levels, which showed statstically no differences as compared to HC samples. Therefore, it is likely the decreased STAT5A levels, results from a post-translational processing mechanism, but the exact mechanism remains to be delineated in future studies. Of note, previous studies from our laboratory have shown that Cathepsin-G can cleave STAT5 proteins (Schuster *et al.*, 2007), and given the aberrant expression of cathepsin-G in naïve CD4 T cells in GPA, it is possible that this protease can cleave STAT5A here. However, cathepsin-G is not selective for STAT5A versus STAT5B (Schuster et al, 2007) and therefore is unlikley to be involved in the decrease in STAT5A levels observed in GPA naïve CD4+ T cells. Neverthless, the decreased IL2-induced STAT5 signalling would be favourable for Tfh differentiation, and is consistent with other gene expression changes noted in these cells, that are characteristic of Tfh cells, such as increased BCL6 and IL21 expression. In contrast, there was no change in STAT3 activation or STAT3 protein levels in GPA naive CD4+ T cells compared to HC. Thus, naïve CD4+ T cells in GPA appear to be set at a basal state that limits STAT5 activity, while maintaining normal STAT3 activity. The functional implications of this imbalance will be discussed in more detail in Chapter 7.

To conclude, naive CD4+ T cells from GPA patients exhibit a significantly different profile of gene expression compared to HC, and show reduced STAT5 pathway activation. These observations may point to an underlying mechanism promoting increased Tfh-like phenotypes in GPA.

5. Chapter 5: Investigation of Treg phenotype and function in GPA

5.1. Introduction

In Chapter 3, the frequencies of Tregs in peripheral blood as assessed by flow cytometry (either $CD25^{high}CD127^{low}$ or $CD25^{high}$Foxp3+) were comparable between GPA and HC (Figure 3.1b). However, the ability of GPA Tregs to suppress effector T cell activation and proliferation has not been addressed. In the healthy condition, Tregs can be classified into different subsets based on phenotypic markers but $CD25^{high}$ $CD127^{low}$ and Foxp3+ CD4+ T cells are widely accepted as Tregs. Moreover, although the most activated Tregs are memory cells, naive Tregs have also been shown to have suppressive function *in vitro* (Safinia *et al.*, 2015; Wing *et al.*, 2019).

In autoimmune disease, the frequency of Tregs reported in studies depends upon the phenotypic markers used, and studies do not always assess the suppressive function of these cells (Abdulahad *et al.*, 2007; Grant *et al.*, 2015; Wing *et al.*, 2019). Therefore, a focus of this chapter will be to assess the suppressive function of Tregs in GPA to understand the potential role these cell subsets may play in the development of GPA pathogenesis.

An increase in the frequency of naive CD4+ CD25+ (CD45RA+CD25+ within Teff) T cells was observed in GPA patients (Figure 3.2e). The contribution of this cell subset to development of disease in GPA is not yet understood. Although it was

observed that naive CD4+ T cells from GPA have a modified IL-2/STAT5 pathway that leads them to adopt a Tfh-like phenotype (Chaper 4), it is still possible that these naive CD25+CD4+ T cells may also possess suppressive function.

Recently, follicular regulatory T cells (Tfrs) have been newly identified and these cells express both Treg and Tfh phenotypic markers such as CXCR5 and PD1. Tfrs also have both memory and naïve phenotypic characteristics and can be found in peripheral blood (cTfrs) (Wing *et al.*, 2019). However, the levels of expression of these phenotypic markers on Tfr/cTfr differ from conventional Tregs. It has been reported that Tfrs have down-regulated CD25 expression compared to Tregs in both humans and mice (Ritvo *et al.*, 2017). Moreover, deficiency of PD1 in Tfrs leads to reduction of CD25 expression but enhances their suppressive function in mice (Sage *et al.*, 2013). In Chapter 3, lower expression of PD1 in total GPA CD4+ T cells (including Tregs and T effectors) was observed in GPA (Figure 3.1e), perhaps implying that these naive CD25+CD4+ T cells may be Tfr cells that are expressing lower CD25 levels than conventional Tregs.

This chapter will investigate the function of Tregs ($CD25^{high}CD127^{low}$) in GPA patients. It will also aim to address whether naive CD25+CD4+ T cells (of which there are higher frequencies in GPA) are Tfrs, which exhibit altered phenotypic marker expression but retain their suppressive function in GPA and HC.

5.2. Results

5.2.1. Expression of Foxp3, PD1 and CXCR5 on Tregs and naive CD25+ CD4+ T cells in GPA.

Transcription factor, Foxp3 is a critical phenotypic marker for Treg cells, and expression of Foxp3 tends to correlate with suppressive function (Wing *et al.*, 2019). To investigate Foxp3 expression in Treg (CD25highCD127low) and naive CD25+CD4+ (CD45RA+CD25+ within Teff as defined in Chapter 3) T cells, percentages of Foxp3 expressing cells within each subset were measured by flow cytometry.

There were no differences in the frequencies of Foxp3+ Tregs (Figure 5.1a) or Foxp3+ naive CD25+CD4+ T cells (Figure 5.1d) between GPA and HC. However, while the mean percentage of Foxp3+ cells within the Treg (CD25highCD127low) subset was over 70% in both GPA and HC, the mean frequency of Foxp3+ cells with naive CD25+CD4+ T cell subset was only approximately 2% in both GPA and HC. This finding indicates that these naïve CD25+CD4+T cells may not have or have lower suppressive function.

To investigate Tfr phenotypic marker expression, frequencies of PD1 and CXCR5 were also measured in Tregs and naive CD25+CD4+ T cells. There were no differences in the frequency of PD1+ and CXCR5+ cells within the Treg subset between GPA and HC (Figure 5.1b and c). Strikingly, there was a significant decrease in PD1 expression on naive CD25+CD4+ T cells from GPA patients compared to HC (Figure 5.1e) but no difference in CXCR5 expression (Figure 5.1f).

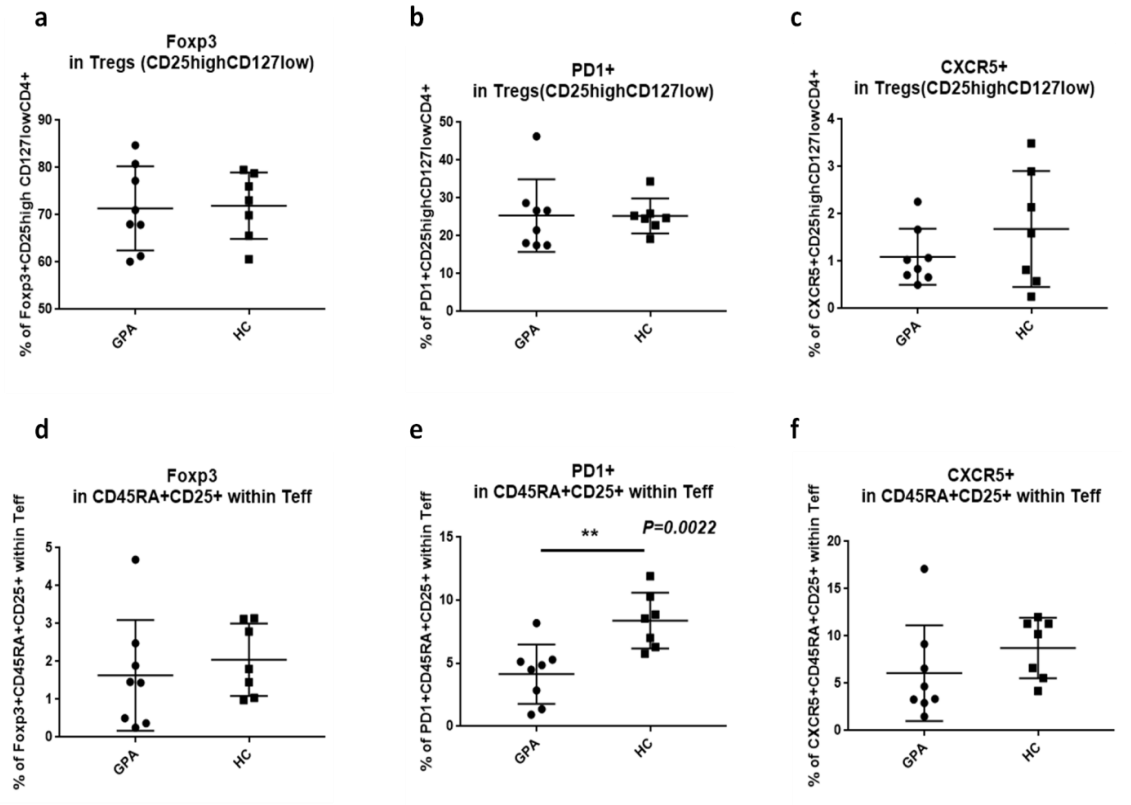

Figure 5.1 Foxp3, PD1 and CXCR5 expression in Tregs and naive CD25+CD4+ T cells. Tregs and naive CD25+CD4+ T cells were classified as described in Figure 3.1b bottom row, and Figure 3.2c respectively. Frequencies of **(a)** Foxp3+, **(b)** PD1+ and **(c)** CXCR5+ Tregs in GPA and HC are shown. Frequencies of **(d)** Foxp3+, **(e)** PD1+ and **(f)** CXCR5+ CD45RA+CD25+ T cells in GPA and HC are shown. Data show mean frequencies of cell subsets, and statistical analysis performed by Mann Whitney test. GPA n=8, HC n=7.

5.2.2. *In vitro* T cell suppression assay using Cell Trace Violet dye dilution.

To test the suppression function of Tregs and naive CD25+CD4+ T cells from GPA patients, an *in vitro* suppression assay was performed by measuring dilution of a dye, Cell Trace Violet (CTV), upon T cell proliferation. To perform this experiment, three T cells subsets were isolated by FACS; activated Treg (CD25+++CD45RA-

within Tregs), naive CD25+CD4+ T cells (CD45RA+CD25+ within Teff) and T responders (Tresp: CD25- within Teff) (Figure 5.2a, b, c). Activated Tregs have been shown to exhibit the strongest suppressive function among Treg subsets (Safinia *et al.*, 2015; Wing *et al.*, 2019). The initial design for this experiment included two Treg subsets; activated Tregs and naive Tregs (CD25++CD45RA+ within Tregs). However, due to limited cell numbers of the naïve CD4+CD25+ population, only activated Tregs were isolated in sufficient numbers to perform the assay.

During the experiment, Tresp cells were labelled with CTV prior to culture with activated Tregs or naive CD25+CD4+ T cells and the level of proliferation of Tresp cells was measured by dye dilution using flow cytometry. The experiment scheme is shown in Figure 5.2a, b and c. The gating strategy for assessing Tresp proliferation by CTV dilution is shown in Figure 5.2d. Overall, as expected, culture of Tresp cells with activated Tregs from either GPA and HC reduced proliferation of Tresp cells, therefore demonstrating that these activated Tregs exhibit a suppressive function (Figure 5.2d). To assess whether there were differences in the rate of cell proliferation in this assay between GPA and HC, frequencies of cells in each of the proliferative peaks shown in Figure 5.2d were calculated using FlowJo software (sFigure 9.9). This analysis showed that there was no difference in the rate of cell proliferation in this assay between GPA and HC.

However, there was variability in the assay and difficulties with reproducibility associated with the requirement for large cell numbers together with the limited availability of PBMCs from GPA patient samples. An alternative assay to measure suppression of T cell function was therefore required.

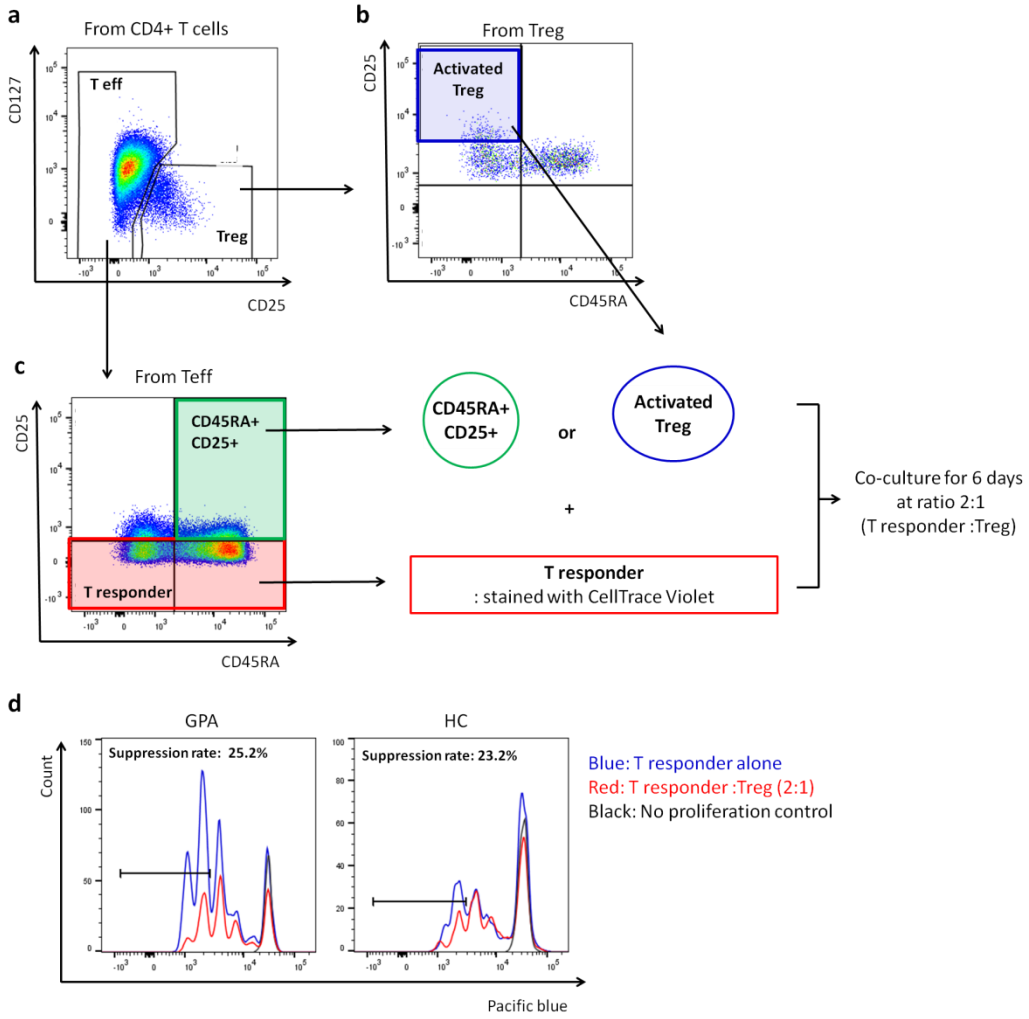

Figure 5.2 Treg and naive CD25+CD4+ cells suppression functional assay by flow cytometry assay. Cryopreserved PBMCs from GPA and HC were stained using a panel of fluorescent conjugated antibodies for cell sorting by FACS. **(a)** Tregs and Teff were gated from CD4+ T cells following the same gating strategy described in Figure 3.1a. **(b)** Activated Tregs were gated based on CD45RA and CD25 expression. Activated Tregs were defined as CD25+++CD45RA- Tregs (highlighted in blue). **(c)** T responders (Tresp) and naive CD25+CD4+ T cells (labelled as CD45RA+CD25+) were gated from the Teff subset based on CD45RA and CD25 expression. Tresp are CD25- Teff (highlighted in red) and CD45RA+CD25+ T cells are highlighted in green. Sorted Tresp were labelled with

CTV dye prior cell culture. Tresp (2,000 cells per reaction) were co-cultured with Tregs or CD45RA+CD25+ T cells at a ratio of 2:1 Tresp:Treg for 6 days with anti-CD3 and anti-CD28. **(d)** Histogram showing CTV dilution by flow cytometry. The two most diluted CTV peaks (demonstrating proliferation of Tresp cells) from GPA and HC after 6 days co-culture were gated to represent the frequency of proliferated cells.

5.2.3. Analysis of Treg ($CD25^{high}CD127^{low}$) function: *in vitro* micro-suppression assay using ^{3}H-thymidine incorporation.

To overcome the limitation regarding cell numbers, a micro-suppression assay using ^{3}H-thymidine incorporation was designed. In this assay, 500 Tresp cells were required per reaction, compared to 2000 in the previous assay. Also, in this experiment, Treg cells and Tresp cells were gated differently (Figure 5.3a and Figure 5.3b respectively). The experiment scheme is shown in Figure 5.3. Tresp cells and Tregs cells were sorted (according to the indicated ratios) directly into 96-well plates with media instead of bulk cell sorting.

First, to test the assay, autologous Treg and Tresp cells from the same donor were isolated and co-cultured (Figure 5.3 c-d). As expected, upon increasing the ratio of Tresp to Treg (reducing the number of Tregs in the assay), the level of suppression of Tresp proliferation was reduced. This phenomenon was observed using cells from both GPA patients and HC (Figure 5.3c and Figure 5.3d respectively). There were no apparent differences in the rate of Treg mediated suppression between GPA and HC.

To test whether Treg populations from one donor can suppress proliferation of Tresp from a different donor in a cross co-culture assay. Tregs and Tresp from different donors were co-cultured at various ratios, in a cross co-culture assay as in Fig 5.3e-f. Data from this cross co-culture study showed that the suppression rate of Tregs from GPA patients on Tresp from HC was comparable that of HC Tregs on Tresp from GPA patients (Figure 5.3e and f). Thus, taken together these results indicate that GPA Tregs and Tresp have no defect in the process of immunoregulation of cell proliferation.

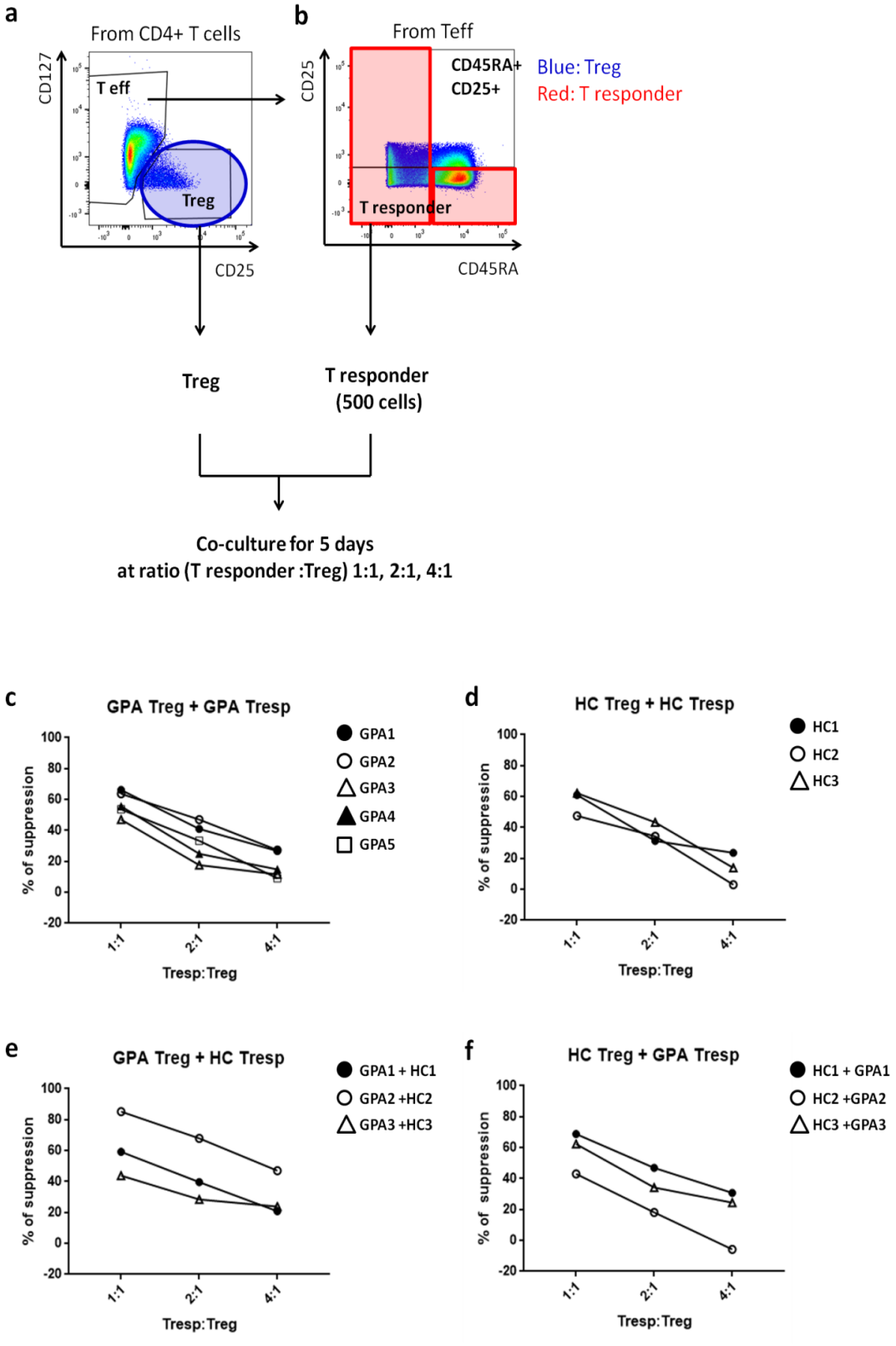

Figure 5.3 Treg micro-suppression assay. Cryopreserved PBMCs from GPA and HC were stained by panel of fluorescent conjugated antibodies for cell sorting by FACS. **(a)** Tregs and Teff were gated from CD4+ T cells by following the same

gating strategy described in Figure 3.1a. Tregs are highlighted in blue. **(b)** T responders were gated from Teff based on CD45RA and CD25 expression. Here Tresp constitute the remainder of the Teff population excluding CD45RA+CD25+ cells (highlighted in red). Sorted Tresp cells (500 cells per reaction) and Tregs were co-cultured at ratio 1:1, 2:1 and 4:1 (Tresp:Treg) for 5 days with anti-CD3 and anti-CD28. For 18h prior to harvesting, cells were pulsed with radioactive ^{3}H-thymidine. Percentage suppression (relative to proliferation of 500 Tresp cells alone) was calculated as described in methods. Suppression rate of **(c)** GPA Tregs on Tresp from same GPA patient n=5, **(d)** HC Tregs on Tresp from same HC n=3, **(e)** GPA Tregs on Tresp from HC n=3 and **(f)** HC Tregs on Tresp from GPA patient n=3.

5.2.4. Analysis of naive CD25+CD4+ T cell function: in-vitro micro-suppression assay using ^{3}H-thymidine incorporation.

To investigate the suppression function of the naive CD25+CD4+ T cell subset, a similar experiment to the one described in Figure 5.3 was performed. The experiment was repeated with three sets of donors; in the first experiment the highest ratio of Tresp:CD45RA+CD25+ cells was 1:1 but since the observed level of suppression was lower than for Tregs, an additional ratio of 0.5:1 was included for the subsequent two repeats to ensure that any suppression at higher ratios of naïve CD25+CD4+ T cells are also detected.

To test the assay, autologous naive CD25+CD4+ T cells and Tresp from the same donor were isolated and co-cultured (Figure 5.4 c-d). However, suppression of T cell proliferation upon co-culture with naive CD25+CD4+ T cells was only observed in one out of three GPA patient samples (GPA2) and none of the healthy controls.

Interestingly, in a cross co-culture assay, suppression of healthy Tresp proliferation was observed upon co-culture with naive CD25+CD4+ T cells from GPA patients when higher numbers of naive CD25+CD4+ T cells were included in the assay (ratios 0.5:1 and 1:1). In contrast, negligible or no suppression activity was observed when HC naive CD25+CD4+ T cells were co-cultured with Tresp from GPA patients at all cell ratios tested (Figure 5.4e and f). Thus, GPA naïve CD25+CD4+ T cells are capable of suppression of proliferation, albeit only at the higher cell ratios as compared to conventional Tregs (Figure 5.3 c and e vs. Figure 5.4 c and e). However, further GPA samples need to be evaluated in order to firmly conclude about the suppressive role of the naïve CD4+CD25+ cell subset.

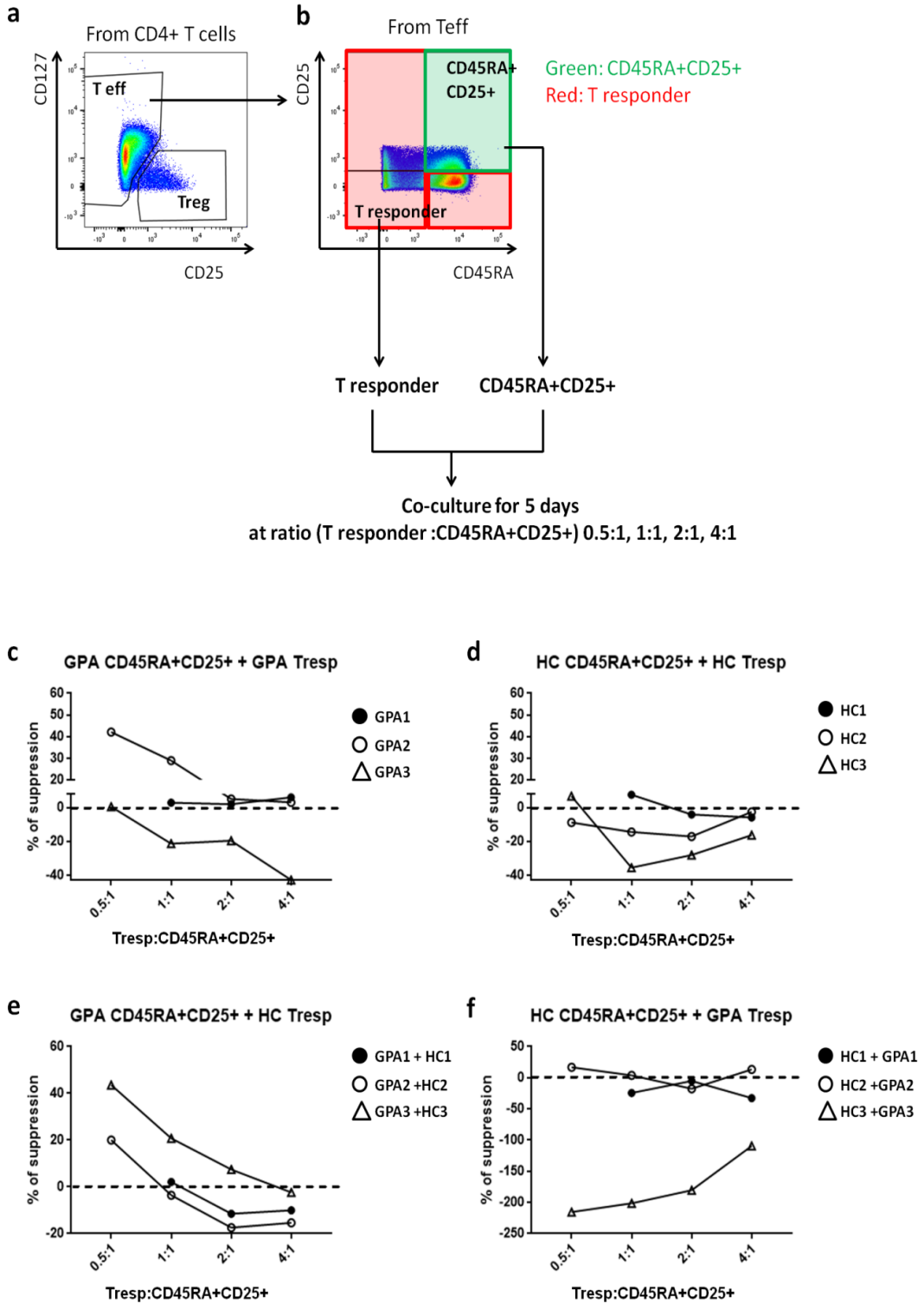

Figure 5.4. Naive CD25+CD4+ T cells micro-suppression assay. Samples prepared and cells isolated as described in Figure 5.3. **(a)** Teff was gated from CD4+ T cells by following the same gating strategy described in Figure 3.1a. **(b)** T responder cells (Tresp, highlighted in red) and naive CD25+CD4+ T cells (here

called CD45RA+CD25+: highlighted in green) were gated from Teff based on CD45RA and CD25 expression. Sorted Tresp (500 cells per reaction) and CD45RA+CD25+ were co-cultured at ratios 0.5:1, 1:1, 2:1 and 4:1 (Tresp: CD45RA+CD25+) for 5 days with anti-CD3 and anti-CD28. Suppression rate of **(c)** GPA CD45RA+CD25+ on Tresp from same GPA patient n=3, **(d)** HC CD45RA+CD25+ on Tresp from same HC n=3, **(e)** GPA CD45RA+CD25+ on Tresp from HC n=3 and **(f)** HC CD45RA+CD25+ on Tresp from GPA patient n=3.

5.2.5. Are naive CD25+CD4+ T cells suppressive or proliferative?

Data described above suggest that at higher ratios, GPA naive CD25+CD4+ T cells may be capable of suppressing HC and GPA Tresp proliferation, under co-culture conditions. However, it was possible that this observed effect was due to an artefact of the high-density cell culture environment. Moreover, if naive CD25+CD4+ T cells are proliferative with TCR stimulation alone, unlike conventional Tregs, for which this assay was originally developed, that would increase the total cell number per condition, confounding reliable measurement of suppressive function (Mcmurchy and Levings, 2012). To investigate this issue, ^{3}H-thymidine incorporation of 500 naive CD25+CD4+ T cells (CD45RA+CD25+) or 500 Tresp cells after 5-day culture with anti-CD3 and anti-CD28 from two GPA patients and two healthy controls was measured (Figure 5.5a). These data suggest that the proliferation of naive CD25+CD4+ T cells is similar to Tresp cells under these culture conditions. Proliferation was also affected by total cell numbers in this assay; Figure 5.5b shows that incorporation of ^{3}H-thymidine in wells containing 1500 Tresp cells is lower than those containing 500 Tresp cells. Therefore, these data suggest that the suppression results observed with naive CD25+CD4+ T cell

(Figure 5.4 c-e) could potentially be influenced by the their proliferative potential and / or cell numbers in each well.

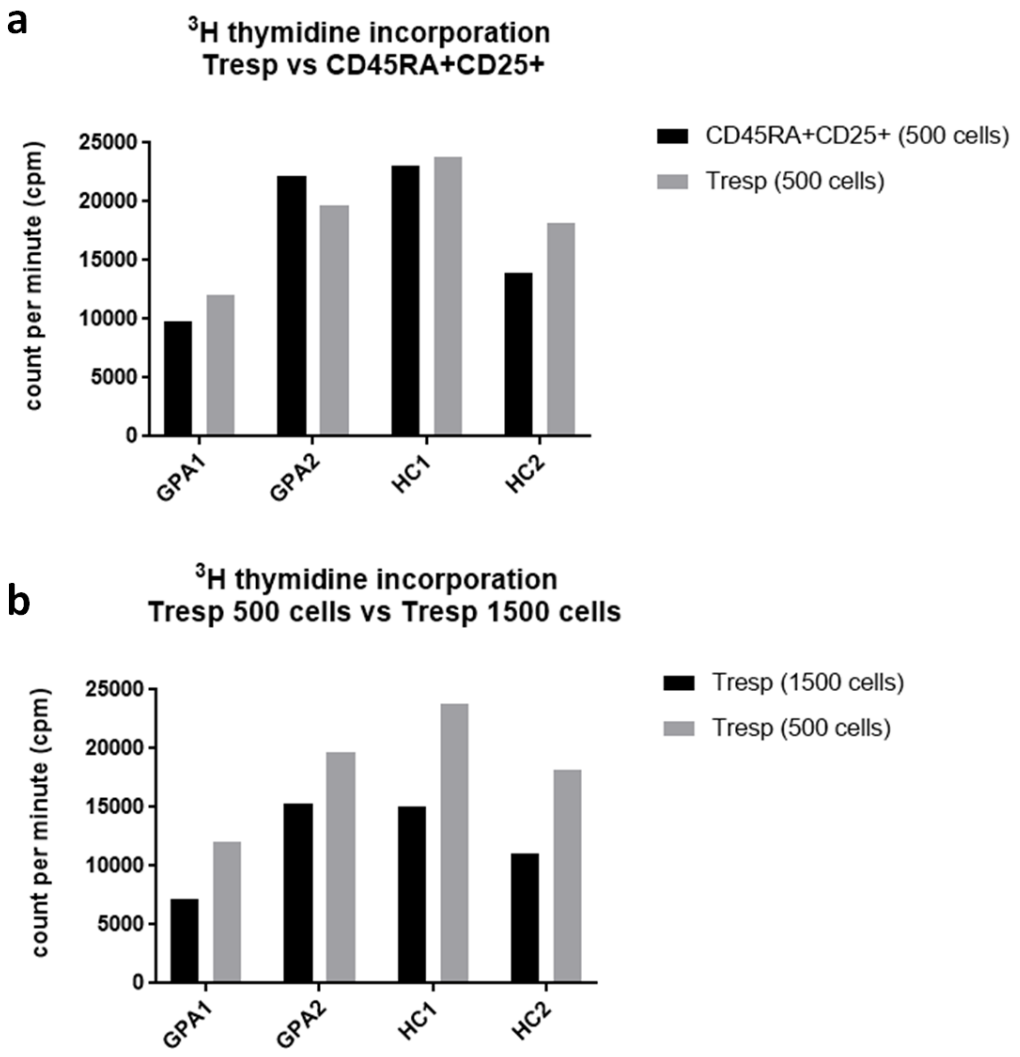

Figure 5.5. Comparison of 3H thymidine incorporation by T responders and naïve CD25+CD4+ T cells. (a) ^{3}H-thymidine incorporation by 500 Tresp alone or 500 naïve CD25+CD4+ T cells under culture conditions described in Figure 5.3 from two GPA patients and two HC. **(b)** ^{3}H-thymidine incorporation by 500 Tresp alone or 1500 Tresp alone (data from the same samples as in a).

5.2.6. Cytokine production from *in vitro* suppression assay.

The main caveat of the suppression assays described above, is that ^{3}H-thymidine incorporation cannot be specifically attributed to the Tresp population – other proliferative cell types will also be labelled. Although Tregs were shown to be non-proliferative in the absence of IL-2 (Levings *et al.*, 2001), it is still possible that Tregs become proliferative upon secretion of by IL-2 from Tresp in the co-culture system. Moreover, naive CD25+CD4+ T cells have been shown to incorporate ^{3}H-thymidine to comparable rates to Tresp (Figure 5.5).

To investigate other 'regulatory functions' of Tregs and naive CD25+CD4+ T cells, the production of cytokines in cell culture supernatants from Tresp alone, and Tresp co-cultured with Tregs, or Tresp co-cultured with naive CD25+CD4+ T cells was measured. Figure 5.6 shows concentrations of cytokines in culture supernatants for each autologous co-culture condition from GPA patient samples and HC samples.

Mean IL-2 concentration in culture supernatants were comparable between GPA and HC in all three conditions (Figure 5.6a,b and c) while IL-10 level tended to be lower in GPA compared to HC (Figure 5.6d,e and f) but differences were not statistically significant.

Interestingly, GM-CSF was statistically significantly higher in GPA culture supernatant after co-culture of Tresp and naive CD25+CD4+ T cells compared to HC (Figure 5.6i), and a trend in the same direction was also observed in GPA culture supernatants from Tresp alone and co-cultured with GPA Tregs (Figure

5.6g and h). There was a trend towards higher IL-13 and TNFα in GPA compared to HC in culture supernatants from Tresp alone or co-cultured with naive CD25+ CD4+ T cells (Figure 5.6k and l, and Figure 5.6q and r). In contrast, there was a strong trend towards lower levels of IFN-γ in supernatant from GPA Tresp compared to HC. No difference in production of other cytokines (IL-4, IL-27, IL-1β, IL-5, IL-6, IL-12, IL-9, IL-23 and IL-18) was observed between GPA and HC. Levels of IL-17A, IL-21 and IL-22 were below the limit of detection (see appendix sFigure 9.5).

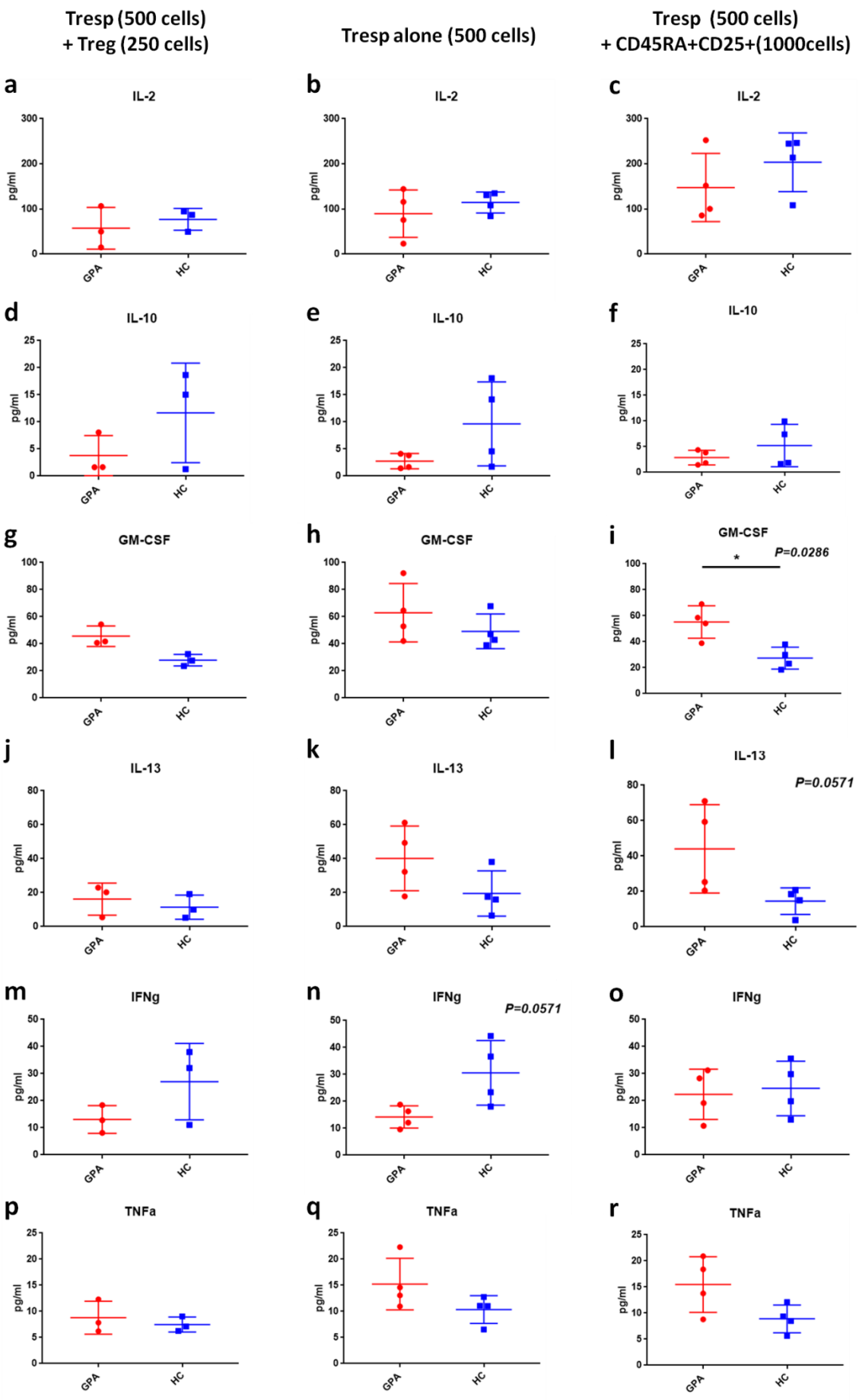
Tresp (500 cells)
+ Treg (250 cells)
Tresp alone (500 cells)
Tresp (500 cells)
+ CD45RA+CD25+(1000cells)
a
IL-2
b
IL-2
c
IL-2
d
IL-10
e
IL-10
f
IL-10
g
GM-CSF
h
GM-CSF
i
GM-CSF
*
P=0.0286
j
IL-13
k
IL-13
l
IL-13
P=0.0571
m
IFNg
n
IFNg
P=0.0571
o
IFNg
p
TNFa
q
TNFa
r
TNFa
pg/ml
GPA
HC

Figure 5.6 Cytokine concentration after Tresp culture alone or Tresp co-culture with Treg or naive CD25+CD4+ T cells. Supernatants from the same experiment described in Figure 5.3 and Figure 5.4 harvested and the level of cytokines were measured by Luminex. **(a,d,g,j,m and p)** Supernatants from cell culture with 500 Tresp and 250 Tregs (GPA n=3, HC n=3). **(b,e,h,k,n and q)** Supernatants from cell culture with 500 Tresp alone (GPA n=4, HC n=4). **(c,f,i,l,o and r)** Supernatants from cell culture with 500 Tresp and 1000 naive CD25+CD4+ T cells (GPA n=4, HC n=4). Cytokine measured as follows **(a,b and c)** IL-2, **(d,e and f)** IL-10, **(g,h and i)**GM-CSF, **(j,k and l)** IL-13, **(m,n and o)** IFNγ and **(p,q and r)** TNFα. Data show mean concentration of cytokine in culture supernatants, and statistical analysis performed by Mann Whitney test.

5.2.7. Changes in cytokine production upon co-culture of Tresp with Treg or CD45RA+CD25+ T cells.

To understand whether Tregs or naive CD25+CD4+ T cells positively or negatively regulated cytokine production upon co-culture with Tresp, fold change in cytokine production between Tresp cultured alone (reference condition) and Tresp co-cultured with Treg or naive CD25+CD4+ T cells were calculated for each individual sample from the data presented in Figure 5.6 (Figure 5.7).

Fold reduction in the levels of most cytokines (Il-2, IL-13, IFNγ and TNFα) in supernatant from before and after Tresp co-culture with Tregs from both GPA and HC was similar (Figure 5.7a, g, i and k). This observation indicates that Tregs from GPA patients have a similar ability to regulate production of these cytokines compared to Tregs from HC. However, there was a trend towards a smaller

reduction in GM-CSF secretion upon culture with GPA Treg compared to HC Treg (mean fold change in levels of GM-CSF from Tresp before and after co-culture with Tregs; GPA= 0.86 and HC= 0.55, p=0.1 (Figure 5.7e)). This observation indicates that GPA Tregs may have a reduced ability to suppress GM-CSF production by Tresp.

Upon co-culture of Tresp with naive CD25+CD4+ T cells, the levels of most of cytokines; IL-13, IFNγ , IL-10 and GM-CSF from HC supernatant were slightly lower compared to Tresp alone (fold change <1, Figure 5.7h, j, d and f). There was little difference in the ability of CD25+CD4+ T cells from GPA patients and HC to suppress production of these cytokines. However, strikingly, IFNγ production was increased upon co-culture of GPA Tresp and CD25+CD4+ T cells compared to Tresp culture alone (fold change >1), while IFNγ production was reduced after co-culture of HC Tresp and CD25+CD4+ T cells compared to Tresp culture alone (fold change <1); differences between GPA and HC co-culture groups were statistically significant (Figure 5.7j).

In sum, Tregs from HC suppress Tresp proinflammatory cytokine production. Tregs from GPA also exhibited suppression of most proinflammatory cytokines production, but failed to suppress production of GM-CSF. Interestingly, co-culture with naive CD4+CD25+ T cells from HC had little effect on cytokine production from Tresp. However, naive CD4+CD25+ T cells from GPA tended to increase the levels of cytokines in co-culture supernatant, especially IFNγ.

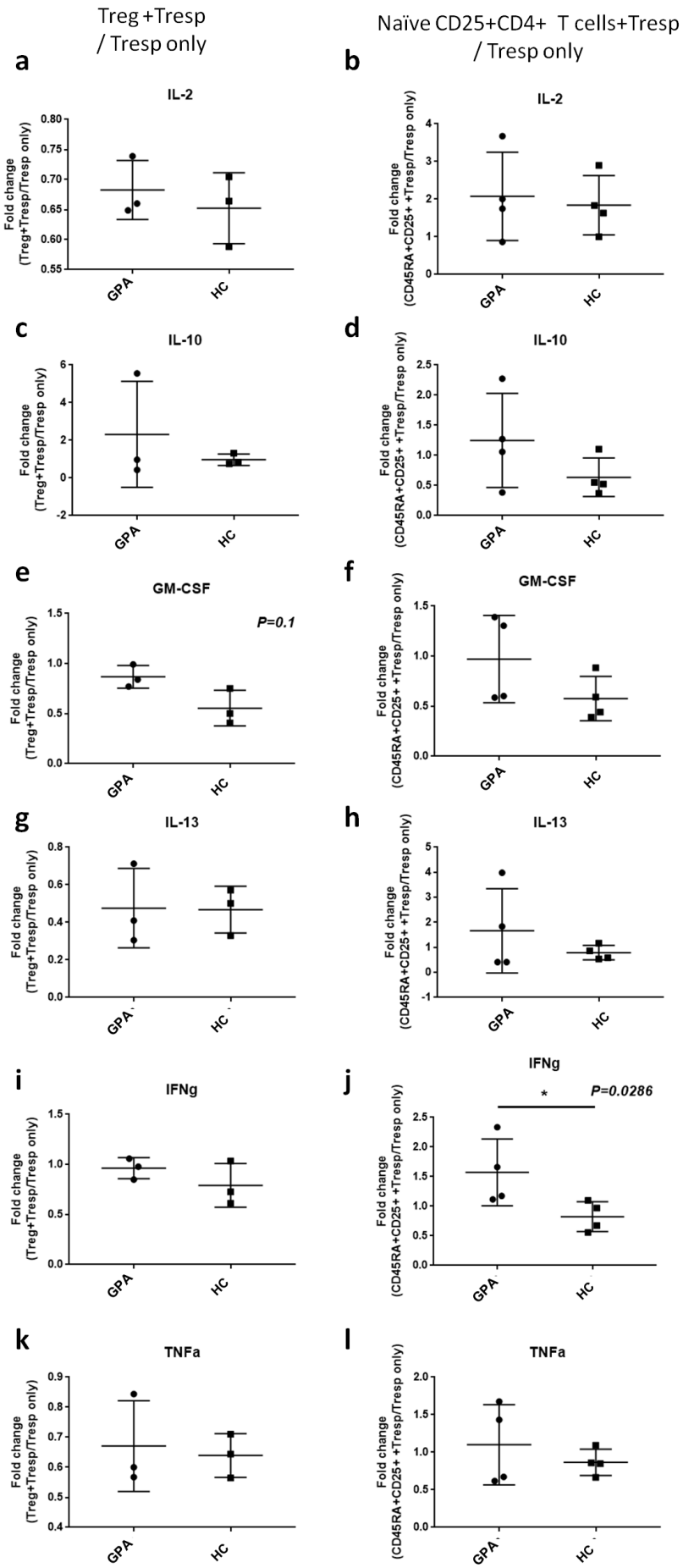
Treg +Tresp
/ Tresp only
Naïve CD25+CD4+ T cells+Tresp
/ Tresp only
a
b
IL-2
IL-2
Fold change (Treg+Tresp/Tresp only)
Fold change (CD45RA+CD25+ +Tresp/Tresp only)
GPA
HC
c
d
IL-10
IL-10
e
f
GM-CSF
GM-CSF
P=0.1
g
h
IL-13
IL-13
i
j
IFNg
IFNg
*
P=0.0286
k
l
TNFa
TNFa

Figure 5.7 Fold change in cytokine concentration after Tresp co-culture with Tregs or navie CD25+CD4+ T cells compared to Tresp culture alone. Using the data described in Figure 5.6, fold change was calculated by dividing concentration of cytokine in co-culture condition by concenetration of cytokine in Tresp alone. **(a,c,e,g,i and k)** Fold change in cytokine concentration after 500 Tresp co-culture with 250 Tregs compared to 500 Tresp culture alone. **(b,d,f,h,j, and l)** Fold change in cytokine concentration after 500 Tresp co-culture with 1000 naive CD25+CD4+ T cells compared to 500 Tresp culture alone. Cytokine measured as follows **(a and b)** IL-2, **(c and d)** IL-10, **(e and f)**GM-CSF, **(g and h)** IL-13, **(i and j)** IFNγ and **(k and l)** TNFα. Data show mean fold change in cytokine concentration and statistical analysis performed by Mann Whitney test.

5.3.Discussion

Data from this study have confirmed that Tregs from GPA patients can suppress proliferation of Teff cells (or Tresp) from both GPA patients and HCs. This finding is in agreement with a previous study in which a Treg suppression assay was also performed (Zhao *et al.*, 2014). However, the most interesting observation was that GPA Tregs showed a decreased capacity to reduce production of GM-CSF in supernatant from co-culture with Tresp while levels of other cytokines were reduced (Figure 5.7). One possibility, is that GM-CSF is produced by Tregs from GPA patients. Moreover, the production of GM-CSF from Tresp and naive CD25+CD4+ T cells from GPA patients is higher than that from HC (Figure 5.6), which suggests that GM-CSF production in CD4+ T cells from GPA may dysregulated.

GM-CSF is a cytokine produced by all types of CD4+ T cells (Zhu, 2018), and an important role of this cytokine is to activate neutrophils (Smith *et al.*, 1995). As activation of neutrophils is believed to be one of the core mechanisms in GPA pathogenesis (Nakazawa *et al.*, 2019), this finding implies that a loss of Treg mediated regulation, specifically of GM-CSF production, may contribute to the underlying mechanism of GPA pathogenesis. However, the data from this study need to be strengthened by increasing sample sizes (limited statistical power with n=3). It will also be important to investigate which of the CD4+ T cell subsets (including Tregs) are responsible for the increase in GM-CSF production.

The assignment of suppressive function to the naïve CD4+CD25+ T cell population proved to be more problematic. Unfortunately, due to limitations in patient sample availability and isolation of sufficient naïve CD4+Cd25+ T cells by cell sorting, the

more favourable method of using CTV staining for assaying suppression of proliferation was not possible. Therefore, the microsuppression assay was employed, but this assay was not ideal because, both naive CD25+CD4+ T cells from GPA and HC have comparable proliferative potential to Teff cells (Tresp) (Figure 5.5) in response to TCR stimulation, unlike conventional Tregs, which only proliferate in the presence of increased IL-2 concentrations (Levings *et al.*, 2001). With this caveat, which applies equally to both HC and GPA (Figure 5.5) the naïve CD4+CD25+ T cell population in GPA, but not from healthy donors suppressed proliferation of Tresp, albeit only at higher cell ratios, as compared to conventional Tregs (Figures 5.3 and 5.4). Further studies need to be conducted in future, using another method such as the CTV labelling method, to confirm the aberrant suppressive function of the naïve CD4+CD25+ T cell population in GPA. The mechanism(s) of suppression by GPA naïve CD4+CD25+ T cells also remains to be elucidated, but may involve immunosuppressive cytokine production, as with conventional Tregs.

The comparison of cytokine production between Tresp cells cultured alone and co-cultured with naive CD25+CD4+ T cells revealed that naive CD25+CD4+ T cells from HC tended to contribute to a slight reduction in cytokine production, while this was not typically the case for GPA. Perhaps naive CD25+CD4+ T cells from HC may have cytokine regulatory functions, that is absent or decreased in GPA patients. The exact nature of the suppressive function and mechanism of naïve CD4+CD25+ T cells in health and disease will need to be addressed in future studies, through development of an alternative T cell suppression assay along with and cytokine-blocking and cell-contact (transwell) assays.

On the other hand, naive CD25+CD4+ T cells from GPA patients may initiate an increase in cytokine production. Of note, Tresp from GPA exhibited lower expression of IFNγ compared to HC when cultured alone (Figure 5.6n), but upon co-culture with naive CD25+CD4+ T cells IFNγ production was increased (Figure 5.7). These finding suggest that the observed positive suppression rate of naive CD25+CD4+ T cells from GPA on Tresp from HC (Figure 5.4) may be more likely due to the high cell number per condition (Figure 5.5) rather than their inherent suppressive function. Again, this hypothesis must be investigated further using an alternative T cell suppression assay.

In conclusion, this study showed that Tregs from GPA have an ability to suppress proliferation of Tresp. However, it would appear that GPA Tregs lack the ability to regulate production of GM-CSF during co-culture with Tresp. Taken together, the data from this study would suggest that naïve CD25+CD4+ T cells in GPA appear functionally different to conventional Tregs. However, an assessment of the ability of naive CD25+CD4+ T cells from either GPA and HC to suppress T cell proliferation should be determined in further studies.

6. Chapter 6. Identification of extracellular factors in plasma that may affect CD4+ T cell phenotype in GPA.

6.1. Introduction

Thus far, data from this study suggest that isolated CD4+ T cells from GPA patients exhibit intrinsic changes in gene expression compared to healthy controls that may contribute to the imbalance in CD4+ T cells subsets observed in GPA. However, in an *in vivo* setting, factors in the extracellular environment in plasma, such as the cytokine mileu, lipids, antibodies, complement, hormones, glycoproteins and various metabolites could significantly influence T cell differentiation programmes (Dupage and Bluestone, 2016; Hess and Kemper, 2016; Howie *et al.*, 2017).

As T cell mediated immune responses play an important role in the pathogenesis of GPA, a number of studies have surveyed the cytokine profiles of these cells in blood, PBMC or isolated cells (Abdulahad *et al.*, 2008; Abdulahad *et al.*, 2013; Lilliebladh *et al.*, 2018). However, these studies are still limited to providing insights into cell intrinsic perturbations in GPA.

Circulating cytokine profiles have been evaluated in serum of AAV patients, which have identified distinct differences between PR3-AAV and MPO-AAV, suggesting heterogeneity in disease pathogenesis (Berti *et al.*, 2018). Moreover, while a study showed higher levels of IL-17 in GPA serum (Rani *et al.*, 2015), another recent

study showed higher levels of IL-10 and GM-CSF in serum from active GPA patients compared to HC, but failed to detect IL-17 in these samples (Szczeklik *et al.*, 2017).

Here we aim to evaluate the circulating plasma cytokines in GPA patients to gain an understanding of whether there is a cytokine dysregulation that may be specifically skewing cells towards a Tfh phenotype. However, cytokines are just one class of inflammatory mediators that influence cellular behaviour. Especially, extracellular cues such as metabolities, lipids and microbial molecules may have an important role in balancing between Tregs and Tfh cells. Some *in vitro* studies have suggested that lipid mediators such as arachidonate 5-lipoxyganase (Alox5) and lipoxinA4 (LXA4) (Nagaya *et al.*, 2017), and extracellular matrix protein 1 induced Tfh differentiation (He *et al.*, 2018). More interestingly, TLR activation in Tregs leads to an upregulation of glucose transporter, Glut1, and subsequent reduction in expression of CD25 and Foxp3 and also a decrease in the ability of these cells to suppress T cell proliferation (Gerriets *et al.*, 2016). In contrast to this, high expression of Glut1 enhanced the generation of Tfh like cells (Zeng *et al.*, 2016) (Glut1 gene *Slc2a1* was highly expressed in GPA naive CD4+ T cells after TCR activation (Figure 4.5d)). Since persistent infection is common in GPA patients, extracellular factor(s) including TLR agonists may induce Tregs (and even naive CD4+ T cells) to become polarised towards a Tfh like phenotype. Also, Figure 4.5 showed that genes involved in metabolism were dysregulated in GPA naive CD4+ T cells and other studies have shown that changes in levels of certain metabolites can affect T cell function in autoimmune diseases (Grigorian *et al.*, 2007; Kupcova Skalnikova *et al.*, 2017).

Therefore, to obtain a more comprehensive picture of the circulating extracellular factors that could drive the observed T cell dysregulation in GPA patients, an unbiased interrogation of circulating factors in plasma is highly desirable. Additionally, proteomic studies could provide a window into the pathophysiological status of patients that sheds light on clinical symptoms. Indeed, proteomic studies have been performed using mass spectrometry with plasma samples to identify biomarkers and analyse the metabolome for diagnosis in other diseases such as lupus, lung and prostate cancer, type 2 diabetes and diabetic kidney disease(Lokhov *et al.*, 2009; Lokhov *et al.*, 2014; Lokhov *et al.*, 2016; Bringans *et al.*, 2017; Geyer *et al.*, 2017; Madda *et al.*, 2018).

In this chapter, cytokine profiles from GPA plasma will be compared with plasma from healthy individuals, and mass spectrometry will be employed to assess differences in protein content in plasma from GPA patients compared to healthy controls. In addition, to test whether extracellular factors alone can drive the observed dysregulation of CD4+ T cell function in GPA, CD4+ T cells from healthy donors will be cultured with plasma from GPA patients and changes in the phenotypes and function of these cells investigated. Through these studies, the contribution of extracellular factor(s) in GPA plasma to the dysregulation of CD4+ T cell subset differentiation observed in GPA will be evaluated.

6.2.Results

6.2.1. Cytokine levels in GPA plasma.

To address whether the plasma cytokine profiles differ between GPA and HC, plasma concentration of a range of cytokines was measured by both Cytometric Bead Array (CBA) and Luminex Cytokine Assay. The CBA assay showed a higher concentration of IL-10 in GPA plasma compare to HC (Figure 6.1a). However, the CBA assay was not deemed to be sensitive enough to detect levels of other cytokines in these plasma samples (see appendix sFigure 9.6). For greater sensitivity, and to test a larger range of cytokines, a Luminex Cytokine Assay was subsequently used. In the Luminex assay, there was a trend towards higher IL-10 in GPA plasma but the difference was not statistically significant (Figure 6.1b). There was however, a statistically significant positive correlation between the IL-10 levels measured by CBA and Luminex assays (Figure 6.1c).

Interestingly IL-18 was also significantly higher in GPA plasma compared to HC (Figure 6.1d). However, there were no statistically significant differences in levels of other cytokines including IL-2, IL-17, IL-21, IFNγ, IL-4 and GM-CSF (Figure 6.1e to j). No difference in production of other cytokines (IL-17, TNFα, IL-6, IL-2, IFNγ and IL-4 by CBA, IL-27, IL-1β, IL-5, IL-12, IL-13, TNFα, IL-9, IL-23, IL-22 and IL6 by Luminex) was observed between GPA and HC (see appendix sFigure 9.6).

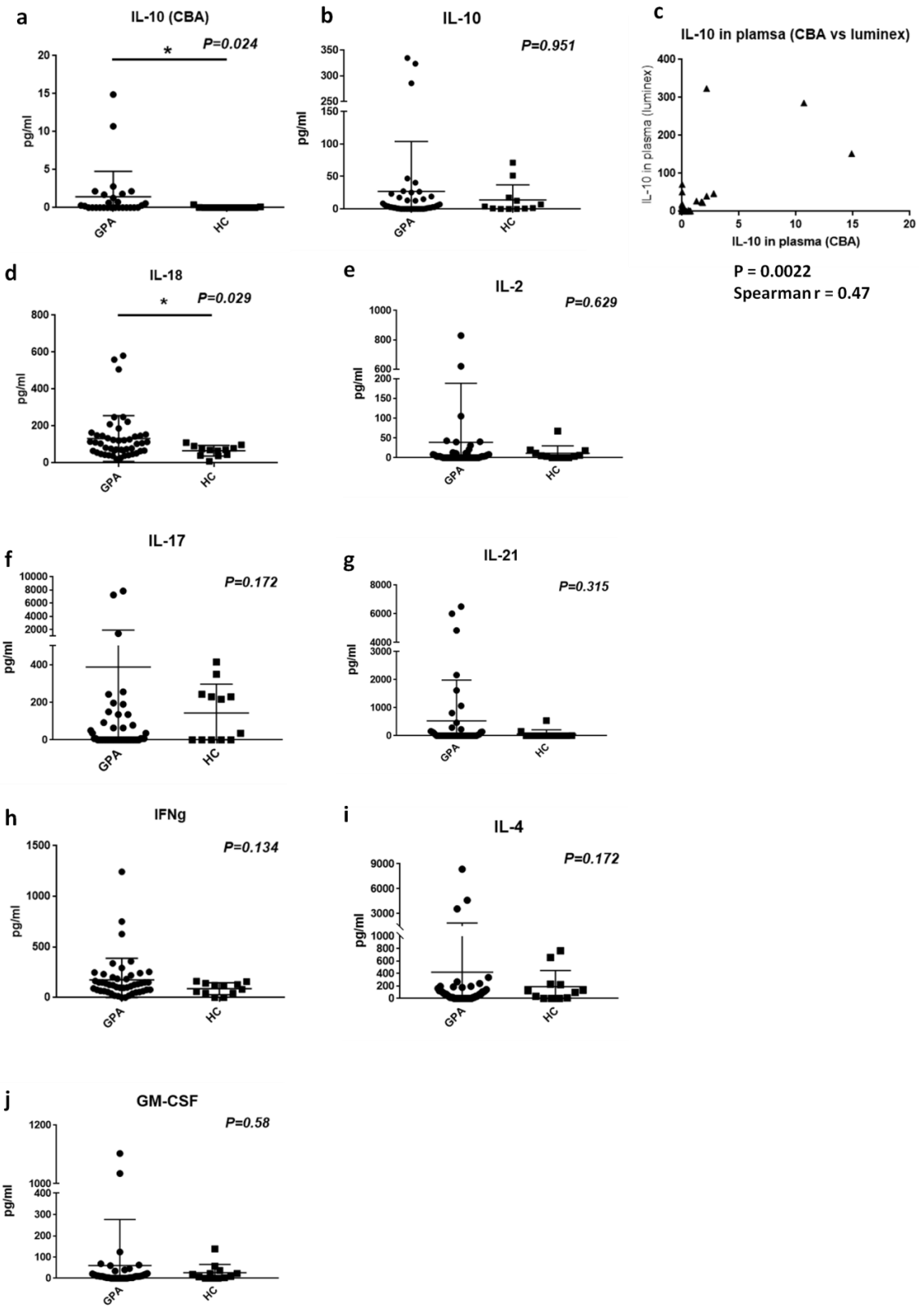

Figure 6.1 Cytokine concentration in GPA and HC plasma. Plasma samples from GPA and HC blood were prepared and cryo-preserved at -80°C until the assay was performed. CBA and Luminex assays were used to measure cytokine concentration

in plasma samples **(a)** IL-10 concentration in GPA and HC plasma as measured by CBA assay GPA n=28, HC n=13. **(b)** IL-10 concentration in GPA and HC plasma was measured by Luminex assay GPA n=47, HC n=12. **(c)** Correlation of IL-10 concentration in the same plasma samples measured by CBA and Luminex assays n= 40. Luminex assays were used to measure concentrations of the following cytokines in GPA and HC plasma; **(d)** IL-18, **(e)** IL-2, **(f)** IL-17, **(g)** IL-21, **(h)** IFNγ, **(i)** IL-4 and **(j)** GM-CSF. GPA n=47, HC n=12. Data show mean concentrations of cytokine in plasma, and statistical analysis performed by Mann Whitney test. Statistical analysis for correlation performed by Spearman correlation. Spearman r=1 indicates perfect positive correlation and Spearman r =-1 indicates perfect negative correlation.

6.2.2. Phenotypic changes in healthy PBMCs upon co-culture with GPA plasma.

To understand the effect, if any, of extracellular factors in GPA plasma on the phenotype of CD4+ T cells, experiments involving co-culture of healthy PBMCs with plasma obtained from GPA patients were performed. Figure 6.2a shows the experimental scheme; in brief, PBMC from a healthy control donor was cultured in media containing different plasma samples from either GPA patients or healthy controls. Five days after culture, supernatants were collected for cytokine measurement and cells were stained with a panel of antibodies (Figure 2.2i) to assess Treg and Tfh cell phenotypes by flow cytometry.

To exclude the donor variation, PBMCs from two healthy donors were tested (HC1 and HC2). There were no differences in the frequencies of Tregs

($CD25^{high}CD127^{low}CD4+$ T cells) in either set of healthy PBMCs after culture with GPA or HC plasmas (Figure 6.2b and c). However, the frequency of Tfh (CXCR5+PD1+CD4+ T cells) cells significantly increased in HC1 PBMCs after culture with GPA plasma samples compare to HC plasma, while there was no statistically significant difference in Tfh frequencies induced by GPA or HC plasmas with HC2 PBMC (Figure 6.2d and e). Of note, the cell frequencies obtained with HC2 were generally lower than HC1, irrespective of treatment conditions, in these and subsequent analyses.

Therefore, we can conclude that factor(s) present in plasma from GPA patients did not affect frequencies of Tregs in healthy PBMCs, but can potentially increase frequencies of Tfh cells.

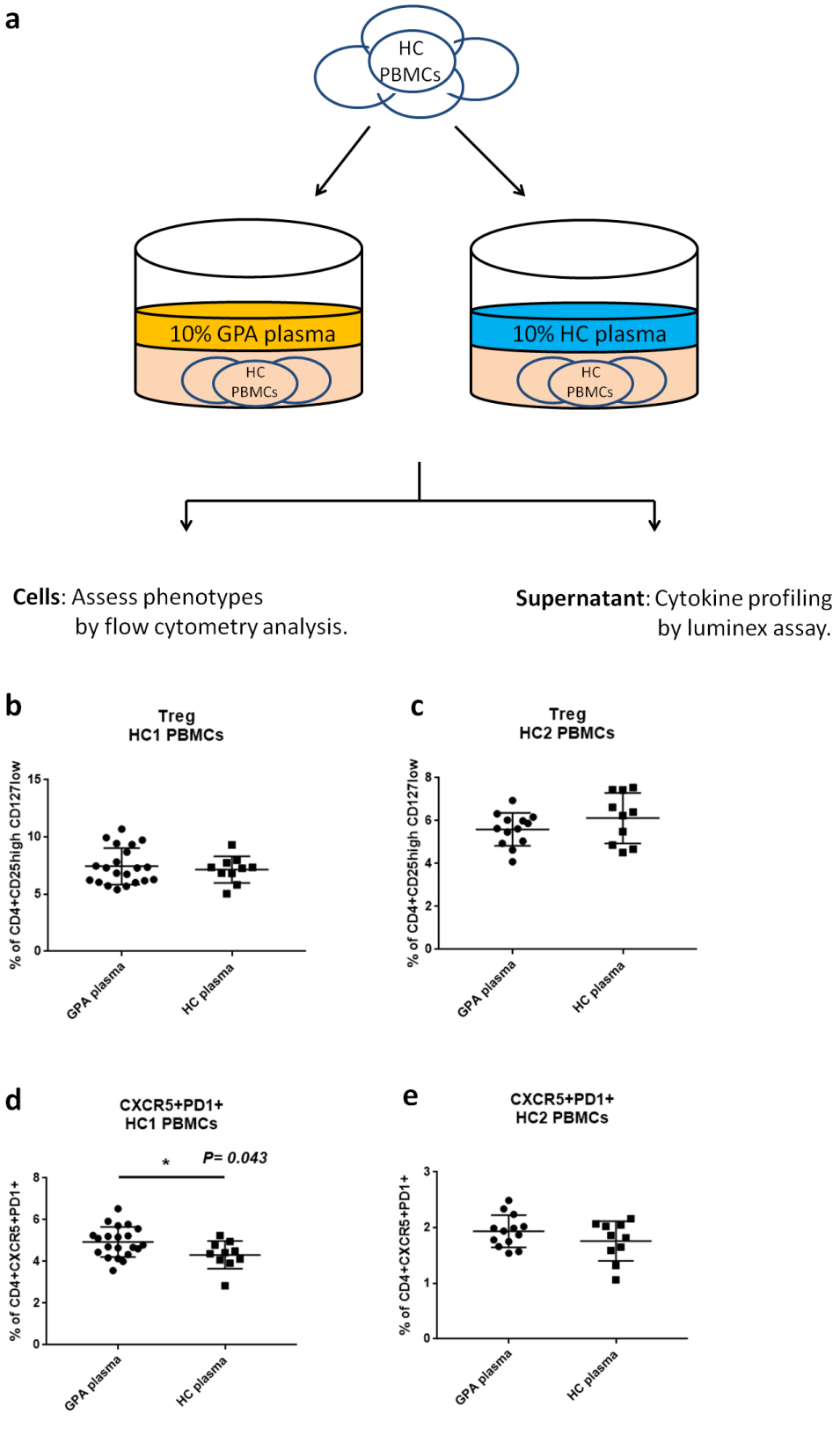

Figure 6.2 Frequency of Treg and Tfh cells in healthy PBMCs after co-culture with GPA or HC plasma. (a) Cryopreserved healthy PBMCs (from one of two different donors, HC1 or HC2) were cultured in media including 10% GPA or HC

plasma. Five days after co-culture, cells were harvested and phenotypic analysis performed by flow cytometry. Culture supernatant was stored at -80°C for cytokine analysis by Luminex assay. **(b-c)** Treg ($CD4^{+}CD25^{high}CD127^{low}$) identification was performed following previous gating strategy from Figure 3.1a and b bottom row. Frequencies of Tregs in **(b)** HC1 or **(c)** HC2 PBMC were assessed after co-culture with GPA plasma (n=21 for HC1, n=13 for HC2) and HC plasma (n=10). **(d-e)** cTfh cells ($CD4^{+}$CXCR5 +PD1+) were identified following a previous gating strategy from Figure 4.1b. The frequencies of cTfh cells in **(d)** HC1 or **(e)** HC2 PBMCs were assessed after them co-culture with GPA plasma or HC plasma. Data shows mean frequencies of cell subsets and statistical analysis performed by Mann Whitney test.

6.2.3. Correlation between CD25 expression and IL-10 concentration in plasma after co-culture of healthy PBMCs with GPA plasma.

Interestingly, after five days co-culture of HC1 PBMCs with GPA plasma, there was a significant increase in CD25 expression on CD4+ T cells (excluding Tregs) (Figure 6.3a). HC2 PBMCs also showed a similar trend to HC1, but differences in CD25 expression were not statistically significant (Figure 6.3d). This might be due to the lower number of plasma samples tested with HC2 PBMCs (hence lower statistical power) compared to the HC1 experiments, and the generally lower cell frequencies observed with HC2 after five days of co-culture. Thus, extracellular factor(s) present in GPA plasma can potentially induce phenotypic changes in HC CD4 T cells that phenocopy GPA CD4 T cells, namely the increased CD25 expression and increased cTfh cell surface markers.

To understand if any cytokine(s) in GPA plasma may be inducing CD25 expression on CD4 Teff cells, the cytokine levels in the various GPA plasmas were correlated to the CD25 expression on CD4 Teff obtained with each GPA plasma co-culture. Interestingly, the correlation analyses revealed a strong positive correlation specifically with the level of IL-10 and CD25 expression in the GPA plasma samples. This phenomenon was observed in both HC1 and HC2 PBMC experiments (Figure 6.3b and e). However, when HC PBMCs were cultured with HC plasma samples, there was no correlation between CD25 expression and IL-10 plasma concentration (Figure 6.3 c and f).

In summary, those GPA plasma samples with high levels of IL-10, induced higher CD25 expression on CD4+ T cells from healthy PBMCs after five-day co-culture.

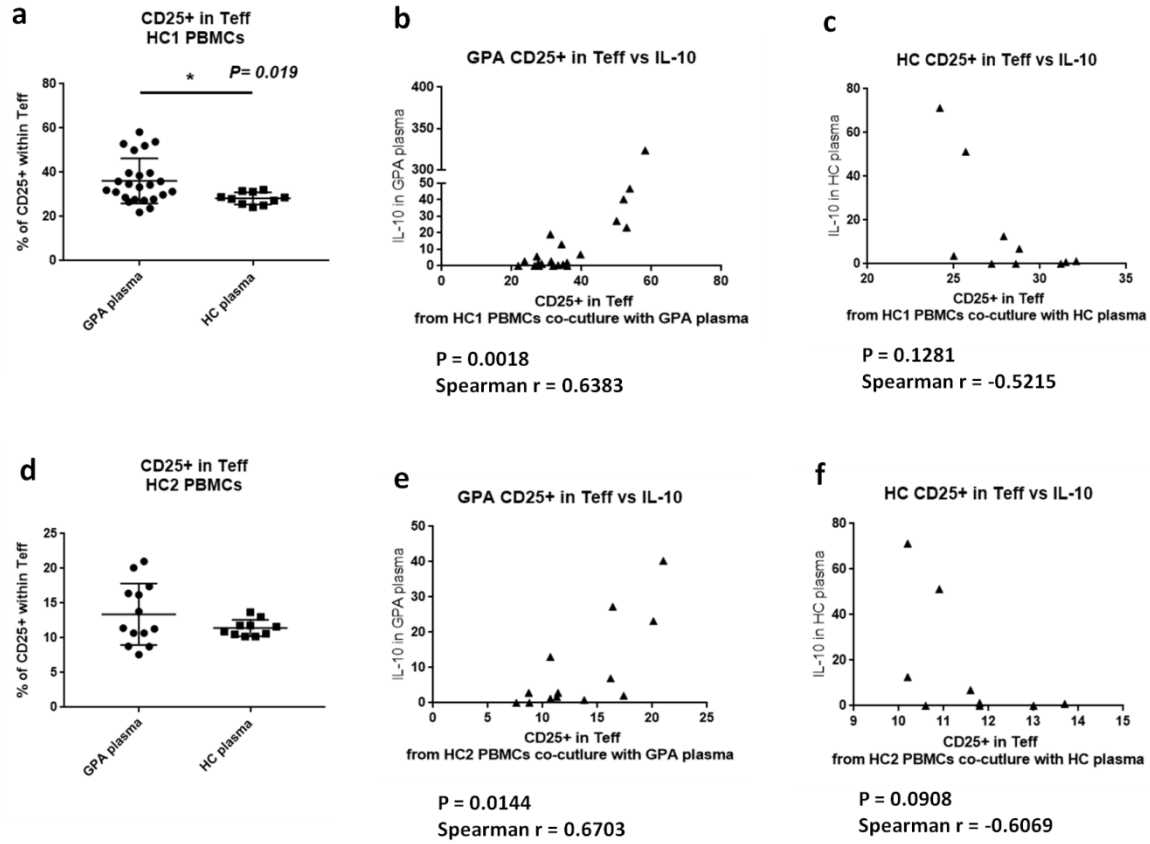

Figure 6.3 Frequencies of healthy CD25+ Teff cells after co-culture with GPA plasma. Data from the same experiment as shown in Figure 6.2 were re-analysed to assess frequencies of CD25+ Teff cells. **(a and d)** CD25+ Teff cells were identified by following a previous gating strategy shown in Figure 3.2c. Frequencies of CD25+ Teff cells in **(a)** HC1 or **(d)** HC2 PBMC were assessed after them co-culture with GPA plasma (n=21 for HC1, n=13 for HC2) or HC plasma (n=10). **(b and e)** Correlation of IL-10 concentration in GPA plasma samples and the frequency of CD25+in Teff cells from **(b)** HC1 or **(e)** HC2 PBMCs after co-culture with the same GPA plasma. **(c and f)** Correlation of IL-10 concentrations in HC plasma and the frequency of CD25+ in Teff cells from **(b)** HC1 or **(e)** HC2 PBMCs after co-culture with the same HC plasma. Data shows mean frequencies of cell subsets and statistical analysis performed by Mann Whitney test (a and d). Statistical analysis for correlation was performed by Spearman correlation (b,c,e andf).

6.2.4. Is IL-10 in GPA plasma the causative factor for CD25 upregulation on CD4+ T cells?

As the IL-10 concentration in GPA plasma positively correlated with CD25 expression on CD4+ T cells in HC PBMCs after co-culture, one hypothesis could be that the IL-10 in GPA plasma induces the observed up-regulation in CD25 expression, as previous studies have shown this to be an immunomodulatory function of IL-10 (Cohen et al, 1994). To address this hypothesis, a similar co-culture experiment with or without additional IL-10 was performed. However, in these experiments, there was no effect of addition of IL-10 on frequencies of CD25+ Teff cells, either in plasma already containing IL-10

(that induced CD25 after co-culture) or plasma not containing IL-10 (that did not induce CD25 after co-culture) (Figure 6.4). Therefore, IL-10, in itself, does not promote CD25 upregulation.

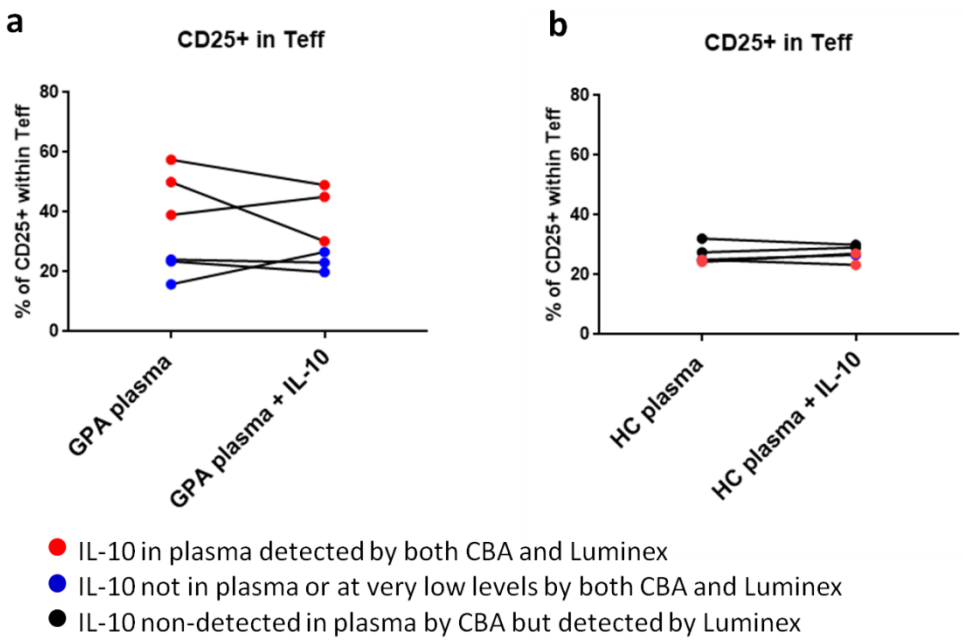

Figure 6.4 Effect of IL-10 supplementation on frequencies of healthy CD25+ Teff in PBMCs after co-culture with GPA or HC plasma. (a) Frequency of CD25+ Teff cells in HC PBMCs co-cultured with GPA plasma alone or GPA plasma plus addition of recombinant IL-10 (2ng/ml). **(b)** Frequency of CD25+ Teff cells in HC PBMCs co-cultured with HC plasma alone or HC plasma plus addition of recombinant IL-10. Paired data points from each donor sample are connected by a line. No statistically significant differences were observed between GPA/HC plasma alone and GPA/HC plasma plus additional IL-10 conditions by Wilcoxon matched pairs signed rank test.

6.2.5. Cytokine concentration in culture supernatants after co-culture of HC PBMCS with GPA plasma.

Cytokine concentrations in culture supernatants from HC PBMCs after co-culture with GPA plasma or HC plasma were compared; there were no statistically significant differences in concentrations of any of the cytokines tested including GM-CSF, IFNγ, TNFα, IL-13, IL-17A, IL-1b, IL-2, , IL-27, IL-6, IL-9 (Figure 6.5, and see appendix sFigure 9.7). Levels of IL-12p7, IL-4, IL-5, IL-22 and IL-23 were below the limit of detection. 0However, an interesting observation was that IL-21 concentration in the co-culture supernatant samples directly correlated with IL-21 concentration in GPA plasma prior to co-culture (Figure 6.5b). Specifically, plasma samples in which IL-21 concentration was above the limit of detection (Figure 6.5a) stimulated IL-21 production in co-culture supernatants despite plasma samples being added at a 1:10 dilution (Figure 6.5b and c). There was no detectable IL-21 in co-culture supernatants from HC PBMCs cultured with HC plasma. In contrast, there was a negative correlation between IL-10 concentrations in the input GPA plasma, and cytokine levels in supernatants after five-day co-culture with HC PBMCs (Figure 6.1d).

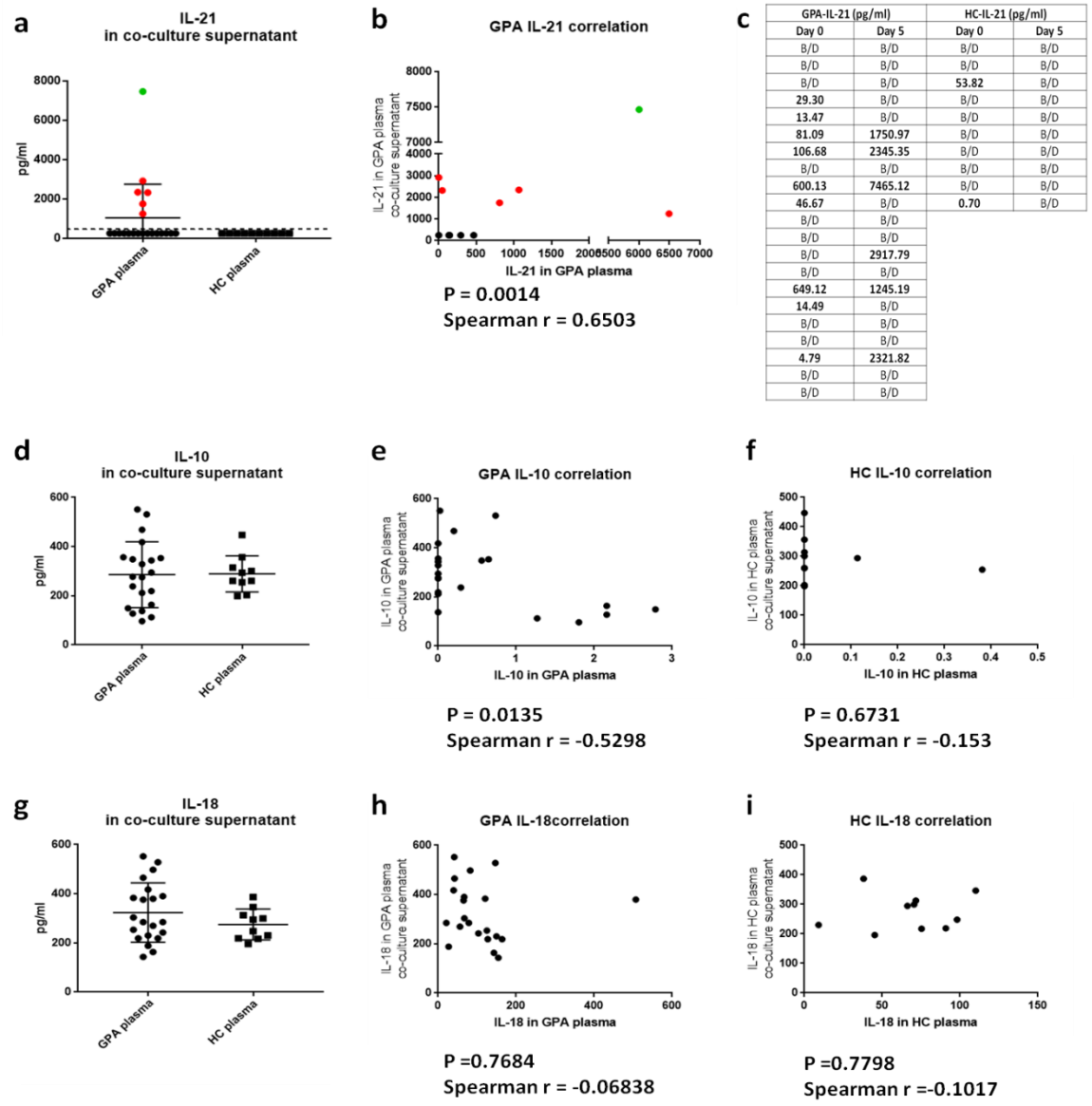

GPA-IL-21 (pg/ml)		HC-IL-21 (pg/ml)	
Day 0	Day 5	Day 0	Day 5
B/D	B/D	B/D	B/D
B/D	B/D	B/D	B/D
B/D	B/D	53.82	B/D
29.30	B/D	B/D	B/D
13.47	B/D	B/D	B/D
81.09	1750.97	B/D	B/D
106.68	2345.35	B/D	B/D
B/D	B/D	B/D	B/D
600.13	7465.12	B/D	B/D
46.67	B/D	0.70	B/D
B/D	B/D		
B/D	B/D		
B/D	2917.79		
B/D	B/D		
649.12	1245.19		
14.49	B/D		
B/D	B/D		
B/D	B/D		
4.79	2321.82		
B/D	B/D		
B/D	B/D		

Figure 6.5 Cytokine concentrations in supernatants from healthy PBMCs co-cultured with GPA plasma.

Cytokine concentrations in supernatants from the experiment described in Figure 6.2 were measured by Luminex assay; **(a)** IL-21, **(d)** IL-10 and **(g)** IL-18. **(b)** Correlation between initial IL-21 concentration in GPA plasma samples and IL-21 in co-culture supernatant from healthy PBMCs co-cultured with GPA plasma. In a and b, samples with IL-21 concentration above limit of detection shown in red, sample with highest IL-21 concentration in green **(c)** IL-21 concentration in culture supernatant from day 0 and day 5 post culture. Day 0 (input) IL-21 concentration is 10% of IL-21 plasma concentration from Figure 6.1g (B/D**:** below

detection). **(e)** Correlation between initial IL-10 concentration in GPA plasma and IL-10 concentration in supernatant from healthy PBMCs co-cultured with GPA plasma **(f)** Correlation between IL-10 concentration in HC plasma and IL-10 concentration in supernatant from healthy PBMCs co-cultured with HC plasma **(h)** Correlation between IL-18 concentration in GPA plasma and IL-18 concentration in supernatant from healthy PBMCs co-cultured with GPA plasma **(i)** Correlation between IL-18 concentration in HC plasma and IL-18 concentration in supernatant from healthy PBMCs co-cultured with HC plasma. Data show mean concentration of cytokine in co-culture supernatant, and no statistically significant differences were observed by Mann Whitney test (a,c and f). Statistical analysis for correlation performed by Spearman correlation (b, d,e,g and h).

6.2.6. Mass spec analysis of GPA plasma compared to HC plasma.

To gain an understanding of potential factor(s) that could be directing the observed phenotypic changes in healthy CD4+ T cells cultured in GPA plasma, mass-spectrometry analysis of GPA and HC plasma was performed. Liquid chromatography (LC) with mass spectrometry (MS)/MS analysis was used to identify and quantify the peptide/protein content in six GPA and three HC plasma samples. Fold change in peptide/protein levels in GPA plasma compared to HC plasma (and the associated p-values) were calculated using Microsoft Excel. To identify potentially dysregulated biological pathways, a list of peptides/proteins that were differentially expressed in GPA patients verses HC was analysed in an Ingenuity Pathway Analysis (IPA). It was shown that acute phase proteins including plasminogen, haptoglobin, alpha-1- antichymotripsin and alpha-2-antiplasmin were highly abundant in GPA plasma compared to HC (Figure 6.6a). However, immunoglobulin related peptides were lower in GPA plasmas than HC

(Figure 6.6a). Interestingly, levels of proteins related to lipid metabolism appeared abnormal in GPA compared to HC plasma; long-chain-fatty–acid CoA ligase, apolipoprotein D (APOD) were more abundant while apolipoprotein(a) (LPA) and apolipoprotein F (APOF) were less abundant in GPA plasma (Figure 6.6a). In the IPA analysis, IL-6 signalling was predicted to be more active in GPA plasma compared to HC plasma (Figure 6.6b).

In sum, mass spectrometry analysis showed dysregulation of proteins involved in lipid metabolism in GPA plasma compared to HC plasma. Also, an abundance of acute phase proteins but lower levels of immunoglobulin proteins were observed in GPA plasma compared to HC plasma.

a

Protein	Fold change
DmX-like protein 2 GN=DMXL2	2.946
cDNA FLJ53691, highly similar to Serotransferrin	2.433
Alpha-1-acid glycoprotein 1 GN=ORM1	2.040
Long-chain-fatty-acid--CoA ligase ACSBG2 GN=ACSBG2	1.725
Ubiquitin-conjugating enzyme E2 GN=UBE2E1	1.723
Probable tRNA(His) guanylyltransferase GN=THG1L	1.598
IGL@ protein GN=IGL@	1.596
Haptoglobin-related protein GN=HPR	1.559
Plasminogen GN=PLG	1.549
Haptoglobin GN=HP	1.539
cDNA FLJ41552 fis, highly similar to Protein Tro alpha1 H	1.411
N-acetyltransferase 5 GN=NAA20	1.383
E3 ubiquitin-protein ligase RFWD2 GN=RFWD2	1.379
General transcription factor IIi isoform E GN=GTF2I	1.366
Complement factor H-related protein 1 GN=CFHR1	1.325
Apolipoprotein D GN=APOD	1.296
Complement component C9 GN=C9	1.264
Protein AHNAK2 GN=AHNAK2	1.244
Properdin GN=CFP	1.243
Alpha-1-antichymotrypsin GN=SERPINA3	1.213
Schlafen family member 11 GN=SLFN11	1.205
Complement component C8 alpha chain GN=C8A	1.186
Centrosomal protein of 89 kDa GN=CEP89	1.183
Hemopexin GN=HPX	1.178
Alpha-2-antiplasmin GN=SERPINF2	1.162
Ig alpha-1 chain C region GN=IGHA1	-1.440
Ig kappa chain C region GN=IGKC	-1.445
Obscurin GN=OBSCN	-1.447
Ig kappa chain V-III region WOL	-1.449
Ig heavy chain V-III region GA	-1.458
Putative uncharacterized protein DKFZp686O16217 GN=DKFZp686O16217	-1.466
Immunoglobulin J chain GN=JCHAIN	-1.469
Protein FAM184A GN=FAM184A	-1.471
Ig kappa chain V-II region Cum	-1.473
IgG H chain	-1.481
Protein IGKV3D-20 GN=IGKV3D-20	-1.482
Single-chain Fv GN=scFv	-1.498
Alpha-1-syntrophin GN=SNTA1	-1.514
Kelch-like protein 40 GN=KLHL40	-1.521
Rheumatoid factor RF-IP12	-1.528
Ig kappa chain V-III region VG	-1.542
Ig kappa chain V-III region POM	-1.553
Uncharacterized protein GN=IGHV3OR16-9	-1.559
Ig heavy chain V-III region CAM GN=IGHM	-1.559
VH3 protein GN=VH3	-1.559
Keratin, type I cytoskeletal 14 GN=KRT14	-1.560
Ig gamma-4 chain C region GN=IGHG4	-1.589
V3-4 protein GN=V3-4	-1.603
Hemoglobin subunit alpha GN=HBA1	-1.675
Hemoglobin subunit beta GN=HBB	-1.711

b Top upstream regulators

Upstream Regulator	Molecule Type	Activation z-score	p-value of overlap	Target molecules in dataset
IL22	cytokine		0.0000299	ABCG1,HP,KRT1
ALB	transporter		0.000168	AGT,ALB
IL6	cytokine	1.342	0.000183	AGT,ALB,HP,ORM1,PLG
mir-634	microrna		0.00035	OPA1,TFAM
HNF1A	transcription regulator		0.00196	AHSG,ALB,C4BPA,ITIH4

Figure 6.6 Mass spectometry analysis: protein levels in GPA plasma compared to plasma from healthy donors. (a) List of top 50 proteins 'dysregulated' in GPA and their fold difference in GPA plasma compared to HC plasma. **(b)** Ingenuity Pathway Analysis (IPA); top five predicted upstream regulators in GPA plasma by 'activation z-score'; a positive z-score indicating predicted activation of an upstream regulator, a negative z-score indicating inhibition.

6.2.7. Mass spectrometry analysis of GPA plasma, stratifying by CD25 upregulation in co-culture.

To specifically investigate what factor(s) in GPA plasma contribute to upregulation of CD25 on healthy CD4+ T cells upon co-culture with GPA plasma, the same dataset was re-analysed by stratifying GPA plasma into those samples that induced CD25 upregulation and those that did not (Figure 6.7). In the dataset, three GPA plasma samples induced CD25 on HC CD4+ T cells (CD25 inducing plasma), and three GPA plasmas did not induce CD25 on HC CD4+ T cells (CD25 non-inducing plasma, CD25 levels after co-culture were comparable to HC plasma co-culture). Figure 6.7a shows the frequencies of CD4+CD25+ T cells from HC PBMCs after co-culture with 'CD25 inducing' GPA plasma, 'CD25 non-inducing' GPA plasma or HC plasma (experiment and data from Figure 6.3a).

In a canonical pathway analysis, the top four predicted canonical pathways (Dendritic cell maturation, Phospholipase C Signaling, Macrophage production of ROS, LXR/RXR activation) all had negative z-scores (indicating reduced pathway activation) in all three GPA plasma groups (all GPA, CD25 inducing only, and CD25 non-inducing only) compared to HC plasma (Figure 6.7b). However, interestingly, the acute phase response signalling pathway was predicted to be activated (positive z-score) in CD25 inducing GPA plasma compared to HC, but not in CD25 non-inducing GPA plasma. In contrast, the complement system pathway was only predicted to be active in CD25 non-inducing GPA plasmas (Figure 6.7b). In an IPA analysis, interestingly, a down-regulation of lipid metabolism was predicted in CD25 inducing plasma samples compared to HC plasma (Figure 6.7c).

In summary, lipid metabolism was predicted to be less active in GPA by IPA analysis. In contrast, acute phase response signalling is predicted to be more active in GPA, specifically in those samples conferring up-regulation of CD25 on CD4+ T cells from healthy PBMCs, perhaps implying a role for this process in CD25 up-regulation.

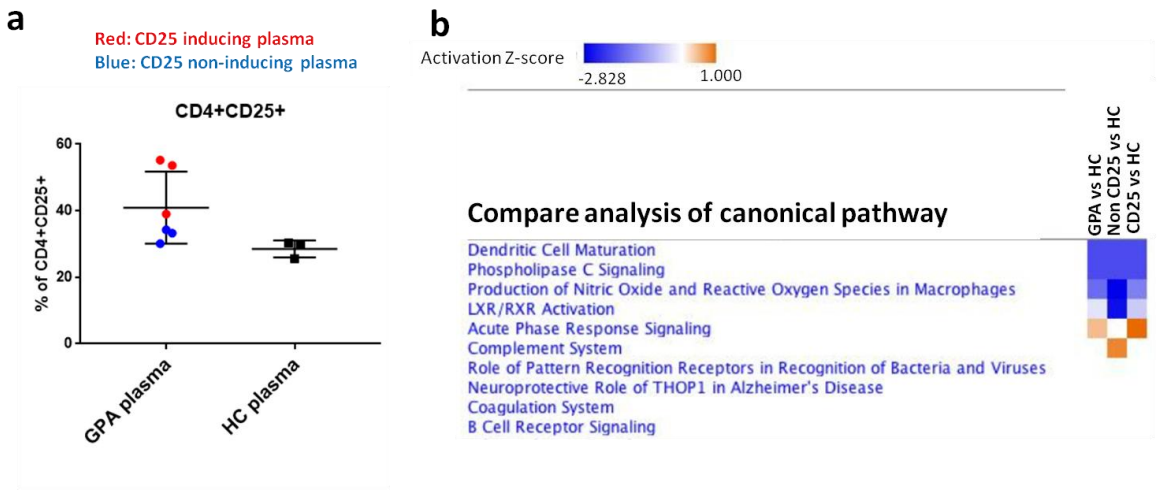

c Top diseases and biofunctions in CD25 inducing plasma vs HC plasma

Categories	Diseases or Functions Annotation	p-Value	Activation z-score	Molecules
Lipid Metabolism, Molecular Transport, Small Molecule Biochemistry	Release of lipid	0.0000358	-1.4	AGT,ALB,APOD,PLG, SNTA1
Lipid Metabolism, Molecular Transport, Small Molecule Biochemistry	Release of cholesterol	0.000288		PLG,SNTA1
Endocrine System Development and Function, Lipid Metabolism, Small Molecule Biochemistry, Vitamin and Mineral Metabolism	Synthesis of pregnenolone	0.000855		AGT,OPA1
Lipid Metabolism, Molecular Transport, Small Molecule Biochemistry	Concentration of lipid	0.00107	-0.243	ABCG1,AGT,ALB,APOD,LPA,PON1
Lipid Metabolism, Molecular Transport, Small Molecule Biochemistry	Concentration of fatty acid	0.00159		APOD,LPA,PON1

Figure 6.7 Mass spectrometry analysis; predicted canonical pathways dysregulated in GPA after stratification of GPA plasma samples by CD25 induction on HC CD4+ T cells. Proteins differing in abundance by a factor of 1.3 or greater between GPA and HC plasma were used for an IPA analysis. **(a)** Frequency of CD4+CD25+ T cells in HC PBMCs after co-culture with GPA plasma or HC plasma – data from Figure 6.3a. For data analysis in the current figure, GPA plasma samples were divided into two groups; three samples inducing CD25 expression on healthy CD4+ T cells to higher levels than HC plasma ('CD25 inducing', highlighted in red) and the other three samples did not enhance CD25 expression on healthy CD4+ T cells ('CD25 non-inducing', highlighted in blue). **(b)** Top predicted canonical pathways between either; all six GPA samples compared to HC (GPA vs HC), 'CD25 inducing' GPA plasmas versus HC (CD25 vs HC), or 'CD25

non-inducing' GPA plasmas compared to HC (Non CD25 vs HC). **(c)** Top predicted diseases and dysregulated biofunctions in CD25 induced GPA plasma in IPA analysis.

6.3. Discussion

The focus of this chapter was to investigate whether there are extracellular factors present in GPA plasma that have the potential to promote phenotypic changes in CD4+ T cells. To test this hypothesis, CD4+ T cells (from healthy donor PBMCs) were co-cultured in plasma from GPA patients (or healthy donors as a control) and phenotypic changes after a five-day culture were assessed. Frequencies of Tregs did not change upon co-culture with GPA plasma (Figure 6.2b and c). Interestingly, co-culture with GPA plasma increased CD25 expression on HC CD4+ T cells, and this increase strongly correlated with initial (day 0) levels of IL-10 in GPA plasma samples (Figure 6.3). Although IL-10 is an immunosuppressive cytokine, paradoxically it is also known to upregulate CD25 expression on T cells, in the presence of TCR activation (Cohen *et al.*, 1994). Given the correlation between ex-vivo IL-10 levels in GPA plasma and CD25 expression following co-culture, it seemed plausible that IL-10 may be a key factor in increasing CD25 expression. However, the results obtained here showed that addition of recombinant IL-10 to either healthy or GPA plasma co-cultures did not significantly upregulate CD25 expression, on CD4+ T cells (Figure 6.4).

An alternative explanation for the observed correlation between IL-10 and CD25 expression could be that the increased IL-10 levels in GPA plasma are indicative of a counterbalance response to the inflammatory cellular activation associated with GPA pathogenesis, while an alternative factor(s) is responsible for increasing CD25 expression on HC CD4+ T cells. Moreover, it was shown that IL-10 can be induced by steroid treatment (John *et al.*, 1998; Mozo *et al.*, 2004) and this has been shown in autoimmune diseases such as multiple sclerosis (MS) and systemic lupus erythematosus (SLE) (Gayo *et al.*, 1998; Godsell *et al.*, 2016). It therefore seems

plausible that the observed increase in IL-10 levels in GPA plasma may be due to steroid treatment rather than a pathophysiological change. Although anti-inflammatory IL-10 levels are elevated in GPA, studies have shown either reduced numbers and/or function of Tregs in GPA (Abdulahad *et al.*, 2007; Zhao *et al.*, 2014), suggesting that these IL-10 levels may be insufficient to suppress the inflammation associated with GPA pathogenesis.

Another explanation could be that GPA patients may be less responsive to IL-10 or that IL-10 may only partially suppress pro-inflammatory immune responses, leading to weakened immune response against infections. Consistent with the notion of underlying persistent inflammation in patients, is the earlier observation of antimicrobial gene expression specifically in GPA patients (Chapter 4), and here the observation that levels of the pro-inflammatory cytokine IL-18 was significantly elevated in GPA plasma (Figure 6.1d). IL-18 is produced by monocytes/macrophages in response to TLR mediated inflammasome activation by pathogenic danger signals and together with IL6, can lead to the induction of acute phase response (Colafrancesco *et al.*, 2012; Slaats *et al.*, 2016). Indeed, IPA analysis of data from mass spectrometry of plasma samples predicted an activation of the proinflammatory acute phase response signalling in GPA plasma samples that induced increased CD25 expression on CD4+ T cells during co-culture. Furthermore, IL-6 was predicted as an activated upstream regulator in the IPA analysis of GPA plasma (Figure 6.6b), most likely due to the elevated expression of acute phase proteins in GPA plasma. -Of note here, acute phase response signalling is mediated by the activation of STAT3 (Akira *et al.*, 1994), which can also induce

CD25 gene expression (Li *et al.*, 2017). Thus, the increased CD25 levels maybe a marker of proinflammatory T cell activation by acute phase proteins in plasma.

The other observation from the co-culture experiments was the potential increase in CXCR5+PD1+ Tfh-like cells. However, as only one of two healthy donor PBMCs tested showed higher frequencies of CXCR5+PD1+ T cells after co-culture with GPA plasma, a firm conclusion cannot be drawn about whether factors present in GPA plasma can drive cTfh differentiation/expansion (Figure 6.2d and e). The caveat to this was that the HC2 donor had very low overall viable T cell frequencies after co-culture, which may have contributed to the results not reaching statistical significance, despite a similar trend in increase of CXCR5+PD1+ in GPA as with HC1. The signature cytokine produced by Tfh cells is IL-21. However, IL-21 concentration in co-culture supernatants was not significantly increased by the presence of GPA plasma (Figure 6.5a). Interestingly, the six GPA plasma co-culture supernatants with increased IL-21 levels, positively correlated with the presence of IL-21 in these GPA plasma samples prior to co-culture (Figure 6.5b), suggesting a positive feedback loop for IL-21 expression. This observation is consistent with previous studies describing autocrine regulation of IL-21 in T cells (Caprioli *et al.*, 2008). In contrast, this positive correlation between initial cytokine concentration and concentration post co-culture was not observed for other cytokines such as IL-10 and IL-18 (Figure 6.5e and h). The source of IL-21 in these PBMC cultures is unclear as cells other than T cells (Tfh or Th17), such as NKT cells also produce IL-21 (Coquet *et al.*, 2007). Future experiments to investigate the cellular source of IL-21 could be performed using flow cytometry and intracellular cytokine staining (ICS).

Mass spectrometry analysis comparing GPA and HC plasma samples revealed several unexpected differences. For instance, lower levels of immunoglobulin proteins were detected in GPA plasma (Figure 6.61). However, this observation may be due to immunosuppressive medications often prescribed to GPA patients. Previous studies have shown that immunosuppressive drug treatment reduced immunoglobulin levels in IgA nephropathy (Kim *et al.*, 2016).

Dysregulation of lipid metabolism in GPA is a novel and exciting observation from the IPA analysis of the mass spectrometry data (Figure 6.6a and Figure 6.7b). Down-regulation of the LXR/RXR activation pathway was predicted in GPA (Figure 6.6a). LXR/RXR activation is one of the critical mechanisms in lipid homeostasis in mammals. Oxidized low-density lipoprotein (LDL) is internalised by scavenger receptors on macrophages such as CD36, which activates the LXR/RXR pathway leading to high density lipoprotein (HDL) efflux (Freeman and Moore, 2003; Calkin and Tontonoz, 2012). The role of HDL in inflammatory disease has been critically established in a number of studies, indicating the importance of metabolic reprogramming in disease pathology. HDL modulates Th1 and Th17 activation in autoimmune disease by reducing DC maturation (Tiniakou *et al.*, 2015) and prevents Treg to Tfh switching during atherosclerosis by reducing intracellular cholesterol levels in Tregs (Gaddis *et al.*, 2018). LXR/RXR pathway activation also has an anti-inflammatory function by suppressing production of proinflammatory cytokines such IL-6 and IL-1β (Freeman and Moore, 2003). The identification of dysregulation of lipid metabolism in GPA could potentially provide an alternative mechanism to explain the imbalance in CD4+ T cell subsets in GPA. Future studies could be performed to investigate the role of lipid metabolism in Tfh differentiation in GPA using inhibitors and/or agonists of this pathway. (and may

provide useful insights into potential therapeutic benefits of these in the treatment of GPA.)

Mass-spectrometry data also predicted a down-regulation of both DC maturation and phospholipase C (PLC) signalling pathways in GPA. Activation of PLC signalling is important for increasing intracellular calcium concentration, and calcium signalling is involved in immune cell activation and proliferation. Therefore down-regulation in PLC signalling may imply reduced DC and / or T cell activation. A previous study showed that calcium signalling, activated through PLC, is critical for DC maturation and activation (Bagley *et al.*, 2004). Moreover, GPA patients with active disease have lower frequencies of circulating DCs, and TLR activation on GPA DCs *in vitro* failed to induce IL-12 expression but did induce abundant type I IFN (Braudeau *et al.*, 2017). The same study also suggested that lower frequencies of circulating DCs in GPA, leads to lower frequencies of Th1 cells. Therefore, it is possible that down-regulation of PLC signalling may ultimately lead to an imbalance in the frequencies of CD4+ T cell subsets.

In conclusion, it would appear that cell-extrinsic factors present in GPA plasma may contribute to the phenotypic changes in CD4+ T cells observed in GPA. In particular, mass spectrometry analysis of GPA plasma has revealed that. dysregulation of lipid metabolism could provide an alternative mechanism to explain the underlying cause of GPA pathogenesis, although further studies will be required to address this hypothesis.

7. Chapter 7. Final discussion

This study has aimed to understand the functional imbalance in CD4+ T cell subsets in GPA by addressing two major questions; i) what factor(s) cause an increase in Tfh cells in GPA and ii) what factor(s) lead to reduction in function or frequency of Tregs.

7.1. STAT5 activation and differentiation of GPA CD4+ T cells.

One interesting observation was that STAT5 activation was reduced in GPA naïve CD4+ T cells, but not STAT3. As STAT5 is an inhibitory signal of Tfh and Th17 differentiation (Laurence *et al.*, 2007; Nurieva *et al.*, 2012), this could explain the increased Tfh phenotype of GPA CD4+ T cells observed in this study. However, no corresponding increases in Th17/IL-17 production were observed, although it is possible that the *in vitro* stimulation conditions used in this study were not sufficient to induce Th17 phenotypes. Several previous studies have shown an increase in Th17/IL-17 production in GPA blood with PMA/Ionomycin stimulation (Abdulahad *et al.*, 2008; Rani *et al.*, 2015) Therefore, further work will be required to address Th17 differentiation in GPA.

Of note, the reduction of levels of active phosphorylated STAT5 was driven by a reduction in STAT5 protein level rather than a specific reduction of phospho-STAT5 in GPA naive CD4+ T cells (Figure 4.10 and Figure 4.11a). Moreover, comparing the levels of STAT5A and STAT5B, only STAT5A exhibited lower protein levels by western blotting in GPA (Figure 4.10). Reduction in STAT5A and STAT5B mRNA expression was less obvious (Figure 4.8a and b) suggesting that negative regulation of STAT5A in GPA occurs after transcription. As discussed in Chapter 4,

STAT5 protein may be cleaved by a protease, Cathepsin G, the mRNA of which was shown to be highly abundant in GPA naive CD4+ T cells (Figure 4.5c and Figure 4.5d). However it is unclear how Cathepsin G targets STAT5A specifically. Further investigation will be required to determine whether additional factors such as STAT5A specific targeting micro-RNAs are expressed in GPA naive CD4+ T cells. Previous studies have suggested that STAT5B is more relevant to Treg function in both humans and mouse models (Cohen *et al.*, 2006; Jenks *et al.*, 2013; Kanai *et al.*, 2014; Villarino *et al.*, 2016). The observation that STAT5A but not STAT5B is down-regulated therefore suggests that normal Treg development and function might be retained in GPA.

7.2. Treg function in GPA.

The reduction of STAT5 activation was only observed in naive CD4+ T cells, not total CD4+ T cells. Since STAT5 is important in survival and proliferation of CD4+ T cells, our observations suggest that STAT5 related defects in GPA may affect differentiation of naïve CD4+ T cells but not the function/phenotype of differentiated cells. Importantly, full STAT5 activation levels in total CD4+ T cells implies normal Treg cell development in GPA. Loss of STAT5 has previously been shown to reduce frequency and function of Tregs (Cohen *et al.*, 2006; Jenks *et al.*, 2013; Kanai *et al.*, 2014; Villarino *et al.*, 2016). Moreover, in this study, the proliferative ability, suppressive function, and frequencies of Tregs were comparable between GPA PBMCs and HC. Importantly, these observations suggest that treatment strategies that aim to increase Treg frequencies would be unlikely to offer an effective solution for GPA patients. Indeed, in a small clinical trial, Rapamycin (an mTOR inhibitor that expands iTregs) was used to treat GPA patients but resulted in limited clinical efficacy (Koening *et al.*, 2009; Battaglia *et*

al., 2012)., 2012 That said, cytokine profiles from the T cell suppression assay suggested that despite GPA Tregs retaining their suppressive function on Tresp proliferation, they did appear to exhibit defective suppression of pro-inflammatory cytokine (GM-CSF) production. This observation is particularly interesting since GM-CSF is a key cytokine for activation of neutrophils, and a previous study showed that GM-CSF induces high levels of PR3 surface expression on isolated healthy polymorphonuclear neutrophils (PMN) (Hellmich *et al.*, 2000). Since high expression of PR3 on neutrophil surfaces is associated with an increased risk of developing ANCA vasculitis (Witko-Sarsat and Thieblemont, 2018), dysregulation of GM-CSF production may be a critical mechanism in GPA pathogenesis. Although further studies are required to assess whether pro-inflammatory cytokines produced in this assay are from Tregs or Tresp, the data suggest that a successful future therapy may need to increase the quality of Tregs in GPA patients, rather than their quantity.

7.3. Increase in Tfh like cells in GPA.

The data from this study consistently reported an increase in Tfh phenotypes in GPA patients, both in naive CD4+ T cells and within total CD4+ T cell populations. Since GPA is an autoimmune disease associated with production of auto-antibodies, Tfh/cTfh like cell types are of particular interest given their role in providing T cell help to support the production of antibodies by B cells. In addition to lower levels of active STAT5, an increase in BCL6 expression (in both total CD4+ T cells and naive CD4+ T cells) and an increase in production of IL-21 (in total CD4+ T cells and potentially also in naive CD4+ T cells) was observed in GPA. Levels of active STAT3 in GPA were comparable to HC after both IL-2 and IL-6 stimulation. Expression of TRIM8, a positive regulator of STAT3 activation (Okumura *et al.*,

2010), was high in GPA, perhaps helping to maintain STAT3 activation. STAT3 has been shown to be critical for Tfh differentiation (Weinstein *et al.*, 2014).

It is notable that the observed increase in Tfh phenotypes in GPA upon *in vitro* culture of CD4+ T cells did not require additional cytokine stimulation, only TCR activation. Perhaps, as other experiments have suggested, GPA CD4+ T cells have a pre-disposition to be become differentiated towards a Tfh phenotype, so do not require additional signals typically required for Tfh differentiation such as IL-12 and TGF-β (Schmitt *et al.*, 2014; Qi, 2016). However, future studies are required to determine the contribution of these Tfh cells to the accumulation of pathogenic ANCA in GPA.

7.4. Aberrant expression of PD1 on GPA CD4+ T cells.

Although the increase Tfh like cell phenotype was observed, experiments involving flow cytometry to phenotype Tfh cells using surface marker staining were unable to detect differences in homeostatic cTfh frequencies between GPA and HC PBMCs. One potential reason for this discrepancy may involve the observed reduction in PD1 expression on GPA CD4+ T cells, since PD1 is a key marker for Tfh subsets. As discussed in Chapter 3, lower PD1 expression may reflect a reduction in exhausted T cells in GPA. *In vitro* differentiation data from Chapter 5 suggests that reduction in PD1 expression in GPA naïve CD4+ T cells may be due to the presence of extracellular factors (perhaps activating TLR signalling) *in vivo* since the intrinsic ability of these cells to express PD1 *in vitro* was comparable between GPA and HC (Figure 4.1d). Recent studies have shown that PD1 expression on CD8+ T cells is reduced upon TCR and TLR activation, and TLR4 activation has also been shown to increase the efficacy of PD-1 blockade therapy for prevention of T cell exhaustion

in cancer (Zahm *et al.*, 2018; Wang *et al.*, 2019). In contrast to cancer immunotherapy, which relies upon active T cells to target malignant tissue, T cell exhaustion tends to improve prognosis in autoimmune diseases. Mounting evidence from a number of studies suggests that in some autoimmune diseases, including GPA, pathogenic infection can initiate or contribute towards the severity of disease symptoms (Cartin-Ceba *et al.*, 2012; Mckinney *et al.*, 2014). In GPA, continuous infection (particularly with *Staphylococcus. aureus*) has been reported, and incidence of infection is related to increased risk of disease relapse (Popa *et al.*, 2007). The balance between reducing disease symptoms and maintaining immunocompetence is a major issue in GPA treatment; while immune suppressive drugs and steroid treatments dampen down activation of T effector cells, the patient has reduced capacity to clear infections. One problem for detection of disease relapse in the clinic is that the symptoms associated with initiation of relapse are similar to infection. Therefore, there is an important unmet need for the identification of biomarkers of disease relapse, which could be used be used in clinical diagnosis to begin treatment before disease symptoms worsen.

7.5. Could elevated CD25 expression in GPA be caused by a TLR agonist in plasma?

CD25 upregulation on naïve CD4 T cells is a hallmark feature of GPA, identified in this study, which could be phenocopied in healthy CD4+ T cells by co-culture with GPA plasma (Chapter 3 and 6), If activation of TLR signalling is involved in reducing T cell exhaustion in GPA, and the responsible factor is also a component of GPA plasma that correlates with upregulation of CD25 on CD4+ T cells, then identification of that factor could be critical for understanding disease pathogenesis and improving treatment. An increase in acute phase proteins and

IL-18 levels in plasma, and higher expression of antimicrobial genes in naive CD4+ T cells, together with predicted activation of TLR signalling in total CD4+ T cells (Kerstein *et al.*, 2017) might all be indicators of underlying infection. Interestingly, in co-culture experiments IL-10 levels in GPA plasma correlated with upregulation of CD25 on healthy CD4+ T cells, although later experiments indicated that IL-10 in itself was not the factor responsible for this phenotype.

Perhaps the CD25-inducing factor(s) is a PAMP / TLR agonist? TLR agonists have been shown to induce IL-10 production directly from innate cells and indirectly from Tregs cells (Lu, 2014). One caveat for this hypothesis was that during co-culture with GPA plasma there was no change in PD1 expression on CD4+ T cells. It is possible that co-culture for longer than five-days and/or exposure to PR3/PR3-ANCA at patho-physiological levels may be required to observe the expected reduction in PD1 expression. Plasma exchange treatment has been proposed and tested in a clinical trial setting for highly active AAV patients (MPA and GPA patients) to prevent end-stage renal disease (Walsh *et al.*, 2013). However plasma exchange treatment is expensive, labour intensive and due to lack of strong scientific evidence there is uncertainty regarding which patients would be most suited to this treatment. Therefore, identification of factor(s) in plasma that may contribute to GPA pathogenesis would represent significant improvement in understanding disease progression.

7.6. What is the function of the naive CD25+CD4+ T cell subset, increased in GPA?

As discussed previously, increased frequencies of naive CD25+CD4+ T cells were observed in PBMCs from GPA patients compared to HC, but the functional capacity

of these cells remains unclear. One hypothesis was that these cells may have Treg function, so to address this hypothesis a T cell suppression assay was performed. However, since cell numbers were limiting, an assay based on ^{3}H thymidine incorporation had to be used instead of a flow cytometry based dye dilution technique assay, and the results were difficult to interpret as it became apparent that both Tresp cells and naïve CD25+CD4+ T cells were proliferative in this assay. However, despite the caveats, cytokine profiles from supernatants after co-culture with Tresp suggest that naïve CD25+CD4+ T cells in GPA may possess different functional characteristics to conventional Tregs (Chapter 5). It is possible that this 'naive CD25+CD4+ T cell' subset may represent T cells in the process of becoming activated or differentiated towards a Tfh-like phenotype. Further studies will be required to confirm the functional characteristics of these cells. More extensive phenotyping of these naive CD25+CD4+ T cell subset by flow cytometry using additional markers of T cell activation such as CD69 (Amlot *et al.*, 1996) would likely be informative. Perhaps more importantly, functional assays will be required, including a redesigned T cell suppression assay that enables measurement of Tresp proliferation specifically, by dye dilution. Due to cell number limitations, it was not feasible to specifically isolate sufficient numbers of the naïve CD25+CD4+ T cell subset for studies other than the microsuppression assay. In future, isolation of these cells would enable a number of further studies including measurement of cytokine production under different conditions, and comprehensive global gene expression profiling using RNA-sequencing methods.

7.7. Limitations and future direction of study.

In addition to the caveats and challenges of interpreting data from limited patient samples from a rare disease, there are broader challenges in studying a

heterogeneous autoimmune disorder with patients on a variety of different treatment regimens. GPA patient samples used in this study are from individuals who have had active disease for some time (as opposed to those in remission after Rituximab (RTX) treatment, or having recently relapsed). GPA is a highly heterogeneous autoimmune disease and is life-threatening without treatment. However, due to an absence of clear diagnosis criteria, diagnosis of GPA remains challenging (Houben *et al.*, 2016). For this reason, when patients are first diagnosed with GPA, most of them have already been prescribed medications such as steroids, immunosuppressive drugs and antibiotics. Therefore, interpreting scientific data from GPA patient samples is challenging because it is often not clear whether observations are the result of GPA pathogenesis or the effects of medication. Indeed, all patients in this study were given combinations of steroids, immunosuppressive drugs and antibiotics (but they had either not received RTX, or had received RTX but relapsed). Therefore, it will be critical to include additional groups of patients who are in remission or who have recently relapsed in future studies.

It will also be important to compare observations in GPA with other autoimmune diseases such as lupus where patients may have similar medication histories but the disease pathology is different. One interesting finding from this study was that lipid metabolism may be dysregulated in GPA (Chapter 6). However, the fact that steroid treatment has been shown to affect lipid metabolism should be considered (Basdevant, 1992). That said, a previous study has associated AAV disease activity with metabolic syndrome (MetS), low levels of HDL, high triglyceride levels, hypertension, central obesity, and high glucose levels. The authors show that those AAV patients with MetS had high levels of inflammation markers such as C-reactive

protein (CRP) (Petermann Smits *et al.*, 2013), and importantly they also showed that their observations were independent of steroid treatment. High levels of acute phase proteins were also observed in GPA in this study, and therefore dysregulation of metabolism may represent an underlying cause of GPA pathology. However, since some SLE patients have also been associated with MetS (Mobini *et al.*, 2018), further work is required to determine whether these changes in metabolism are specific to GPA or represent a broader hallmark of inflammatory autoimmune disease.

Another major (but largely unavoidable) limitation of data from this study is that CD4+ T cells were obtained from peripheral blood not inflammatory tissues. In chronic inflammation, it is expected that effector CD4+ T cells will be recruited to inflammatory tissues (Austrup *et al.*, 1997; Suzuki *et al.*, 1999; Hamann and Syrbe, 2000) so the balance between CD4+ T cell subsets in inflammatory tissues may differ from peripheral blood. In this study, gut homing receptor ITGB7 was shown to be highly expressed in GPA naive CD4+ T cells (Figure 4.5d). In addition, it has been reported that phenotypes of circulating Tregs may differ from tissue resident Tregs (Pesenacker *et al.*, 2015). Studies using peripheral blood may not re-create the local inflammatory environment within a granuloma, which may affect phenotypes and functions of CD4+ T cells. Within a granuloma, the following mechanism for CD4+ T cell polarisation has been proposed; PR3 positive apoptotic neutrophils become engulfed by macrophages, leading to production of pro-inflammatory cytokines such as IL-1β and IL-6 (phagocytic macrophages typically secrete both pro- and anti-inflammatory cytokines (Millet *et al.*, 2015)). IL-1β and IL-6 induce Th2/Th17 polarisation of CD4+ T cells and moreover, these macrophages also secrete granulocyte-colony stimulating factor (G-CSF),

recruiting more neutrophils to the granuloma (Millet *et al.*, 2015). That said, the study by Millet *et al* was performed *in vitro* using co-culture models. And since GM-CSF has been shown to upregulate PR3 on neutrophils more effectively than G-CSF (Hellmich *et al.*, 2000), the current study extends this hypothesis, since GPA Tregs appear to lack the ability to suppress GM-CSF production by CD4+ T cells.

Therefore, the observations from the current study should be interpreted bearing in mind the caveats discussed above. Ultimately, future studies with inflammatory tissue from GPA patients may be required to fully understand the pathogenesis of this disease.

7.8. Conclusion

In conclusion, the work presented in this thesis has shown that there is a functional imbalance between Tregs and Tfh cell subsets in GPA and has sought to understand the mechanisms responsible for this imbalance. There is evidence that intrinsic molecular changes to signalling pathways and metabolism within naïve CD4+ T cells in GPA may be driving this imbalance. Reduced activation of STAT5 (but normal activation of STAT3) was observed in naive CD4+ T cells in GPA, potentially leading these cells to adopt Tfh like phenotypes by increasing BCL6 and IL-21 expression (Figure 7.1a). Analysis of Treg function in GPA indicated that while there were no increases in Treg numbers and GPA Tregs can efficiently suppress the proliferation of effector T cells (Figure 7.1b), significantly, they fail to inhibit the expression of a specific pro-inflammatory cytokine GM-CSF (Figure 7.1c). These observations could provide a framework to address the functional imbalance between Tregs and Tfh subsets therapeutically. This study has also shown that naive CD4+ cells in GPA have higher expression of CD25 compared to

those from healthy individuals (Figure 7.1d), and that these naive CD25+CD4+ T cells are unlikely a subset of Tregs although their function needs to be further investigated.

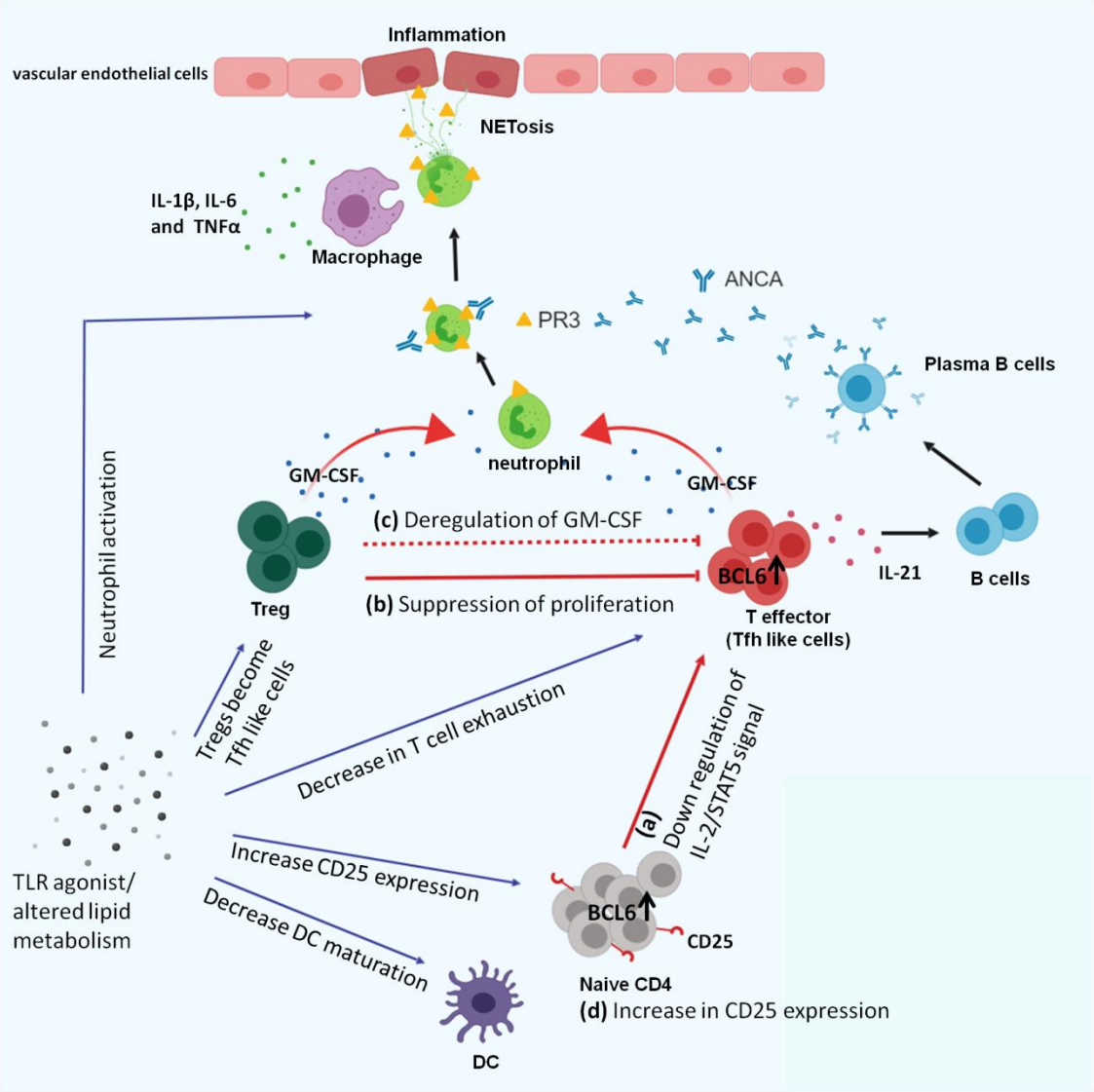

Figure 7.1 Schematic of GPA pathology highlighting contributions from this study.

Red arrows represent data from this study analysing phenotype and function of GPA CD4+ T cells. Blue arrows represent hypothetical outcomes based on preliminary data from analysis of GPA plasma.

8. References

ABBAS, A. K. et al. Revisiting IL-2: Biology and therapeutic prospects. **Sci Immunol,** v. 3, n. 25, Jul 6 2018. ISSN 2470-9468 (Electronic)
2470-9468 (Linking). Available at: < https://www.ncbi.nlm.nih.gov/pubmed/29980618 >.

ABDULAHAD, W. H. et al. Increased frequency of circulating IL-21 producing Th-cells in patients with granulomatosis with polyangiitis (GPA). **Arthritis Res Ther,** v. 15, n. 3, p. R70, 2013. ISSN 1478-6362 (Electronic)
1478-6354 (Linking). Available at: < http://www.ncbi.nlm.nih.gov/pubmed/23799890 >.

ABDULAHAD, W. H.; STEGEMAN, C. A.; KALLENBERG, C. G. Review article: The role of CD4(+) T cells in ANCA-associated systemic vasculitis. **Nephrology (Carlton),** v. 14, n. 1, p. 26-32, Feb 2009. ISSN 1440-1797 (Electronic)
1320-5358 (Linking). Available at: < https://www.ncbi.nlm.nih.gov/pubmed/19143940 >.

ABDULAHAD, W. H. et al. Skewed distribution of Th17 lymphocytes in patients with Wegener's granulomatosis in remission. **Arthritis Rheum,** v. 58, n. 7, p. 2196-205, Jul 2008. ISSN 0004-3591 (Print)
0004-3591 (Linking). Available at: < http://www.ncbi.nlm.nih.gov/pubmed/18576340 >.

ABDULAHAD, W. H. et al. Functional defect of circulating regulatory CD4+ T cells in patients with Wegener's granulomatosis in remission. **Arthritis Rheum,** v. 56, n. 6, p. 2080-91, Jun 2007. ISSN 0004-3591 (Print)
0004-3591 (Linking). Available at: < http://www.ncbi.nlm.nih.gov/pubmed/17530650 >.

ABDULAHAD, W. H. et al. Persistent expansion of CD4+ effector memory T cells in Wegener's granulomatosis. **Kidney Int,** v. 70, n. 5, p. 938-47, Sep 2006. ISSN 0085-2538 (Print)
0085-2538 (Linking). Available at: < http://www.ncbi.nlm.nih.gov/pubmed/16837919 >.

ADALID-PERALTA, L. et al. Mechanisms underlying the induction of regulatory T cells and its relevance in the adaptive immune response in parasitic infections. **Int J Biol Sci,** v. 7, n. 9, p. 1412-26, 2011. ISSN 1449-2288 (Electronic). Available at: < http://www.ncbi.nlm.nih.gov/pubmed/22110392 >.

AFZALI, B. et al. CD161 expression characterizes a subpopulation of human regulatory T cells that produces IL-17 in a STAT3-dependent manner. **Eur J Immunol,** v. 43, n. 8, p. 2043-54, Aug 2013. ISSN 1521-4141 (Electronic)
0014-2980 (Linking). Available at: < http://www.ncbi.nlm.nih.gov/pubmed/23677517 >.

AI, W. et al. Optimal method to stimulate cytokine production and its use in immunotoxicity assessment. **Int J Environ Res Public Health,** v. 10, n. 9, p. 3834-42, Aug 27 2013. ISSN 1660-4601 (Electronic)
1660-4601 (Linking). Available at: < https://www.ncbi.nlm.nih.gov/pubmed/23985769 >.

AKIRA, S. et al. Molecular cloning of APRF, a novel IFN-stimulated gene factor 3 p91-related transcription factor involved in the gp130-mediated signaling pathway. **Cell,** v. 77, n. 1, p. 63-71, Apr 8 1994. ISSN 0092-8674 (Print)
0092-8674 (Linking). Available at: < https://www.ncbi.nlm.nih.gov/pubmed/7512451 >.

AMLOT, P. L. et al. Activation antigen expression on human T cells. I. Analysis by two-colour flow cytometry of umbilical cord blood, adult blood and lymphoid tissue. **Clin Exp Immunol,** v. 105, n. 1, p. 176-82, Jul 1996. ISSN 0009-9104 (Print)
0009-9104 (Linking). Available at: < https://www.ncbi.nlm.nih.gov/pubmed/8697627 >.

AUSTRUP, F. et al. P- and E-selectin mediate recruitment of T-helper-1 but not T-helper-2 cells into inflammed tissues. **Nature,** v. 385, n. 6611, p. 81-3, Jan 2 1997. ISSN 0028-0836 (Print)
0028-0836 (Linking). Available at: < https://www.ncbi.nlm.nih.gov/pubmed/8985251 >.

AVRAMEAS, S. Autopolyreactivity Confers a Holistic Role in the Immune System. **Scand J Immunol,** v. 83, n. 4, p. 227-34, Apr 2016. ISSN 1365-3083 (Electronic)
0300-9475 (Linking). Available at: < https://www.ncbi.nlm.nih.gov/pubmed/26808310 >.

AVRAMEAS, S.; ALEXOPOULOS, H.; MOUTSOPOULOS, H. M. Natural Autoantibodies: An Undersugn Hero of the Immune System and Autoimmune Disorders-A Point of View. **Front Immunol,** v. 9, p. 1320, 2018. ISSN 1664-3224 (Print)
1664-3224 (Linking). Available at: < https://www.ncbi.nlm.nih.gov/pubmed/29946320 >.

BACH, J. F. The hygiene hypothesis in autoimmunity: the role of pathogens and commensals. **Nat Rev Immunol,** v. 18, n. 2, p. 105-120, Feb 2018. ISSN 1474-1741 (Electronic)
1474-1733 (Linking). Available at: < https://www.ncbi.nlm.nih.gov/pubmed/29034905 >.

BAGLEY, K. C. et al. Calcium signaling through phospholipase C activates dendritic cells to mature and is necessary for the activation and maturation of dendritic cells induced by diverse agonists. **Clin Diagn Lab Immunol,** v. 11, n. 1, p. 77-82, Jan 2004. ISSN 1071-412X (Print)
1071-412X (Linking). Available at: < https://www.ncbi.nlm.nih.gov/pubmed/14715548 >.

BALLESTEROS-TATO, A. et al. Interleukin-2 inhibits germinal center formation by limiting T follicular helper cell differentiation. **Immunity,** v. 36, n. 5, p. 847-56, May 25 2012. ISSN 1097-4180 (Electronic)
1074-7613 (Linking). Available at: < https://www.ncbi.nlm.nih.gov/pubmed/22464171 >.

BANTUG, G. R. et al. The spectrum of T cell metabolism in health and disease. **Nat Rev Immunol,** v. 18, n. 1, p. 19-34, Jan 2018. ISSN 1474-1741 (Electronic)
1474-1733 (Linking). Available at: < https://www.ncbi.nlm.nih.gov/pubmed/28944771 >.

BASDEVANT, A. Steroids and lipid metabolism: mechanism of action. **Int J Fertil,** v. 37 Suppl 2, p. 93-7, 1992. ISSN 0020-725X (Print)
0020-725X (Linking). Available at: < https://www.ncbi.nlm.nih.gov/pubmed/1354664 >.

BATISTA, F. D.; HARWOOD, N. E. The who, how and where of antigen presentation to B cells. **Nat Rev Immunol,** v. 9, n. 1, p. 15-27, Jan 2009. ISSN 1474-1741 (Electronic)
1474-1733 (Linking). Available at: < https://www.ncbi.nlm.nih.gov/pubmed/19079135 >.

BATTAGLIA, M.; STABILINI, A.; TRESOLDI, E. Expanding human T regulatory cells with the mTOR-inhibitor rapamycin. **Methods Mol Biol,** v. 821, p. 279-93, 2012. ISSN 1940-6029 (Electronic)
1064-3745 (Linking). Available at: < https://www.ncbi.nlm.nih.gov/pubmed/22125072 >.

BERDEN, A. E. et al. Cellular immunity in Wegener's granulomatosis: characterizing T lymphocytes. **Arthritis Rheum,** v. 60, n. 6, p. 1578-87, Jun 2009. ISSN 0004-3591 (Print)
0004-3591 (Linking). Available at: < http://www.ncbi.nlm.nih.gov/pubmed/19479864 >.

BERTI, A. et al. Brief Report: Circulating Cytokine Profiles and Antineutrophil Cytoplasmic Antibody Specificity in Patients With Antineutrophil Cytoplasmic Antibody-Associated Vasculitis. **Arthritis Rheumatol,** v. 70, n. 7, p. 1114-1121, Jul 2018. ISSN 2326-5205 (Electronic)
2326-5191 (Linking). Available at: < https://www.ncbi.nlm.nih.gov/pubmed/29693324 >.

BORIES, D. et al. Down-regulation of a serine protease, myeloblastin, causes growth arrest and differentiation of promyelocytic leukemia cells. **Cell,** v. 59, n. 6, p. 959-68, Dec 22 1989. ISSN 0092-8674 (Print)
0092-8674 (Linking). Available at: < https://www.ncbi.nlm.nih.gov/pubmed/2598267 >.

BRAUDEAU, C. et al. Dysregulated Responsiveness of Circulating Dendritic Cells to Toll-Like Receptors in ANCA-Associated Vasculitis. **Front Immunol,** v. 8, p. 102, 2017. ISSN 1664-3224 (Print)
1664-3224 (Linking). Available at: < https://www.ncbi.nlm.nih.gov/pubmed/28232832 >.

BRINGANS, S. D. et al. Comprehensive mass spectrometry based biomarker discovery and validation platform as applied to diabetic kidney disease. **EuPA Open Proteom,** v. 14, p. 1-10, Mar 2017. ISSN 2212-9685 (Electronic)
2212-9685 (Linking). Available at: < https://www.ncbi.nlm.nih.gov/pubmed/29900119 >.

BROEDERS, S. et al. Revised 2017 international consensus on ANCA testing in small vessel vasculitis: support from an external quality assessment. **Ann Rheum Dis**, Sep 5 2018. ISSN 1468-2060 (Electronic)
0003-4967 (Linking). Available at: < https://www.ncbi.nlm.nih.gov/pubmed/30185413 >.

BRUSTLE, A. et al. The development of inflammatory T(H)-17 cells requires interferon-regulatory factor 4. **Nat Immunol,** v. 8, n. 9, p. 958-66, Sep 2007. ISSN 1529-2908 (Print)
1529-2908 (Linking). Available at: < https://www.ncbi.nlm.nih.gov/pubmed/17676043 >.

BUCK, M. D.; O'SULLIVAN, D.; PEARCE, E. L. T cell metabolism drives immunity. **J Exp Med,** v. 212, n. 9, p. 1345-60, Aug 24 2015. ISSN 1540-9538 (Electronic)
0022-1007 (Linking). Available at: < https://www.ncbi.nlm.nih.gov/pubmed/26261266 >.

CALKIN, A. C.; TONTONOZ, P. Transcriptional integration of metabolism by the nuclear sterol-activated receptors LXR and FXR. **Nat Rev Mol Cell Biol,** v. 13, n. 4, p. 213-24, Mar 14 2012. ISSN 1471-0080 (Electronic)
1471-0072 (Linking). Available at: < https://www.ncbi.nlm.nih.gov/pubmed/22414897 >.

CAPRIOLI, F. et al. Autocrine regulation of IL-21 production in human T lymphocytes. **J Immunol,** v. 180, n. 3, p. 1800-7, Feb 1 2008. ISSN 0022-1767 (Print)
0022-1767 (Linking). Available at: < https://www.ncbi.nlm.nih.gov/pubmed/18209077 >.

CARTIN-CEBA, R.; PEIKERT, T.; SPECKS, U. Pathogenesis of ANCA-associated vasculitis. **Curr Rheumatol Rep,** v. 14, n. 6, p. 481-93, Dec 2012. ISSN 1534-6307 (Electronic)
1523-3774 (Linking). Available at: < http://www.ncbi.nlm.nih.gov/pubmed/22927039 >.

CERUTTI, A.; COLS, M.; PUGA, I. Marginal zone B cells: virtues of innate-like antibody-producing lymphocytes. **Nat Rev Immunol,** v. 13, n. 2, p. 118-32, Feb 2013. ISSN 1474-1741 (Electronic)
1474-1733 (Linking). Available at: < https://www.ncbi.nlm.nih.gov/pubmed/23348416 >.

CHAVELE, K. M.; MERRY, E.; EHRENSTEIN, M. R. Cutting edge: circulating plasmablasts induce the differentiation of human T follicular helper cells via IL-6 production. **J Immunol,** v. 194, n. 6, p. 2482-5, Mar 15 2015. ISSN 1550-6606 (Electronic)

0022-1767 (Linking). Available at: < https://www.ncbi.nlm.nih.gov/pubmed/25681343 >.

CHEN, G. et al. The NF-kappaB transcription factor c-Rel is required for Th17 effector cell development in experimental autoimmune encephalomyelitis. **J Immunol,** v. 187, n. 9, p. 4483-91, Nov 1 2011. ISSN 1550-6606 (Electronic)
0022-1767 (Linking). Available at: < https://www.ncbi.nlm.nih.gov/pubmed/21940679 >.

CHEN, L.; FLIES, D. B. Molecular mechanisms of T cell co-stimulation and co-inhibition. **Nat Rev Immunol,** v. 13, n. 4, p. 227-42, Apr 2013. ISSN 1474-1741 (Electronic)
1474-1733 (Linking). Available at: < https://www.ncbi.nlm.nih.gov/pubmed/23470321 >.

CHOI, Y. S.; YANG, J. A.; CROTTY, S. Dynamic regulation of Bcl6 in follicular helper CD4 T (Tfh) cells. **Curr Opin Immunol,** v. 25, n. 3, p. 366-72, Jun 2013. ISSN 1879-0372 (Electronic)
0952-7915 (Linking). Available at: < http://www.ncbi.nlm.nih.gov/pubmed/23688737 >.

CHRISTIE, D.; ZHU, J. Transcriptional regulatory networks for CD4 T cell differentiation. **Curr Top Microbiol Immunol,** v. 381, p. 125-72, 2014. ISSN 0070-217X (Print)
0070-217X (Linking). Available at: < https://www.ncbi.nlm.nih.gov/pubmed/24839135 >.

COHEN, A. C. et al. Cutting edge: Decreased accumulation and regulatory function of CD4+ CD25(high) T cells in human STAT5b deficiency. **J Immunol,** v. 177, n. 5, p. 2770-4, Sep 1 2006. ISSN 0022-1767 (Print)
0022-1767 (Linking). Available at: < https://www.ncbi.nlm.nih.gov/pubmed/16920911 >.

COHEN, S. B. et al. IL-10 enhances expression of the IL-2 receptor alpha chain on T cells. **Immunology,** v. 83, n. 3, p. 329-32, Nov 1994. ISSN 0019-2805 (Print)
0019-2805 (Linking). Available at: < https://www.ncbi.nlm.nih.gov/pubmed/7835955 >.

COLAFRANCESCO, S. et al. IL-18 Serum Level in Adult Onset Still's Disease: A Marker of Disease Activity. **Int J Inflam,** v. 2012, p. 156890, 2012. ISSN 2042-0099 (Electronic)
2042-0099 (Linking). Available at: < https://www.ncbi.nlm.nih.gov/pubmed/22762008 >.

COOLEY, I. D.; READ, K. A.; OESTREICH, K. J. Trans-presentation of IL-15 modulates STAT5 activation and Bcl-6 expression in TH1 cells. **Sci Rep,** v. 5, p. 15722, Oct 26 2015. ISSN 2045-2322 (Electronic)
2045-2322 (Linking). Available at: < https://www.ncbi.nlm.nih.gov/pubmed/26500048 >.

COQUET, J. M. et al. IL-21 is produced by NKT cells and modulates NKT cell activation and cytokine production. **J Immunol,** v. 178, n. 5, p. 2827-34, Mar 1 2007. ISSN 0022-1767 (Print)
0022-1767 (Linking). Available at: < https://www.ncbi.nlm.nih.gov/pubmed/17312126 >.

COX, M. A.; ZAJAC, A. J. Shaping successful and unsuccessful CD8 T cell responses following infection. **J Biomed Biotechnol,** v. 2010, p. 159152, 2010. ISSN 1110-7251 (Electronic)
1110-7243 (Linking). Available at: < https://www.ncbi.nlm.nih.gov/pubmed/20379363 >.

CRAWFORD, A. et al. Molecular and transcriptional basis of CD4(+) T cell dysfunction during chronic infection. **Immunity,** v. 40, n. 2, p. 289-302, Feb 20 2014. ISSN 1097-4180 (Electronic)
1074-7613 (Linking). Available at: < https://www.ncbi.nlm.nih.gov/pubmed/24530057 >.

CROTTY, S.; JOHNSTON, R. J.; SCHOENBERGER, S. P. Effectors and memories: Bcl-6 and Blimp-1 in T and B lymphocyte differentiation. **Nat Immunol,** v. 11, n. 2, p. 114-20, Feb 2010. ISSN 1529-2916 (Electronic)
1529-2908 (Linking). Available at: < https://www.ncbi.nlm.nih.gov/pubmed/20084069 >.

CSERNOK, E.; LAMPRECHT, P.; GROSS, W. L. Clinical and immunological features of drug-induced and infection-induced proteinase 3-antineutrophil cytoplasmic antibodies and myeloperoxidase-antineutrophil cytoplasmic antibodies and vasculitis. **Curr Opin Rheumatol,** v. 22, n. 1, p. 43-8, Jan 2010. ISSN 1531-6963 (Electronic)
1040-8711 (Linking). Available at: < https://www.ncbi.nlm.nih.gov/pubmed/19770659 >.

CUADRADO, E. et al. Proteomic Analyses of Human Regulatory T Cells Reveal Adaptations in Signaling Pathways that Protect Cellular Identity. **Immunity,** v. 48, n. 5, p. 1046-1059 e6, May 15 2018. ISSN 1097-4180 (Electronic)
1074-7613 (Linking). Available at: < https://www.ncbi.nlm.nih.gov/pubmed/29752063 >.

DANG, E. V. et al. Control of T(H)17/T(reg) balance by hypoxia-inducible factor 1. **Cell,** v. 146, n. 5, p. 772-84, Sep 2 2011. ISSN 1097-4172 (Electronic)
0092-8674 (Linking). Available at: < https://www.ncbi.nlm.nih.gov/pubmed/21871655 >.

DE BONT, C. M.; BOELENS, W. C.; PRUIJN, G. J. M. NETosis, complement, and coagulation: a triangular relationship. **Cell Mol Immunol,** v. 16, n. 1, p. 19-27, Jan 2019. ISSN 2042-0226 (Electronic)
1672-7681 (Linking). Available at: < https://www.ncbi.nlm.nih.gov/pubmed/29572545 >.

DE ROSA, S. C. et al. 11-color, 13-parameter flow cytometry: identification of human naive T cells by phenotype, function, and T-cell receptor diversity. **Nat Med,** v. 7, n. 2, p. 245-8, Feb 2001. ISSN 1078-8956 (Print)
1078-8956 (Linking). Available at: < https://www.ncbi.nlm.nih.gov/pubmed/11175858 >.

DELGADO-RIZO, V. et al. Neutrophil Extracellular Traps and Its Implications in Inflammation: An Overview. **Front Immunol,** v. 8, p. 81, 2017. ISSN 1664-3224 (Print)
1664-3224 (Linking). Available at: < https://www.ncbi.nlm.nih.gov/pubmed/28220120 >.

DI MARTINO, A.; MERLINI, L.; FALDINI, C. Autoimmunity in intervertebral disc herniation: from bench to bedside. **Expert Opin Ther Targets,** v. 17, n. 12, p. 1461-70, Dec 2013. ISSN 1744-7631 (Electronic)
1472-8222 (Linking). Available at: < https://www.ncbi.nlm.nih.gov/pubmed/23991673 >.

DIAS, S. et al. Effector Regulatory T Cell Differentiation and Immune Homeostasis Depend on the Transcription Factor Myb. **Immunity,** v. 46, n. 1, p. 78-91, Jan 17 2017. ISSN 1097-4180 (Electronic)
1074-7613 (Linking). Available at: < https://www.ncbi.nlm.nih.gov/pubmed/28099866 >.

DIEHL, S. A. et al. IL-6 triggers IL-21 production by human CD4+ T cells to drive STAT3-dependent plasma cell differentiation in B cells. **Immunol Cell Biol,** v. 90, n. 8, p. 802-11, Sep 2012. ISSN 1440-1711 (Electronic)
0818-9641 (Linking). Available at: < https://www.ncbi.nlm.nih.gov/pubmed/22491065 >.

DITORO, D. et al. Differential IL-2 expression defines developmental fates of follicular versus nonfollicular helper T cells. **Science,** v. 361, n. 6407, Sep 14 2018. ISSN 1095-9203 (Electronic)
0036-8075 (Linking). Available at: < https://www.ncbi.nlm.nih.gov/pubmed/30213884 >.

DUMITRU, C.; KABAT, A. M.; MALOY, K. J. Metabolic Adaptations of CD4(+) T Cells in Inflammatory Disease. **Front Immunol,** v. 9, p. 540, 2018. ISSN 1664-3224 (Print)
1664-3224 (Linking). Available at: < https://www.ncbi.nlm.nih.gov/pubmed/29599783 >.

DUNKELBERGER, J. R.; SONG, W. C. Complement and its role in innate and adaptive immune responses. **Cell Res,** v. 20, n. 1, p. 34-50, Jan 2010. ISSN 1748-7838 (Electronic)
1001-0602 (Linking). Available at: < https://www.ncbi.nlm.nih.gov/pubmed/20010915 >.

DUPAGE, M.; BLUESTONE, J. A. Harnessing the plasticity of CD4 T cells to treat immune-mediated disease. **Nat Rev Immunol**, Feb 15 2016. ISSN 1474-1741 (Electronic)
1474-1733 (Linking). Available at: < http://www.ncbi.nlm.nih.gov/pubmed/26875830 >.

DURANT, S. et al. Apoptosis-induced proteinase 3 membrane expression is independent from degranulation. **J Leukoc Biol,** v. 75, n. 1, p. 87-98, Jan 2004. ISSN 0741-5400 (Print)
0741-5400 (Linking). Available at: < https://www.ncbi.nlm.nih.gov/pubmed/14525959 >.

EYERICH, K.; EYERICH, S. Th22 cells in allergic disease. **Allergo J Int,** v. 24, n. 1, p. 1-7, 2015. ISSN 2197-0378 (Print)
2197-0378 (Linking). Available at: < https://www.ncbi.nlm.nih.gov/pubmed/26120541 >.

FAHEY, L. M. et al. Viral persistence redirects CD4 T cell differentiation toward T follicular helper cells. **J Exp Med,** v. 208, n. 5, p. 987-99, May 9 2011. ISSN 1540-9538 (Electronic)
0022-1007 (Linking). Available at: < https://www.ncbi.nlm.nih.gov/pubmed/21536743 >.

FLOSSMANN, O. et al. Development of comprehensive disease assessment in systemic vasculitis. **Postgrad Med J,** v. 84, n. 989, p. 143-52, Mar 2008. ISSN 1469-0756 (Electronic)
0032-5473 (Linking). Available at: < https://www.ncbi.nlm.nih.gov/pubmed/18372486 >.

FONSECA, V. R. et al. Human blood Tfr cells are indicators of ongoing humoral activity not fully licensed with suppressive function. **Sci Immunol,** v. 2, n. 14, Aug 11 2017. ISSN 2470-9468 (Electronic)
2470-9468 (Linking). Available at: < https://www.ncbi.nlm.nih.gov/pubmed/28802258 >.

FREEMAN, M. W.; MOORE, K. J. eLiXiRs for restraining inflammation. **Nat Med,** v. 9, n. 2, p. 168-9, Feb 2003. ISSN 1078-8956 (Print)
1078-8956 (Linking). Available at: < https://www.ncbi.nlm.nih.gov/pubmed/12563335 >.

GADDIS, D. E. et al. Apolipoprotein AI prevents regulatory to follicular helper T cell switching during atherosclerosis. **Nat Commun,** v. 9, n. 1, p. 1095, Mar 15 2018. ISSN 2041-1723 (Electronic)
2041-1723 (Linking). Available at: < https://www.ncbi.nlm.nih.gov/pubmed/29545616 >.

GANZ, T. Defensins: antimicrobial peptides of innate immunity. **Nat Rev Immunol,** v. 3, n. 9, p. 710-20, Sep 2003. ISSN 1474-1733 (Print)
1474-1733 (Linking). Available at: < https://www.ncbi.nlm.nih.gov/pubmed/12949495 >.

GAYO, A. et al. Glucocorticoids increase IL-10 expression in multiple sclerosis patients with acute relapse. **J Neuroimmunol,** v. 85, n. 2, p. 122-30, May 15 1998. ISSN 0165-5728 (Print)
0165-5728 (Linking). Available at: < https://www.ncbi.nlm.nih.gov/pubmed/9630160 >.

GEETHA, D. et al. Current therapy of granulomatosis with polyangiitis and microscopic polyangiitis: the role of rituximab. **J Nephrol,** v. 28, n. 1, p. 17-27, Feb 2015. ISSN 1724-6059 (Electronic)
1121-8428 (Linking). Available at: < https://www.ncbi.nlm.nih.gov/pubmed/25185728 >.

GERMAIN, R. N. T-cell development and the CD4-CD8 lineage decision. **Nat Rev Immunol,** v. 2, n. 5, p. 309-22, May 2002. ISSN 1474-1733 (Print)

1474-1733 (Linking). Available at: < https://www.ncbi.nlm.nih.gov/pubmed/12033737 >.

GERRIETS, V. A. et al. Foxp3 and Toll-like receptor signaling balance Treg cell anabolic metabolism for suppression. **Nat Immunol,** v. 17, n. 12, p. 1459-1466, Dec 2016. ISSN 1529-2916 (Electronic)
1529-2908 (Linking). Available at: < https://www.ncbi.nlm.nih.gov/pubmed/27695003 >.

GEYER, P. E. et al. Revisiting biomarker discovery by plasma proteomics. **Mol Syst Biol,** v. 13, n. 9, p. 942, Sep 26 2017. ISSN 1744-4292 (Electronic)
1744-4292 (Linking). Available at: < https://www.ncbi.nlm.nih.gov/pubmed/28951502 >.

GODSELL, J. et al. Clinical associations of IL-10 and IL-37 in systemic lupus erythematosus. **Sci Rep,** v. 6, p. 34604, Oct 6 2016. ISSN 2045-2322 (Electronic)
2045-2322 (Linking). Available at: < https://www.ncbi.nlm.nih.gov/pubmed/27708376 >.

GONZALEZ-NAVAJAS, J. M. et al. Immunomodulatory functions of type I interferons. **Nat Rev Immunol,** v. 12, n. 2, p. 125-35, Jan 6 2012. ISSN 1474-1741 (Electronic)
1474-1733 (Linking). Available at: < https://www.ncbi.nlm.nih.gov/pubmed/22222875 >.

GRANT, C. R. et al. Regulatory T-cells in autoimmune diseases: challenges, controversies and--yet--unanswered questions. **Autoimmun Rev,** v. 14, n. 2, p. 105-16, Feb 2015. ISSN 1873-0183 (Electronic)
1568-9972 (Linking). Available at: < https://www.ncbi.nlm.nih.gov/pubmed/25449680 >.

GRANUCCI, F. et al. Early IL-2 production by mouse dendritic cells is the result of microbial-induced priming. **J Immunol,** v. 170, n. 10, p. 5075-81, May 15 2003. ISSN 0022-1767 (Print)
0022-1767 (Linking). Available at: < https://www.ncbi.nlm.nih.gov/pubmed/12734352 >.

GRAYSON, P. C. et al. Neutrophil-Related Gene Expression and Low-Density Granulocytes Associated With Disease Activity and Response to Treatment in Antineutrophil Cytoplasmic Antibody-Associated Vasculitis. **Arthritis Rheumatol,** v. 67, n. 7, p. 1922-32, Jul 2015. ISSN 2326-5205 (Electronic)
2326-5191 (Linking). Available at: < https://www.ncbi.nlm.nih.gov/pubmed/25891759 >.

GRECZMIEL, U. et al. Sustained T follicular helper cell response is essential for control of chronic viral infection. **Sci Immunol,** v. 2, n. 18, Dec 1 2017. ISSN 2470-9468 (Electronic)
2470-9468 (Linking). Available at: < https://www.ncbi.nlm.nih.gov/pubmed/29196449 >.

GRIGORIAN, A. et al. Control of T Cell-mediated autoimmunity by metabolite flux to N-glycan biosynthesis. **J Biol Chem,** v. 282, n. 27, p. 20027-35, Jul 6 2007. ISSN 0021-9258 (Print)
0021-9258 (Linking). Available at: < https://www.ncbi.nlm.nih.gov/pubmed/17488719 >.

GROVER, S. P.; MACKMAN, N. Neutrophils, NETs, and immunothrombosis. **Blood,** v. 132, n. 13, p. 1360-1361, Sep 27 2018. ISSN 1528-0020 (Electronic)
0006-4971 (Linking). Available at: < https://www.ncbi.nlm.nih.gov/pubmed/30262582 >.

HAMANN, A.; SYRBE, U. T-cell trafficking into sites of inflammation. **Rheumatology (Oxford),** v. 39, n. 7, p. 696-9, Jul 2000. ISSN 1462-0324 (Print)
1462-0324 (Linking). Available at: < https://www.ncbi.nlm.nih.gov/pubmed/10908685 >.

HE, J. et al. Circulating precursor CCR7(lo)PD-1(hi) CXCR5(+) CD4(+) T cells indicate Tfh cell activity and promote antibody responses upon antigen reexposure. **Immunity,** v. 39, n. 4, p. 770-81, Oct 17 2013. ISSN 1097-4180 (Electronic)

1074-7613 (Linking). Available at: < http://www.ncbi.nlm.nih.gov/pubmed/24138884 >.

HE, L. et al. Extracellular matrix protein 1 promotes follicular helper T cell differentiation and antibody production. **Proc Natl Acad Sci U S A,** v. 115, n. 34, p. 8621-8626, Aug 21 2018. ISSN 1091-6490 (Electronic)
0027-8424 (Linking). Available at: < https://www.ncbi.nlm.nih.gov/pubmed/30087185 >.

HEESTERS, B. A. et al. Antigen Presentation to B Cells. **Trends Immunol,** v. 37, n. 12, p. 844-854, Dec 2016. ISSN 1471-4981 (Electronic)
1471-4906 (Linking). Available at: < https://www.ncbi.nlm.nih.gov/pubmed/27793570 >.

HELLMICH, B. et al. Granulocyte-macrophage colony-stimulating factor (GM-CSF) but not granulocyte colony-stimulating factor (G-CSF) induces plasma membrane expression of proteinase 3 (PR3) on neutrophils in vitro. **Clin Exp Immunol,** v. 120, n. 2, p. 392-8, May 2000. ISSN 0009-9104 (Print)
0009-9104 (Linking). Available at: < https://www.ncbi.nlm.nih.gov/pubmed/10792393 >.

HESS, C.; KEMPER, C. Complement-Mediated Regulation of Metabolism and Basic Cellular Processes. **Immunity,** v. 45, n. 2, p. 240-54, Aug 16 2016. ISSN 1097-4180 (Electronic)
1074-7613 (Linking). Available at: < https://www.ncbi.nlm.nih.gov/pubmed/27533012 >.

HOUBEN, E. et al. Diagnosing ANCA-associated vasculitis in ANCA positive patients: A retrospective analysis on the role of clinical symptoms and the ANCA titre. **Medicine (Baltimore),** v. 95, n. 40, p. e5096, Oct 2016. ISSN 1536-5964 (Electronic)
0025-7974 (Linking). Available at: < https://www.ncbi.nlm.nih.gov/pubmed/27749588 >.

HOWIE, D. et al. The Role of Lipid Metabolism in T Lymphocyte Differentiation and Survival. **Front Immunol,** v. 8, p. 1949, 2017. ISSN 1664-3224 (Print)
1664-3224 (Linking). Available at: < https://www.ncbi.nlm.nih.gov/pubmed/29375572 >.

HSIEH, C. S.; LEE, H. M.; LIO, C. W. Selection of regulatory T cells in the thymus. **Nat Rev Immunol,** v. 12, n. 3, p. 157-67, Feb 10 2012. ISSN 1474-1741 (Electronic)
1474-1733 (Linking). Available at: < https://www.ncbi.nlm.nih.gov/pubmed/22322317 >.

IANNELLA, G. et al. Granulomatosis with polyangiitis and facial palsy: Literature review and insight in the autoimmune pathogenesis. **Autoimmun Rev,** v. 15, n. 7, p. 621-31, Jul 2016. ISSN 1873-0183 (Electronic)
1568-9972 (Linking). Available at: < https://www.ncbi.nlm.nih.gov/pubmed/26851550 >.

ISE, W. et al. The transcription factor BATF controls the global regulators of class-switch recombination in both B cells and T cells. **Nat Immunol,** v. 12, n. 6, p. 536-43, Jun 2011. ISSN 1529-2916 (Electronic)
1529-2908 (Linking). Available at: < https://www.ncbi.nlm.nih.gov/pubmed/21572431 >.

JAMESON, S. C.; MASOPUST, D. Understanding Subset Diversity in T Cell Memory. **Immunity,** v. 48, n. 2, p. 214-226, Feb 20 2018. ISSN 1097-4180 (Electronic)
1074-7613 (Linking). Available at: < https://www.ncbi.nlm.nih.gov/pubmed/29466754 >.

JENKS, J. A. et al. Differentiating the roles of STAT5B and STAT5A in human CD4+ T cells. **Clin Immunol,** v. 148, n. 2, p. 227-36, Aug 2013. ISSN 1521-7035 (Electronic)
1521-6616 (Linking). Available at: < https://www.ncbi.nlm.nih.gov/pubmed/23773921 >.

JENNETTE, J. C. et al. 2012 revised International Chapel Hill Consensus Conference Nomenclature of Vasculitides. **Arthritis Rheum,** v. 65, n. 1, p. 1-11, Jan 2013. ISSN 1529-0131 (Electronic)
0004-3591 (Linking). Available at: < https://www.ncbi.nlm.nih.gov/pubmed/23045170 >.

JIN, W.; DONG, C. IL-17 cytokines in immunity and inflammation. **Emerg Microbes Infect,** v. 2, n. 9, p. e60, Sep 2013. ISSN 2222-1751 (Electronic)
2222-1751 (Linking). Available at: < http://www.ncbi.nlm.nih.gov/pubmed/26038490 >.

JOGDAND, G. M.; MOHANTY, S.; DEVADAS, S. Regulators of Tfh Cell Differentiation. **Front Immunol,** v. 7, p. 520, 2016. ISSN 1664-3224 (Print)
1664-3224 (Linking). Available at: < https://www.ncbi.nlm.nih.gov/pubmed/27933060 >.

JOHN, M. et al. Inhaled corticosteroids increase interleukin-10 but reduce macrophage inflammatory protein-1alpha, granulocyte-macrophage colony-stimulating factor, and interferon-gamma release from alveolar macrophages in asthma. **Am J Respir Crit Care Med,** v. 157, n. 1, p. 256-62, Jan 1998. ISSN 1073-449X (Print)
1073-449X (Linking). Available at: < https://www.ncbi.nlm.nih.gov/pubmed/9445307 >.

JOHNSTON, R. J. et al. STAT5 is a potent negative regulator of TFH cell differentiation. **J Exp Med,** v. 209, n. 2, p. 243-50, Feb 13 2012. ISSN 1540-9538 (Electronic)
0022-1007 (Linking). Available at: < http://www.ncbi.nlm.nih.gov/pubmed/22271576 >.

JOHNSTON, R. J. et al. Bcl6 and Blimp-1 are reciprocal and antagonistic regulators of T follicular helper cell differentiation. **Science,** v. 325, n. 5943, p. 1006-10, Aug 21 2009. ISSN 1095-9203 (Electronic)
0036-8075 (Linking). Available at: < https://www.ncbi.nlm.nih.gov/pubmed/19608860 >.

JORCH, S. K.; KUBES, P. An emerging role for neutrophil extracellular traps in noninfectious disease. **Nat Med,** v. 23, n. 3, p. 279-287, Mar 7 2017. ISSN 1546-170X (Electronic)
1078-8956 (Linking). Available at: < https://www.ncbi.nlm.nih.gov/pubmed/28267716 >.

KALLENBERG, C. G.; TADEMA, H. Vasculitis and infections: contribution to the issue of autoimmunity reviews devoted to "autoimmunity and infection". **Autoimmun Rev,** v. 8, n. 1, p. 29-32, Oct 2008. ISSN 1873-0183 (Electronic)
1568-9972 (Linking). Available at: < https://www.ncbi.nlm.nih.gov/pubmed/18703171 >.

KANAI, T. et al. Identification of STAT5A and STAT5B target genes in human T cells. **PLoS One,** v. 9, n. 1, p. e86790, 2014. ISSN 1932-6203 (Electronic)
1932-6203 (Linking). Available at: < https://www.ncbi.nlm.nih.gov/pubmed/24497979 >.

KANAMORI, M. et al. Induced Regulatory T Cells: Their Development, Stability, and Applications. **Trends Immunol,** v. 37, n. 11, p. 803-811, Nov 2016. ISSN 1471-4981 (Electronic)
1471-4906 (Linking). Available at: < https://www.ncbi.nlm.nih.gov/pubmed/27623114 >.

KANTARI, C. et al. Proteinase 3, the Wegener autoantigen, is externalized during neutrophil apoptosis: evidence for a functional association with phospholipid scramblase 1 and interference with macrophage phagocytosis. **Blood,** v. 110, n. 12, p. 4086-95, Dec 1 2007. ISSN 0006-4971 (Print)
0006-4971 (Linking). Available at: < https://www.ncbi.nlm.nih.gov/pubmed/17712045 >.

KERSTEIN, A. et al. Environmental factor and inflammation-driven alteration of the total peripheral T-cell compartment in granulomatosis with polyangiitis. **J Autoimmun,** v. 78, p. 79-91, Mar 2017. ISSN 1095-9157 (Electronic)
0896-8411 (Linking). Available at: < https://www.ncbi.nlm.nih.gov/pubmed/28040323 >.

KHAN, D.; ANSAR AHMED, S. Regulation of IL-17 in autoimmune diseases by transcriptional factors and microRNAs. **Front Genet,** v. 6, p. 236, 2015. ISSN 1664-8021 (Print)
1664-8021 (Linking). Available at: < https://www.ncbi.nlm.nih.gov/pubmed/26236331 >.

KIEBACK, E. et al. Thymus-Derived Regulatory T Cells Are Positively Selected on Natural Self-Antigen through Cognate Interactions of High Functional Avidity. **Immunity,** v. 44, n. 5, p. 1114-26, May 17 2016. ISSN 1097-4180 (Electronic)
1074-7613 (Linking). Available at: < https://www.ncbi.nlm.nih.gov/pubmed/27192577 >.

KIM, H. P.; IMBERT, J.; LEONARD, W. J. Both integrated and differential regulation of components of the IL-2/IL-2 receptor system. **Cytokine Growth Factor Rev,** v. 17, n. 5, p. 349-66, Oct 2006. ISSN 1359-6101 (Print)
1359-6101 (Linking). Available at: < https://www.ncbi.nlm.nih.gov/pubmed/16911870 >.

KIM, J. I. et al. The transcription factor c-Maf controls the production of interleukin-4 but not other Th2 cytokines. **Immunity,** v. 10, n. 6, p. 745-51, Jun 1999. ISSN 1074-7613 (Print)
1074-7613 (Linking). Available at: < https://www.ncbi.nlm.nih.gov/pubmed/10403649 >.

KIM, M. J. et al. Effect of Immunosuppressive Drugs on the Changes of Serum Galactose-Deficient IgA1 in Patients with IgA Nephropathy. **PLoS One,** v. 11, n. 12, p. e0166830, 2016. ISSN 1932-6203 (Electronic)
1932-6203 (Linking). Available at: < https://www.ncbi.nlm.nih.gov/pubmed/27930655 >.

KITAGAWA, Y.; SAKAGUCHI, S. Molecular control of regulatory T cell development and function. **Curr Opin Immunol,** v. 49, p. 64-70, Dec 2017. ISSN 1879-0372 (Electronic)
0952-7915 (Linking). Available at: < https://www.ncbi.nlm.nih.gov/pubmed/29065384 >.

KLEINEWIETFELD, M.; HAFLER, D. A. The plasticity of human Treg and Th17 cells and its role in autoimmunity. **Semin Immunol,** v. 25, n. 4, p. 305-12, Nov 15 2013. ISSN 1096-3618 (Electronic)
1044-5323 (Linking). Available at: < http://www.ncbi.nlm.nih.gov/pubmed/24211039 >.

KNIGHT, A.; SANDIN, S.; ASKLING, J. Risks and relative risks of Wegener's granulomatosis among close relatives of patients with the disease. **Arthritis Rheum,** v. 58, n. 1, p. 302-7, Jan 2008. ISSN 0004-3591 (Print)
0004-3591 (Linking). Available at: < https://www.ncbi.nlm.nih.gov/pubmed/18163522 >.

KOENING, C. L. et al. Limited utility of rapamycin in severe, refractory Wegener's granulomatosis. **J Rheumatol,** v. 36, n. 1, p. 116-9, Jan 2009. ISSN 0315-162X (Print)
0315-162X (Linking). Available at: < https://www.ncbi.nlm.nih.gov/pubmed/19012360 >.

KOMOCSI, A. et al. Peripheral blood and granuloma CD4(+)CD28(-) T cells are a major source of interferon-gamma and tumor necrosis factor-alpha in Wegener's granulomatosis. **Am J Pathol,** v. 160, n. 5, p. 1717-24, May 2002. ISSN 0002-9440 (Print)
0002-9440 (Linking). Available at: < https://www.ncbi.nlm.nih.gov/pubmed/12000723 >.

KUPCOVA SKALNIKOVA, H. et al. Advances in Proteomic Techniques for Cytokine Analysis: Focus on Melanoma Research. **Int J Mol Sci,** v. 18, n. 12, Dec 13 2017. ISSN 1422-0067 (Electronic)

1422-0067 (Linking). Available at: < https://www.ncbi.nlm.nih.gov/pubmed/29236046 >.

KUSAM, S. et al. Inhibition of Th2 differentiation and GATA-3 expression by BCL-6. **J Immunol,** v. 170, n. 5, p. 2435-41, Mar 1 2003. ISSN 0022-1767 (Print)
0022-1767 (Linking). Available at: < https://www.ncbi.nlm.nih.gov/pubmed/12594267 >.

LAMPRECHT, P. et al. Heterogeneity of CD4 and CD8+ memory T cells in localized and generalized Wegener's granulomatosis. **Arthritis Res Ther,** v. 5, n. 1, p. R25-31, 2003. ISSN 1478-6362 (Electronic)
1478-6354 (Linking). Available at: < http://www.ncbi.nlm.nih.gov/pubmed/12716450 >.

LAURENCE, A. et al. Interleukin-2 signaling via STAT5 constrains T helper 17 cell generation. **Immunity,** v. 26, n. 3, p. 371-81, Mar 2007. ISSN 1074-7613 (Print)
1074-7613 (Linking). Available at: < https://www.ncbi.nlm.nih.gov/pubmed/17363300 >.

LAWAND, M.; DECHANET-MERVILLE, J.; DIEU-NOSJEAN, M. C. Key Features of Gamma-Delta T-Cell Subsets in Human Diseases and Their Immunotherapeutic Implications. **Front Immunol,** v. 8, p. 761, 2017. ISSN 1664-3224 (Print)
1664-3224 (Linking). Available at: < https://www.ncbi.nlm.nih.gov/pubmed/28713381 >.

LEE, M. S. et al. Gene expression profiles during human CD4+ T cell differentiation. **Int Immunol,** v. 16, n. 8, p. 1109-24, Aug 2004. ISSN 0953-8178 (Print)
0953-8178 (Linking). Available at: < https://www.ncbi.nlm.nih.gov/pubmed/15210650 >.

LEE, W.; LEE, G. R. Transcriptional regulation and development of regulatory T cells. **Exp Mol Med,** v. 50, n. 3, p. e456, Mar 9 2018. ISSN 2092-6413 (Electronic)
1226-3613 (Linking). Available at: < https://www.ncbi.nlm.nih.gov/pubmed/29520112 >.

LEGOUX, F. P. et al. CD4+ T Cell Tolerance to Tissue-Restricted Self Antigens Is Mediated by Antigen-Specific Regulatory T Cells Rather Than Deletion. **Immunity,** v. 43, n. 5, p. 896-908, Nov 17 2015. ISSN 1097-4180 (Electronic)
1074-7613 (Linking). Available at: < https://www.ncbi.nlm.nih.gov/pubmed/26572061 >.

LEPSE, N. et al. Immune regulatory mechanisms in ANCA-associated vasculitides. **Autoimmun Rev,** v. 11, n. 2, p. 77-83, Dec 2011. ISSN 1873-0183 (Electronic)
1568-9972 (Linking). Available at: < https://www.ncbi.nlm.nih.gov/pubmed/21856453 >.

LEVINGS, M. K.; SANGREGORIO, R.; RONCAROLO, M. G. Human cd25(+)cd4(+) t regulatory cells suppress naive and memory T cell proliferation and can be expanded in vitro without loss of function. **J Exp Med,** v. 193, n. 11, p. 1295-302, Jun 4 2001. ISSN 0022-1007 (Print)
0022-1007 (Linking). Available at: < https://www.ncbi.nlm.nih.gov/pubmed/11390436 >.

LEVY, R. et al. Genetic, immunological, and clinical features of patients with bacterial and fungal infections due to inherited IL-17RA deficiency. **Proc Natl Acad Sci U S A,** v. 113, n. 51, p. E8277-E8285, Dec 20 2016. ISSN 1091-6490 (Electronic)
0027-8424 (Linking). Available at: < https://www.ncbi.nlm.nih.gov/pubmed/27930337 >.

LI, P. et al. STAT5-mediated chromatin interactions in superenhancers activate IL-2 highly inducible genes: Functional dissection of the Il2ra gene locus. **Proc Natl Acad Sci U S A,** v. 114, n. 46, p. 12111-12119, Nov 14 2017. ISSN 1091-6490 (Electronic)
0027-8424 (Linking). Available at: < https://www.ncbi.nlm.nih.gov/pubmed/29078395 >.

LIAO, W. et al. Modulation of cytokine receptors by IL-2 broadly regulates differentiation into helper T cell lineages. **Nat Immunol,** v. 12, n. 6, p. 551-9, Jun 2011. ISSN 1529-2916 (Electronic)
1529-2908 (Linking). Available at: < https://www.ncbi.nlm.nih.gov/pubmed/21516110 >.

LIAO, W. et al. Priming for T helper type 2 differentiation by interleukin 2-mediated induction of interleukin 4 receptor alpha-chain expression. **Nat Immunol,** v. 9, n. 11, p. 1288-96, Nov 2008. ISSN 1529-2916 (Electronic)
1529-2908 (Linking). Available at: < https://www.ncbi.nlm.nih.gov/pubmed/18820682 >.

LILLIEBLADH, S. et al. Phenotypic Characterization of Circulating CD4(+) T Cells in ANCA-Associated Vasculitis. **J Immunol Res,** v. 2018, p. 6984563, 2018. ISSN 2314-7156 (Electronic)
2314-7156 (Linking). Available at: < https://www.ncbi.nlm.nih.gov/pubmed/30510966 >.

LIN, J. X. et al. Cloning of human Stat5B. Reconstitution of interleukin-2-induced Stat5A and Stat5B DNA binding activity in COS-7 cells. **J Biol Chem,** v. 271, n. 18, p. 10738-44, May 3 1996. ISSN 0021-9258 (Print)
0021-9258 (Linking). Available at: < https://www.ncbi.nlm.nih.gov/pubmed/8631883 >.

LIO, C. W.; HSIEH, C. S. A two-step process for thymic regulatory T cell development. **Immunity,** v. 28, n. 1, p. 100-11, Jan 2008. ISSN 1074-7613 (Print)
1074-7613 (Linking). Available at: < https://www.ncbi.nlm.nih.gov/pubmed/18199417 >.

LIU, X. et al. Genome-wide Analysis Identifies Bcl6-Controlled Regulatory Networks during T Follicular Helper Cell Differentiation. **Cell Rep,** v. 14, n. 7, p. 1735-1747, Feb 23 2016. ISSN 2211-1247 (Electronic). Available at: < https://www.ncbi.nlm.nih.gov/pubmed/26876184 >.

LOCCI, M. et al. Erratum: Activin A programs the differentiation of human TFH cells. **Nat Immunol,** v. 17, n. 10, p. 1235, Sep 20 2016. ISSN 1529-2916 (Electronic)
1529-2908 (Linking). Available at: < https://www.ncbi.nlm.nih.gov/pubmed/27648551 >.

LOKHOV, P. G. et al. Mass spectrometric signatures of the blood plasma metabolome for disease diagnostics. **Biomed Rep,** v. 4, n. 1, p. 122-126, Jan 2016. ISSN 2049-9434 (Print)
2049-9434 (Linking). Available at: < https://www.ncbi.nlm.nih.gov/pubmed/26870348 >.

LOKHOV, P. G. et al. [Metabolic fingerprinting of blood plasma for patients with prostate cancer]. **Biomed Khim,** v. 55, n. 3, p. 247-54, May-Jun 2009. ISSN 2310-6972 (Print)
2310-6905 (Linking). Available at: < https://www.ncbi.nlm.nih.gov/pubmed/19663000 >.

LOKHOV, P. G. et al. Diagnosing impaired glucose tolerance using direct infusion mass spectrometry of blood plasma. **PLoS One,** v. 9, n. 9, p. e105343, 2014. ISSN 1932-6203 (Electronic)
1932-6203 (Linking). Available at: < https://www.ncbi.nlm.nih.gov/pubmed/25202985 >.

LONG, D. et al. Clinical significance and immunobiology of IL-21 in autoimmunity. **J Autoimmun**, Feb 14 2019. ISSN 1095-9157 (Electronic)
0896-8411 (Linking). Available at: < https://www.ncbi.nlm.nih.gov/pubmed/30773373 >.

LU, H. TLR Agonists for Cancer Immunotherapy: Tipping the Balance between the Immune Stimulatory and Inhibitory Effects. **Front Immunol,** v. 5, p. 83, 2014. ISSN 1664-3224 (Print)
1664-3224 (Linking). Available at: < https://www.ncbi.nlm.nih.gov/pubmed/24624132 >.

LUTALO, P. M.; D'CRUZ, D. P. Diagnosis and classification of granulomatosis with polyangiitis (aka Wegener's granulomatosis). **J Autoimmun,** v. 48-49, p. 94-8, Feb-Mar 2014. ISSN 1095-9157 (Electronic)
0896-8411 (Linking). Available at: < http://www.ncbi.nlm.nih.gov/pubmed/24485158 >.

LYONS, P. A. et al. Genetically distinct subsets within ANCA-associated vasculitis. **N Engl J Med,** v. 367, n. 3, p. 214-23, Jul 19 2012. ISSN 1533-4406 (Electronic)
0028-4793 (Linking). Available at: < https://www.ncbi.nlm.nih.gov/pubmed/22808956 >.

MA, C. S. et al. The origins, function, and regulation of T follicular helper cells. **J Exp Med,** v. 209, n. 7, p. 1241-53, Jul 2 2012. ISSN 1540-9538 (Electronic)
0022-1007 (Linking). Available at: < http://www.ncbi.nlm.nih.gov/pubmed/22753927 >.

MADDA, R. et al. Plasma proteomic analysis of systemic lupus erythematosus patients using liquid chromatography/tandem mass spectrometry with label-free quantification. **PeerJ,** v. 6, p. e4730, 2018. ISSN 2167-8359 (Print)
2167-8359 (Linking). Available at: < https://www.ncbi.nlm.nih.gov/pubmed/29761050 >.

MALHOTRA, D. et al. Tolerance is established in polyclonal CD4(+) T cells by distinct mechanisms, according to self-peptide expression patterns. **Nat Immunol,** v. 17, n. 2, p. 187-95, Feb 2016. ISSN 1529-2916 (Electronic)
1529-2908 (Linking). Available at: < https://www.ncbi.nlm.nih.gov/pubmed/26726812 >.

MANSI, I. A.; OPRAN, A.; ROSNER, F. ANCA-associated small-vessel vasculitis. **Am Fam Physician,** v. 65, n. 8, p. 1615-20, Apr 15 2002. ISSN 0002-838X (Print)
0002-838X (Linking). Available at: < https://www.ncbi.nlm.nih.gov/pubmed/11989638 >.

MARINAKI, S. et al. Abnormalities of CD4 T cell subpopulations in ANCA-associated vasculitis. **Clin Exp Immunol,** v. 140, n. 1, p. 181-91, Apr 2005. ISSN 0009-9104 (Print)
0009-9104 (Linking). Available at: < http://www.ncbi.nlm.nih.gov/pubmed/15762890 >.

MARTINEZ, G. J.; DONG, C. BATF: bringing (in) another Th17-regulating factor. **J Mol Cell Biol,** v. 1, n. 2, p. 66-8, Dec 2009. ISSN 1759-4685 (Electronic)
1759-4685 (Linking). Available at: < https://www.ncbi.nlm.nih.gov/pubmed/19726487 >.

MATLOUBIAN, M.; CONCEPCION, R. J.; AHMED, R. CD4+ T cells are required to sustain CD8+ cytotoxic T-cell responses during chronic viral infection. **J Virol,** v. 68, n. 12, p. 8056-63, Dec 1994. ISSN 0022-538X (Print)
0022-538X (Linking). Available at: < https://www.ncbi.nlm.nih.gov/pubmed/7966595 >.

MATZARAKI, V. et al. The MHC locus and genetic susceptibility to autoimmune and infectious diseases. **Genome Biol,** v. 18, n. 1, p. 76, Apr 27 2017. ISSN 1474-760X (Electronic)
1474-7596 (Linking). Available at: < https://www.ncbi.nlm.nih.gov/pubmed/28449694 >.

MCDYER, J. F. et al. IL-2 receptor blockade inhibits late, but not early, IFN-gamma and CD40 ligand expression in human T cells: disruption of both IL-12-dependent and -independent pathways of IFN-gamma production. **J Immunol,** v. 169, n. 5, p. 2736-46, Sep 1 2002. ISSN 0022-1767 (Print)
0022-1767 (Linking). Available at: < https://www.ncbi.nlm.nih.gov/pubmed/12193748 >.

MCHEYZER-WILLIAMS, M. et al. Molecular programming of B cell memory. **Nat Rev Immunol,** v. 12, n. 1, p. 24-34, Dec 9 2011. ISSN 1474-1741 (Electronic)
1474-1733 (Linking). Available at: < https://www.ncbi.nlm.nih.gov/pubmed/22158414 >.

MCKINNEY, E. F. et al. T-cell exhaustion, co-stimulation and clinical outcome in autoimmunity and infection. **Nature,** v. 523, n. 7562, p. 612-6, Jul 30 2015. ISSN 1476-4687 (Electronic) 0028-0836 (Linking). Available at: < https://www.ncbi.nlm.nih.gov/pubmed/26123020 >.

MCKINNEY, E. F. et al. The immunopathology of ANCA-associated vasculitis. **Semin Immunopathol,** v. 36, n. 4, p. 461-78, Jul 2014. ISSN 1863-2300 (Electronic) 1863-2297 (Linking). Available at: < http://www.ncbi.nlm.nih.gov/pubmed/25056155 >.

MCMURCHY, A. N.; LEVINGS, M. K. Suppression assays with human T regulatory cells: a technical guide. **Eur J Immunol,** v. 42, n. 1, p. 27-34, Jan 2012. ISSN 1521-4141 (Electronic) 0014-2980 (Linking). Available at: < https://www.ncbi.nlm.nih.gov/pubmed/22161814 >.

MEDZHITOV, R. Recognition of microorganisms and activation of the immune response. **Nature,** v. 449, n. 7164, p. 819-26, Oct 18 2007. ISSN 1476-4687 (Electronic) 0028-0836 (Linking). Available at: < https://www.ncbi.nlm.nih.gov/pubmed/17943118 >.

MELANDRI, D. et al. The gammadeltaTCR combines innate immunity with adaptive immunity by utilizing spatially distinct regions for agonist selection and antigen responsiveness. **Nat Immunol,** v. 19, n. 12, p. 1352-1365, Dec 2018. ISSN 1529-2916 (Electronic) 1529-2908 (Linking). Available at: < https://www.ncbi.nlm.nih.gov/pubmed/30420626 >.

MIAO, T. et al. Early growth response gene-2 controls IL-17 expression and Th17 differentiation by negatively regulating Batf. **J Immunol,** v. 190, n. 1, p. 58-65, Jan 1 2013. ISSN 1550-6606 (Electronic) 0022-1767 (Linking). Available at: < https://www.ncbi.nlm.nih.gov/pubmed/23203924 >.

MILLET, A. et al. Proteinase 3 on apoptotic cells disrupts immune silencing in autoimmune vasculitis. **J Clin Invest,** v. 125, n. 11, p. 4107-21, Nov 2 2015. ISSN 1558-8238 (Electronic) 0021-9738 (Linking). Available at: < https://www.ncbi.nlm.nih.gov/pubmed/26436651 >.

MITRA, S.; LEONARD, W. J. Biology of IL-2 and its therapeutic modulation: Mechanisms and strategies. **J Leukoc Biol,** v. 103, n. 4, p. 643-655, Apr 2018. ISSN 1938-3673 (Electronic) 0741-5400 (Linking). Available at: < https://www.ncbi.nlm.nih.gov/pubmed/29522246 >.

MIYARA, M. et al. Functional delineation and differentiation dynamics of human CD4+ T cells expressing the FoxP3 transcription factor. **Immunity,** v. 30, n. 6, p. 899-911, Jun 19 2009. ISSN 1097-4180 (Electronic) 1074-7613 (Linking). Available at: < https://www.ncbi.nlm.nih.gov/pubmed/19464196 >.

MOBINI, M. et al. Metabolic syndrome in patients with systemic lupus erythematosus: Association with disease activity, disease damage and age. **Int J Rheum Dis,** v. 21, n. 5, p. 1023-1030, May 2018. ISSN 1756-185X (Electronic) 1756-1841 (Linking). Available at: < https://www.ncbi.nlm.nih.gov/pubmed/29611288 >.

MOGENSEN, T. H. Pathogen recognition and inflammatory signaling in innate immune defenses. **Clin Microbiol Rev,** v. 22, n. 2, p. 240-73, Table of Contents, Apr 2009. ISSN 1098-6618 (Electronic) 0893-8512 (Linking). Available at: < https://www.ncbi.nlm.nih.gov/pubmed/19366914 >.

MORGAN, M. D. et al. Anti-neutrophil cytoplasm-associated glomerulonephritis. **J Am Soc Nephrol,** v. 17, n. 5, p. 1224-34, May 2006. ISSN 1046-6673 (Print) 1046-6673 (Linking). Available at: < https://www.ncbi.nlm.nih.gov/pubmed/16624931 >.

MORGAN, M. D. et al. CD4+CD28- T cell expansion in granulomatosis with polyangiitis (Wegener's) is driven by latent cytomegalovirus infection and is associated with an increased risk of infection and mortality. **Arthritis Rheum,** v. 63, n. 7, p. 2127-37, Jul 2011. ISSN 1529-0131 (Electronic)
0004-3591 (Linking). Available at: < https://www.ncbi.nlm.nih.gov/pubmed/21437878 >.

MOZO, L.; SUAREZ, A.; GUTIERREZ, C. Glucocorticoids up-regulate constitutive interleukin-10 production by human monocytes. **Clin Exp Allergy,** v. 34, n. 3, p. 406-12, Mar 2004. ISSN 0954-7894 (Print)
0954-7894 (Linking). Available at: < https://www.ncbi.nlm.nih.gov/pubmed/15005734 >.

MUELLER, A. et al. Germinal centre-like structures in Wegener's granuloma: the morphological basis for autoimmunity? **Rheumatology (Oxford),** v. 47, n. 8, p. 1111-3, Aug 2008. ISSN 1462-0332 (Electronic)
1462-0324 (Linking). Available at: < http://www.ncbi.nlm.nih.gov/pubmed/18515866 >.

MURPHY, K. et al. **Janeway's immunobiology**. 7th ed. / Kenneth Murphy, Paul Travers, Mark Walport ; with contributions by Michael Ehrenstein ... [et al.]. New York: Garland Science ; London : Taylor & Francis [distributor], 2008. ISBN 9780815341239 (pbk.) : ¹42.99
9780815342908 (pbk: international student edition) : no price
0815341237 (pbk.) : ¹42.99
081534290X (pbk: international student edition) : no price. Available at: < Table of contents only http://www.loc.gov/catdir/toc/ecip079/2007002499.html
Publisher description http://www.loc.gov/catdir/enhancements/fy0828/2007002499-d.html >.

NAGAYA, T. et al. Lipid mediators foster the differentiation of T follicular helper cells. **Immunol Lett,** v. 181, p. 51-57, Jan 2017. ISSN 1879-0542 (Electronic)
0165-2478 (Linking). Available at: < https://www.ncbi.nlm.nih.gov/pubmed/27838468 >.

NAKAZAWA, D. et al. Author Correction: Pathogenesis and therapeutic interventions for ANCA-associated vasculitis. **Nat Rev Rheumatol,** v. 15, n. 2, p. 123, Feb 2019. ISSN 1759-4804 (Electronic)
1759-4790 (Linking). Available at: < https://www.ncbi.nlm.nih.gov/pubmed/30655606 >.

NAUGLER, W. E.; KARIN, M. The wolf in sheep's clothing: the role of interleukin-6 in immunity, inflammation and cancer. **Trends Mol Med,** v. 14, n. 3, p. 109-19, Mar 2008. ISSN 1471-4914 (Print)
1471-4914 (Linking). Available at: < https://www.ncbi.nlm.nih.gov/pubmed/18261959 >.

NEURATH, M. F.; KAPLAN, M. H. Th9 cells in immunity and immunopathological diseases. **Semin Immunopathol,** v. 39, n. 1, p. 1-4, Jan 2017. ISSN 1863-2300 (Electronic)
1863-2297 (Linking). Available at: < https://www.ncbi.nlm.nih.gov/pubmed/27900451 >.

NISTALA, K.; WEDDERBURN, L. R. Th17 and regulatory T cells: rebalancing pro- and anti-inflammatory forces in autoimmune arthritis. **Rheumatology (Oxford),** v. 48, n. 6, p. 602-6, Jun 2009. ISSN 1462-0332 (Electronic)
1462-0324 (Linking). Available at: < http://www.ncbi.nlm.nih.gov/pubmed/19269955 >.

NUNES, J. A. et al. Signal transduction by CD28 costimulatory receptor on T cells. B7-1 and B7-2 regulation of tyrosine kinase adaptor molecules. **J Biol Chem,** v. 271, n. 3, p. 1591-8, Jan 19 1996. ISSN 0021-9258 (Print)
0021-9258 (Linking). Available at: < https://www.ncbi.nlm.nih.gov/pubmed/8576157 >.

NURIEVA, R. I. et al. STAT5 protein negatively regulates T follicular helper (Tfh) cell generation and function. **J Biol Chem,** v. 287, n. 14, p. 11234-9, Mar 30 2012. ISSN 1083-351X (Electronic) 0021-9258 (Linking). Available at: < https://www.ncbi.nlm.nih.gov/pubmed/22318729 >.

O'SHEA, J. J. et al. The JAK-STAT pathway: impact on human disease and therapeutic intervention. **Annu Rev Med,** v. 66, p. 311-28, 2015. ISSN 1545-326X (Electronic) 0066-4219 (Linking). Available at: < https://www.ncbi.nlm.nih.gov/pubmed/25587654 >.

OKUMURA, F. et al. TRIM8 modulates STAT3 activity through negative regulation of PIAS3. **J Cell Sci,** v. 123, n. Pt 13, p. 2238-45, Jul 1 2010. ISSN 1477-9137 (Electronic) 0021-9533 (Linking). Available at: < https://www.ncbi.nlm.nih.gov/pubmed/20516148 >.

OLSEN, I.; SOLLID, L. M. Pitfalls in determining the cytokine profile of human T cells. **J Immunol Methods,** v. 390, n. 1-2, p. 106-12, Apr 30 2013. ISSN 1872-7905 (Electronic) 0022-1759 (Linking). Available at: < https://www.ncbi.nlm.nih.gov/pubmed/23416458 >.

OOI, J. D. et al. The immunodominant myeloperoxidase T-cell epitope induces local cell-mediated injury in antimyeloperoxidase glomerulonephritis. **Proc Natl Acad Sci U S A,** v. 109, n. 39, p. E2615-24, Sep 25 2012. ISSN 1091-6490 (Electronic) 0027-8424 (Linking). Available at: < https://www.ncbi.nlm.nih.gov/pubmed/22955884 >.

OWEN, D. L.; FARRAR, M. A. STAT5 and CD4 (+) T Cell Immunity. **F1000Res,** v. 6, p. 32, 2017. ISSN 2046-1402 (Print) 2046-1402 (Linking). Available at: < https://www.ncbi.nlm.nih.gov/pubmed/28163905 >.

PADRINES, M. et al. Interleukin-8 processing by neutrophil elastase, cathepsin G and proteinase-3. **FEBS Lett,** v. 352, n. 2, p. 231-5, Sep 26 1994. ISSN 0014-5793 (Print) 0014-5793 (Linking). Available at: < https://www.ncbi.nlm.nih.gov/pubmed/7925979 >.

PANAGOULIAS, I. et al. Transcription Factor Ets-2 Acts as a Preinduction Repressor of Interleukin-2 (IL-2) Transcription in Naive T Helper Lymphocytes. **J Biol Chem,** v. 291, n. 52, p. 26707-26721, Dec 23 2016. ISSN 1083-351X (Electronic) 0021-9258 (Linking). Available at: < https://www.ncbi.nlm.nih.gov/pubmed/27815505 >.

PANDIYAN, P.; ZHU, J. Origin and functions of pro-inflammatory cytokine producing Foxp3 regulatory T cells. **Cytokine**, Jul 9 2015. ISSN 1096-0023 (Electronic) 1043-4666 (Linking). Available at: < http://www.ncbi.nlm.nih.gov/pubmed/26165923 >.

PAPAYANNOPOULOS, V. Neutrophil extracellular traps in immunity and disease. **Nat Rev Immunol,** v. 18, n. 2, p. 134-147, Feb 2018. ISSN 1474-1741 (Electronic) 1474-1733 (Linking). Available at: < https://www.ncbi.nlm.nih.gov/pubmed/28990587 >.

PAPILLION, A. M. et al. IL-6 counteracts IL-2-dependent suppression of T follicular helper cell responses. **The Journal of Immunology,** v. 200, n. 1 Supplement, p. 110.13-110.13, 2018.

PARK, H. et al. A distinct lineage of CD4 T cells regulates tissue inflammation by producing interleukin 17. **Nat Immunol,** v. 6, n. 11, p. 1133-41, Nov 2005. ISSN 1529-2908 (Print) 1529-2908 (Linking). Available at: < http://www.ncbi.nlm.nih.gov/pubmed/16200068 >.

PESENACKER, A. M.; BROADY, R.; LEVINGS, M. K. Control of tissue-localized immune responses by human regulatory T cells. **Eur J Immunol,** v. 45, n. 2, p. 333-43, Feb 2015. ISSN 1521-4141 (Electronic)

0014-2980 (Linking). Available at: < https://www.ncbi.nlm.nih.gov/pubmed/25378065 >.

PETERMANN SMITS, D. R. et al. Metabolic syndrome in ANCA-associated vasculitis. **Rheumatology (Oxford),** v. 52, n. 1, p. 197-203, Jan 2013. ISSN 1462-0332 (Electronic)
1462-0324 (Linking). Available at: < https://www.ncbi.nlm.nih.gov/pubmed/23192910 >.

PHAM, D. et al. Opposing roles of STAT4 and Dnmt3a in Th1 gene regulation. **J Immunol,** v. 191, n. 2, p. 902-11, Jul 15 2013. ISSN 1550-6606 (Electronic)
0022-1767 (Linking). Available at: < https://www.ncbi.nlm.nih.gov/pubmed/23772023 >.

PISSANI, F.; STREECK, H. Emerging concepts on T follicular helper cell dynamics in HIV infection. **Trends Immunol,** v. 35, n. 6, p. 278-86, Jun 2014. ISSN 1471-4981 (Electronic)
1471-4906 (Linking). Available at: < http://www.ncbi.nlm.nih.gov/pubmed/24703588 >.

POPA, E. R. et al. Staphylococcal toxic-shock-syndrome-toxin-1 as a risk factor for disease relapse in Wegener's granulomatosis. **Rheumatology (Oxford),** v. 46, n. 6, p. 1029-33, Jun 2007. ISSN 1462-0324 (Print)
1462-0324 (Linking). Available at: < https://www.ncbi.nlm.nih.gov/pubmed/17409134 >.

POPAT, R. J. et al. Anti-myeloperoxidase antibodies attenuate the monocyte response to LPS and shape macrophage development. **JCI Insight,** v. 2, n. 2, p. e87379, Jan 26 2017. ISSN 2379-3708 (Print)
2379-3708 (Linking). Available at: < https://www.ncbi.nlm.nih.gov/pubmed/28138552 >.

QI, H. T follicular helper cells in space-time. **Nat Rev Immunol,** v. 16, n. 10, p. 612-25, Oct 2016. ISSN 1474-1741 (Electronic)
1474-1733 (Linking). Available at: < https://www.ncbi.nlm.nih.gov/pubmed/27573485 >.

RANI, L. et al. Predominance of PR3 specific immune response and skewed TH17 vs. T-regulatory milieu in active granulomatosis with polyangiitis. **Cytokine,** v. 71, n. 2, p. 261-7, Feb 2015. ISSN 1096-0023 (Electronic)
1043-4666 (Linking). Available at: < http://www.ncbi.nlm.nih.gov/pubmed/25461407 >.

READ, K. A.; POWELL, M. D.; OESTREICH, K. J. T follicular helper cell programming by cytokine-mediated events. **Immunology,** v. 149, n. 3, p. 253-261, Nov 2016. ISSN 1365-2567 (Electronic)
0019-2805 (Linking). Available at: < https://www.ncbi.nlm.nih.gov/pubmed/27442976 >.

RITVO, P. G. et al. Tfr cells lack IL-2Ralpha but express decoy IL-1R2 and IL-1Ra and suppress the IL-1-dependent activation of Tfh cells. **Sci Immunol,** v. 2, n. 15, Sep 8 2017. ISSN 2470-9468 (Electronic)
2470-9468 (Linking). Available at: < https://www.ncbi.nlm.nih.gov/pubmed/28887367 >.

ROSENBLUM, M. D.; REMEDIOS, K. A.; ABBAS, A. K. Mechanisms of human autoimmunity. **J Clin Invest,** v. 125, n. 6, p. 2228-33, Jun 2015. ISSN 1558-8238 (Electronic)
0021-9738 (Linking). Available at: < https://www.ncbi.nlm.nih.gov/pubmed/25893595 >.

ROVEDATTI, L. et al. Differential regulation of interleukin 17 and interferon gamma production in inflammatory bowel disease. **Gut,** v. 58, n. 12, p. 1629-36, Dec 2009. ISSN 1468-3288 (Electronic)
0017-5749 (Linking). Available at: < http://www.ncbi.nlm.nih.gov/pubmed/19740775 >.

RUTH, A. J. et al. Anti-neutrophil cytoplasmic antibodies and effector CD4+ cells play nonredundant roles in anti-myeloperoxidase crescentic glomerulonephritis. **J Am Soc Nephrol,** v. 17, n. 7, p. 1940-9, Jul 2006. ISSN 1046-6673 (Print)
1046-6673 (Linking). Available at: < https://www.ncbi.nlm.nih.gov/pubmed/16769746 >.

SAFINIA, N. et al. Regulatory T Cells: Serious Contenders in the Promise for Immunological Tolerance in Transplantation. **Front Immunol,** v. 6, p. 438, 2015. ISSN 1664-3224 (Print)
1664-3224 (Linking). Available at: < https://www.ncbi.nlm.nih.gov/pubmed/26379673 >.

SAGE, P. T. et al. The receptor PD-1 controls follicular regulatory T cells in the lymph nodes and blood. **Nat Immunol,** v. 14, n. 2, p. 152-61, Feb 2013. ISSN 1529-2916 (Electronic)
1529-2908 (Linking). Available at: < https://www.ncbi.nlm.nih.gov/pubmed/23242415 >.

SAHOO, A. et al. Batf is important for IL-4 expression in T follicular helper cells. **Nat Commun,** v. 6, p. 7997, 2015. ISSN 2041-1723 (Electronic)
2041-1723 (Linking). Available at: < http://www.ncbi.nlm.nih.gov/pubmed/26278622 >.

SAKAGUCHI, S. et al. FOXP3+ regulatory T cells in the human immune system. **Nat Rev Immunol,** v. 10, n. 7, p. 490-500, Jul 2010. ISSN 1474-1741 (Electronic)
1474-1733 (Linking). Available at: < https://www.ncbi.nlm.nih.gov/pubmed/20559327 >.

SAKAGUCHI, S.; WING, K.; MIYARA, M. Regulatory T cells - a brief history and perspective. **Eur J Immunol,** v. 37 Suppl 1, p. S116-23, Nov 2007. ISSN 0014-2980 (Print)
0014-2980 (Linking). Available at: < http://www.ncbi.nlm.nih.gov/pubmed/17972355 >.

SAKAGUCHI, S. et al. Regulatory T cells and immune tolerance. **Cell,** v. 133, n. 5, p. 775-87, May 30 2008. ISSN 1097-4172 (Electronic)
0092-8674 (Linking). Available at: < http://www.ncbi.nlm.nih.gov/pubmed/18510923 >.

SALLUSTO, F.; GEGINAT, J.; LANZAVECCHIA, A. Central memory and effector memory T cell subsets: function, generation, and maintenance. **Annu Rev Immunol,** v. 22, p. 745-63, 2004. ISSN 0732-0582 (Print)
0732-0582 (Linking). Available at: < https://www.ncbi.nlm.nih.gov/pubmed/15032595 >.

SANJABI, S. et al. Anti-inflammatory and pro-inflammatory roles of TGF-beta, IL-10, and IL-22 in immunity and autoimmunity. **Curr Opin Pharmacol,** v. 9, n. 4, p. 447-53, Aug 2009. ISSN 1471-4973 (Electronic)
1471-4892 (Linking). Available at: < https://www.ncbi.nlm.nih.gov/pubmed/19481975 >.

SCHMITT, E. G.; WILLIAMS, C. B. Generation and function of induced regulatory T cells. **Front Immunol,** v. 4, p. 152, 2013. ISSN 1664-3224 (Print)
1664-3224 (Linking). Available at: < https://www.ncbi.nlm.nih.gov/pubmed/23801990 >.

SCHMITT, N. et al. The cytokine TGF-beta co-opts signaling via STAT3-STAT4 to promote the differentiation of human TFH cells. **Nat Immunol,** v. 15, n. 9, p. 856-65, Sep 2014. ISSN 1529-2916 (Electronic)
1529-2908 (Linking). Available at: < https://www.ncbi.nlm.nih.gov/pubmed/25064073 >.

SCHULTZ, B. T. et al. Circulating HIV-Specific Interleukin-21(+)CD4(+) T Cells Represent Peripheral Tfh Cells with Antigen-Dependent Helper Functions. **Immunity,** v. 44, n. 1, p. 167-78, Jan 19 2016. ISSN 1097-4180 (Electronic)
1074-7613 (Linking). Available at: < http://www.ncbi.nlm.nih.gov/pubmed/26795249 >.

SCHUSTER, B. et al. Purification and identification of the STAT5 protease in myeloid cells. **Biochem J,** v. 404, n. 1, p. 81-7, May 15 2007. ISSN 1470-8728 (Electronic)
0264-6021 (Linking). Available at: < https://www.ncbi.nlm.nih.gov/pubmed/17300217 >.

SHEKHAR, S.; YANG, X. The darker side of follicular helper T cells: from autoimmunity to immunodeficiency. **Cell Mol Immunol,** v. 9, n. 5, p. 380-5, Sep 2012. ISSN 2042-0226 (Electronic)
1672-7681 (Linking). Available at: < http://www.ncbi.nlm.nih.gov/pubmed/22885524 >.

SHENG, W. et al. STAT5 programs a distinct subset of GM-CSF-producing T helper cells that is essential for autoimmune neuroinflammation. **Cell Res,** v. 24, n. 12, p. 1387-402, Dec 2014. ISSN 1748-7838 (Electronic)
1001-0602 (Linking). Available at: < https://www.ncbi.nlm.nih.gov/pubmed/25412660 >.

SIMON, S.; LABARRIERE, N. PD-1 expression on tumor-specific T cells: Friend or foe for immunotherapy? **Oncoimmunology,** v. 7, n. 1, p. e1364828, 2017. ISSN 2162-4011 (Print)
2162-4011 (Linking). Available at: < https://www.ncbi.nlm.nih.gov/pubmed/29296515 >.

SLAATS, J. et al. IL-1beta/IL-6/CRP and IL-18/ferritin: Distinct Inflammatory Programs in Infections. **PLoS Pathog,** v. 12, n. 12, p. e1005973, Dec 2016. ISSN 1553-7374 (Electronic)
1553-7366 (Linking). Available at: < https://www.ncbi.nlm.nih.gov/pubmed/27977798 >.

SMITH, W. B. et al. Neutrophils activated by granulocyte-macrophage colony-stimulating factor express receptors for interleukin-3 which mediate class II expression. **Blood,** v. 86, n. 10, p. 3938-44, Nov 15 1995. ISSN 0006-4971 (Print)
0006-4971 (Linking). Available at: < https://www.ncbi.nlm.nih.gov/pubmed/7579364 >.

SNANOUDJ, R. et al. The blockade of T-cell co-stimulation as a therapeutic stratagem for immunosuppression: Focus on belatacept. **Biologics,** v. 1, n. 3, p. 203-13, Sep 2007. ISSN 1177-5475 (Print)
1177-5475 (Linking). Available at: < https://www.ncbi.nlm.nih.gov/pubmed/19707331 >.

SOFI, M. H. et al. Elevated IL-6 expression in CD4 T cells via PKCtheta and NF-kappaB induces Th2 cytokine production. **Mol Immunol,** v. 46, n. 7, p. 1443-50, Apr 2009. ISSN 1872-9142 (Electronic)
0161-5890 (Linking). Available at: < https://www.ncbi.nlm.nih.gov/pubmed/19181387 >.

SPOLSKI, R.; GROMER, D.; LEONARD, W. J. The gamma c family of cytokines: fine-tuning signals from IL-2 and IL-21 in the regulation of the immune response. **F1000Res,** v. 6, p. 1872, 2017. ISSN 2046-1402 (Print)
2046-1402 (Linking). Available at: < https://www.ncbi.nlm.nih.gov/pubmed/29123649 >.

SPOLSKI, R.; LI, P.; LEONARD, W. J. Biology and regulation of IL-2: from molecular mechanisms to human therapy. **Nat Rev Immunol,** v. 18, n. 10, p. 648-659, Oct 2018. ISSN 1474-1741 (Electronic)
1474-1733 (Linking). Available at: < https://www.ncbi.nlm.nih.gov/pubmed/30089912 >.

STONIER, S. W.; SCHLUNS, K. S. Trans-presentation: a novel mechanism regulating IL-15 delivery and responses. **Immunol Lett,** v. 127, n. 2, p. 85-92, Jan 4 2010. ISSN 1879-0542 (Electronic)
0165-2478 (Linking). Available at: < https://www.ncbi.nlm.nih.gov/pubmed/19818367 >.

STRITESKY, G. L. et al. The transcription factor STAT3 is required for T helper 2 cell development. **Immunity,** v. 34, n. 1, p. 39-49, Jan 28 2011. ISSN 1097-4180 (Electronic)
1074-7613 (Linking). Available at: < https://www.ncbi.nlm.nih.gov/pubmed/21215659 >.

SUZUKI, N. et al. Selective accumulation of CCR5+ T lymphocytes into inflamed joints of rheumatoid arthritis. **Int Immunol,** v. 11, n. 4, p. 553-9, Apr 1999. ISSN 0953-8178 (Print)
0953-8178 (Linking). Available at: < https://www.ncbi.nlm.nih.gov/pubmed/10323208 >.

SZCZEKLIK, W. et al. Skewing toward Treg and Th2 responses is a characteristic feature of sustained remission in ANCA-positive granulomatosis with polyangiitis. **Eur J Immunol,** v. 47, n. 4, p. 724-733, Apr 2017. ISSN 1521-4141 (Electronic)
0014-2980 (Linking). Available at: < https://www.ncbi.nlm.nih.gov/pubmed/28155222 >.

TAKABA, H.; TAKAYANAGI, H. The Mechanisms of T Cell Selection in the Thymus. **Trends Immunol,** v. 38, n. 11, p. 805-816, Nov 2017. ISSN 1471-4981 (Electronic)
1471-4906 (Linking). Available at: < https://www.ncbi.nlm.nih.gov/pubmed/28830733 >.

TARZI, R. M.; PUSEY, C. D. Current and future prospects in the management of granulomatosis with polyangiitis (Wegener's granulomatosis). **Ther Clin Risk Manag,** v. 10, p. 279-93, 2014. ISSN 1176-6336 (Print)
1176-6336 (Linking). Available at: < http://www.ncbi.nlm.nih.gov/pubmed/24790453 >.

TIAN, Y. et al. Unique phenotypes and clonal expansions of human CD4 effector memory T cells re-expressing CD45RA. **Nat Commun,** v. 8, n. 1, p. 1473, Nov 13 2017. ISSN 2041-1723 (Electronic)
2041-1723 (Linking). Available at: < https://www.ncbi.nlm.nih.gov/pubmed/29133794 >.

TIAN, Y.; ZAJAC, A. J. IL-21 and T Cell Differentiation: Consider the Context. **Trends Immunol,** v. 37, n. 8, p. 557-568, Aug 2016. ISSN 1471-4981 (Electronic)
1471-4906 (Linking). Available at: < https://www.ncbi.nlm.nih.gov/pubmed/27389961 >.

TINIAKOU, I. et al. High-density lipoprotein attenuates Th1 and th17 autoimmune responses by modulating dendritic cell maturation and function. **J Immunol,** v. 194, n. 10, p. 4676-87, May 15 2015. ISSN 1550-6606 (Electronic)
0022-1767 (Linking). Available at: < https://www.ncbi.nlm.nih.gov/pubmed/25870241 >.

TRIPATHI, S. K.; LAHESMAA, R. Transcriptional and epigenetic regulation of T-helper lineage specification. **Immunol Rev,** v. 261, n. 1, p. 62-83, Sep 2014. ISSN 1600-065X (Electronic)
0105-2896 (Linking). Available at: < https://www.ncbi.nlm.nih.gov/pubmed/25123277 >.

VAN DEN BROEK, T.; BORGHANS, J. A. M.; VAN WIJK, F. The full spectrum of human naive T cells. **Nat Rev Immunol,** v. 18, n. 6, p. 363-373, Jun 2018. ISSN 1474-1741 (Electronic)
1474-1733 (Linking). Available at: < https://www.ncbi.nlm.nih.gov/pubmed/29520044 >.

VELLA, L. A.; HERATI, R. S.; WHERRY, E. J. CD4(+) T Cell Differentiation in Chronic Viral Infections: The Tfh Perspective. **Trends Mol Med,** v. 23, n. 12, p. 1072-1087, Dec 2017. ISSN 1471-499X (Electronic)
1471-4914 (Linking). Available at: < https://www.ncbi.nlm.nih.gov/pubmed/29137933 >.

VILLARINO, A. et al. Signal transducer and activator of transcription 5 (STAT5) paralog dose governs T cell effector and regulatory functions. **Elife,** v. 5, Mar 21 2016. ISSN 2050-084X (Electronic)
2050-084X (Linking). Available at: < https://www.ncbi.nlm.nih.gov/pubmed/26999798 >.

VINUESA, C. G.; CYSTER, J. G. How T cells earn the follicular rite of passage. **Immunity,** v. 35, n. 5, p. 671-80, Nov 23 2011. ISSN 1097-4180 (Electronic)
1074-7613 (Linking). Available at: < https://www.ncbi.nlm.nih.gov/pubmed/22118524 >.

VINUESA, C. G. et al. Follicular Helper T Cells. **Annu Rev Immunol,** v. 34, p. 335-68, May 20 2016. ISSN 1545-3278 (Electronic)
0732-0582 (Linking). Available at: < https://www.ncbi.nlm.nih.gov/pubmed/26907215 >.

VROOM, T. M. et al. Tissue distribution of human gamma delta T cells: no evidence for general epithelial tropism. **J Clin Pathol,** v. 44, n. 12, p. 1012-7, Dec 1991. ISSN 0021-9746 (Print)
0021-9746 (Linking). Available at: < https://www.ncbi.nlm.nih.gov/pubmed/1838746 >.

WALSH, M. et al. Plasma exchange and glucocorticoid dosing in the treatment of anti-neutrophil cytoplasm antibody associated vasculitis (PEXIVAS): protocol for a randomized controlled trial. **Trials,** v. 14, p. 73, Mar 14 2013. ISSN 1745-6215 (Electronic)
1745-6215 (Linking). Available at: < https://www.ncbi.nlm.nih.gov/pubmed/23497590 >.

WANG, L.; WANG, F. S.; GERSHWIN, M. E. Human autoimmune diseases: a comprehensive update. **J Intern Med,** v. 278, n. 4, p. 369-95, Oct 2015. ISSN 1365-2796 (Electronic)
0954-6820 (Linking). Available at: < https://www.ncbi.nlm.nih.gov/pubmed/26212387 >.

WANG, Y. et al. TLR4 signaling improves PD-1 blockade therapy during chronic viral infection. **PLoS Pathog,** v. 15, n. 2, p. e1007583, Feb 2019. ISSN 1553-7374 (Electronic)
1553-7366 (Linking). Available at: < https://www.ncbi.nlm.nih.gov/pubmed/30726291 >.

WEBB, L. M. C.; LINTERMAN, M. A. Signals that drive T follicular helper cell formation. **Immunology,** v. 152, n. 2, p. 185-194, Oct 2017. ISSN 1365-2567 (Electronic)
0019-2805 (Linking). Available at: < https://www.ncbi.nlm.nih.gov/pubmed/28628194 >.

WEINSTEIN, J. S. et al. Global transcriptome analysis and enhancer landscape of human primary T follicular helper and T effector lymphocytes. **Blood,** v. 124, n. 25, p. 3719-29, Dec 11 2014. ISSN 1528-0020 (Electronic)
0006-4971 (Linking). Available at: < https://www.ncbi.nlm.nih.gov/pubmed/25331115 >.

WHERRY, E. J. T cell exhaustion. **Nat Immunol,** v. 12, n. 6, p. 492-9, Jun 2011. ISSN 1529-2916 (Electronic)
1529-2908 (Linking). Available at: < https://www.ncbi.nlm.nih.gov/pubmed/21739672 >.

WHERRY, E. J.; KURACHI, M. Molecular and cellular insights into T cell exhaustion. **Nat Rev Immunol,** v. 15, n. 8, p. 486-99, Aug 2015. ISSN 1474-1741 (Electronic)
1474-1733 (Linking). Available at: < https://www.ncbi.nlm.nih.gov/pubmed/26205583 >.

WILDE, B. et al. Abnormal expression pattern of the IL-2 receptor beta-chain on CD4+ T cells in ANCA-associated vasculitis. **Dis Markers,** v. 2014, p. 249846, 2014a. ISSN 1875-8630 (Electronic)
0278-0240 (Linking). Available at: < http://www.ncbi.nlm.nih.gov/pubmed/24648606 >.

_____. Signal tranducers and activators of transcription: expression and function in anti-neutrophil cytoplasmic antibody-associated vasculitis. **Mol Med Rep,** v. 9, n. 6, p. 2316-20, Jun 2014b. ISSN 1791-3004 (Electronic)
1791-2997 (Linking). Available at: < https://www.ncbi.nlm.nih.gov/pubmed/24676862 >.

WILDE, B. et al. Aberrant expression of the negative costimulator PD-1 on T cells in granulomatosis with polyangiitis. **Rheumatology (Oxford),** v. 51, n. 7, p. 1188-97, Jul 2012. ISSN 1462-0332 (Electronic)
1462-0324 (Linking). Available at: < https://www.ncbi.nlm.nih.gov/pubmed/22447882 >.

WILDE, B. et al. Th17 expansion in granulomatosis with polyangiitis (Wegener's): the role of disease activity, immune regulation and therapy. **Arthritis Res Ther,** v. 14, n. 5, p. R227, 2012. ISSN 1478-6362 (Electronic)
1478-6354 (Linking). Available at: < http://www.ncbi.nlm.nih.gov/pubmed/23079279 >.

WING, J. B.; TANAKA, A.; SAKAGUCHI, S. Human FOXP3(+) Regulatory T Cell Heterogeneity and Function in Autoimmunity and Cancer. **Immunity,** v. 50, n. 2, p. 302-316, Feb 19 2019. ISSN 1097-4180 (Electronic)
1074-7613 (Linking). Available at: < https://www.ncbi.nlm.nih.gov/pubmed/30784578 >.

WITKO-SARSAT, V.; THIEBLEMONT, N. Granulomatosis with polyangiitis (Wegener granulomatosis): A proteinase-3 driven disease? **Joint Bone Spine,** v. 85, n. 2, p. 185-189, Mar 2018. ISSN 1778-7254 (Electronic)
1297-319X (Linking). Available at: < https://www.ncbi.nlm.nih.gov/pubmed/28495524 >.

WU, H. et al. Molecular Control of Follicular Helper T cell Development and Differentiation. **Front Immunol,** v. 9, p. 2470, 2018. ISSN 1664-3224 (Electronic)
1664-3224 (Linking). Available at: < https://www.ncbi.nlm.nih.gov/pubmed/30410493 >.

YANG, Y. et al. T-bet and eomesodermin play critical roles in directing T cell differentiation to Th1 versus Th17. **J Immunol,** v. 181, n. 12, p. 8700-10, Dec 15 2008. ISSN 1550-6606 (Electronic)
0022-1767 (Linking). Available at: < https://www.ncbi.nlm.nih.gov/pubmed/19050290 >.

ZAHM, C. D. et al. TLR Stimulation during T-cell Activation Lowers PD-1 Expression on CD8(+) T Cells. **Cancer Immunol Res,** v. 6, n. 11, p. 1364-1374, Nov 2018. ISSN 2326-6074 (Electronic)
2326-6066 (Linking). Available at: < https://www.ncbi.nlm.nih.gov/pubmed/30201735 >.

ZENG, H. et al. mTORC1 and mTORC2 Kinase Signaling and Glucose Metabolism Drive Follicular Helper T Cell Differentiation. **Immunity,** v. 45, n. 3, p. 540-554, Sep 20 2016. ISSN 1097-4180 (Electronic)
1074-7613 (Linking). Available at: < https://www.ncbi.nlm.nih.gov/pubmed/27637146 >.

ZHANG, F.; MENG, G.; STROBER, W. Interactions among the transcription factors Runx1, RORgammat and Foxp3 regulate the differentiation of interleukin 17-producing T cells. **Nat Immunol,** v. 9, n. 11, p. 1297-306, Nov 2008. ISSN 1529-2916 (Electronic)
1529-2908 (Linking). Available at: < https://www.ncbi.nlm.nih.gov/pubmed/18849990 >.

ZHAO, Y. et al. Circulating T follicular helper cell and regulatory T cell frequencies are influenced by B cell depletion in patients with granulomatosis with polyangiitis. **Rheumatology (Oxford),** v. 53, n. 4, p. 621-30, Apr 2014. ISSN 1462-0332 (Electronic)
1462-0324 (Linking). Available at: < http://www.ncbi.nlm.nih.gov/pubmed/24357812 >.

ZHOU, L. et al. IL-6 programs T(H)-17 cell differentiation by promoting sequential engagement of the IL-21 and IL-23 pathways. **Nat Immunol,** v. 8, n. 9, p. 967-74, Sep 2007. ISSN 1529-2908 (Print)
1529-2908 (Linking). Available at: < https://www.ncbi.nlm.nih.gov/pubmed/17581537 >.

ZHU, J. T Helper Cell Differentiation, Heterogeneity, and Plasticity. **Cold Spring Harb Perspect Biol,** v. 10, n. 10, Oct 1 2018. ISSN 1943-0264 (Electronic)
1943-0264 (Linking). Available at: < https://www.ncbi.nlm.nih.gov/pubmed/28847903 >.

9.Appendix

					Chapter 3								Chapter 3				
Medication	Type of ANCA	Subject	Age	Gender	Figure 3.1, Figure 3.4, Figure 3.6	Figure 3.2	Figure 3.3a	Figure 3.3b	Figure 3.5	Subject	Age	Gender	Figure 3.1, Figure 3.4, Figure 3.6	Figure 3.2	Figure 3.3a	Figure 3.3b	Figure 3.5
S, I , A	c	GPA1	48	M	o	o				H1	27	F	o	o	o		
S, PRE-RTX	-	GPA2	55	M			o			H2	31	F	o	o	o	o	
S, H	c	GPA3	71	F	o	o	o			H3	70	F	o	o	o		
S, I, A	p	GPA4	45	F						H4	31	M	o	o			
S, I, A	c	GPA5	23	F	o	o				H5	60	M	o	o	o		
S, I, A	c	GPA6	35	F	o	o	o			H6	45	M	o	o			
S, I, A	c	GPA7	68	M						H7	43	M	o	o			o
S, PRE-RTX	c	GPA8	59	M	o	o				H8	54	F	o	o			o
S, I, A	c	GPA9	30	M	o	o				H9	55	F					
S, PRE-RTX	p	GPA10	46	M	o	o			o	H10	45	F				o	
S, PRE-RTX, H	p	GPA11	55	F	o	o		o	o	H11	45	M					
S, PRE-RTX, A	c	GPA12	65	F						H12	55	M			o		
S, I, A	p	GPA13	73	M						H13	58	F		o			
S, I, H	p	GPA14	43	M						H14	57	F		o			
S, I, A	p	GPA15	44	F						H15	26	F				o	
S, I, A, D	p	GPA16	58	M						H16	49	F		o		o	
S, I, A, H, PRE-RTX	p	GPA17	60	F						H17	52	F				o	
S, I, D	c	GPA18	44	M		o				H18	57	F				o	
S, I, A	c	GPA19	48	M						H19	73	F					
S, I, A, H	c	GPA20	65	F			o			H20	38	F				o	
PRE-RTX	c	GPA21	39	M													
S	c	GPA22	49	M													
S	p	GPA23	43	M													
I	c	GPA24	50	F		o											
S, I, A,D	c	GPA25	69	F			o										
S, I, D	c	GPA26	47	M				o									
S, I, H	p	GPA27	66	F			o										
S, I, A	c	GPA28	25	F			o										
PRE-RTX, I	c	GPA29	47	F				o									
S, I, A	c	GPA30	36	F		o	o	o									
S, PRE-RTX, H	p	GPA31	56	F				o									
S, A, D	c	GPA32	46	F				o									
S, H	p	GPA33	45	F				o									
PRE-RTX, A, S	c	GPA34	53	M		o											
PRE-RTX, I, S,A	c	GPA35	43	M													
S, I, A	c	GPA36	56	F													
S, I, A	p	GPA37	44	F		o		o									
S, I, A, H, PRE-RTX	p	GPA38	61	F													
S, A	c	GPA39	48	F				o									
S, A	c	GPA40	34	F				o									
S, I, D	c	GPA41	44	M				o									
I	-	GPA42	56	M													
S, I, A	-	GPA43	50	F													
S, I, A, D	c	GPA44	44	M													
S, I	c	GPA45	50	F													
S	c	GPA46	49	M													
PRE-RTX, A	-	GPA47	45	F													
S, I, A,H, D	p	GPA48	39	F													
S, I, A,H, D	-	GPA49	61	F													
S, I, A	c	GPA50	50	F													

sTable 9.1. Patient and healthy control samples used in Chapter 3.

Abbreviation of medication; Steroids (S), Immunosuppressive drugs (I), Antibiotics (A), Vitamin D (D), Hydroxychloroquine (H), previously Rituximab treated (PRE-RTX).

					Chapter 4				
Medication	Type of ANCA	Subject	Age	Gender	Figure 4.1-Figure 4.4	Figure 4.5 - Figure 4.8	Figure 4.9	Figure 4.10 Figure 4.11	Figure 4.12
S, I , A	c	GPA1	48	M			o		
S, PRE-RTX	-	GPA2	55	M					
S, H	c	GPA3	71	F					
S, I, A	p	GPA4	45	F					
S, I, A	c	GPA5	23	F			o		
S, I, A	c	GPA6	35	F			o		
S, I, A	c	GPA7	68	M					
S, PRE-RTX	c	GPA8	59	M					
S, I, A	c	GPA9	30	M					
S, PRE-RTX	p	GPA10	46	M	o		o		
S, PRE-RTX, H	p	GPA11	55	F			o		
S, PRE-RTX, A	c	GPA12	65	F	o				
S, I, A	p	GPA13	73	M					
S, I, H	p	GPA14	43	M					
S, I, A	p	GPA15	44	F	o	o (Group2)			
S, I, A, D	p	GPA16	58	M		o			
S, I, A, H, PRE-RTX	p	GPA17	60	F		o (Group2)			
S, I, D	c	GPA18	44	M	o	o			
S, I, A	c	GPA19	48	M		o			
S, I, A, H	c	GPA20	65	F		o			
PRE-RTX	c	GPA21	39	M	o	o			
S	c	GPA22	49	M		o			
S	p	GPA23	43	M	o				
I	c	GPA24	50	F					
S, I, A,D	c	GPA25	69	F	o				
S, I, D	c	GPA26	47	M	o				
S, I, H	p	GPA27	66	F					
S, I, A	c	GPA28	25	F					
PRE-RTX, I	c	GPA29	47	F					
S, I, A	c	GPA30	36	F					
S, PRE-RTX, H	p	GPA31	56	F					
S, A, D	c	GPA32	46	F					
S, H	p	GPA33	45	F				o	o
PRE-RTX, A, S	c	GPA34	53	M	o				
PRE-RTX, I, S,A	c	GPA35	43	M					
S, I, A	c	GPA36	56	F					
S, I, A	p	GPA37	44	F				o	o
S, I, A, H, PRE-RTX	p	GPA38	61	F					
S, A	c	GPA39	48	F				o	o
S, A	c	GPA40	34	F					
S, I, D	c	GPA41	44	M					
I	-	GPA42	56	M					
S, I, A	-	GPA43	50	F					
S, I, A, D	c	GPA44	44	M					
S, I	c	GPA45	50	F					
S	c	GPA46	49	M					
PRE-RTX, A	-	GPA47	45	F					
S, I, A,H, D	p	GPA48	39	F					
S, I, A,H, D	-	GPA49	61	F					
S, I, A	c	GPA50	50	F					

			Chapter 4				
Subject	Age	Gender	Figure 4.1-Figure 4.4	Figure 4.5-Figure 4.8	Figure 4.9	Figure 4.10-Figure 4.11	Figure 4.12
H1	27	F					
H2	31	F	o				
H3	70	F	o		o		
H4	31	M			o		
H5	60	M			o		
H6	45	M	o				
H7	43	M					
H8	54	F					
H9	55	F		o			
H10	45	F		o			
H11	45	M		o			
H12	55	M	o	o			
H13	58	F		o			
H14	57	F	o				
H15	26	F	o				
H16	49	F				o	o
H17	52	F					
H18	57	F				o	o
H19	73	F					
H20	38	F					

sTable 9.2. Patient and healthy control samples used in Chapter 4.

Abbreviation of medication; Steroids (S), Immunosuppressive drugs (I), Antibiotics (A), Vitamin D (D), Hydroxychloroquine (H), previously Rituximab treated (PRE-RTX).

					Chapter 5						Chapter 5		
Medication	Type of ANCA	Subject	Age	Gender	Figure 5.1	Figure 5.3-Figure 5.5	Figure 5.6	Subject	Age	Gender	Figure 5.1	Figure 5.3-Figure 5.5	Figure 5.6
S, I , A	c	GPA1	48	M	o			H1	27	F	o		
S, PRE-RTX	-	GPA2	55	M				H2	31	F	o		
S, H	c	GPA3	71	F	o			H3	70	F	o		
S, I, A	p	GPA4	45	F				H4	31	M	o		
S, I, A	c	GPA5	23	F	o			H5	60	M	o		
S, I, A	c	GPA6	35	F	o			H6	45	M	o		
S, I, A	c	GPA7	68	M				H7	43	M	o		
S, PRE-RTX	c	GPA8	59	M	o			H8	54	F	o		
S, I, A	c	GPA9	30	M	o			H9	55	F			
S, PRE-RTX	p	GPA10	46	M	o			H10	45	F			
S, PRE-RTX, H	p	GPA11	55	F	o			H11	45	M			
S, PRE-RTX, A	c	GPA12	65	F				H12	55	M			
S, I, A	p	GPA13	73	M				H13	58	F		o	o
S, I, H	p	GPA14	43	M				H14	57	F		o	
S, I, A	p	GPA15	44	F				H15	26	F			
S, I, A, D	p	GPA16	58	M				H16	49	F		o	o
S, I, A, H, PRE-RTX	p	GPA17	60	F				H17	52	F			
S, I, D	c	GPA18	44	M				H18	57	F			o
S, I, A	c	GPA19	48	M				H19	73	F			
S, I, A, H	c	GPA20	65	F				H20	38	F			o
PRE-RTX	c	GPA21	39	M									
S	c	GPA22	49	M									
S	p	GPA23	43	M									
I	c	GPA24	50	F			o						
S, I, A,D	c	GPA25	69	F									
S, I, D	c	GPA26	47	M									
S, I, H	p	GPA27	66	F									
S, I, A	c	GPA28	25	F									
PRE-RTX, I	c	GPA29	47	F		o							
S, I, A	c	GPA30	36	F									
S, PRE-RTX, H	p	GPA31	56	F									
S, A, D	c	GPA32	46	F		o	o						
S, H	p	GPA33	45	F									
PRE-RTX, A, S	c	GPA34	53	M									
PRE-RTX, I, S,A	c	GPA35	43	M									
S, I, A	c	GPA36	56	F		o							
S, I, A	p	GPA37	44	F									
S, I, A, H, PRE-RTX	p	GPA38	61	F									
S, A	c	GPA39	48	F			o						
S, A	c	GPA40	34	F			o						
S, I, D	c	GPA41	44	M									
I	-	GPA42	56	M									
S, I, A	-	GPA43	50	F									
S, I, A, D	c	GPA44	44	M									
S, I	c	GPA45	50	F									
S	c	GPA46	49	M									
PRE-RTX, A	-	GPA47	45	F									
S, I, A,H, D	p	GPA48	39	F									
S, I, A,H, D	-	GPA49	61	F									
S, I, A	c	GPA50	50	F									

sTable 9. 3. Patient and healthy control samples used in Chapter 5.

Abbreviation of medication; Steroids (S), Immunosuppressive drugs (I), Antibiotics (A), Vitamin D (D), Hydroxychloroquine (H), previously Rituximab treated (PRE-RTX).

					Chapter 6 (plasma samples)								Chapter 6 (plasma samples)				
Medication	Type of ANCA	Subject	Age	Gender	Figure 6.1a	Figure 6.1b-j	Figure 6.2, Figure 6.3, Figure 6.5	Figure 6.4	Figure 6.6	Subject	Age	Gender	Figure 6.1a	Figure 6.1b-j	Figure 6.2, Figure 6.3, Figure 6.5	Figure 6.4	Figure 6.6
S, I , A	c	GPA1	48	M	o	o	o			H1	27	F	o	o			
S, PRE-RTX	-	GPA2	55	M	o	o	o			H2	31	F	o	o	o		
S, H	c	GPA3	71	F	o	o	o	o		H3	70	F	o	o	o	o	
S, I, A	p	GPA4	45	F	o	o	o			H4	31	M	o	o	o		o
S, I, A	c	GPA5	23	F	o	o	o	o	o	H5	60	M	o	o	o		
S, I, A	c	GPA6	35	F	o	o	o		o	H6	45	M	o	o	o		
S, I, A	c	GPA7	68	M	o	o	o	o	o	H7	43	M	o	o	o	o	o
S, PRE-RTX	c	GPA8	59	M	o	o	o	o	o	H8	54	F	o	o			
S, I, A	c	GPA9	30	M	o	o	o			H9	55	F	o				
S, PRE-RTX	p	GPA10	46	M	o	o	o			H10	45	F	o	o	o	o	
S, PRE-RTX, H	p	GPA11	55	F	o	o	o			H11	45	M	o	o	o	o	
S, PRE-RTX, A	c	GPA12	65	F	o	o	o	o		H12	55	M	o	o	o	o	
S, I, A	p	GPA13	73	M	o	o	o			H13	58	F	o	o	o		o
S, I, H	p	GPA14	43	M	o	o	o			H14	57	F					
S, I, A	p	GPA15	44	F	o	o	o			H15	26	F					
S, I, A, D	p	GPA16	58	M	o	o	o			H16	49	F					
S, I, A, H, PRE-RTX	p	GPA17	60	F	o	o	o			H17	52	F					
S, I, D	c	GPA18	44	M	o	o	o			H18	57	F					
S, I, A	c	GPA19	48	M	o	o	o		o	H19	73	F					
S, I, A, H	c	GPA20	65	F	o	o	o		o	H20	38	F					
PRE-RTX	c	GPA21	39	M	o	o	o										
S	c	GPA22	49	M	o	o	o	o									
S	p	GPA23	43	M		o											
I	c	GPA24	50	F		o											
S, I, A,D	c	GPA25	69	F		o											
S, I, D	c	GPA26	47	M		o											
S, I, H	p	GPA27	66	F		o											
S, I, A	c	GPA28	25	F		o											
PRE-RTX, I	c	GPA29	47	F		o											
S, I, A	c	GPA30	36	F		o											
S, PRE-RTX, H	p	GPA31	56	F		o											
S, A, D	c	GPA32	46	F		o											
S, H	p	GPA33	45	F		o											
PRE-RTX, A, S	c	GPA34	53	M		o											
PRE-RTX, I, S,A	c	GPA35	43	M		o											
S, I, A	c	GPA36	56	F		o											
S, I, A	p	GPA37	44	F		o											
S, I, A, H, PRE-RTX	p	GPA38	61	F		o											
S, A	c	GPA39	48	F													
S, A	c	GPA40	34	F													
S, I, D	c	GPA41	44	M													
I	-	GPA42	56	M	o	o											
S, I, A	-	GPA43	50	F	o	o											
S, I, A, D	c	GPA44	44	M	o	o											
S, I	c	GPA45	50	F		o											
S	c	GPA46	49	M		o											
PRE-RTX, A	-	GPA47	45	F		o											
S, I, A,H, D	p	GPA48	39	F		o											
S, I, A,H, D	-	GPA49	61	F		o											
S, I, A	c	GPA50	50	F		o											

sTable 9.4. Patient and healthy control samples used in Chapter 6.

Abbreviation of medication; Steroids (S), Immunosuppressive drugs (I), Antibiotics (A), Vitamin D (D), Hydroxychloroquine (H), previously Rituximab treated (PRE-RTX).

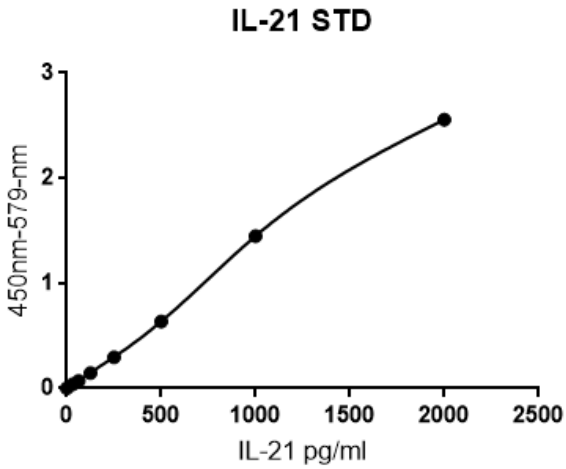

sFigure 9.1. IL-21 ELISA standard curve.

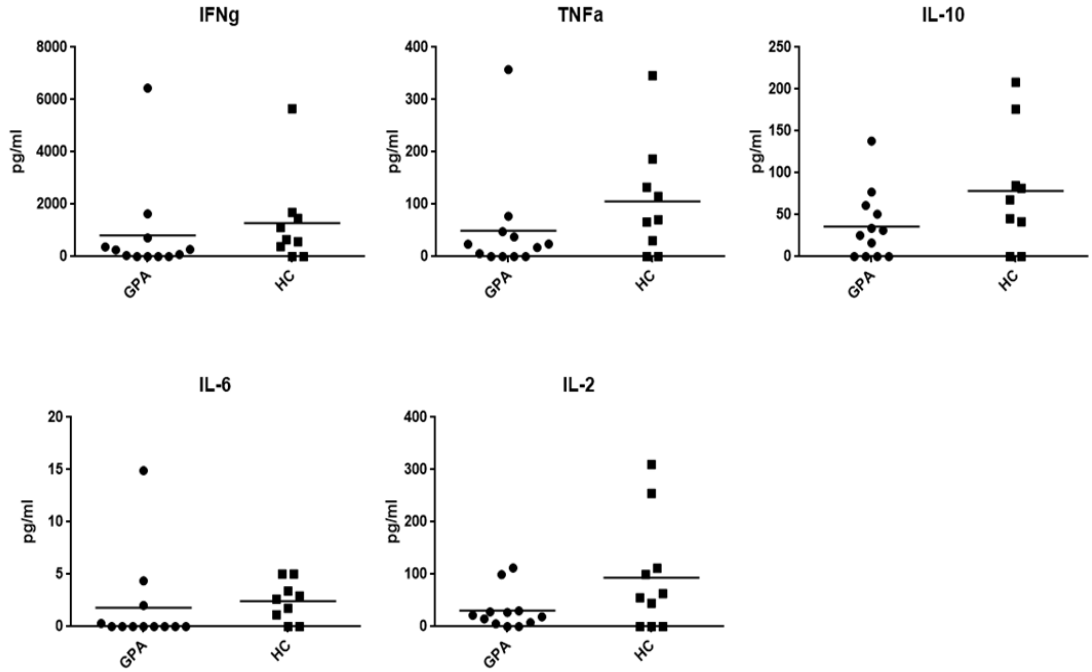

sFigure 9.2. Cytokine production in TCR stimulated CD4+ T cell culture supernatants.

$CD4^+$ T cells from GPA patients or healthy controls were cultured for 4 days in the presence of anti-CD3 and anti-CD28 to mimic TCR stimulation. Cytokines were measured by CBA assay.

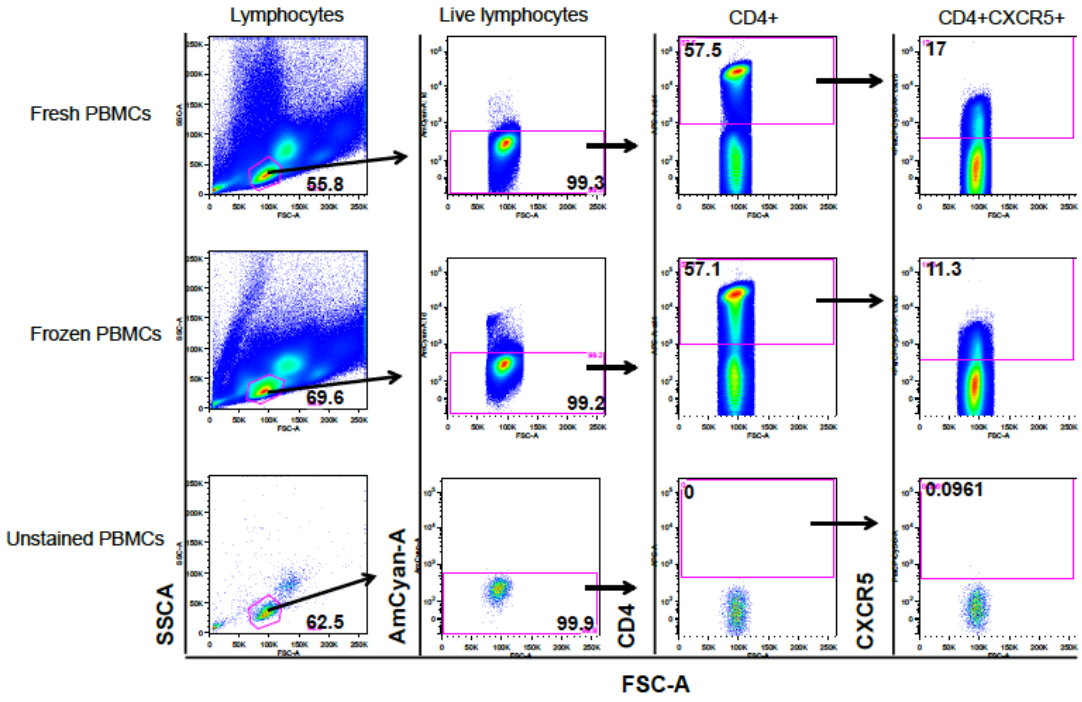

sFigure 9.3. CXCR5 expression in the CD4+ T-lymphocyte population in fresh and frozen PBMCs.1 million freshly isolated (Fresh) or cryopreserved (frozen) PBMCs were stained with CD4-eFluor780 and CXCR5-PerCP/Cy5.5 antibodies diluted at 1 in 50. Fresh unstained PBMC was used as a negative control (unstained PBMCs) and dead cells were excluded by Amcyan staining.

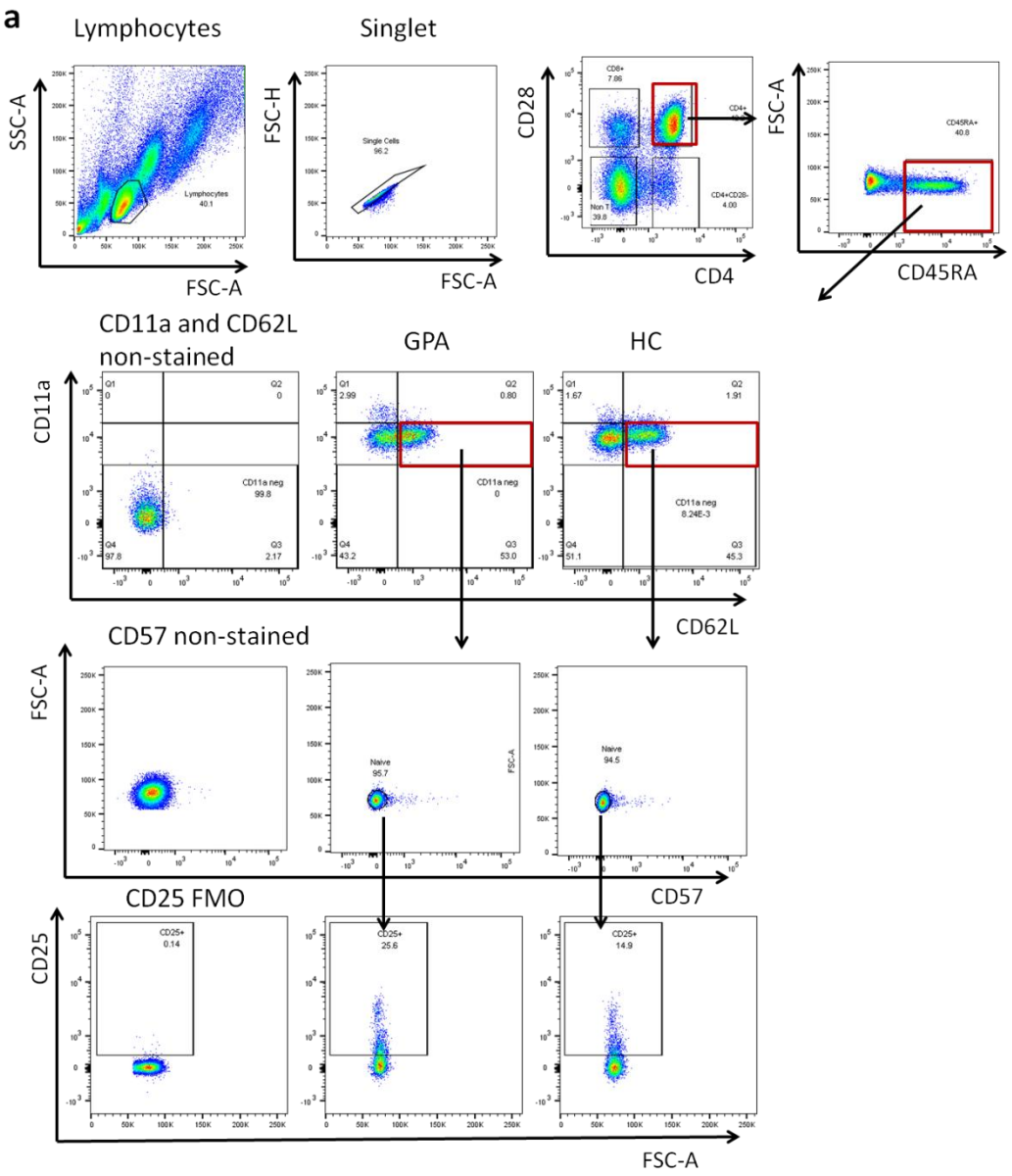
a
Lymphocytes
Singlet
SSC-A
FSC-A
FSC-H
FSC-A
CD28
CD4
FSC-A
CD45RA
CD11a and CD62L
non-stained
GPA
HC
CD11a
CD62L
CD57 non-stained
FSC-A
CD57
CD25 FMO
CD25
FSC-A

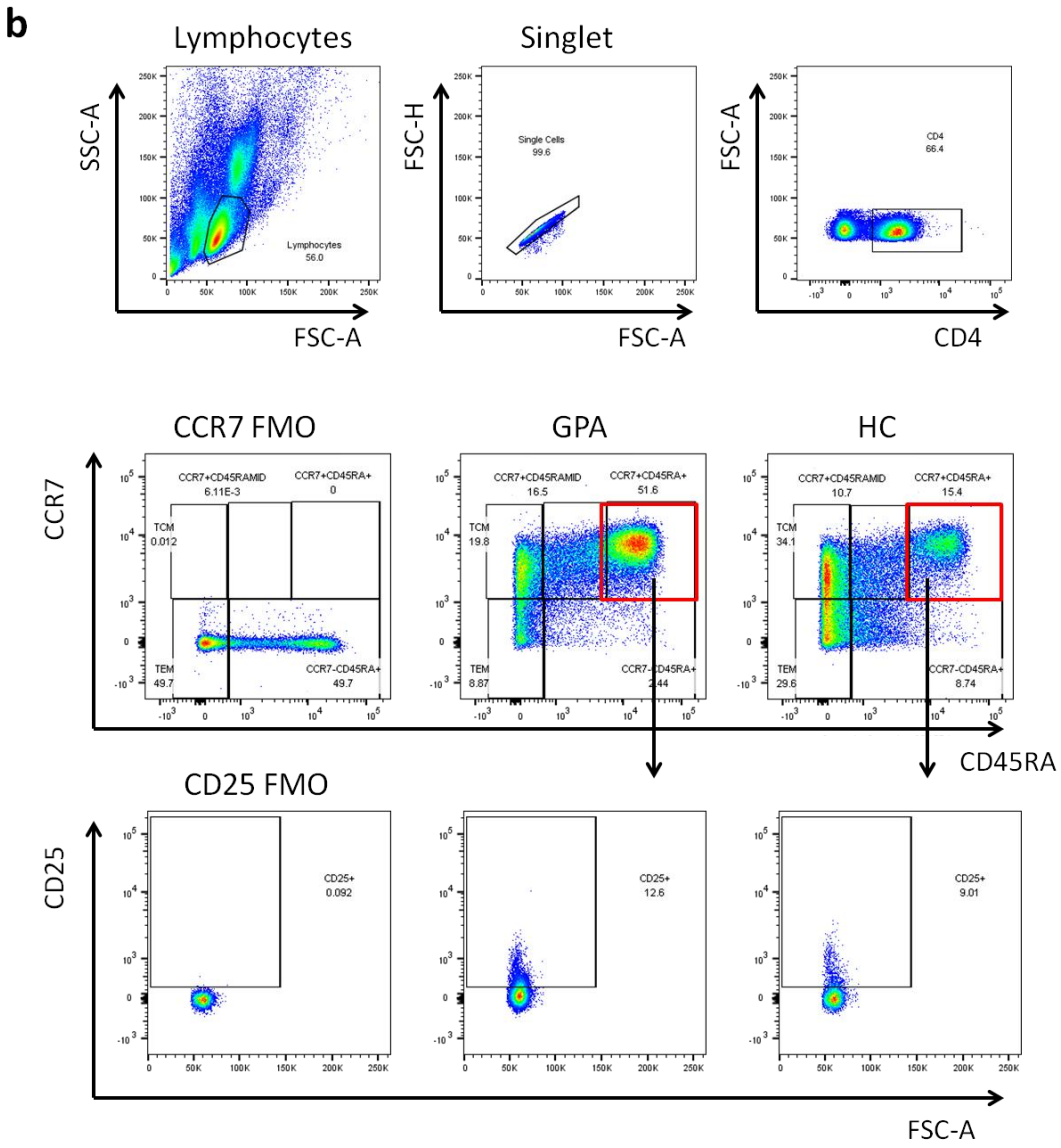

sFigure 9.4 CD25 expression on comprehensively phenotyped naive CD4+ T cells. **(a)** Gating strategy for detection of CD25 expression on naïve (CD4+CD28+CD45RA+CD62L+CD11a^{dim}CD57-) T cells from GPA and HC PBMC by flow cytometry. **(b)** Gating strategy for detection of CD25 expression on naive (CD4+CCR7+CD45RA+) T cells from GPA and HC PBMC by flow cytometry.

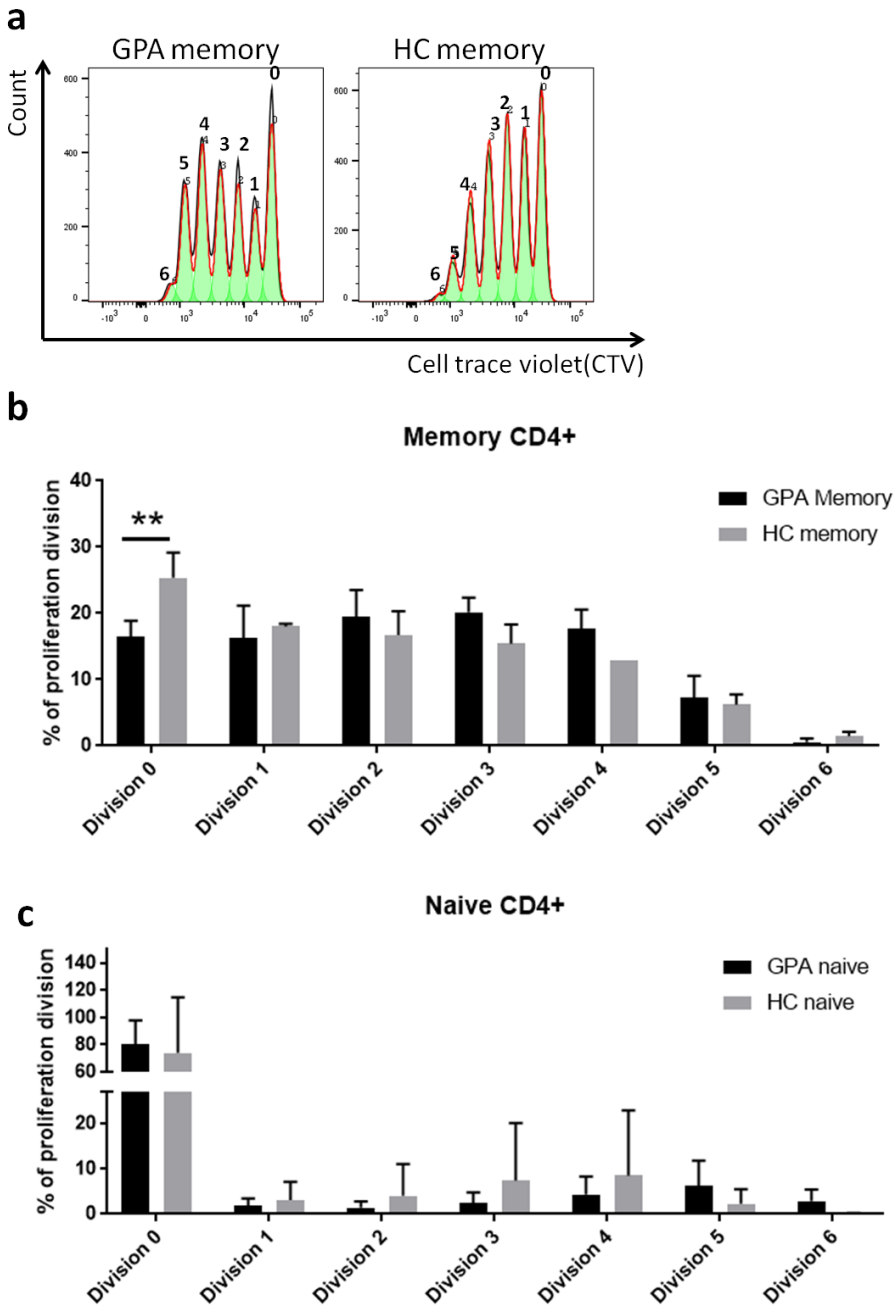

sFigure 9.5 Frequency of CD4+ T cells at each cycle of cell division. **(a)** The frequency of cells in each proliferative peak of the histogram shown in Figure 3.5b were calculated using Flowjo software. No. of divisions of cells in each peak is indicated. Division 0 represents the undivided population. Percentage of **(b)** memory and **(c)** naive CD4+ T cells from GPA and HC cells in each proliferative peak (GPA n=3, HC n=3). Data show mean and standard deviation, and statistical analysis performed by two-way ANOVA (Sidak's multiple comparison test).

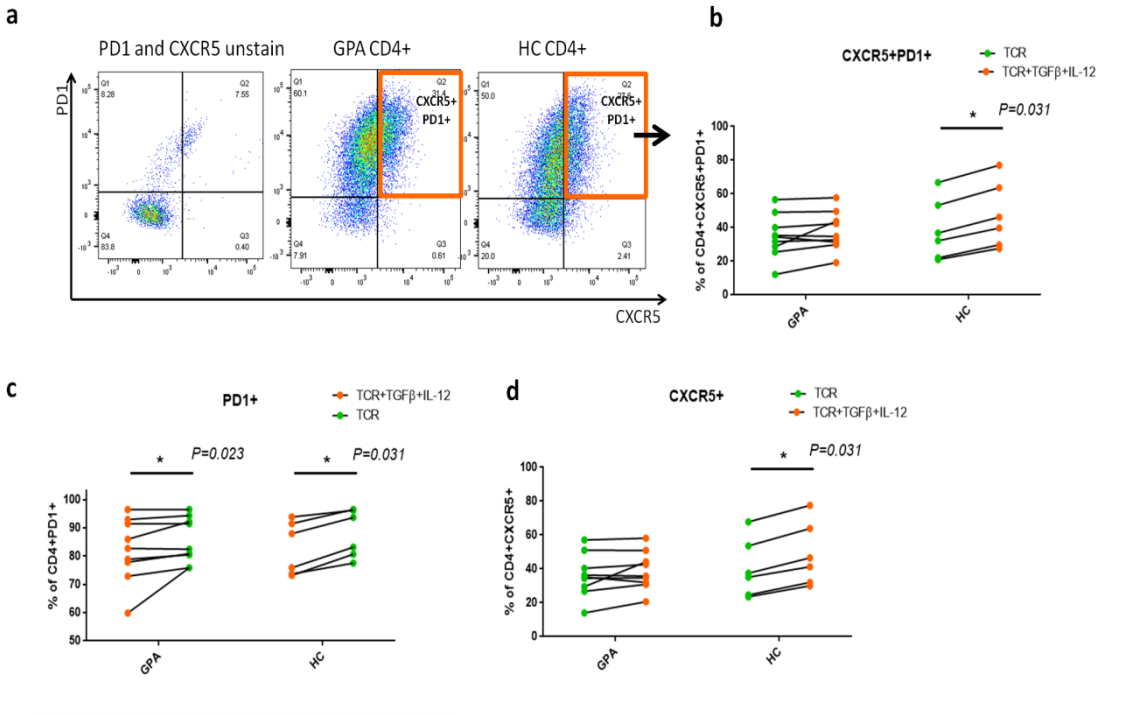

sFigure 9.6 CXCR5+PD1+CD4+ T cells after Th0 (TCR) and Tfh (TCR+ TGFβ+IL-12) in vitro differentiation. (a) CXCR5+PD1+CD4+ T cells were identified using an alternative gating to the method described in Figure 4.1a. In this analysis, only the cells with the lowest signal in the PE-Cy7 (PD1) and PerCP-Cy5.5 (CXCR5) channels in the unstained control were excluded from the analysis.. The frequencies of **(b)** CXCR5+PD1+CD4+ T cells, **(c)** PD1+CD4+ T cells and **(d)** CXCR5+CD4+ T cells were compared between GPA patients and HC naive CD4+ T cells cultured with TCR alone (green dot) or TCR+TGFβ+IL-21 (orange dot). Statistical analysis was performed by Wilcoxon matched pairs signed rank test. n=9 (GPA) and n=6 (HC).

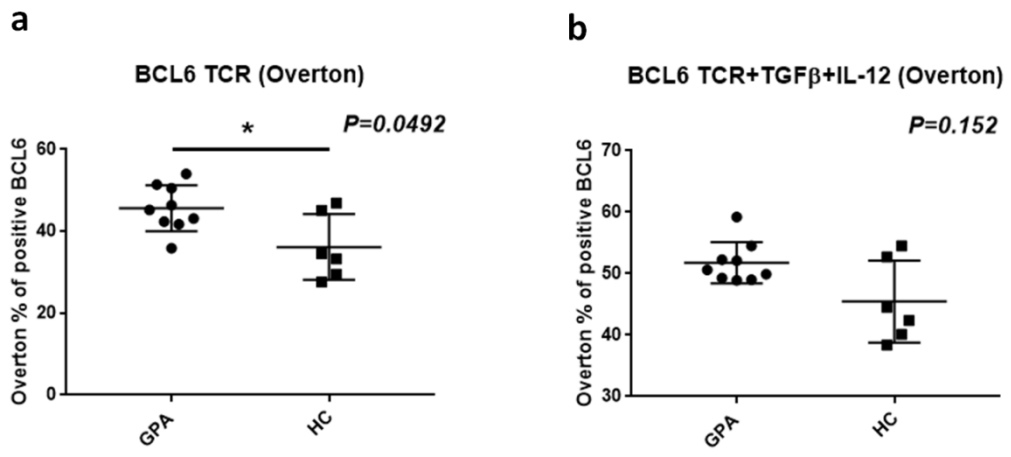

sFigure 9.7 Intracellular expression of BCL6 in CD4+ T cells after Th0 and Tfh in vitro differentiation, calculated by Overton subtraction. Isolated naive CD4+ T cells from GPA patients or healthy controls were cultured for 5 days under Th0 (TCR alone) or Tfh (TCR+TGFβ+IL-12) differentiation conditions. **(a and b)** The Overton percentage of BCL6 positive cells was determined by subtracting the area of the isotype control histogram from the area of the BCL6^{+}CD4+ T cell histogram (representative histograms shown in Figure 4.2a). Overton % of BCL6+ cells were compared between GPA and HC naive CD4+ T cells cultured under **(a)** Th0 (TCR) or **(b)** Tfh (TCR+TGFβ+IL-12) differentiation conditions. Data show mean frequencies of cell subsets, and statistical analysis performed by Mann Whitney test. GPA n=9 HC n=6.

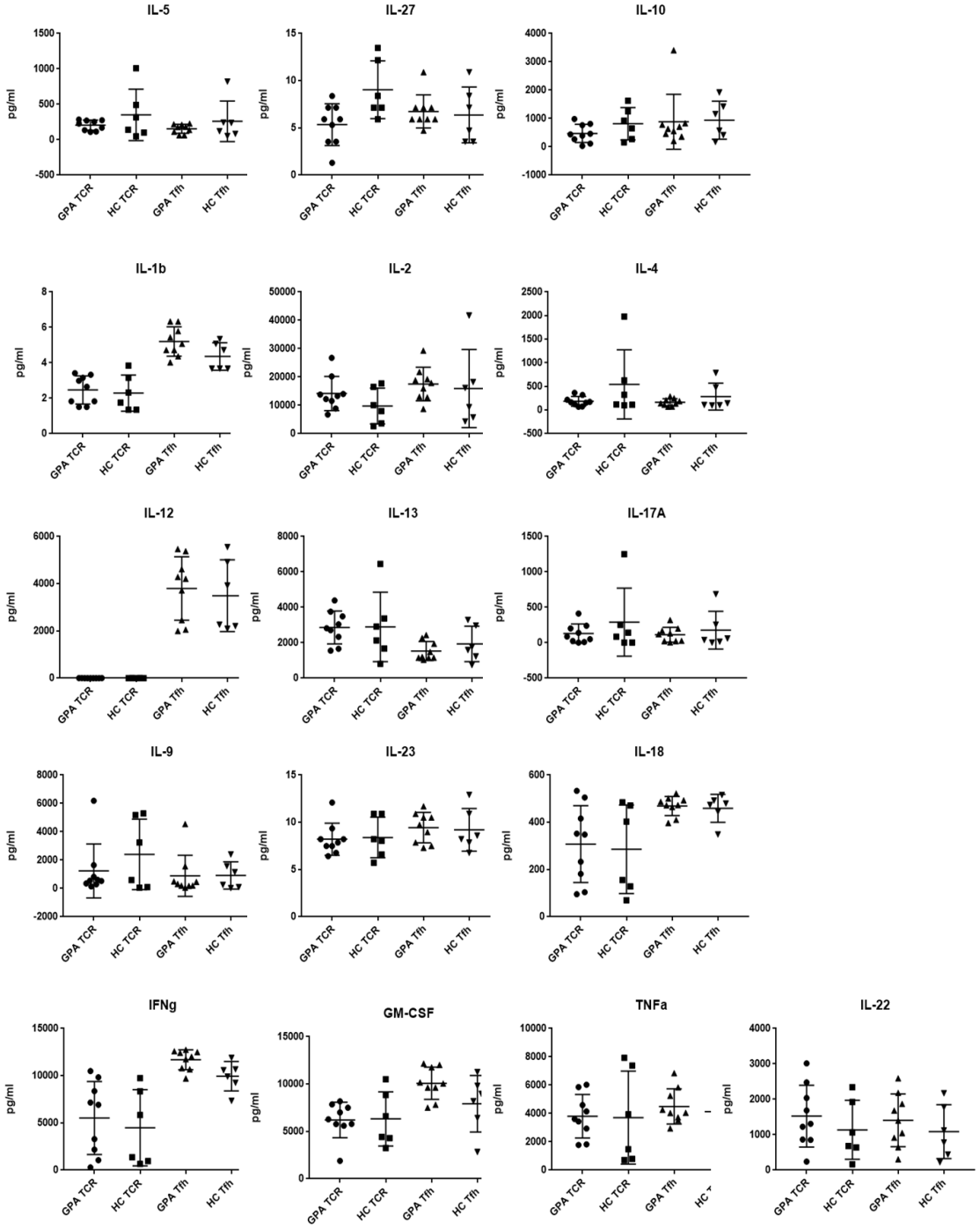

sFigure 9.8 Secreted cytokine levels from naive CD4+ T cells after in vitro Th0 (TCR) and Tfh differentiation (Tfh). Isolated naive CD4+ T cells from GPA patients or healthy controls were cultured for 5 days under Th0 (TCR alone) or Tfh (TCR+TGFβ+IL-12) differentiation conditions. Concentration of cytokines in cell culture supernatants was measured by Luminex assay.

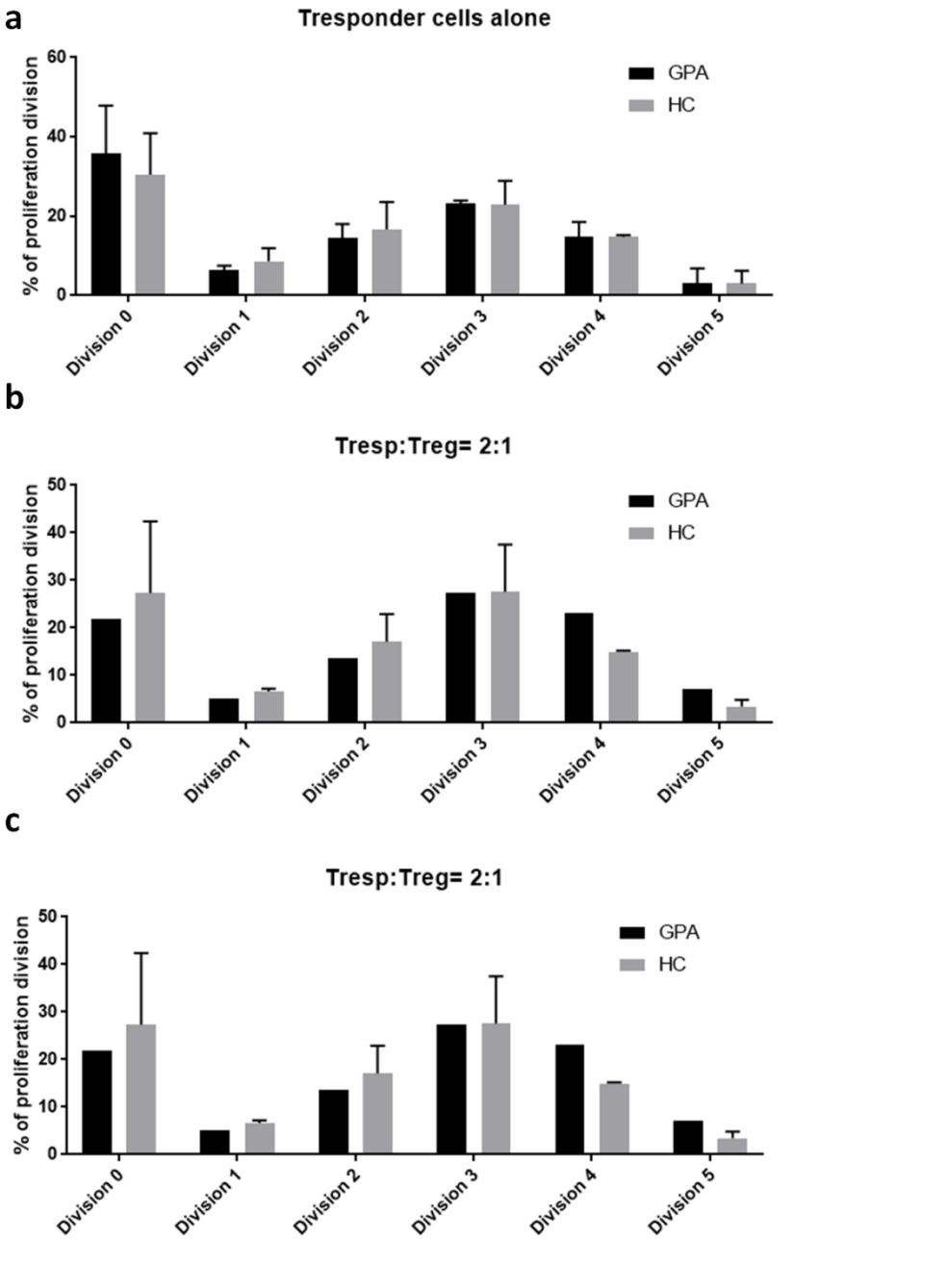

sFigure 9.9 Frequency of T responder cells at each cycle of cell division. The frequency of cells in each proliferative peak was calculated using Flowjo software. No. of cell divisions is indicated. Division 0 represents the undivided population. Percentage of **(a)** T responder cells cultured alone **(b)** Tresp cells and Tregs were co-cultured at ratio 2:1 for 6 days with anti-CD3 and anti-CD28 (GPA n=1, HC n=2). **(c)** Tresp cells and CD25+naive CD4+ T cells were co-cultured at ratio 2:1 (GPA n=2, HC n=2).

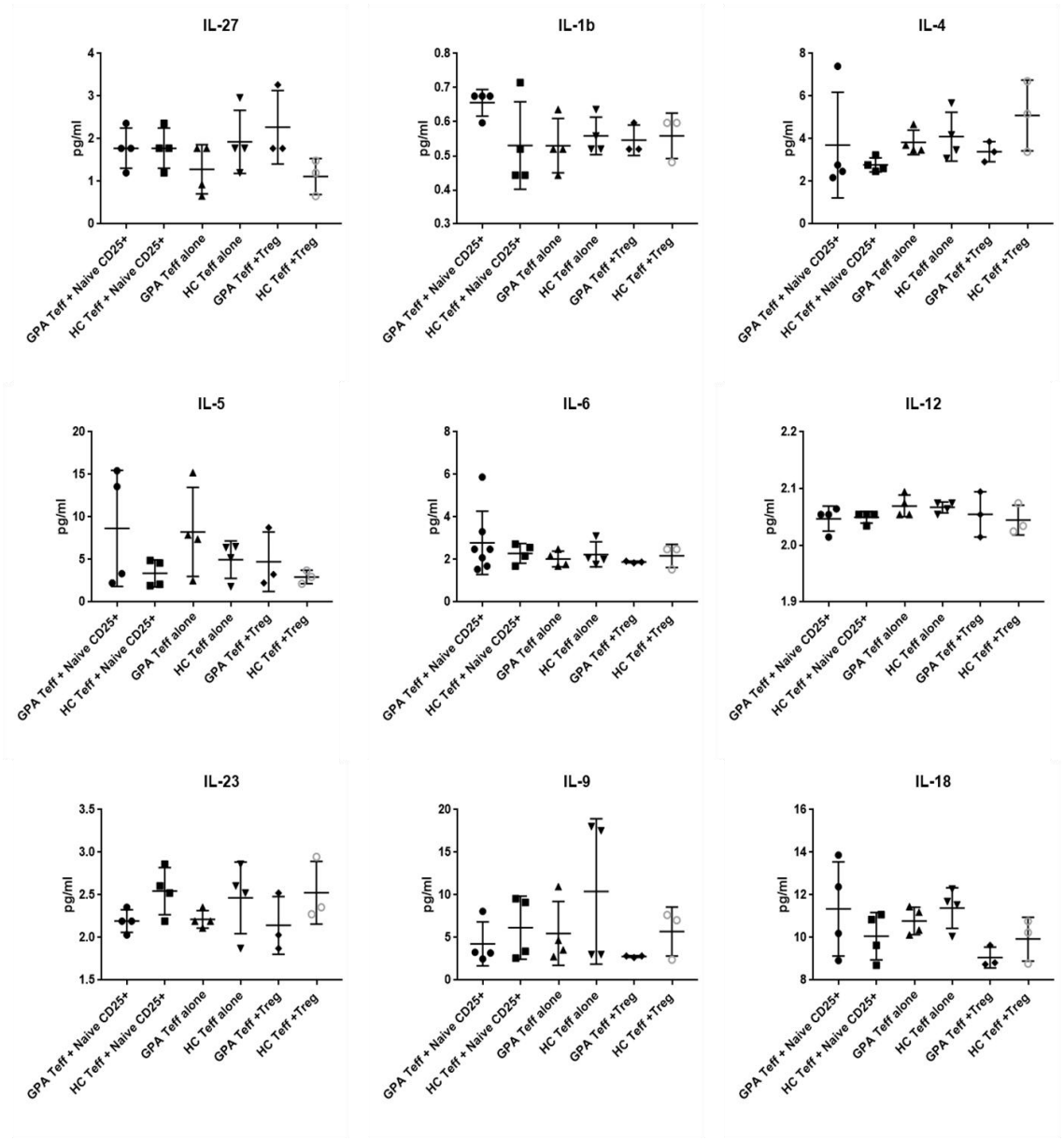

sFigure 9.10 Cytokine concentration after Tresp culture alone or Tresp co-culture with Treg or naive CD25+CD4+ T cells. Supernatants from the same experiment described in Figure 5.3 and Figure 5.4 harvested and the level of cytokines were measured by Luminex. Supernatants from cell culture with 500 Tresp and 1000 naive CD25+CD4+ T cells (Teff + naive CD25+). Supernatants from cell culture with 500 Tresp alone (Teff alone). Supernatants from cell culture with 500 Tresp and 250 Tregs (Teff + Treg).

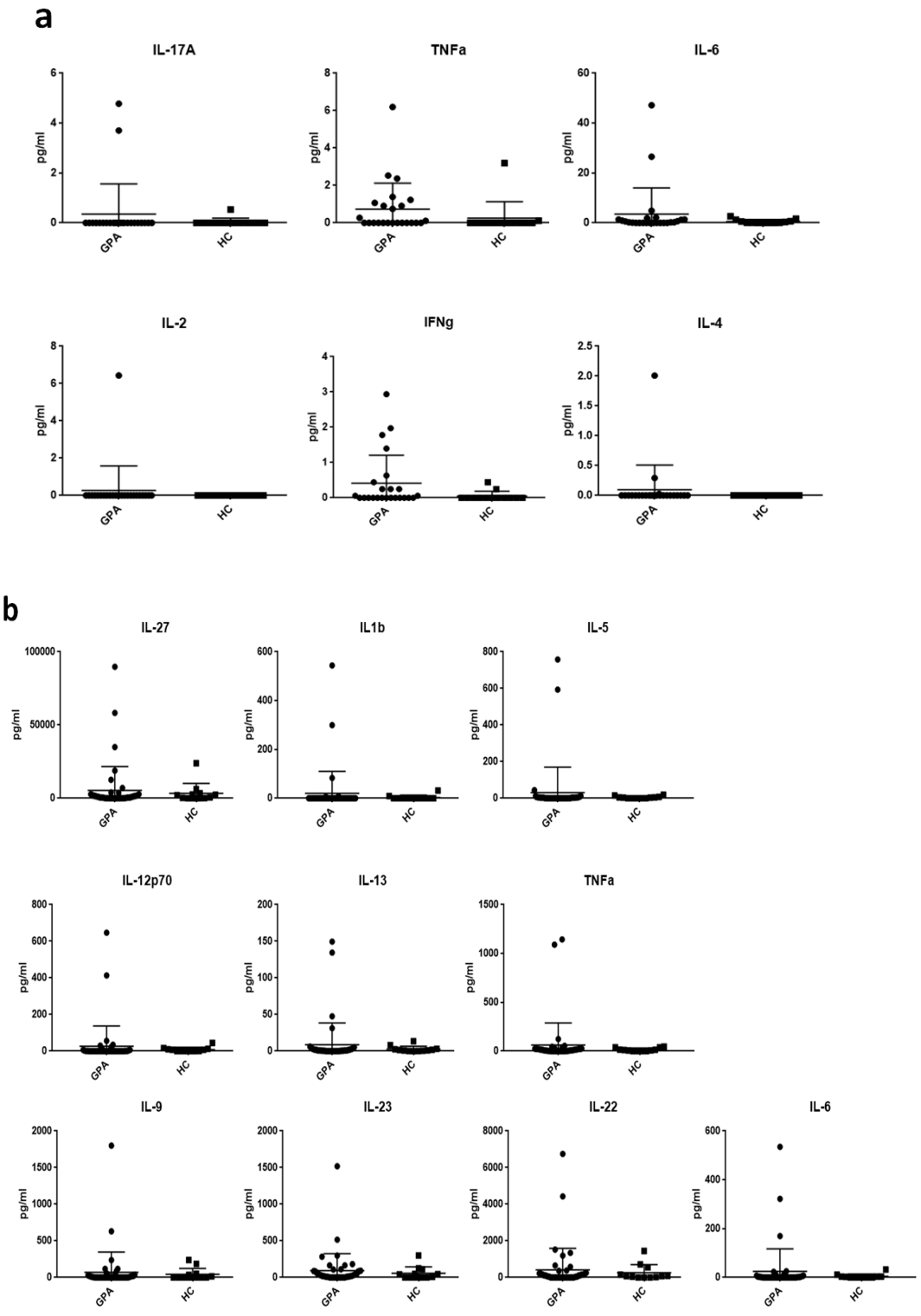

sFigure 9.11. Figure 6.1 Cytokine concentration in GPA and HC plasma.

(a) Cytokines measured by CBA **(b)** Cytokine measured by Luminex.

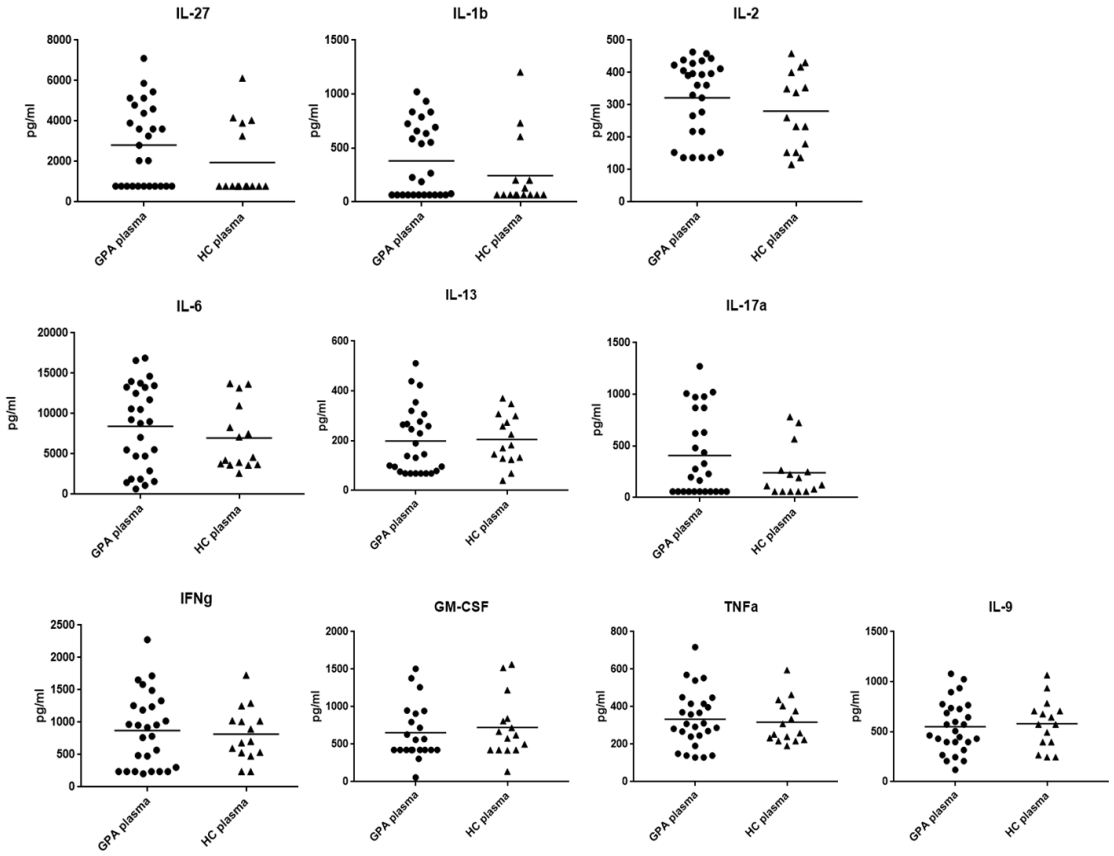

sFigure 9.12 Cytokine concentrations in supernatants from healthy PBMCs co-cultured with GPA plasma. Cytokine concentrations in supernatants from the experiment described in Figure 6.2 were measured by Luminex assay.

sTable 9.5 Gene list from Figure 4.5c.

List of differently expressed genes in rested naive CD4+ T cells from GPA patients compare to HC (Figure 4.5c)								
Rested naive CD4+ T cells (All GPA)			Rested naive CD4+ T cells (GPA group1)			Rested naive CD4+ T cells (GPA group2)		
Gene	p-value	Fold-Change	Gene	p-value	Fold-Change	Gene	p-value	Fold-Change
GLYR1	0.0020	2.9757	DEFA1	0.0001	3.9065	KATNBL1	0.0003	4.2933
DEFA1	0.0304	2.7785	DEFA1B	0.0001	3.5562	SYMPK	0.0024	4.1715
DEFA1B	0.0255	2.6332	DEFA3	0.0002	3.5140	CYP27A1	0.0437	4.1098
DEFA3	0.0268	2.6147	MCEMP1	0.0117	3.2884	NDUFA5	0.0381	3.8960
LOC653600	0.0266	2.3688	S100A8	0.0029	3.1763	MMP9	0.0194	3.5066
CTSG	0.0469	2.2834	LOC653600	0.0001	3.1334	ATF5	0.0129	3.4484
MS4A3	0.0116	2.2682	MS4A3	0.0000	3.0458	TMC6	0.0463	3.4130
KLHL34	0.0413	2.0806	CTSG	0.0076	3.0417	HS.544833	0.0000	3.2662
OLFM4	0.0144	2.0241	GLYR1	0.0032	2.9583	COA1	0.0385	3.0515
HEBP2	0.0144	1.9772	CAMP	0.0233	2.8889	GLYR1	0.0146	3.0197
LOC643695	0.0475	1.9735	GCA	0.0453	2.6268	KRT18P28	0.0003	3.0075
QARS	0.0146	1.9621	S100A9	0.0136	2.6113	KLHDC8B	0.0070	2.9435
SNORD35B	0.0118	1.9405	OLFM4	0.0003	2.6049	WDR73	0.0222	2.9362
SSU72	0.0245	1.8903	ASGR1	0.0429	2.4800	CSF1R	0.0340	2.9227
POLR3C	0.0191	1.8579	KLHL34	0.0228	2.4682	SAAL1	0.0407	2.7939
DDX27	0.0476	1.8403	SNRNP35	0.0184	2.4138	ZBTB12	0.0070	2.7868
SRP72	0.0098	1.7970	QARS	0.0031	2.3594	GON7	0.0034	2.7377
CHUK	0.0109	1.7952	SNORD35B	0.0022	2.3254	DCAF8	0.0042	2.6594
GYG1	0.0020	1.7683	CEACAM8	0.0007	2.2543	ELAVL1	0.0342	2.6095
ZFYVE21	0.0437	1.7296	LOC650646	0.0375	2.2071	HS.542413	0.0033	2.6045
LOC339879	0.0348	1.7136	MYPOP	0.0447	2.2067	RNF181	0.0021	2.5970
NKIRAS1	0.0462	1.7070	SFXN5	0.0339	2.1571	MDC1	0.0043	2.5760
NEIL2	0.0279	1.7009	RRAGC	0.0286	2.1104	CHCHD3	0.0384	2.5515
CLPP	0.0116	1.7005	TMEM209	0.0297	2.0943	VASH2	0.0001	2.5244
UGCG	0.0323	1.6934	DDX27	0.0198	2.0531	AKT2	0.0152	2.4940
TSEN34	0.0136	1.6792	HEBP2	0.0254	2.0195	OBFC1	0.0000	2.4897
CORO1C	0.0432	1.6783	UBE2O	0.0434	1.9580	IFI30	0.0482	2.4857
LOC642489	0.0191	1.6669	COMMD7	0.0199	1.9515	FAM105B	0.0431	2.4662
MBLAC1	0.0449	1.6608	POLR3C	0.0123	1.9486	SRP72	0.0046	2.4654
TJAP1	0.0056	1.6534	CHUK	0.0092	1.9377	LOC100132287	0.0097	2.4566
OSTF1	0.0129	1.6395	RPS26P11	0.0432	1.9269	RASGRP3	0.0209	2.4472
CTSH	0.0241	1.6312	UGCG	0.0128	1.9136	LOC646434	0.0091	2.3823
OBFC1	0.0068	1.6018	PIK3R5	0.0305	1.9094	NCKAP5L	0.0055	2.3481
WDR36	0.0176	1.6011	ALG5	0.0250	1.8932	WDR36	0.0013	2.3330
NDUFS7	0.0251	1.6010	LOC644934	0.0297	1.8875	HS.250648	0.0094	2.3303
RPS26P10	0.0464	1.5985	SSU72	0.0377	1.8668	ZNF512	0.0332	2.3252
CAPZA2	0.0498	1.5920	CMAS	0.0064	1.8606	NDUFB11	0.0465	2.3141
ZNF232	0.0289	1.5873	LCN2	0.0462	1.8574	ADA	0.0042	2.2857
LASP1	0.0369	1.5807	ESRRAP2	0.0149	1.8344	TSPAN33	0.0196	2.2779
CMAS	0.0387	1.5756	DNTTIP1	0.0281	1.8285	COPRS	0.0193	2.2663
PSMD5	0.0188	1.5718	LOC1001319	0.0400	1.8075	ATP5EP2	0.0296	2.2634

SPDYE2	0.0333	1.5710
RPL36AL	0.0409	1.5680
XPA	0.0106	1.5515
EIF3K	0.0103	1.5507
GNPNAT1	0.0008	1.5491
LOC643138	0.0467	1.5435
TTC1	0.0218	1.5357
RFWD2	0.0100	1.5256
FCN1	0.0448	1.5222
TALDO1	0.0054	1.5215
ITGAM	0.0026	1.5170
HCLS1	0.0053	1.5130
NARS	0.0404	1.5126
ACTL6A	0.0129	1.4948
PAF1	0.0376	1.4943
LOC645116	0.0498	1.4905
COX20	0.0453	-1.4917
LRRC37A	0.0325	-1.4928
IFIT2	0.0261	-1.4955
RELT	0.0236	-1.4955
COPB2	0.0241	-1.4983
LOC401623	0.0102	-1.5025
HS.541829	0.0056	-1.5026
HS.552082	0.0027	-1.5078
LOC100128274	0.0317	-1.5079
HARS	0.0467	-1.5125
LOC442113	0.0027	-1.5126
IFFO1	0.0006	-1.5155
FBXO38	0.0218	-1.5177
ANXA11	0.0365	-1.5209
DYRK2	0.0007	-1.5231
LOC651213	0.0473	-1.5232
HEATR1	0.0281	-1.5241
LOC646093	0.0003	-1.5245
MICU2	0.0159	-1.5246
MAPKAPK5	0.0313	-1.5293
TAF1	0.0397	-1.5297
MYC	0.0266	-1.5299
HS.566647	0.0098	-1.5308
LOC284297	0.0001	-1.5317
LOC732450	0.0018	-1.5357
ZNHIT2	0.0251	-1.5369
ZNF276	0.0061	-1.5408
TOX	0.0105	-1.5428

71		
GADD45GIP1	0.0264	1.7917
FCN1	0.0069	1.7898
CLPP	0.0146	1.7767
TMEM204	0.0492	1.7764
CEACAM3	0.0220	1.7744
RPS26P10	0.0308	1.7536
NDUFS7	0.0153	1.7460
EML4	0.0243	1.7411
GALNS	0.0347	1.7224
GNPNAT1	0.0000	1.7182
GYG1	0.0047	1.7172
ZNF232	0.0225	1.7147
TJAP1	0.0088	1.7011
NEIL2	0.0497	1.6894
LOC642489	0.0328	1.6891
SPDYE2	0.0298	1.6764
ITGAM	0.0002	1.6748
TSEN34	0.0290	1.6704
HK3	0.0474	1.6667
APH1A	0.0126	1.6610
RPL36AL	0.0411	1.6536
RAB31	0.0304	1.6488
CEBPE	0.0343	1.6484
ACTL6A	0.0048	1.6390
TFAM	0.0427	1.6352
HIST1H2BE	0.0479	1.6339
HS.577098	0.0157	1.6327
GTSCR1	0.0280	1.6320
PSMD5	0.0282	1.6122
UBXN6	0.0457	1.6102
PTEN	0.0217	1.6032
RPL13	0.0357	1.5990
LOC100132317	0.0179	1.5953
CTSH	0.0470	1.5907
DDX49	0.0363	1.5905
SRP72	0.0460	1.5834
FRAT2	0.0472	1.5812
EIF3K	0.0156	1.5811
LYZ	0.0051	1.5781
PDE3B	0.0251	1.5774
CUTC	0.0071	1.5745
NARS	0.0460	1.5580
OSTF1	0.0394	1.5578
LOC100128265	0.0274	1.5576

EIF4ENIF1	0.0159	2.2587
ZRSR2	0.0137	2.2559
NRD1	0.0031	2.2512
ABRACL	0.0311	2.2337
RPA3	0.0030	2.2270
SNAPIN	0.0359	2.2190
ZFYVE21	0.0367	2.2174
IPO9	0.0224	2.2113
EXOSC6	0.0095	2.2087
ASB13	0.0013	2.1982
ZRSR2	0.0153	2.1784
HS.105636	0.0494	2.1736
AHSA2	0.0086	2.1687
BTG2	0.0181	2.1654
POM121C	0.0367	2.1526
FUK	0.0092	2.1329
C6ORF136	0.0166	2.1213
NBEAL1	0.0068	2.1070
HAVCR2	0.0092	2.1063
GPNMB	0.0432	2.0946
LOC391073	0.0058	2.0783
LOC643817	0.0092	2.0745
ROM1	0.0067	2.0710
FGFR1OP2	0.0089	2.0706
PNN	0.0071	2.0678
LOC641710	0.0166	2.0664
HS.38894	0.0067	2.0645
SLC45A4	0.0214	2.0556
HS.565491	0.0035	2.0448
SLC35A1	0.0098	2.0408
SNORA40	0.0115	2.0355
SNRP70	0.0205	2.0350
PARP14	0.0335	2.0350
HS.164406	0.0244	2.0294
AGO1	0.0143	2.0241
RPN1	0.0105	2.0228
LOC54103	0.0284	2.0220
ADAM23	0.0003	2.0159
LOC100130919	0.0448	2.0041
DNAJC11	0.0023	2.0037
MRPL17	0.0043	2.0014
SP140L	0.0447	1.9966
RFWD2	0.0016	1.9944
LOC730316	0.0435	1.9940

LOC400713	0.0018	-1.5432
LOC644256	0.0075	-1.5462
LOC649635	0.0121	-1.5478
LOC440354	0.0085	-1.5505
CROT	0.0007	-1.5524
LOC653752	0.0348	-1.5576
FBRS	0.0104	-1.5617
RBM39	0.0242	-1.5625
CHD2	0.0361	-1.5651
CNOT3	0.0152	-1.5655
MCUR1	0.0179	-1.5657
LSM8	0.0421	-1.5690
ELP2	0.0052	-1.5696
LOC645974	0.0033	-1.5698
HS.353387	0.0039	-1.5724
SNORD66	0.0181	-1.5737
PMS2P5	0.0422	-1.5743
MX2	0.0356	-1.5798
C2CD3	0.0434	-1.5810
IFT20	0.0207	-1.5820
HS.575696	0.0112	-1.5854
C5ORF44	0.0427	-1.5857
COX5A	0.0223	-1.5883
HINT2	0.0424	-1.5884
AP1G2	0.0433	-1.5885
MIS18BP1	0.0291	-1.5896
MAPK13	0.0455	-1.5914
ENTPD6	0.0282	-1.5954
HMHA1	0.0099	-1.5961
ABHD10	0.0066	-1.5962
LOC100132324	0.0129	-1.5985
LOC648729	0.0263	-1.5990
KDM5C	0.0271	-1.6006
LOC644642	0.0001	-1.6028
GMFB	0.0335	-1.6042
PLCD1	0.0148	-1.6070
UBE2E2	0.0124	-1.6074
HS.580797	0.0017	-1.6133
POLR2J3	0.0422	-1.6167
UBAP1	0.0133	-1.6175
LOC123688	0.0095	-1.6206
MRPL37	0.0162	-1.6219
SLC25A37	0.0059	-1.6233
ANKRD12	0.0275	-1.6304
LOC1001305	0.0359	-1.6397
CD177	0.0456	1.5544
SRP54	0.0403	1.5535
NCF1	0.0402	1.5533
TTC1	0.0286	1.5442
ANAPC16	0.0169	1.5408
LOC442590	0.0497	1.5388
XPA	0.0272	1.5274
ADPGK	0.0046	1.5271
MYO5A	0.0435	1.5265
LOC100132247	0.0403	1.5244
NUMB	0.0178	1.5241
S100P	0.0343	1.5200
C2ORF49	0.0470	1.5164
MOB1A	0.0457	1.5111
RPS26	0.0483	1.5056
LOC100134379	0.0472	1.5049
OR10AD1	0.0217	-1.4915
CLC	0.0486	-1.4916
IFIT2	0.0494	-1.4930
DGKQ	0.0326	-1.4945
RELT	0.0436	-1.4977
DYRK2	0.0010	-1.4977
MCHR2	0.0015	-1.4981
NFATC2	0.0494	-1.5006
AP1B1	0.0146	-1.5014
LOC644790	0.0359	-1.5016
LOC646093	0.0008	-1.5023
FBXO38	0.0448	-1.5043
MEF2C	0.0354	-1.5049
C2ORF68	0.0093	-1.5050
ADCY7	0.0405	-1.5056
Ssc5d	0.0005	-1.5066
LOC400986	0.0081	-1.5073
MBTPS1	0.0187	-1.5080
SFRS18	0.0116	-1.5105
HS.541829	0.0124	-1.5129
CNOT3	0.0408	-1.5145
LOC647834	0.0020	-1.5150
LOC442113	0.0051	-1.5202
SELL	0.0363	-1.5204
MCUR1	0.0409	-1.5214
CYBASC3	0.0456	-1.5225
LOC100130604	0.0124	-1.5236
LOC645332	0.0239	-1.5244
MORF4L1	0.0182	-1.5247
ZMYND19	0.0231	1.9919
RTTN	0.0153	1.9911
AP1S2	0.0319	1.9875
RALB	0.0352	1.9835
HS.8038	0.0300	1.9813
TMEM87A	0.0328	1.9766
LOC643138	0.0295	1.9720
AIFM2	0.0154	1.9717
BPHL	0.0281	1.9667
RHOU	0.0361	1.9621
ZNF746	0.0247	1.9564
PELI2	0.0052	1.9557
LOC100134703	0.0144	1.9513
MON2	0.0111	1.9497
SLC27A3	0.0498	1.9458
BEX2	0.0489	1.9457
LOC647873	0.0107	1.9456
TPD52L2	0.0461	1.9448
TYMS	0.0009	1.9448
UTP15	0.0184	1.9404
GJB2	0.0000	1.9350
LOC648057	0.0270	1.9347
MAU2	0.0022	1.9249
SH3BP2	0.0446	1.9232
MRPL36	0.0002	1.9180
CCDC134	0.0101	1.9076
BPTF	0.0129	1.9069
TALDO1	0.0020	1.9056
PPAN	0.0173	1.9036
GYG1	0.0081	1.9026
MARCKS	0.0445	1.9026
RRP15	0.0034	1.9020
ACIN1	0.0119	1.9001
DEDD2	0.0212	1.8970
SMIM19	0.0038	1.8936
ENY2	0.0115	1.8928
HS.197143	0.0080	1.8890
IQGAP2	0.0353	1.8871
LOC653353	0.0139	1.8862
PSMD6	0.0389	1.8784
SLC38A6	0.0461	1.8757
SGK1	0.0092	1.8747
LOC391157	0.0303	1.8673
PPAN-P2RY11	0.0099	1.8663
METAP2	0.0054	1.8646

61								
NCBP2	0.0016	-1.6401	NOLC1	0.0490	-1.5247	OSTF1	0.0268	1.8627
ERAP2	0.0290	-1.6484	TOX	0.0252	-1.5286	RNF213	0.0168	1.8618
SSTR2	0.0014	-1.6531	HS.566647	0.0216	-1.5292	NAT12	0.0173	1.8544
MNT	0.0111	-1.6544	RTCD1	0.0384	-1.5296	VAMP4	0.0148	1.8541
DESI1	0.0274	-1.6552	LOC649635	0.0250	-1.5311	PAF1	0.0141	1.8476
FUT6	0.0087	-1.6683	RBM39	0.0467	-1.5311	ZNF181	0.0268	1.8458
MED11	0.0081	-1.6716	LOC729780	0.0380	-1.5331	HS.547551	0.0206	1.8457
NAMPT	0.0089	-1.6735	UBAP1	0.0330	-1.5333	PTTG1	0.0397	1.8432
GGCT	0.0124	-1.6768	FLJ40473	0.0178	-1.5339	LOC91431	0.0273	1.8371
UBR1	0.0201	-1.6798	ELP2	0.0147	-1.5342	GHDC	0.0039	1.8364
ID2B	0.0249	-1.6838	TMUB2	0.0280	-1.5362	FAM91A1	0.0000	1.8363
SNF8	0.0015	-1.6879	PSMC2	0.0228	-1.5408	HS.440548	0.0008	1.8321
SLC35F6	0.0177	-1.6894	HS.552082	0.0049	-1.5409	FAM89A	0.0062	1.8293
IL11RA	0.0007	-1.6924	LOC645974	0.0093	-1.5416	SFT2D1	0.0105	1.8236
LIX1L	0.0131	-1.6952	TATDN1	0.0449	-1.5483	ROD1	0.0054	1.8212
CD5	0.0264	-1.6966	HCP5	0.0449	-1.5572	HSPBAP1	0.0338	1.8171
DNAJC25-GNG10	0.0165	-1.6970	NF1	0.0256	-1.5584	WDTC1	0.0012	1.8096
VAMP3	0.0000	-1.7019	NGDN	0.0232	-1.5591	MYO9B	0.0055	1.8065
GALNT3	0.0002	-1.7090	RANGRF	0.0300	-1.5615	PTGR1	0.0171	1.8034
BECN1	0.0211	-1.7093	CROT	0.0022	-1.5649	SENP7	0.0253	1.7948
CABIN1	0.0257	-1.7127	HS.562875	0.0047	-1.5663	ANGEL2	0.0112	1.7943
LOC730953	0.0043	-1.7179	LOC728105	0.0016	-1.5669	SAMHD1	0.0436	1.7904
IARS2	0.0184	-1.7199	LOC391656	0.0302	-1.5693	LOC646572	0.0335	1.7886
FAM86DP	0.0115	-1.7204	LOC644256	0.0140	-1.5705	KIAA1328	0.0070	1.7812
IL2RB	0.0130	-1.7217	MAPKAPK5	0.0407	-1.5772	FAM117A	0.0428	1.7807
INO80D	0.0216	-1.7224	ATP13A3	0.0082	-1.5818	LOC100130123	0.0046	1.7801
RP2	0.0139	-1.7236	ENTPD6	0.0499	-1.5824	AGXT2L2	0.0472	1.7785
LINC00921	0.0224	-1.7237	AKAP9	0.0138	-1.5827	LOC100130790	0.0075	1.7720
CXXC1	0.0161	-1.7288	LOC100128274	0.0295	-1.5845	HS.10862	0.0337	1.7699
C21ORF2	0.0069	-1.7308	LIX1L	0.0438	-1.5865	HS.507449	0.0117	1.7697
KIAA0408	0.0004	-1.7318	KMT2A	0.0108	-1.5869	CAPN5	0.0302	1.7689
MFSD11	0.0345	-1.7376	COPB2	0.0172	-1.5878	LEPREL1	0.0067	1.7672
LOC728942	0.0011	-1.7434	UBE2E2	0.0293	-1.5895	LOC286239	0.0365	1.7668
ITGAL	0.0482	-1.7522	DNAJC25-GNG10	0.0400	-1.5929	RRP1	0.0047	1.7665
CACNB3	0.0263	-1.7545	HS.580797	0.0057	-1.5932	SCARNA10	0.0008	1.7628
SAMM50	0.0141	-1.7592	IFFO1	0.0004	-1.5941	TBCE	0.0064	1.7628
HS.574008	0.0058	-1.7660	DARS2	0.0039	-1.5950	CSTA	0.0420	1.7559
TNFSF8	0.0432	-1.7706	SSTR2	0.0057	-1.5951	CCAR1	0.0002	1.7549
PPDPF	0.0040	-1.7764	PLCD1	0.0279	-1.5961	C3ORF62	0.0271	1.7538
PALLD	0.0105	-1.7766	TAF4B	0.0061	-1.5984	HS.575542	0.0175	1.7516
CTDSP2	0.0290	-1.7790	DNAJB9	0.0274	-1.6031	PIAS3	0.0473	1.7510
CHCHD4	0.0322	-1.7801	LOC644642	0.0003	-1.6042	ADCY6	0.0108	1.7477
C5ORF15	0.0456	-1.7854	GPR68	0.0456	-1.6094	SMG5	0.0332	1.7440
LOC391811	0.0490	-1.7967	HMHA1	0.0091	-1.6129	FBRSL1	0.0244	1.7427

HS.512087	0.0174	-1.7987
LOC729375	0.0095	-1.8037
RBM4B	0.0444	-1.8118
KXD1	0.0276	-1.8145
ZNF696	0.0119	-1.8401
LOC650159	0.0096	-1.8522
CES2	0.0210	-1.8960
RPS6KB1	0.0130	-1.9103
DEXI	0.0221	-1.9161
ST3GAL5	0.0414	-1.9174
CFDP1	0.0019	-1.9237
LOC645600	0.0175	-1.9304
ZNF33B	0.0364	-1.9640
COX8A	0.0257	-1.9693
FHOD1	0.0345	-1.9801
TMEM85	0.0488	-1.9936
HS.572752	0.0018	-1.9987
ZMIZ1	0.0360	-2.0025
SLC30A9	0.0012	-2.0131
TSHZ2	0.0003	-2.0363
LOC644353	0.0008	-2.0538
ECH1	0.0000	-2.0538
March6	0.0024	-2.0805
DNAJC3	0.0183	-2.1561
EBNA1BP2	0.0116	-2.1603
GLA	0.0095	-2.1632
OXA1L	0.0269	-2.2109
NDUFAB1	0.0372	-2.2768
LINC01000	0.0023	-2.3199
S1PR5	0.0093	-2.3214
SAFB2	0.0073	-2.3257
MAP3K11	0.0106	-2.3556
RNF20	0.0356	-2.3683
SLC5A3	0.0075	-2.3992
FADD	0.0032	-2.4174
NOP16	0.0012	-2.4987
STK36	0.0339	-2.6148
CD99L2	0.0005	-2.6541
CD7	0.0016	-2.8295
ISCA2	0.0008	-2.9313

LOC732450	0.0016	-1.6178
VCP	0.0240	-1.6188
SMU1	0.0486	-1.6216
ZNF276	0.0053	-1.6221
MNT	0.0283	-1.6233
SLC25A37	0.0113	-1.6241
SNORD66	0.0249	-1.6246
DDX41	0.0186	-1.6255
SAMHD1	0.0308	-1.6285
CHD2	0.0427	-1.6319
HS.353387	0.0038	-1.6332
LOC100132324	0.0208	-1.6361
SPIRE1	0.0469	-1.6407
MIS18BP1	0.0350	-1.6508
ANXA11	0.0227	-1.6591
DESI1	0.0485	-1.6612
LOC651213	0.0300	-1.6643
RNU6-1	0.0275	-1.6653
LOC100130561	0.0309	-1.6697
HS.575696	0.0117	-1.6747
IL11RA	0.0017	-1.6791
FUT6	0.0174	-1.6807
AP1G2	0.0423	-1.6816
VAMP3	0.0002	-1.6857
LOC728942	0.0048	-1.6881
SLC35F6	0.0348	-1.6914
LINC00921	0.0471	-1.6962
IARS2	0.0403	-1.6976
RP2	0.0324	-1.6999
HYKK	0.0106	-1.7057
GGCT	0.0221	-1.7058
SCARNA5	0.0092	-1.7086
LOC730953	0.0067	-1.7137
NCBP2	0.0016	-1.7232
PPDPF	0.0040	-1.7264
CABIN1	0.0432	-1.7276
GALNT3	0.0005	-1.7348
SAMM50	0.0189	-1.7362
BECN1	0.0310	-1.7369
HEATR1	0.0040	-1.7376
LOC648729	0.0187	-1.7389
ERAP2	0.0213	-1.7471
KANSL3	0.0396	-1.7543
LOC100133510	0.0359	-1.7595
LOC652184	0.0010	-1.7603

ZDHHC2	0.0239	1.7371
CENPC1	0.0147	1.7318
TMEM138	0.0110	1.7280
ADAMDEC1	0.0346	1.7262
PROSER1	0.0127	1.7216
HS.336643	0.0159	1.7206
FCHO1	0.0056	1.7172
RABGEF1	0.0096	1.7131
B3GAT3	0.0023	1.7096
HS.121667	0.0054	1.7071
LOC643167	0.0105	1.7056
PTP4A1	0.0107	1.7014
PDAP1	0.0281	1.6999
ALMS1	0.0069	1.6987
LOC650799	0.0469	1.6983
ZNF319	0.0103	1.6978
NAT15	0.0429	1.6965
GAS7	0.0009	1.6953
PDHX	0.0054	1.6927
GOLGA2	0.0041	1.6857
SEC24B	0.0198	1.6829
ZNF542P	0.0005	1.6816
BRE	0.0325	1.6789
PEX16	0.0267	1.6786
ZNF236	0.0003	1.6773
LOC728263	0.0344	1.6763
LOC644650	0.0025	1.6754
TUBD1	0.0197	1.6745
LOC158301	0.0008	1.6736
TXNL1	0.0426	1.6706
LOC132241	0.0232	1.6618
LOC100128156	0.0305	1.6591
DYNC1I2	0.0266	1.6565
TRK1	0.0488	1.6560
TMCC1	0.0006	1.6544
UPF2	0.0277	1.6533
NDUFA11	0.0156	1.6525
TFPI	0.0067	1.6491
HLX	0.0054	1.6472
FBXL20	0.0336	1.6466
PRDM8	0.0156	1.6436
LOC727805	0.0103	1.6434
LOC100129882	0.0156	1.6431
CBX4	0.0190	1.6410
NEURL4	0.0311	1.6409

MED11	0.0094	-1.7625	PTPN11	0.0496	1.6408
HS.574008	0.0140	-1.7642	PANX2	0.0380	1.6347
NAMPT	0.0048	-1.7800	HDGFRP3	0.0319	1.6331
PALLD	0.0222	-1.7834	HCLS1	0.0157	1.6322
CD5	0.0264	-1.7849	ACP1	0.0177	1.6305
CXXC1	0.0176	-1.7867	LOC647089	0.0067	1.6301
IL2RB	0.0186	-1.7870	CUL4B	0.0128	1.6289
HS.512087	0.0343	-1.7904	TCTEX1D2	0.0190	1.6272
FAM86DP	0.0096	-1.7975	HS.122007	0.0432	1.6219
C21ORF2	0.0097	-1.8013	IKZF3	0.0100	1.6209
TACC1	0.0075	-1.8016	LOC441734	0.0007	1.6208
KIAA0408	0.0003	-1.8033	CCL2	0.0243	1.6204
UBR1	0.0152	-1.8087	RNASEL	0.0352	1.6195
PHF15	0.0221	-1.8105	GP1BA	0.0304	1.6153
ID2B	0.0224	-1.8147	STXBP5	0.0323	1.6150
ANKRD12	0.0138	-1.8160	HS.537779	0.0016	1.6146
ARIH2	0.0142	-1.8165	XPA	0.0494	1.6137
RSC1A1	0.0391	-1.8173	LOC100134524	0.0023	1.6133
PABPC4	0.0293	-1.8252	HS.572883	0.0097	1.6118
MYLIP	0.0203	-1.8294	CREBZF	0.0194	1.6115
MAPK13	0.0150	-1.8352	TLK1	0.0095	1.6084
CFDP1	0.0081	-1.8403	HS.576373	0.0339	1.6035
FBXO34	0.0437	-1.8483	THEM6	0.0215	1.6016
ZNF696	0.0064	-1.8517	UBE2V2	0.0475	1.6009
CHCHD4	0.0407	-1.8609	MRPL22	0.0276	1.5987
SKIV2L	0.0006	-1.8681	AKIP1	0.0273	1.5967
KXD1	0.0390	-1.8775	CXORF21	0.0305	1.5952
SNF8	0.0003	-1.8885	CD300A	0.0000	1.5934
KCTD7	0.0411	-1.8935	HIPK3	0.0353	1.5866
LOC729375	0.0087	-1.8990	ERLEC1	0.0239	1.5861
RABGAP1	0.0159	-1.8994	RINT1	0.0009	1.5859
INO80D	0.0094	-1.9082	PPAT	0.0024	1.5813
GMFB	0.0017	-1.9230	AZI2	0.0011	1.5812
COX16	0.0365	-1.9234	JAKMIP2	0.0074	1.5798
DEXI	0.0387	-1.9263	LOC642732	0.0407	1.5791
COX8A	0.0440	-1.9284	ZNF434	0.0410	1.5779
HS.572752	0.0063	-1.9412	LOC728936	0.0467	1.5773
ZNF252	0.0440	-1.9431	HS.445414	0.0046	1.5736
HS.445036	0.0433	-1.9519	C9ORF57	0.0001	1.5708
SLC30A9	0.0020	-2.0003	COG6	0.0217	1.5675
SNRPA1	0.0296	-2.0149	MEAF6	0.0371	1.5660
RGCC	0.0091	-2.0431	LOC100132572	0.0023	1.5653
LOC650159	0.0010	-2.0511	RSAD1	0.0228	1.5652
ECH1	0.0002	-2.0558	ADM	0.0457	1.5633
CRNKL1	0.0435	-2.0588	RCE1	0.0363	1.5620
LOC644353	0.0026	-2.0635	PI4K2A	0.0102	1.5580

C5ORF15	0.0191	-2.0693
LOC100133692	0.0297	-2.0850
RPS6KB1	0.0095	-2.1061
MEF2D	0.0490	-2.1156
RBM4B	0.0194	-2.1287
LOC645600	0.0134	-2.1440
TSHZ2	0.0005	-2.1663
DNAJC3	0.0322	-2.1965
LINC01000	0.0077	-2.2466
FADD	0.0053	-2.2721
GLA	0.0088	-2.2762
CES2	0.0053	-2.2823
S1PR5	0.0221	-2.2930
MARCH6	0.0011	-2.2952
MAP3K11	0.0145	-2.3244
EBNA1BP2	0.0123	-2.3626
RNF20	0.0397	-2.4177
STK36	0.0445	-2.4303
CD7	0.0081	-2.4544
SLC5A3	0.0144	-2.4662
NOP16	0.0038	-2.4859
SAFB2	0.0072	-2.5405
CD99L2	0.0002	-2.7518
ISCA2	0.0034	-2.8492

LOC648863	0.0400	1.5576
LOC646461	0.0236	1.5576
CSF1	0.0120	1.5574
NKTR	0.0264	1.5537
HS.171171	0.0097	1.5494
HS.31532	0.0101	1.5484
WDR77	0.0236	1.5446
ERGIC2	0.0331	1.5413
SLC10A5	0.0102	1.5404
LOC643850	0.0102	1.5389
LOC728806	0.0140	1.5385
ABCD1	0.0324	1.5371
BTF3P11	0.0007	1.5367
TXNRD1	0.0310	1.5341
COQ7	0.0166	1.5321
CMTM8	0.0000	1.5309
DNAL1	0.0043	1.5239
F5	0.0263	1.5230
C17ORF51	0.0088	1.5221
HLA-B	0.0303	1.5214
LOC440104	0.0424	1.5184
PYGB	0.0437	1.5173
SEC14L1	0.0005	1.5148
IDE	0.0087	1.5147
ASPSCR1	0.0099	1.5141
LOC641992	0.0344	1.5129
CLP1	0.0144	1.5126
RYK	0.0436	1.5105
C10ORF137	0.0200	1.5095
HS.560899	0.0237	1.5094
LOC645015	0.0205	1.5074
LOC100133952	0.0131	1.5054
ZNF514	0.0333	1.5044
MRPL13	0.0150	1.5037
LOC100133438	0.0055	1.5032
TMEM45B	0.0348	1.5017
GTF2H1	0.0109	1.5014
HS.541066	0.0171	1.5003
FTSJ1	0.0024	1.4988
CHST7	0.0149	1.4975
LOC648024	0.0155	1.4967
TFF1	0.0030	1.4961
SFR1	0.0439	1.4957
TMBIM6	0.0293	1.4932
FLJ38717	0.0427	1.4907

THOP1	0.0238	1.4904
LOC442113	0.0287	-1.4937
LOC641298	0.0269	-1.5021
ZNF187	0.0211	-1.5041
LOC100132472	0.0466	-1.5128
TMEM191A	0.0265	-1.5131
TFIP11	0.0498	-1.5190
CHIC1	0.0258	-1.5211
CROT	0.0177	-1.5216
ZHX1	0.0318	-1.5245
ERP27	0.0123	-1.5257
DPP9	0.0067	-1.5313
CYP4V2	0.0386	-1.5351
FLJ11827	0.0389	-1.5430
MMGT1	0.0368	-1.5431
EPN1	0.0237	-1.5506
KRAS	0.0221	-1.5520
AMY1C	0.0110	-1.5536
HMHA1	0.0500	-1.5550
ATP10A	0.0269	-1.5622
KIAA0408	0.0143	-1.5653
CELF2	0.0160	-1.5717
KIAA1671	0.0058	-1.5808
LOC646093	0.0025	-1.5817
FAM120C	0.0018	-1.5824
DYRK2	0.0026	-1.5885
ARHGEF1	0.0090	-1.5918
LOC100134304	0.0104	-1.5945
Ssc5d	0.0014	-1.5963
LOC650909	0.0353	-1.5976
LOC644642	0.0024	-1.5992
GFOD2	0.0184	-1.6094
SLC25A37	0.0423	-1.6212
MICU2	0.0177	-1.6252
LOC646549	0.0153	-1.6262
ADIPOQ	0.0248	-1.6275
KCNK6	0.0015	-1.6293
LOC645974	0.0183	-1.6428
GALNT3	0.0075	-1.6461
EIF3FP2	0.0063	-1.6481
RNF115	0.0114	-1.6488
RNF115	0.0408	-1.6529
NBPF14	0.0394	-1.6577
LOC100129890	0.0350	-1.6609
ELP2	0.0230	-1.6618

HS.580797	0.0157	-1.6647
MCUR1	0.0486	-1.6821
HS.582025	0.0059	-1.6827
RPS8	0.0219	-1.6858
TNRC6B	0.0399	-1.6901
LOC100134372	0.0165	-1.6912
CNOT3	0.0425	-1.7004
LOC400713	0.0056	-1.7119
IL11RA	0.0072	-1.7261
LOC730953	0.0263	-1.7283
MNT	0.0496	-1.7350
VAMP3	0.0011	-1.7432
ZNHIT2	0.0425	-1.7439
TSHZ2	0.0274	-1.7444
MAGED1	0.0019	-1.7472
LOC440354	0.0181	-1.7487
SSNA1	0.0470	-1.7586
FBRS	0.0197	-1.7618
LOC100134047	0.0215	-1.7642
HS.574008	0.0472	-1.7704
FXYD5	0.0297	-1.7991
SSTR2	0.0065	-1.8076
ZNF696	0.0326	-1.8115
SAMM50	0.0436	-1.8180
KDM5C	0.0476	-1.8250
BLMH	0.0108	-1.8262
GZMA	0.0227	-1.8316
MYO18A	0.0288	-1.8338
HARS	0.0416	-1.8378
UBAP1	0.0194	-1.8490
IFT20	0.0217	-1.8792
MYC	0.0186	-1.8844
LOC401623	0.0032	-1.8867
LOC728942	0.0072	-1.8897
LOC401622	0.0090	-1.8915
BTBD2	0.0399	-1.8937
PPDPF	0.0073	-1.9076
RHOH	0.0207	-1.9172
TCF7	0.0456	-1.9180
SPINT2	0.0132	-1.9252
MRPL37	0.0224	-1.9262
ABHD10	0.0057	-1.9512
DNAJC25-GNG10	0.0212	-1.9880
RMRP	0.0084	-1.9923
NOA1	0.0306	-1.9950

LIX1L	0.0215	-2.0008
LOC644353	0.0157	-2.0297
BRI3P1	0.0431	-2.0384
SLC30A9	0.0093	-2.0453
ECH1	0.0021	-2.0489
PRPS1	0.0287	-2.0510
TOMM22	0.0059	-2.0512
IRF2BPL	0.0378	-2.1070
ADAT1	0.0372	-2.1446
CFDP1	0.0097	-2.1490
HS.572752	0.0126	-2.1500
LOC400027	0.0275	-2.1652
LPXN	0.0301	-2.2399
C1ORF162	0.0340	-2.3139
CISD2	0.0110	-2.3871
CD99L2	0.0048	-2.4248
MAP3K11	0.0396	-2.4355
NDUFS3	0.0409	-2.4467
ST3GAL5	0.0483	-2.4743
ACTN1	0.0196	-2.4919
LINC01000	0.0161	-2.5137
NOP16	0.0167	-2.5308
FLT3LG	0.0188	-2.6152
FADD	0.0061	-2.8227
STK36	0.0448	-3.1398
ISCA2	0.0101	-3.1469
RNMT	0.0203	-3.6482
CD7	0.0022	-4.0378
MXD4	0.0321	-4.4923

sTable 9.6 Gene list from Figure 4.5d.

List of differently expressed genes in 2 hour TCR stimulated naive CD4+ T cells from GPA patients compare to HC (Figure 4.5d)								
2 hour TCR naive CD4+ T cells (All GPA)			2 hour TCR naive CD4+ T cells (GPA group1)			2 hour TCR naive CD4+ T cells (GPA group2)		
Gene	p-value	Fold-Change	Gene	p-value	Fold-Change	Gene	p-value	Fold-Change
DEFA1	0.0030	4.4561	DEFA1	0.0000	7.1960	CCL2	0.0000	5.1285
DEFA3	0.0030	3.9214	DEFA3	0.0000	6.0962	GPNMB	0.0002	4.8994
NCF2	0.0048	3.5313	DEFA1B	0.0000	5.4493	THBS1	0.0134	4.8576
DEFA1B	0.0056	3.4926	LOC653600	0.0000	4.3216	DTNB	0.0071	4.2094
ITGB7	0.0006	3.1564	CAMP	0.0046	4.0233	BLVRB	0.0001	4.2011
LOC653600	0.0075	2.9284	NCF2	0.0083	3.7000	CCR1	0.0079	4.0618
GPNMB	0.0041	2.7266	ZNF428	0.0112	3.5263	ZNF787	0.0468	4.0229
CBX1	0.0046	2.6832	S100A9	0.0023	3.5135	DECR1	0.0025	4.0189
ZNF428	0.0452	2.6008	S100A8	0.0031	3.1461	CBX1	0.0038	4.0095
RBM25	0.0133	2.4598	ITGB7	0.0024	3.0828	GPT2	0.0003	3.9739
USP24	0.0400	2.3278	USP24	0.0135	2.9833	TMC6	0.0278	3.9552
TMEM63A	0.0158	2.2864	GCA	0.0304	2.8745	TSN	0.0030	3.5729
DENND4B	0.0031	2.1578	RBM25	0.0180	2.6153	ARHGEF3	0.0086	3.5517
PEA15	0.0336	2.1262	MPO	0.0167	2.6112	CDC37	0.0244	3.5148
FTH1	0.0258	2.1148	CEACAM8	0.0004	2.3528	ITGB7	0.0086	3.3483
GNB1L	0.0069	2.1076	ENY2	0.0002	2.3436	NUDT3	0.0105	3.2845
SKIV2L	0.0019	2.0885	HIGD2A	0.0058	2.2935	PLEKHA3	0.0077	3.2661
IFI30	0.0319	2.0742	CBX1	0.0196	2.2849	HS.540724	0.0001	3.1631
PSMB6	0.0232	2.0219	PEA15	0.0455	2.2014	HIST1H4B	0.0092	3.1431
ENY2	0.0019	2.0157	MS4A3	0.0009	2.2014	LOC648980	0.0113	3.1119
ARHGEF3	0.0488	1.9834	TMEM63A	0.0380	2.1793	TRIM8	0.0010	3.0959
ANP32A	0.0088	1.9785	SKIV2L	0.0001	2.1746	GNB1L	0.0024	3.0864
TRIM56	0.0136	1.9487	FTH1	0.0360	2.1689	TYW3	0.0088	3.0732
TACC1	0.0071	1.9283	GPNMB	0.0095	2.1568	MED1	0.0000	3.0680
MALSU1	0.0422	1.9186	SUCLG1	0.0073	2.0608	PINK1	0.0215	3.0448
STARD3	0.0205	1.9102	NOL12	0.0134	2.0408	CYTH4	0.0299	3.0399
MTR	0.0023	1.8967	BPI	0.0174	2.0351	MTR	0.0000	3.0154
SH3YL1	0.0207	1.8601	B4GALT5	0.0162	2.0307	UBASH3B	0.0402	2.9333
B4GALT5	0.0190	1.8580	FDFT1	0.0129	2.0290	TACC1	0.0005	2.9166
CEACAM8	0.0493	1.8395	HADH2	0.0041	2.0288	RASA2	0.0008	2.8663
CDK9	0.0030	1.8325	BSDC1	0.0263	2.0088	SPIRE1	0.0028	2.8514
CHD4	0.0347	1.8323	STARD3	0.0260	1.9907	LOC649242	0.0033	2.8476
TRIM8	0.0201	1.8302	DENND4B	0.0090	1.9872	TRIM56	0.0035	2.8444
NPEPL1	0.0275	1.8234	CHSY1	0.0254	1.9731	UQCRHL	0.0056	2.8423
C17ORF96	0.0267	1.8204	NSUN5	0.0048	1.9573	CCDC142	0.0097	2.8023
HIGD2A	0.0449	1.8193	SR140	0.0273	1.9202	VRK2	0.0003	2.7927
PELI2	0.0080	1.8166	RFX7	0.0131	1.9143	CLEC4A	0.0004	2.7707
UQCRHL	0.0290	1.8117	S100P	0.0028	1.8949	LYN	0.0400	2.7690
MED1	0.0037	1.8025	HSD17B10	0.0104	1.8819	TSPAN33	0.0057	2.7533
FOSB	0.0178	1.8011	CHMP5	0.0321	1.8672	GOLGA8F	0.0042	2.7360
NSUN5	0.0087	1.8003	TWISTNB	0.0269	1.8661	NBPF14	0.0004	2.7155

BP75	0.0112	1.7833
PRKAR2A	0.0222	1.7813
RFX7	0.0153	1.7683
KIAA0748	0.0193	1.7644
HS.572649	0.0207	1.7484
TRIM25	0.0129	1.7408
ZNF358	0.0471	1.7363
GOLGA8F	0.0314	1.7311
NSUN2	0.0365	1.7301
FAM103A1	0.0365	1.7237
LOC651919	0.0100	1.7144
NOL12	0.0478	1.7130
ABHD10	0.0024	1.7119
HADH2	0.0245	1.7095
GOT1	0.0401	1.7089
NPLOC4	0.0294	1.7081
FAM38A	0.0462	1.7073
NUP85	0.0236	1.6936
MORC3	0.0108	1.6873
TALDO1	0.0010	1.6821
SON	0.0000	1.6667
LOC93622	0.0232	1.6605
STAT4	0.0043	1.6561
FGFR1OP2	0.0479	1.6436
MXD1	0.0250	1.6389
ARHGEF6	0.0427	1.6385
INTS3	0.0109	1.6374
NAMPT	0.0117	1.6373
PRKAB2	0.0152	1.6341
RTCD1	0.0133	1.6331
DOCK11	0.0056	1.6272
APP	0.0302	1.6262
ADAP2	0.0079	1.6194
LYZ	0.0031	1.6162
SDAD1	0.0389	1.6043
TBL1XR1	0.0042	1.6037
HS.122007	0.0081	1.6026
POLS	0.0325	1.6013
TAF15	0.0475	1.5809
MDH1	0.0387	1.5784
ANKRD12	0.0385	1.5760
S100P	0.0484	1.5747
DDX26B	0.0111	1.5743
CNO	0.0286	1.5736
RNF103	0.0004	1.5727
SMC2	0.0403	1.5696

LOC651919	0.0043	1.8648
MAPKAPK3	0.0287	1.8604
SH3YL1	0.0404	1.8562
ANP32A	0.0210	1.8224
GNB1L	0.0261	1.8093
ERMP1	0.0203	1.8086
DHRS3	0.0402	1.8057
LIME1	0.0342	1.7987
SLC2A1	0.0362	1.7977
GOT1	0.0468	1.7928
SUMO1P3	0.0172	1.7913
MDH1	0.0155	1.7857
INTS3	0.0065	1.7782
LOC729769	0.0316	1.7716
TECR	0.0460	1.7578
NAA15	0.0102	1.7551
DCAF7	0.0469	1.7510
CNO	0.0141	1.7469
LOC642033	0.0228	1.7456
KLHDC4	0.0442	1.7411
LYZ	0.0012	1.7389
KARS	0.0045	1.7348
DOCK11	0.0045	1.7307
PRPSAP1	0.0481	1.7285
SCPEP1	0.0146	1.7278
DDX26B	0.0048	1.7254
HS.250648	0.0275	1.7126
MORC3	0.0204	1.7075
HS.122007	0.0064	1.7069
EXOSC6	0.0217	1.6983
RSPH3	0.0184	1.6904
PELI2	0.0049	1.6895
STAT4	0.0067	1.6815
TRIM56	0.0442	1.6751
KIAA0748	0.0461	1.6689
CDK9	0.0158	1.6664
BCL6	0.0001	1.6663
ABHD10	0.0063	1.6653
ANKRD12	0.0324	1.6574
ADSL	0.0412	1.6524
OLFM4	0.0273	1.6510
ADAP2	0.0136	1.6508
TRIM25	0.0381	1.6468
DNAJC8	0.0365	1.6451
CALCOCO2	0.0124	1.6433
TALDO1	0.0022	1.6409

C17ORF96	0.0088	2.7074
C11ORF74	0.0062	2.7062
CEACAM21	0.0484	2.6951
SNRNP35	0.0364	2.6901
ACOT13	0.0008	2.6820
CYBASC3	0.0012	2.6775
FOSB	0.0046	2.6639
HS.566524	0.0061	2.6581
DENND4B	0.0049	2.6508
OFD1	0.0152	2.6437
XPO7	0.0026	2.6380
GBP5	0.0289	2.6217
POMGNT1	0.0296	2.6194
AGAP3	0.0177	2.6053
GK	0.0105	2.5804
TMEM63A	0.0491	2.5780
ARRB1	0.0191	2.5777
HS.572649	0.0023	2.5703
SLC25A4	0.0263	2.5583
HS.423734	0.0179	2.5510
NPLOC4	0.0055	2.5464
URM1	0.0163	2.5349
TUG1	0.0077	2.5288
POU2F1	0.0107	2.5038
TAF15	0.0035	2.4863
DUSP5	0.0142	2.4859
SETD6	0.0044	2.4698
PSMB6	0.0420	2.4556
ASCC1	0.0003	2.4499
ANP32A	0.0098	2.4296
PRKAB2	0.0014	2.4120
MAP3K3	0.0001	2.4063
RGL2	0.0013	2.3983
TMEM111	0.0138	2.3951
LOC493754	0.0210	2.3916
RAD23A	0.0094	2.3835
PIP5K1C	0.0181	2.3785
TPH1	0.0034	2.3732
SPOP	0.0007	2.3660
SAT1	0.0394	2.3638
SOX8	0.0118	2.3569
ATP6V1E1	0.0438	2.3518
BP75	0.0062	2.3441
SNIP1	0.0405	2.3425
NOP10	0.0212	2.3425
FAM38A	0.0265	2.3347

P4HB	0.0002	1.5650
SUMO1P3	0.0498	1.5622
DNAJC8	0.0415	1.5470
LMNA	0.0364	1.5368
ASCC1	0.0268	1.5338
IDH3A	0.0230	1.5336
COX20	0.0338	1.5327
cd28	0.0416	1.5289
GVIN1	0.0489	1.5278
TMEM243	0.0227	1.5235
METAP2	0.0200	1.5202
FKRP	0.0412	1.5190
LOC441253	0.0449	1.5189
NAA15	0.0440	1.5175
SCAF4	0.0395	1.5167
CCNC	0.0133	1.5137
MAPRE1	0.0216	1.5135
RSPH3	0.0437	1.5095
KARS	0.0296	1.5069
AFAP1	0.0123	1.5042
BCL6	0.0017	1.5029
HIPK3	0.0127	1.5020
CECR5	0.0443	1.5020
OCIAD2	0.0427	1.5008
HPS3	0.0054	1.4989
EMC10	0.0232	1.4982
MAP2K1	0.0380	1.4931
SNW1	0.0339	1.4923
EEF2	0.0002	1.4902
NDUFAF7	0.0293	-1.4901
SEC23B	0.0458	-1.4931
SLC25A39	0.0271	-1.4940
EPC2	0.0068	-1.4949
HS.536620	0.0190	-1.5022
FGGY	0.0064	-1.5039
LYRM1	0.0095	-1.5061
LDLRAD1	0.0003	-1.5064
LOC100133130	0.0109	-1.5112
HS.202577	0.0224	-1.5124
KCNA3	0.0430	-1.5160
TMEM115	0.0235	-1.5212
MAP1LC3C	0.0026	-1.5215
PANK2	0.0005	-1.5217
SLC46A3	0.0093	-1.5231
PBDC1	0.0195	-1.5239

TACC1	0.0214	1.6341
BBC3	0.0375	1.6293
MXD1	0.0250	1.6274
SEC11A	0.0451	1.6196
LOC100131031	0.0096	1.6175
GVIN1	0.0441	1.6174
FKRP	0.0374	1.6155
SMIM7	0.0274	1.6113
ZNF691	0.0154	1.6110
FGFR1OP2	0.0229	1.6104
HS.538259	0.0212	1.6056
MIRLET7A1	0.0054	1.5990
BP75	0.0395	1.5986
MORF4L1	0.0101	1.5966
IFT20	0.0275	1.5932
LOC100134047	0.0162	1.5898
PSMD6	0.0486	1.5893
RNF103	0.0011	1.5863
ETS2	0.0053	1.5828
DYRK4	0.0214	1.5815
TBL1XR1	0.0084	1.5808
MTR	0.0081	1.5756
LOC728739	0.0270	1.5755
CD93	0.0470	1.5732
CSNK2A1	0.0114	1.5670
XPO5	0.0228	1.5649
HMHA1	0.0146	1.5549
SON	0.0001	1.5523
RNF115	0.0233	1.5508
METAP2	0.0104	1.5463
LOC728093	0.0127	1.5450
MRPS10	0.0495	1.5440
GDPD3	0.0489	1.5382
TRIM26	0.0293	1.5349
AFAP1	0.0213	1.5273
PEX19	0.0074	1.5215
DEFA4	0.0023	1.5180
P4HB	0.0006	1.5172
HPS3	0.0111	1.5120
FAM50A	0.0472	1.5116
LOC727900	0.0459	1.5095
RNA5S9	0.0379	1.5055
cd28	0.0332	1.5037
AP3S1	0.0187	1.4994
WWC3	0.0160	1.4992

TSPAN17	0.0224	2.3300
CDK9	0.0033	2.3239
C11ORF80	0.0089	2.3144
IDH3A	0.0005	2.3115
CYP1B1	0.0094	2.3056
SLC25A30	0.0033	2.3026
CTNNA1	0.0473	2.2999
ST3GAL1	0.0088	2.2952
LZTR1	0.0374	2.2910
SOS1	0.0377	2.2907
FAM103A1	0.0265	2.2740
HS.568777	0.0376	2.2657
SH2B1	0.0214	2.2648
TTYH3	0.0065	2.2640
MGC12965	0.0027	2.2421
LOC100133163	0.0253	2.2205
METAP1	0.0089	2.2159
COLGALT1	0.0025	2.2119
PRKAR2A	0.0249	2.2108
NAMPT	0.0032	2.2001
IL1B	0.0387	2.1985
LAS1L	0.0250	2.1975
SNORD69	0.0433	2.1948
KYNU	0.0275	2.1786
PELI2	0.0017	2.1776
SLC25A18	0.0062	2.1767
IPO4	0.0307	2.1689
C20ORF66	0.0109	2.1470
LOC728611	0.0072	2.1459
DHPS	0.0020	2.1339
FAM89A	0.0012	2.1314
YAF2	0.0060	2.1312
RASSF4	0.0000	2.1309
LOC441253	0.0081	2.1307
SMARCD3	0.0065	2.1278
LOC100128252	0.0168	2.1260
ACOX3	0.0046	2.1101
SMC2	0.0163	2.1087
POLS	0.0162	2.1059
RPRD2	0.0410	2.1035
NDN	0.0289	2.1011
RTCD1	0.0076	2.1008
C4ORF27	0.0347	2.0989
TMEM243	0.0032	2.0932
CASP8	0.0016	2.0909

RNU1-1	0.0456	-1.5241	CCNC	0.0320	1.4915	JAM3	0.0171	2.0890
ZNF256	0.0343	-1.5252	ABCF2	0.0109	-1.4931	SLAMF8	0.0072	2.0829
HS.444291	0.0265	-1.5368	LOC643167	0.0121	-1.4968	ARL5B	0.0002	2.0827
SLC30A1	0.0202	-1.5398	HS.445843	0.0176	-1.4988	LOC642962	0.0246	2.0821
MEAF6	0.0079	-1.5407	SEMA4D	0.0081	-1.5014	NID1	0.0040	2.0732
IKZF3	0.0027	-1.5430	BCL2L2	0.0148	-1.5166	LPP	0.0082	2.0720
ZNF562	0.0468	-1.5446	BAZ1A	0.0471	-1.5211	DCAF4	0.0453	2.0669
RHOB	0.0170	-1.5455	PANK2	0.0010	-1.5266	ADRB2	0.0007	2.0641
CSF2	0.0046	-1.5474	LOC441154	0.0048	-1.5308	XRN1	0.0310	2.0591
NFYC	0.0388	-1.5540	CCDC28B	0.0197	-1.5312	COX20	0.0114	2.0507
ZC3H11A	0.0250	-1.5555	STX6	0.0381	-1.5343	BANP	0.0437	2.0444
FUNDC2	0.0193	-1.5603	HS.444291	0.0482	-1.5368	CD300LF	0.0437	2.0442
LOC100128140	0.0012	-1.5619	RHOB	0.0267	-1.5370	FLJ32255	0.0277	2.0360
KCTD17	0.0282	-1.5621	REXO1	0.0188	-1.5378	IPO11	0.0304	2.0357
XRCC5	0.0061	-1.5643	NR4A1	0.0171	-1.5380	DNAJC7	0.0462	2.0345
ABCB9	0.0392	-1.5652	TMEM251	0.0389	-1.5382	OCIAD2	0.0110	2.0340
SLC36A3	0.0054	-1.5667	IKZF3	0.0038	-1.5421	CCDC71	0.0276	2.0324
TRMT61A	0.0391	-1.5673	PCCB	0.0105	-1.5422	SSBP2	0.0052	2.0314
BAZ1A	0.0204	-1.5679	SLC30A1	0.0294	-1.5496	THRAP3	0.0463	2.0292
HS.538195	0.0338	-1.5686	LOC644305	0.0280	-1.5522	KIAA0748	0.0345	2.0275
CCDC28B	0.0085	-1.5699	LDLRAD1	0.0004	-1.5553	LOC642414	0.0083	2.0274
HOOK1	0.0361	-1.5701	LOC643943	0.0191	-1.5565	GOLM1	0.0062	2.0271
NEK8	0.0058	-1.5707	LOC100128140	0.0034	-1.5577	LOC442096	0.0414	2.0270
GOSR1	0.0122	-1.5787	LOC100133130	0.0149	-1.5583	ACAP2	0.0216	2.0233
LOC642248	0.0348	-1.5819	SH2D1A	0.0235	-1.5596	NUP85	0.0345	2.0150
SNORA5A	0.0407	-1.5909	LOC100128274	0.0343	-1.5616	SFT2D2	0.0352	2.0037
ZNF185	0.0086	-1.5928	CSF2	0.0102	-1.5623	TRIM25	0.0271	1.9998
ZNF526	0.0385	-1.5957	SEC23B	0.0487	-1.5636	ARID3A	0.0045	1.9979
INTS9	0.0294	-1.5966	NUDT14	0.0481	-1.5639	LOC283050	0.0418	1.9964
LOC441154	0.0009	-1.6099	PRKCB	0.0139	-1.5700	ASCL2	0.0010	1.9950
REXO1	0.0053	-1.6099	ZNF185	0.0201	-1.5709	C16ORF72	0.0095	1.9929
NCSTN	0.0208	-1.6111	CFL1	0.0476	-1.5722	SON	0.0000	1.9912
CASC3	0.0374	-1.6202	MEAF6	0.0090	-1.5741	ARHGEF6	0.0436	1.9829
MAGEH1	0.0134	-1.6257	ZC3H12A	0.0006	-1.5750	LOC642867	0.0135	1.9826
NUP98	0.0436	-1.6276	DNMT3A	0.0134	-1.5772	KLHL23	0.0066	1.9663
IFT46	0.0445	-1.6288	FAM107B	0.0271	-1.5862	ACADM	0.0059	1.9626
LOC642154	0.0042	-1.6344	SLC36A3	0.0101	-1.5912	CDK5RAP2	0.0047	1.9613
LOC644824	0.0401	-1.6428	PBDC1	0.0222	-1.5916	TP53I13	0.0028	1.9604
GPS1	0.0106	-1.6428	GPS1	0.0198	-1.5984	ZFP64	0.0025	1.9582
HLA-DQA1	0.0008	-1.6472	CCR4	0.0178	-1.6063	ATP6V1C1	0.0117	1.9569
ERLIN1	0.0015	-1.6502	LOC642154	0.0104	-1.6087	LOC100133881	0.0101	1.9483
CCR4	0.0057	-1.6526	ZNF562	0.0452	-1.6156	NIPA1	0.0157	1.9378
MB21D1	0.0050	-1.6567	EPC2	0.0019	-1.6160	RANBP6	0.0259	1.9371
LOC652491	0.0386	-1.6568	FUNDC2	0.0218	-1.6344	TIMM8B	0.0444	1.9369
WNK1	0.0155	-1.6573	DDI2	0.0423	-1.6364	LEO1	0.0245	1.9316

USP15	0.0035	-1.6583
LOC645688	0.0214	-1.6705
GCSAML	0.0360	-1.6804
MED30	0.0079	-1.6839
ZNF559	0.0154	-1.6978
GUSB	0.0286	-1.7029
UBE2G2	0.0293	-1.7041
P2RY10	0.0069	-1.7060
LOC729841	0.0074	-1.7077
RFX1	0.0269	-1.7328
WIPI1	0.0293	-1.7336
SNORD35B	0.0319	-1.7343
NDUFA8	0.0104	-1.7410
CFLAR	0.0202	-1.7460
FBXW4	0.0401	-1.7563
LOC100129112	0.0468	-1.7593
HS.483906	0.0044	-1.7599
FAM175B	0.0007	-1.7677
CHES1	0.0447	-1.7733
LOC648366	0.0029	-1.7975
LOC647466	0.0075	-1.8197
LOC646093	0.0000	-1.8202
EOMES	0.0471	-1.8216
ANGPTL4	0.0206	-1.8325
ENDOG	0.0036	-1.8659
LOC647079	0.0023	-1.8674
MRPS28	0.0265	-1.8675
SLC8B1	0.0397	-1.8746
SF1	0.0045	-1.8834
PPP1R10	0.0136	-1.9099
IL18RAP	0.0058	-1.9250
CISD2	0.0134	-1.9321
HARS2	0.0296	-1.9324
PSME4	0.0144	-1.9358
HS.552160	0.0102	-1.9380
TNFAIP8L2	0.0034	-1.9510
SF3B4	0.0067	-2.0113
MRPL51	0.0275	-2.0139
LOC652776	0.0086	-2.0160
IFT27	0.0012	-2.0162
LOC644436	0.0200	-2.0549
HS.137971	0.0081	-2.0599
HS.580229	0.0031	-2.0690
TLCD1	0.0125	-2.1557
SLC18B1	0.0167	-2.1725

C16ORF62	0.0076	-1.6385
LOC100132364	0.0465	-1.6415
ZNF256	0.0243	-1.6499
MED30	0.0200	-1.6634
GTPBP6	0.0465	-1.6707
PLEKHM3	0.0258	-1.6717
HS.538195	0.0184	-1.6814
TRAK2	0.0362	-1.6888
NCSTN	0.0217	-1.6936
MB21D1	0.0070	-1.6976
ERLIN1	0.0025	-1.7052
ZNF559	0.0260	-1.7110
KHNYN	0.0457	-1.7122
LOC646093	0.0001	-1.7206
WNK1	0.0185	-1.7221
USP15	0.0044	-1.7362
HIF1AN	0.0238	-1.7418
FAM175B	0.0026	-1.7471
ZC3H11A	0.0072	-1.7493
IL18RAP	0.0257	-1.7505
GOSR1	0.0047	-1.7511
HS.483906	0.0105	-1.7559
HS.552160	0.0323	-1.7575
HLA-DQA1	0.0005	-1.7592
MAGEH1	0.0087	-1.7721
RFX1	0.0376	-1.7727
LOC647079	0.0099	-1.7764
LOC729841	0.0101	-1.7778
LOC647466	0.0196	-1.7812
NDUFA8	0.0107	-1.7831
LOC648366	0.0055	-1.7868
UBE2G2	0.0311	-1.7912
CFLAR	0.0293	-1.8023
TTC39C	0.0478	-1.8208
LOC652776	0.0222	-1.8226
WBSCR22	0.0322	-1.8318
TNFAIP8L2	0.0123	-1.8643
EFR3A	0.0221	-1.8715
PPP1R10	0.0310	-1.8752
P2RY10	0.0027	-1.8940
ENDOG	0.0077	-1.8977
PSME4	0.0295	-1.9113
LOC645688	0.0044	-1.9136
SF1	0.0092	-1.9197
FBXW4	0.0268	-1.9616

MORC2	0.0192	1.9229
YDJC	0.0012	1.9223
OR2A4	0.0321	1.9211
BRD7P2	0.0023	1.9107
LOC728323	0.0050	1.9098
TUBB2C	0.0402	1.9085
RUSC1	0.0431	1.9076
LSM4	0.0162	1.9042
ARHGEF15	0.0289	1.9025
AFF4	0.0004	1.9005
LOC730358	0.0001	1.8998
HS.543971	0.0242	1.8976
SKIV2L	0.0041	1.8879
BRSK1	0.0051	1.8809
COPG2	0.0298	1.8807
PAF1	0.0121	1.8793
TMEM194A	0.0153	1.8771
AMT	0.0006	1.8767
RBM15	0.0127	1.8729
MGC15705	0.0044	1.8687
PTPMT1	0.0252	1.8586
MTA1	0.0193	1.8552
LOC440341	0.0011	1.8537
TNFRSF14	0.0229	1.8498
FUOM	0.0032	1.8479
PEAK1	0.0155	1.8471
HPCAL4	0.0191	1.8426
AGAP6	0.0414	1.8423
LOC728125	0.0444	1.8416
SEC23IP	0.0005	1.8409
RRP9	0.0142	1.8404
LOC100131330	0.0213	1.8383
TMEM147	0.0054	1.8380
CTSA	0.0041	1.8345
ABHD10	0.0106	1.8343
IFNGR1	0.0290	1.8310
SUMF1	0.0407	1.8304
MPEG1	0.0038	1.8301
C17ORF53	0.0084	1.8277
SNW1	0.0257	1.8257
ANO6	0.0000	1.8240
TXNDC17	0.0098	1.8211
LOC100131480	0.0073	1.8207
CTDSPL2	0.0012	1.8163
EMC10	0.0189	1.8156

SNORD48	0.0494	-2.1971
RANGAP1	0.0035	-2.2368
S1PR5	0.0085	-2.3467
MED6	0.0179	-2.4264
FGF9	0.0485	-2.4826
FAM217B	0.0063	-2.5991
SAC3D1	0.0369	-2.6996
NT5C	0.0091	-2.7904
WDR18	0.0066	-2.8368
SNORA3B	0.0026	-3.0330

STRAP	0.0345	-1.9747
SF3B4	0.0146	-2.0282
HS.137971	0.0176	-2.0641
CISD2	0.0062	-2.0904
TLCD1	0.0258	-2.1457
IFT27	0.0014	-2.1712
HS.580229	0.0048	-2.1815
RANGAP1	0.0089	-2.2134
S1PR5	0.0225	-2.2860
SLC18B1	0.0210	-2.3280
TLE3	0.0472	-2.3633
MED6	0.0392	-2.3761
PMVK	0.0433	-2.4564
FAM217B	0.0146	-2.6012
SNORD48	0.0276	-2.6483
NT5C	0.0101	-2.6544
WDR18	0.0201	-2.6830
FGF9	0.0281	-2.9445
SNORA3B	0.0065	-3.0786

LOC100134100	0.0269	1.8122
PREB	0.0228	1.8098
UTP3	0.0037	1.8055
LOC650737	0.0000	1.7988
HS.20255	0.0013	1.7966
PGRMC1	0.0404	1.7938
RCOR1	0.0049	1.7933
PROZ	0.0418	1.7924
NOL8	0.0436	1.7918
KIAA1551	0.0185	1.7911
TALDO1	0.0043	1.7897
ZDHHC7	0.0051	1.7879
HS.539564	0.0027	1.7856
NIPAL1	0.0072	1.7827
IBTK	0.0094	1.7789
POLRMT	0.0107	1.7771
SNORD14A	0.0013	1.7750
UPF1	0.0063	1.7730
U2AF1	0.0478	1.7728
IQSEC3	0.0021	1.7696
SNORD74	0.0046	1.7692
POP4	0.0011	1.7691
SCAF4	0.0496	1.7668
MYOM2	0.0447	1.7619
IL10RB	0.0406	1.7596
ZNF335	0.0048	1.7586
TNFRSF10D	0.0299	1.7576
ABCA1	0.0329	1.7567
MICU2	0.0074	1.7558
CLPB	0.0013	1.7557
ZNF25	0.0028	1.7490
LOC648434	0.0496	1.7487
CHID1	0.0018	1.7464
MAP2K1	0.0453	1.7420
ECHDC2	0.0052	1.7398
SPTAN1	0.0383	1.7383
OGFR	0.0398	1.7379
PNN	0.0323	1.7376
CSNK2A2	0.0086	1.7355
STX6	0.0386	1.7349
PHC3	0.0261	1.7343
YARS2	0.0220	1.7335
TNFSF13B	0.0000	1.7334
FGFR1OP2	0.0396	1.7294
CYTH3	0.0184	1.7275
LOC652672	0.0011	1.7272

SMARCC1	0.0415	1.7267
LOC652479	0.0056	1.7263
LOC646030	0.0030	1.7249
LOC642546	0.0381	1.7232
GORASP2	0.0424	1.7220
CLIC5	0.0306	1.7192
FLJ13197	0.0105	1.7186
LOC644162	0.0029	1.7167
RGL4	0.0169	1.7159
ZNF696	0.0496	1.7148
HS.545650	0.0086	1.7121
MRPL17	0.0209	1.7073
LOC643503	0.0296	1.7073
MRPS11	0.0168	1.7061
RAPGEF1	0.0412	1.7057
KLF8	0.0442	1.7028
LOC388572	0.0486	1.7021
HS.567480	0.0269	1.6994
LOC100133854	0.0125	1.6983
HS.579870	0.0009	1.6970
RPF1	0.0136	1.6958
P4HB	0.0007	1.6913
LOC283953	0.0184	1.6867
RPS6KA4	0.0238	1.6864
HS.46506	0.0011	1.6859
EIF2S2	0.0151	1.6845
C1ORF35	0.0056	1.6832
SELENOI	0.0118	1.6816
RRP7BP	0.0001	1.6807
ATP1B3	0.0127	1.6800
XAB2	0.0264	1.6798
PISD	0.0099	1.6793
PLIN3	0.0172	1.6733
SNORD14B	0.0000	1.6726
LOC650159	0.0403	1.6725
LOC100129361	0.0127	1.6713
TBL1XR1	0.0200	1.6623
LAGE3	0.0013	1.6622
HS.4986	0.0189	1.6621
PRRT3	0.0209	1.6603
LOC100129936	0.0341	1.6591
CDC25B	0.0091	1.6590
LOC647810	0.0027	1.6582
FTSJ3	0.0002	1.6554
ZDHHC2	0.0371	1.6541

LOC100134300	0.0127	1.6450
PFKM	0.0024	1.6437
DDX20	0.0203	1.6435
ESR2	0.0055	1.6422
SPIB	0.0093	1.6421
TTBK2	0.0187	1.6386
SERINC1	0.0073	1.6379
LOC643167	0.0172	1.6316
MLL3	0.0345	1.6309
HS.572642	0.0499	1.6284
LOC401703	0.0170	1.6226
GOLGA7	0.0049	1.6224
CCRL2	0.0082	1.6219
LIMS1	0.0088	1.6210
RNF11	0.0295	1.6197
NRBF2	0.0278	1.6183
MGC72104	0.0073	1.6181
BOLA2	0.0341	1.6173
PDE12	0.0065	1.6173
RPRD2	0.0470	1.6169
LOC149448	0.0070	1.6167
AIM1	0.0498	1.6163
TCEA3	0.0161	1.6132
GLCCI1	0.0001	1.6119
TAPT1	0.0388	1.6114
LOC100131737	0.0274	1.6106
NCCRP1	0.0386	1.6106
ASPH	0.0314	1.6080
SLC25A32	0.0052	1.6073
IVNS1ABP	0.0246	1.6024
LOC648024	0.0061	1.6008
DIAPH1	0.0404	1.5996
SORL1	0.0093	1.5967
NBPF8	0.0429	1.5963
KIZ	0.0129	1.5956
SOGA1	0.0110	1.5956
LOC440917	0.0199	1.5949
STAT4	0.0458	1.5943
HS.561570	0.0267	1.5937
LOC100131972	0.0164	1.5828
SPPL3	0.0076	1.5786
FXR1	0.0441	1.5785
NDRG2	0.0006	1.5772
LOC100129531	0.0121	1.5769
SERPINE1	0.0002	1.5769

PDP1	0.0136	1.5762
LOC651881	0.0339	1.5758
HLA-DQB1	0.0002	1.5745
LOC653189	0.0290	1.5684
OSBP	0.0017	1.5676
HS.232573	0.0371	1.5646
LOC642093	0.0251	1.5626
PDLIM5	0.0025	1.5617
INVS	0.0388	1.5603
COG7	0.0114	1.5599
PTCD1	0.0445	1.5587
PURA	0.0358	1.5555
EEF2	0.0029	1.5507
ZNF836	0.0291	1.5495
PICALM	0.0002	1.5492
HS.560459	0.0040	1.5475
ZSCAN5A	0.0103	1.5475
VPS37A	0.0163	1.5449
HLA-DRA	0.0055	1.5401
UVSSA	0.0015	1.5399
RNF103	0.0113	1.5392
LOC100133937	0.0113	1.5378
HIPK3	0.0494	1.5324
GPATCH1	0.0349	1.5306
CROP	0.0349	1.5274
NIPBL	0.0332	1.5270
BNIP3L	0.0013	1.5256
DYNLT3	0.0098	1.5238
LINC01137	0.0053	1.5237
HS.565250	0.0013	1.5231
EWSR1	0.0031	1.5228
MTAP	0.0033	1.5218
GPATCH11	0.0380	1.5216
DTWD1	0.0067	1.5167
HS.397465	0.0200	1.5100
DPY19L3	0.0345	1.5072
HS.544017	0.0007	1.5034
PTAFR	0.0436	1.4959
MECR	0.0079	1.4954
STX3	0.0348	1.4941
FAM110B	0.0003	1.4931
LOC653147	0.0187	1.4919
LOC653226	0.0293	-1.4908
RAET1K	0.0235	-1.4925
LOC729362	0.0107	-1.4938
ZNF830	0.0447	-1.4956

LOC100127993	0.0021	-1.4976
LOC643159	0.0468	-1.5000
LOC643319	0.0152	-1.5007
LOC651361	0.0171	-1.5007
ORAOV1	0.0365	-1.5011
LOC100129518	0.0489	-1.5023
HS.59368	0.0402	-1.5025
SESN3	0.0155	-1.5026
LOC653513	0.0366	-1.5039
EIF5	0.0361	-1.5069
RPL37A	0.0296	-1.5071
ZFP92	0.0172	-1.5090
PANK2	0.0082	-1.5096
HLTF	0.0436	-1.5126
LOC727826	0.0036	-1.5143
LOC391126	0.0189	-1.5155
LOC390578	0.0026	-1.5170
MIR1296	0.0233	-1.5200
ERLIN1	0.0449	-1.5204
LOC149069	0.0181	-1.5211
LOC645387	0.0037	-1.5217
NDNL2	0.0024	-1.5220
LOC100134108	0.0285	-1.5319
LOC100133377	0.0014	-1.5354
ORC5	0.0408	-1.5358
XRCC6	0.0419	-1.5363
UBXN2A	0.0329	-1.5381
SNORA5B	0.0391	-1.5388
CXORF30	0.0235	-1.5398
ROCK1	0.0308	-1.5399
COQ2	0.0059	-1.5424
HS.211724	0.0405	-1.5445
IKZF3	0.0181	-1.5452
PAK2	0.0237	-1.5458
RNU1-4	0.0485	-1.5464
LOC100130070	0.0355	-1.5476
HADHB	0.0146	-1.5514
NR1H2	0.0183	-1.5534
RPLP0P2	0.0431	-1.5548
LOC100132488	0.0123	-1.5611
FOXJ2	0.0132	-1.5617
LYRM1	0.0443	-1.5620
FGGY	0.0338	-1.5623
LOC390414	0.0123	-1.5635
LOC649702	0.0494	-1.5677

NARG2	0.0298	-1.5695
PAIP2	0.0033	-1.5719
LOC100128140	0.0153	-1.5723
PMPCA	0.0123	-1.5731
GALNT3	0.0134	-1.5738
GTF2H2C	0.0327	-1.5779
HS.555583	0.0087	-1.5811
THOP1	0.0109	-1.5838
LOC100130015	0.0178	-1.5863
FLJ41562	0.0162	-1.5879
LDHAL6A	0.0273	-1.5920
PTTG1IP	0.0426	-1.5950
LOC441958	0.0118	-1.5955
LOC402221	0.0091	-1.6040
LOC651017	0.0371	-1.6104
LOC646446	0.0004	-1.6162
DYNLRB1	0.0430	-1.6200
LOC441642	0.0010	-1.6205
LOC100131301	0.0148	-1.6252
LOC392522	0.0023	-1.6442
ZNF185	0.0417	-1.6490
C12ORF10	0.0349	-1.6553
HS.571417	0.0373	-1.6585
ZNF391	0.0376	-1.6622
TMEM115	0.0437	-1.6622
NDUFAF7	0.0374	-1.6686
CCDC28B	0.0279	-1.6711
MAP1LC3C	0.0081	-1.6794
LOC100131905	0.0244	-1.6798
RSPRY1	0.0449	-1.6880
GIMAP4	0.0141	-1.6908
COX4I1	0.0167	-1.6925
LOC101060275	0.0331	-1.6953
LOC642154	0.0232	-1.7003
HS.534439	0.0233	-1.7095
NOL12	0.0038	-1.7115
LOC100133329	0.0092	-1.7121
GGPS1	0.0379	-1.7309
MED30	0.0454	-1.7361
MRPS18B	0.0286	-1.7389
HS.536620	0.0241	-1.7504
GPS1	0.0281	-1.7592
HS.483906	0.0370	-1.7700
LOC646966	0.0036	-1.7731
CCR4	0.0249	-1.7744

LOC728453	0.0470	-1.7791
SLC25A39	0.0262	-1.7805
KIAA0408	0.0027	-1.7815
RHOH	0.0366	-1.7836
PARP12	0.0257	-1.7860
ENDOG	0.0478	-1.7885
REXO1	0.0134	-1.8052
RPL26	0.0038	-1.8124
SLC46A3	0.0091	-1.8131
FAM175B	0.0091	-1.8204
ZNF324B	0.0252	-1.8207
KCTD17	0.0351	-1.8209
LOC648366	0.0203	-1.8247
LOC441154	0.0025	-1.8259
HS.536748	0.0499	-1.8390
HOOK1	0.0431	-1.8462
NEK8	0.0051	-1.8943
CASC3	0.0429	-1.9007
LOC647466	0.0374	-1.9196
ZNF526	0.0418	-1.9362
XRCC5	0.0022	-1.9465
CDS2	0.0085	-1.9554
TCP11L2	0.0426	-1.9596
KAT6A	0.0402	-1.9707
IFT46	0.0222	-1.9791
CHCHD2	0.0269	-1.9977
PSMC5	0.0206	-2.0414
SNORD35B	0.0298	-2.0448
ZFP36L2	0.0354	-2.0477
CD99L2	0.0166	-2.0643
ELOF1	0.0038	-2.0698
LOC730288	0.0018	-2.0869
LOC653717	0.0031	-2.0932
LOC646093	0.0000	-2.0952
LOC647079	0.0093	-2.1156
WHAMM	0.0155	-2.1513
FRAT2	0.0131	-2.1557
TNFAIP8L2	0.0144	-2.1859
GCSAML	0.0254	-2.2023
GUSB	0.0163	-2.2693
LOC728973	0.0009	-2.2933
RANGAP1	0.0282	-2.2964
PICK1	0.0275	-2.3522
ANGPTL4	0.0132	-2.4163
IL18RAP	0.0078	-2.4413
CRNKL1	0.0497	-2.4663

HS.552160	0.0101	-2.4743
S1PR5	0.0451	-2.5057
MRPL51	0.0385	-2.5697
LOC652776	0.0067	-2.5943
SNORA3B	0.0346	-2.9220
NT5C	0.0170	-3.1617
LOC644436	0.0049	-3.1767
WDR18	0.0292	-3.2611
CRIP1	0.0064	-3.4121
CD52	0.0024	-3.4999

9.1. Method: Mass spectrometry

CEMS Proteomics Facility – The James Black Centre – King's College London

Research Report Document

From Steve Lynham **Date** 6th September 2017

To Sangmi Kim
Susan John

LC-MS/MS Identification and Quantitative Analysis of Proteins in Plasma PBMCs from Healthy Controls and Patients with Granulomatosis with Polyangitis

Introduction

The aim of this work was to identify proteins with quantifiable differences comparing isolated peripheral blood mononuclear cells (PBMCs) from healthy and patient plasma. The samples were collected in heparin tubes and centrifuged to collect plasma before being processed to isolate PBMC by Ficoll density centrifugation. The samples included three healthy control (HC) plasmas and 6 Granulomatosis with polyangitis (GPA) autoimmune patient plasma samples, of which three GPA could induce CD25 and IL-21 expression when co-cultured with healthy PBMC and three that didn't. The group have seen significant differences in cytokine expression in the GPA plasmas vs. HC, but have not looked for any other proteins. They expect that there may be microbial polypeptides that maybe differentially expressed. They are interested in identifying proteins that might be driving the differential IL-21 expression in the co-culture assay with healthy PBMC, as IL-21 is a key cytokine that promotes Follicular T-helper (Tfh) cell differentiation in GPA,

which can enhance B-cell differentiation and autoantibody production in germinal centers and thus promote disease progression. They also think that there must be proteins that are present in the Il-21 inducing GPA plasmas that maybe missing in the GPA samples that do not induce Il-21.

Samples were provided by Sangmi Kim and Susan John (Department of Immunobiology, King's College London) for a multiplex quantitative experiment using Tandem Mass Tags (TMT) in a 10plex labelling kit, isoelectric focussing separation for peptide/protein identification and quantitation by LC-MS/MS.

Methods

Sample Preparation

Nine plasma samples were provided in labelled tubes, three from healthy individuals, three from patients with GPA that can induce IL21 and CD25 (GPA7, 8 & 26) and three from patients that did not induce IL21 and CD25 from PBMC (GPA5, 6 & 25). Samples were subjected to a protein assay to determine the level of total protein. A volume loading protocol with a set volume load of 100□l per sample was employed instead in this experiment regardless of the protein amount.

Protein Assay

Samples were prepared for assay using the Bradford reagent method. Bovine serum albumin (BSA) standard was prepared to as a stock solution (3 □g/□l in lysis buffer) with a standard curve prepared for microtitre plate assay (Table 1).

Table 1: BSA standard preparation for protein estimation assay.

BSA standard concentration (□g/□l)	Volume of BSA stock (□l)	Volume of Lysis buffer (□l)
0	-	500
0.025	4.22	495.78
0.05	8.45	491.55
0.1	16.89	483.11
0.2	33.78	466.22
0.4	67.57	432.43
0.5	84.46	415.54

10 □l of each appropriate standard was pipetted (on ice, to limit evaporation) in triplicate into microtitre plate wells. All samples were diluted by 1:200 and 1:300 in PBS to determine which dilution was within the range of the standard curve and pipetted in

triplicate into the microtitre plate wells adjacent to the BSA standards. Bradford (Bio-Rad) dye reagent was prepared by diluting 1 part dye with 4 parts 18MΩ water (10 ml dye + 40 ml 18MΩ H_2O). Following the addition of 200 µl Bradford reagent dye to all samples and standards, the plate was read at 595 nm (Figure 1).

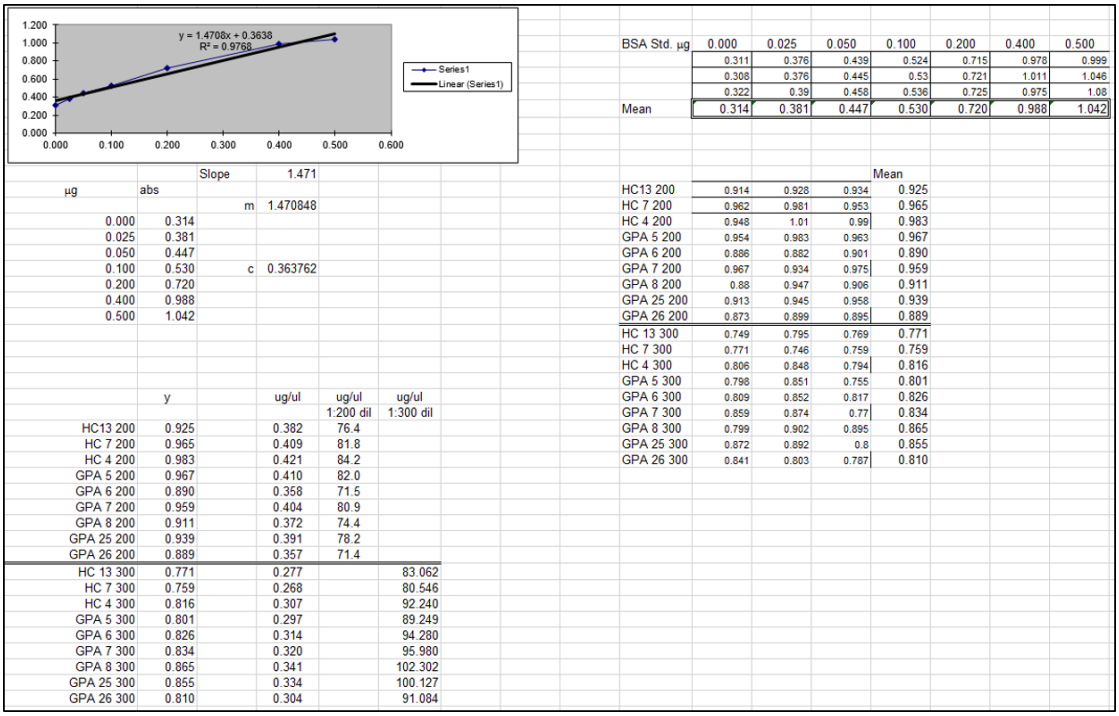

		Slope	1.471										
µg	abs												
		m	1.470848										
0.000	0.314												
0.025	0.381												
0.050	0.447												
0.100	0.530	c	0.363762										
0.200	0.720												
0.400	0.988												
0.500	1.042												
	y		ug/ul	ug/ul 1:200 dil	ug/ul 1:300 dil								
HC13 200	0.925		0.382	76.4									
HC 7 200	0.965		0.409	81.8									
HC 4 200	0.983		0.421	84.2									
GPA 5 200	0.967		0.410	82.0									
GPA 6 200	0.890		0.358	71.5									
GPA 7 200	0.959		0.404	80.9									
GPA 8 200	0.911		0.372	74.4									
GPA 25 200	0.939		0.391	78.2									
GPA 26 200	0.889		0.357	71.4									
HC 13 300	0.771		0.277		83.062								
HC 7 300	0.759		0.268		80.546								
HC 4 300	0.816		0.307		92.240								
GPA 5 300	0.801		0.297		89.249								
GPA 6 300	0.826		0.314		94.280								
GPA 7 300	0.834		0.320		95.980								
GPA 8 300	0.865		0.341		102.302								
GPA 25 300	0.855		0.334		100.127								
GPA 26 300	0.810		0.304		91.084								

BSA Std. µg	0.000	0.025	0.050	0.100	0.200	0.400	0.500
	0.311	0.376	0.439	0.524	0.715	0.978	0.999
	0.308	0.376	0.445	0.53	0.721	1.011	1.046
	0.322	0.39	0.458	0.536	0.725	0.975	1.08
Mean	0.314	0.381	0.447	0.530	0.720	0.988	1.042

				Mean
HC13 200	0.914	0.928	0.934	0.925
HC 7 200	0.962	0.981	0.953	0.965
HC 4 200	0.948	1.01	0.99	0.983
GPA 5 200	0.954	0.983	0.963	0.967
GPA 6 200	0.886	0.882	0.901	0.890
GPA 7 200	0.967	0.934	0.975	0.959
GPA 8 200	0.88	0.947	0.906	0.911
GPA 25 200	0.913	0.945	0.958	0.939
GPA 26 200	0.873	0.899	0.895	0.889
HC 13 300	0.749	0.795	0.769	0.771
HC 7 300	0.771	0.746	0.759	0.759
HC 4 300	0.806	0.848	0.794	0.816
GPA 5 300	0.798	0.851	0.755	0.801
GPA 6 300	0.809	0.852	0.817	0.826
GPA 7 300	0.859	0.874	0.77	0.834
GPA 8 300	0.799	0.902	0.895	0.865
GPA 25 300	0.872	0.892	0.8	0.855
GPA 26 300	0.841	0.803	0.787	0.810

Figure 1: Bradford assay calculation for total protein estimation for all samples

All samples were diluted 1:200 in PBS following the protein assay calculation prior to further processing. A Reference sample containing an equal proportion of each of the nine samples was produced (Figure 2).

Sample	ug/ul	in 10ul	make up to 1ml in Ambic	Take 100ul to make
HC13	76.4	763.60	0.76	76.36
HC 7	81.8	817.99	0.82	81.80
HC 4	84.2	841.56	0.84	84.16
GPA 5	82.0	819.81	0.82	81.98
GPA 6	71.5	715.10	0.72	71.51
GPA 7	80.9	808.93	0.81	80.89
GPA 8	74.4	744.11	0.74	74.41
GPA 25	78.2	781.73	0.78	78.17
GPA 26	71.4	714.20	0.71	71.42
		781.73		Dry down to completion at this point for digest and TMT
			Take 7007.03 and divide by 90 to give:	
Reference is made up of 10ul of each sample (90ul)		7007.03 in 90ul	77.86	this is the value of 1ul and is close to the mean and median so use this
Median	781.7			Take 10uls to make 778.6 and make up to 1ml in Ambic to give 0.778
				Take 100uls of this to give 77.80

Figure 2: Reference sample calculation containing a proportion of all nine samples

A volume loading protocol with a set volume load of 100µl per sample was employed after the dilution. 10µls of each diluted sample was aliquoted into the Reference sample tube. All samples were then dried to completion in a SpeedVac (Thermo Fisher Scientific) prior to enzymatic digestion.

Enzymatic Digestion

Cysteine reduction and alkylation followed by digestion with trypsin were performed on all 10 samples prior to subsequent isobaric mass tag labelling.

Reagents:

200mM TEAB & 0.2% SDS – 1ml 1M TEAB in 3900µl water and 100µl 10% SDS to give 0.2% SDS in 200mM TEAB

100mM TEAB & 0.1% SDS – 500µl 1M TEAB in 4450µl water and 50µl 10%SDS to give 0.1% SDS in 100mM TEAB

100mM TEAB & 0.1% TFA – 500µl 1M TEAB in 4495µl water and 5µl TFA to give 0.1% TFA in 100mM TEAB

8mM TCEP – 22.93mg in 1ml 100mM TEAB & 0.1% SDS for 80mM stock; dilute stock 10-fold

67.5mM IAA – 12.48mg in 1ml 100mM TEAB & 0.1% SDS for 67.5mM stock

0.2µg/µl Trypsin – add 125µl 100mM TEAB & 0.1% TFA to a 25µg vial

1. All 100µl samples were dried to completion in a Speed Vac (ThermoFisherScientific) and made up to 70µl in 100mM TEAB and 0.1% SDS (Table 2).

Table 2: TMT labelling protocol sample volume calculation table

Sample #	Dried Volume Load (µl)	Volume of ddH2O (µl)	Volume of 200mM TEAB & 0.2% SDS (µl)	Total Sample Volume (µl)
Reference	100	35	35	70
HC4	100	35	35	70
HC7	100	35	35	70
HC13	100	35	35	70
GPA5	100	35	35	70
GPA6	100	35	35	70
GPA7	100	35	35	70
GPA8	100	35	35	70
GPA25	100	35	35	70
GPA26	100	35	35	70

2. Reduce the cysteine residues by adding 10µl 8mM TCEP (made up in 100mM TEAB and 0.1% SDS) and incubating samples at 55°C for 1 hour.

3. Cool samples to room temperature then alkylate by adding 10µl of 67.5mM IAA (in 100mM TEAB and 0.1% SDS) and incubating at room temperature in the dark for 30 minutes.

4. Perform trypsin digestion on the samples by adding 10µl of 0.2µg/µl trypsin (in 100mM TEAB and 0.1% TFA). Incubate samples at 37°C overnight.

Peptide Labelling with TMT

Each sample was treated individually with labels added at a 1:1 ratio. The mass tags contain four regions in their structure which includes a mass reporter region, a cleavable linker region, a mass normalisation region and a protein reactive group. The chemical structures of ten tags are identical with the isotopes being substituted at different positions (Figure 3). The tags have the same molecular weight and to compensate for the isotopic variation, the mass reporter and mass normalisation regions have different molecular masses in each tag. This being the case, during chromatographic separation and in MS survey scan mode, the different tags are indistinguishable from each other. Under MS/MS fragmentation however, the reporter ions are distinguishable and quantification data, along with peptide identification are obtained (Figure 4).

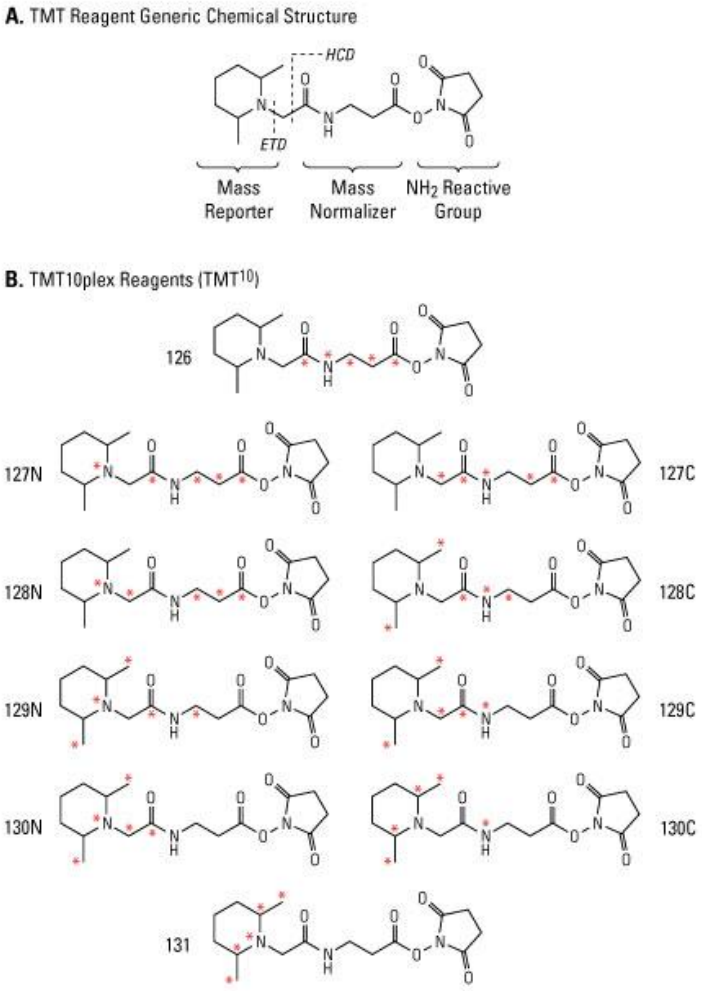

Figure 3: Structure of the amine TMT10plex tags. A. Functional regions of the TMT reagent structure including MS/MS fragmentation sites by higher energy collision dissociation (HCD) and electron transfer dissociation (ETD). B. TMT10plex reagent structures with 13C and 15N heavy isotope positions (red asterisks). (Reproduced from ThermoFisher.com).

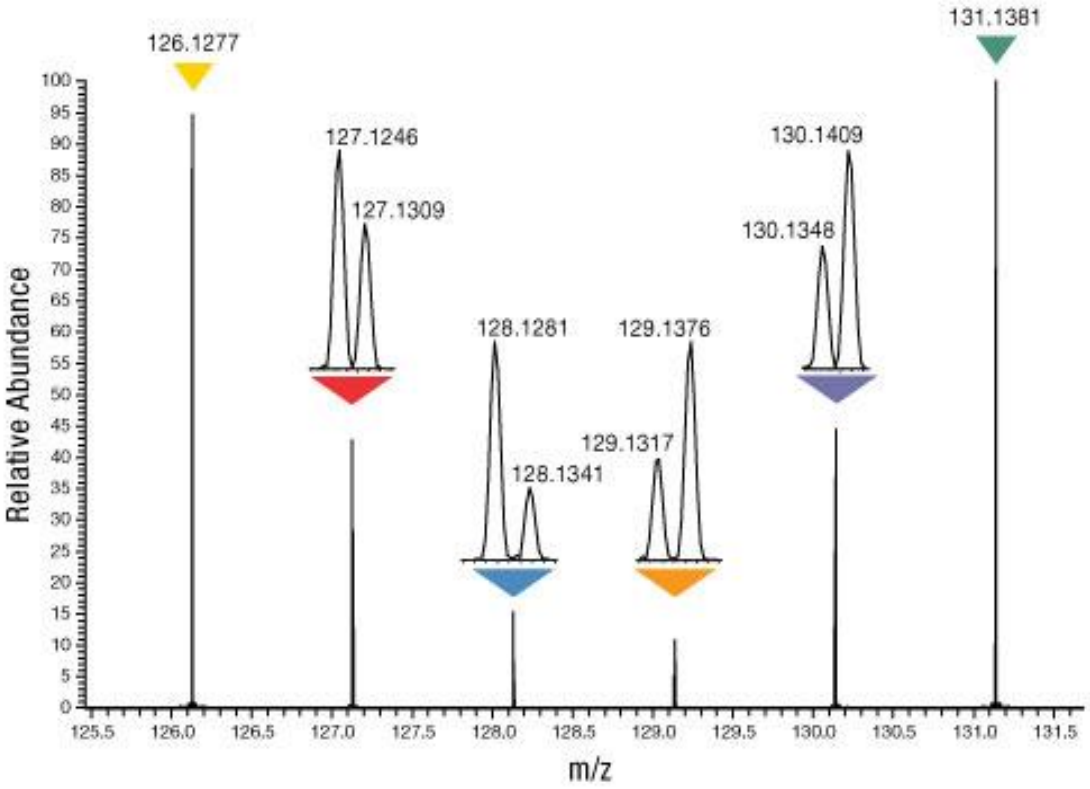

Figure 4: TMT10plex reporter ion ratios following fragmentation. The relative abundance of the target protein or peptide fragment in ten different samples is easily measured by comparing the reporter ions generated by MS/MS fragmentation of the different mass tags (Reproduced from ThermoFisher.com).

Following trypsin digestion, each individual sample was labelled with a unique TMT10plex label (Table 3).

Table 3: Sample labelling strategy for TMT10plex

Sample #	TMT10plex Label	Individual Label Mass (Daltons)
Reference	126	126.1277
HC4	127c	127.1246
HC7	127n	127.1309
HC13	128c	128.1281
GPA5	128n	128.1341
GPA6	129c	129.1317
GPA7	129n	129.1376
GPA8	130c	130.1348
GPA25	130n	130.1409
GPA26	131	131.1381

1. 41µl of appropriate TMT reagent (ThermoFisherScientific, UK; Lot# SC249418Awas added to the appropriate sample, vortexed and briefly centrifuged at 14000rpm before incubation at room temperature for 1 hour.
2. Stop the reaction by adding 8µl of 5% hydroxylamine to each sample and incubating for a further 15 minutes at room temperature.
3. Combine all 10 samples for each TMT10plex and incubate at room temperature for a further 15 minutes.
4. Freeze combined sample at -80°C then dry to completion in a Speed vac.

Sample Fractionation by Isoelectric Focussing

The TMT10plex samples were fractionated using isoelectric focussing (IEF, Agilent Technologies, UK) in a low resolution strip (12 well) with a 3-10 non-linear (NL) gradient. Firstly, the lyophilised samples were resuspended in a stock solution of IPG buffer prior to fractionation. The IEF strips were also rehydrated using a solution containing stock IPG buffer

Reagents:

IPG stock solution - 60µl IPG buffer added to 600µl glycerol and 4340µl ddH_2O water.

Sample resuspension buffer – 1800µl IPG stock solution.

IEF strip rehydration buffer – 560µl IPG stock added to 140µl ddH_2O.

Ampholytes.

1. Rehydrate the IEF strip using the rehydration buffer in the strip tray.
2. Resuspend the sample using the resuspension buffer, vortex and centrifuge for 1min at 14000rpm.
3. Add equal volumes (150µl) of the sample to each of the 12 sample wells across the strip
4. Place wicks, electrodes and mineral oil to the ends of the strips and tray
5. Set 100kVh method and start (Figure 5).
6. Once complete, remove each fraction to a separate tube and label accordingly. Wash each well with 100µl 49.9%/50%/0.1% (H_2O/Acetonitrile/Formic acid). Remove the solution and pool with the respective sample tubes.
7. Dry to completion in a Speed vac and store at -80°C until analysed by mass spectrometry

Figure 5: Isoelectric focussing run time information. Full separation over 20kVh completed in just over 18 hours.

Sample clean up

Separated fractions contain glycerol as an ingredient of the IEF buffer which must be removed prior to mass spectrometry analysis. The glycerol was removed using C18 reversed-phase Zip-Tips (Millipore) to bind the labelled peptides and wash the contaminant to waste. Zip-Tips were primed with 100% acetonitrile (ACN) and equilibrated with 0.1% trifluoroacetic acid (TFA) as an ion-pairing agent to help bind the peptides. Peptides were bound to the C18 packing and washed with 0.1% TFA before elution with 50% ACN/0.1% Formic acid. Peptide eluates were dried to completion in a SpeedVac.

LC-MS/MS tandem mass spectrometry

The fractionated TMT labelled peptide samples were resuspended in 15µL of 50mM ammonium bicarbonate before pooling fractions together with a total volume of 30□l. Fraction 1 was pooled with Fraction 7, Fraction 2 was pooled with Fraction 8 and so on. Six samples were analysed by LC-MS/MS. Chromatographic separations were performed using an EASY NanoLC system (ThermoFisherScientific, UK). Peptides were resolved by reversed phase chromatography on a 75 µm C18 column using a three step linear gradient of acetonitrile in 0.1% formic acid. The gradient was delivered to elute the peptides at a flow rate of 300 nL/min over 180 min. The eluate was ionised by electrospray ionisation using an Orbitrap Velos Pro (ThermoFisherScientific, UK) operating under Xcalibur v2.2. The instrument was programmed to acquire in automated data-dependent switching mode, selecting precursor ions based on their intensity for sequencing Higher-energy C-trap dissociation (HCD) for peptide identification and reporter ion fragmentation. The

instrument was operated in automated data-dependent switching mode, selecting precursor ions based on their intensity for sequencing by HCD in a Top 10 method. The MS/MS analyses were conducted using higher than normal collision energy profiles that were chosen based on the mass-to-charge ratio (m/z) and the charge state of the peptide.

Database Searching

Raw mass spectrometry data were processed into peak list files using Proteome Discoverer (ThermoScientific; v1.4) (Figure 6).

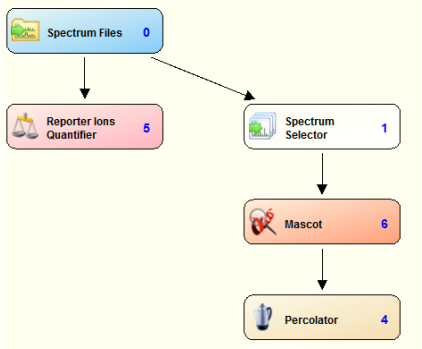

Figure 6: Proteome discoverer nodal workflow for raw data processing method 'Steve_TMT10plex_LotNo.SC249418A_TMT_SK_SJ_HT.

Spectrum Selector

Min. Precursor mass:	350 Da
Max. Precursor mass:	10000 Da
S/N Threshold (FT-only):	1.5

Mascot

Database:	Uniprot
Enzyme:	Trypsin
Missed cleavage:	2
Precursor mass tol:	20 ppm
Fragment mass tol:	0.05 Da
Dynamic modifications:	TMT6plex (K)
	TMT6plex (N-Term)
	Carbamidomethyl (C)
	Oxidation (M)

Peptide validator

Target FDR (strict):	0.01
Target FDR (relaxed):	0.05

Reporter ion quantifier

Integration window tol.:	20 ppm
Integration method:	Most confident centroid

Each of the six pooled fraction raw data files were searched individually and also processed together as one TMT10plex experiment and searched as a 'Mudpit' using the Mascot search algorithm (www.matrixscience.com) against Human Taxonomy only in the Uniprot database (Table 4).

Table 4: LC/MS/MS reference table. Up = Uniprot Database; HT = Human Taxonomy.

Sample	**LC/MS/MS Ref.**	**Date Analysed**	**Mascot Search Ref.**
PR474_SK1_7_TMT10plex_HT	20112017	20/11/2017	45779up HT
PR474_SK1_7_TMT10plex_HT	20112017	20/11/2017	45780up HT
PR474_SK1_7_TMT10plex_HT	20112017	20/11/2017	45781up HT
PR474_SK1_7_TMT10plex_HT	20112017	20/11/2017	45782up HT
PR474_SK1_7_TMT10plex_HT	20112017	20/11/2017	45783up HT
PR474_SK1_7_TMT10plex_HT	20112017	20/11/2017	45787up HT
PR474_SK1_7_TMT10plex_Mudpit_HT	20112017	20/11/2017	45788up HT

Results

LC-MS/MS analysis has successfully identified many proteins from the TMT10plex experiment comparing samples of healthy control PBMC and PBMC with inducing and non-inducing PGA. Samples were searched using the Uniprot database selecting Human Taxonomy (HT). Database generated files were uploaded into Scaffold 4 (v4.8.4) software (www.proteomesoftware.com) to create a .sfd file (PR474 SK1_7_6_12_mudpit_HTup_20171122_EDIT; Figure 7).

Scaffold allows statistical filtering of the data at the protein and peptide level. These filters were applied to the data at various confidence levels for protein identification with a minimum of three peptides, and also a lower stringency of one peptide (Table 4). High stringency filters of 95% confidence interval (CI) for minimum protein, 1 peptide and 0% CI for peptide values was applied (bold numbers; boxed area; Table 3). Mascot applies a 95% probability CI in the MOWSE scoring algorithm that is an identification threshold. This threshold is calculated as described on the Matrix Science website:

"Given an absolute probability that a match is random, and knowing the size of the sequence database being searched, it becomes possible to provide an objective measure of the significance of a result. A commonly accepted threshold is that an event is significant if it would be expected to occur at random with a frequency of less than 5%."

Any protein that is above this identity threshold is deemed significant.

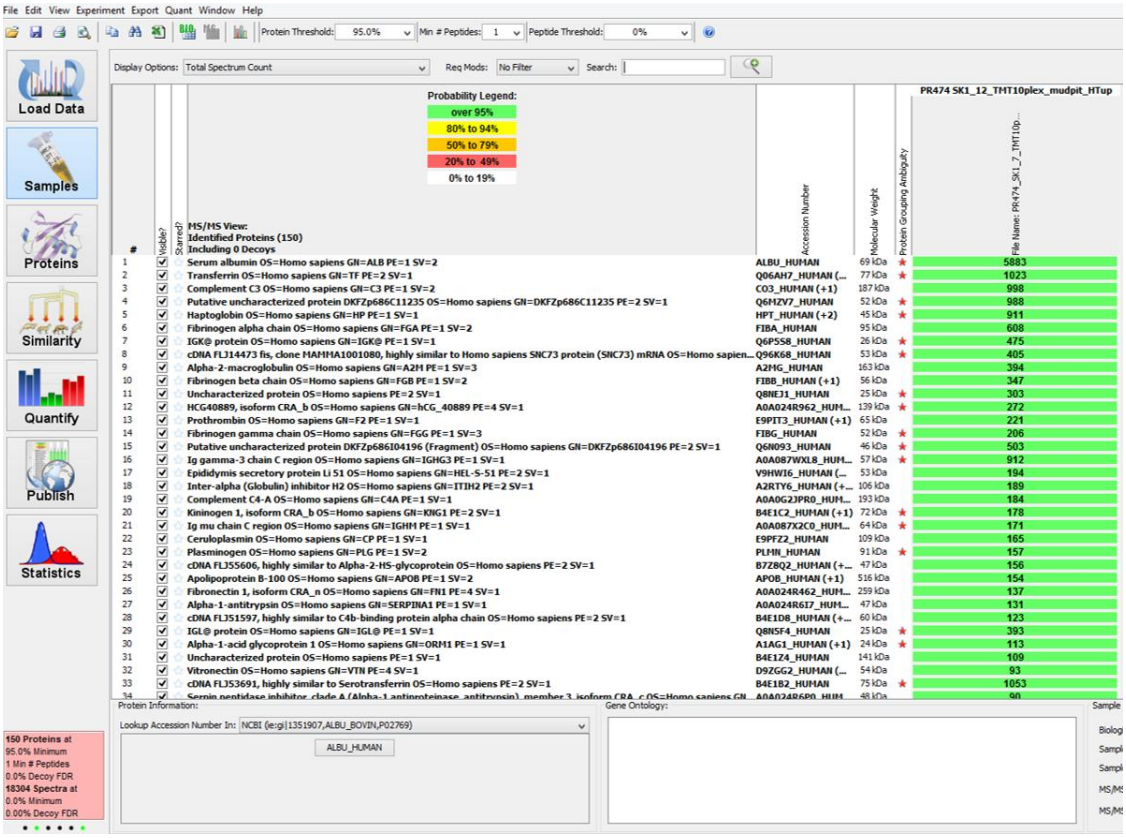

Figure 7: Scaffold sample view representing total qualitative protein identifications from the TMT10plex experiment following database searching against the Human portion of the Uniprot database.

Table 5: Qualitative protein assignments from sequence data following LC-MS/MS analysis

Filter Stringency	PR474 SK1_7_6_12_mudpit_HTup (3 pep/1 pep)
99%	93/130
95%	106/**150**
90%	110/165
80%	117/218

50%	148/538
20%	148/1383

150 proteins were detected in the PR474 SK1_7_6_12_mudpit_HTup sample following database searching and 95% CI filtering. These are numbers of total proteins identified from the Human portion of the Uniprot database. A further filter was applied to the data in the Scaffold software which allows a specific search for proteins that contain a TMT label. This can be used to check for labelling efficiency at the protein level as we assume that every peptide is labelled to 100% efficiency. Figure 8 represents the Scaffold TMT filtering for the same data set.

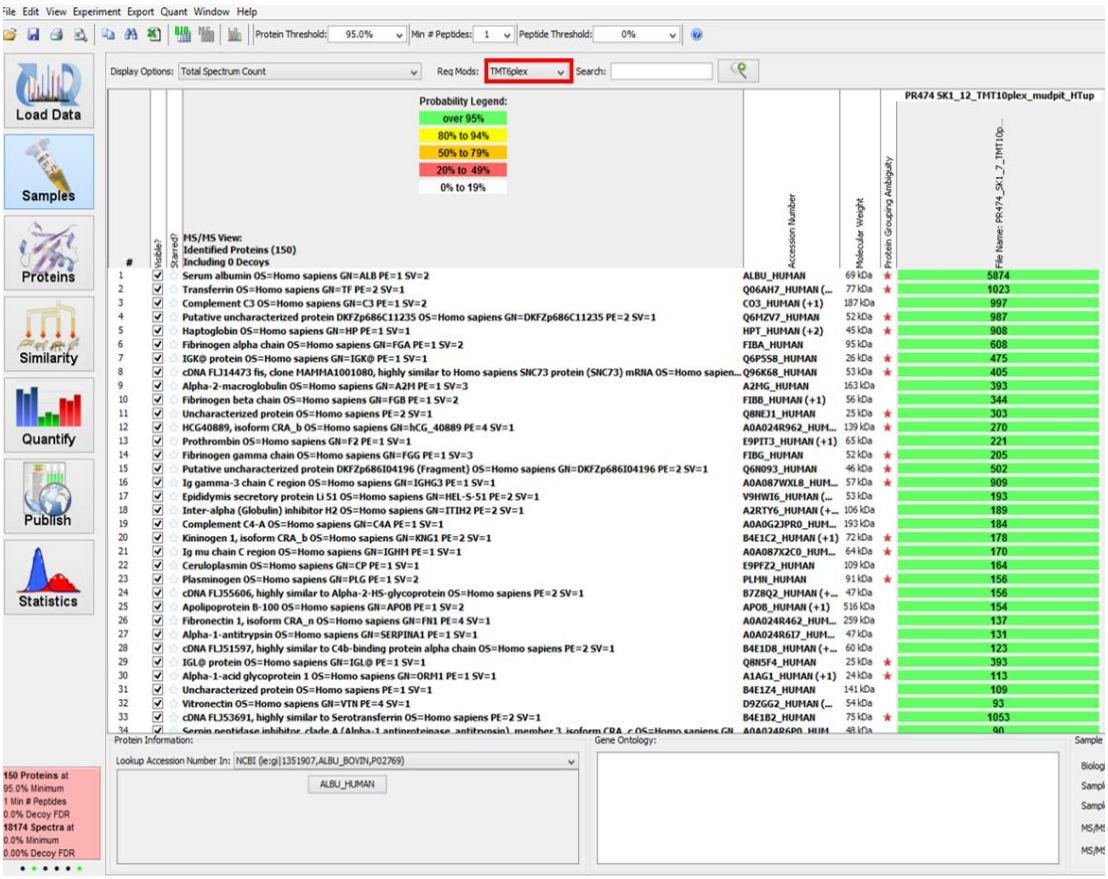

Figure 8: Scaffold sample view representing the protein identifications after filtering for proteins containing a TMT label (red box).

Table 6: Qualitative protein assignments after Scaffold filtering for TMT labelled proteins only.

Filter Stringency	R474 SK1_7_6_12_mudpit_HTup (3 pep/1 pep)

99%	93/130
95%	106/**150**
90%	110/163
80%	117/205
50%	143/453
20%	147/983

Overall, a slightly lower number of proteins were detected after applying the TMT label filter (Table 6) although the same number of proteins (150) were detected after the filter was applied. When compared to the total number of proteins identified this shows that there was a 100% labelling efficiency at the protein level (95% CI).

Quantitative protein measurements

Quantitative measurement filters in the Proteome Discoverer software were set to the low stringency (p=0.05) when extracting the quantitative data to be in-line with the Scaffold qualitative data. The TMT reporter ion signal (area under the peak) was used to measure the abundance between the detected peptides across the TMT10plex. The reporter ion signal can be seen in Figure 9 at the low end of the fragmentation spectra. The value for each peptide in a protein was summed into one measurement for the fold-change calculation to determine an up or down-regulation of the identified proteins.

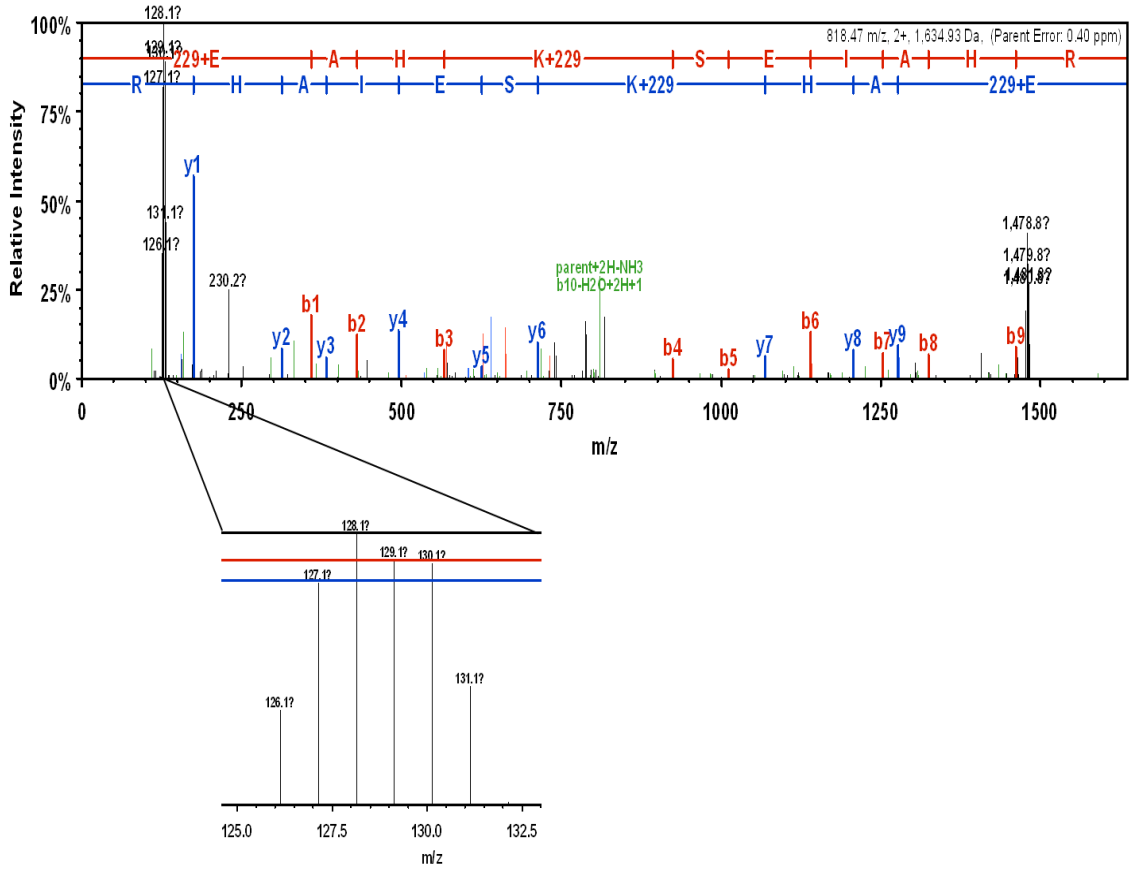

Figure 9: Representation of an LC-MS/MS peptide fragmentation spectra displaying the TMT reporter ion peaks at the low mass end of the spectra. Absolute ion intensity value of the area under the peak of the reporter ions was used in calculation of fold-change differences between the peptides.

Proteome Discoverer quantitative output

Following the data processing method highlighted in Figure 6, Proteome Discoverer (v1.4) was used to extract the absolute peak area of the TMT reporter ions for every labelled peptide. To be considered for comparison, every peptide must have been identified in the database search, have a reporter ion value and a database assigned TMT modification. All peptides that are missing either of these parameters are removed prior to data processing steps.